Survey and comparison of petroleum well electrologging tools

Khemarat Kunsuik-Mengrai

SURVEY AND COMPARISON OF PETROLEUM WELL ELECTROLOGGING TOOLS

BY
KHEMARAT KUNSUIK-MENGRAI

Thesis submitted for the degree of M.Sc.

To

The University of Durham
School of Engineering and Applied Science
July 1989

ABSTRACT

The principles used in the design of electrologging tools used in the petroleum industry are reviewed. Examples of tools and methods are taken from Gearhart Industries, Schlumberger Ltd and Western Atlas Ltd who are the three major electrologging companies accounting for 93% of the world market share. The survey and comparison of the tools in each of the category used both during the exploration and development stage of a well and reservoir are made. The results are presented and discussed. Furthermore an insight to the future of this industry is presented.

CONTENTS

TABLE OF FIGURES

TABLES

CHARTS

GLOSSARY OF TERMS

The following is a list of commonly used words found in this thesis:-

Annulus - When there is casing within the well, the space between the outer casing wall and the formation is often referred to as the "annulus". In a multi-string completion, the space between the outer tubing wall and the inner casing wall can also be referred to as the "annulus".

API - American Petroleum Institute.

Bed - A layer of geological formation is also termed a "bed".

Bit - The drill-bit used to make the hole.

Borehole - The hole of the well.

Bowspring - A spring device attached to a logging tool to help eccentering the tool to one side of the borehole wall.

Cable - The link between the downhole tools and the surface processing computer, through which the signals are transmitted.

Cartridge - Part of the logging tool which contains the electronics to power the sensors, process the resulting measurement signals, and transmit the signals up the cable to the truck.

Casing - Pipe of various sizes, usually 30, 20, 13, 9, 7, or 5 inches which is lowered into the well to stop the the borehole from collapsing.

Cement - Seals the casing in-place within a well.

Cuttings - The drilled particles of rock formation.

Dual calipers - When a logging tool has four caliper arms, the two opposite arms generally work together to give the borehole diameter. Hence, four caliper arms will give two borehole diameters at 90° to each other. A tool having four caliper arms is commonly known to provide "dual calipers".

Flushed zone - The zone which has been flushed out by the filtrate of the drilling mud.

Formation - The structure of rocks which surrounds the borehole.

Gas-oil ratio - The ratio of oil to gas produced in a well, often referred to as "GOR".

Log	-	A graph of resistivity, porosity, etc., made with the logging tool stationary, or versus the formaton depth which is permanently recorded on tape, film, or print paper is referred to as a "log".
Mud	-	The fluid used within a well, generally while drilling, to contain the borehole pressure, to lubricate the drilling bit, to transport the drilled cuttings to surface. The common fluid base can be freshwater, seawater, or diesel, and the chemicals added can be for example: barite, potassium chloride, sodium chloride, etc..
Mud filtrate	-	The solvent of the mud fluid.
Mud-cake	-	The solute of the mud fluid, generally left on the borehole wall as the filtrate invades into the formation.
Sanding	-	When a sandstone reservoir is forced to produce too fast, the formation will tend to collapse, and the sand matrix will flow out into the wellbore too. This causes both hole-fill and plugging of the producing perforated holes.
Sonde	-	The part of the logging tool which contains the sensors used in making the measurements.
TVD	-	True vertical depth.
Virgin zone	-	The part of the formation surrounding the borehole which has been invaded by the mud filtrate. It is also referred to as the "uninvaded zone".
Water cut	-	Measured in percentage (%), it is the fraction of the water out of the total volume of fluids produced in a well.
Zone of transition	-	The zone between the flushed zone and the virgin zone, and can also be called the "annulus".

SYMBOLS

The following is a list of symbols used in this thesis (refer to figure S-1):

Symbols	Description	Customary Units or Relation
a	electrical activity	moles per litre
a	coefficient in F-ϕ relation	$F = a/\phi^m$
A	atomic weight	atomic mass units
C	electric conductivity	millimhos per metre (mmhos/m)
C_p	sonic compaction factor	$\phi_{SV\,COR} = C_p\ \phi_{SV}$
D	depth	feet (ft) or metres (m)
d	diameter	inches (in.)
E	electromotive force	millivolts (mV)
F	formation resistivity factor	$F = a/\phi^m$
G	geometrical factor (function of d_i)	dimensionless
H	hydrogen index	dimensionless
h	thickness (bed, mud-cake,etc.)	feet, metres, inches
I	index	dimensionless
J	pseudo geometrical factor	dimensionless
K	electrochemical SP coefficent	$E_c = K \log (a_w/a_{mf})$
k	permeability, absolute (fluid flow)	millidarcies (md)
m	porosity (cementation) exponent	$F = a/\phi_m$
p	pressure	pounds/sq.inch (psi)
R	resistivity	ohm-metres (ohm-m)
r	radial distance from hole axis	inches
S	saturation	fraction or percent of pore volume
T	temperature	degrees (°F or °C), or kelvin (K)
t	time	microseconds (ms), seconds (s)
V	Volume	cubic centimetres (cc), cubic feet, etc.
Z	atomic number	dimensionless
ϕ	porosity	fraction or percentage of bulk volume, porosity unit (p.u.)

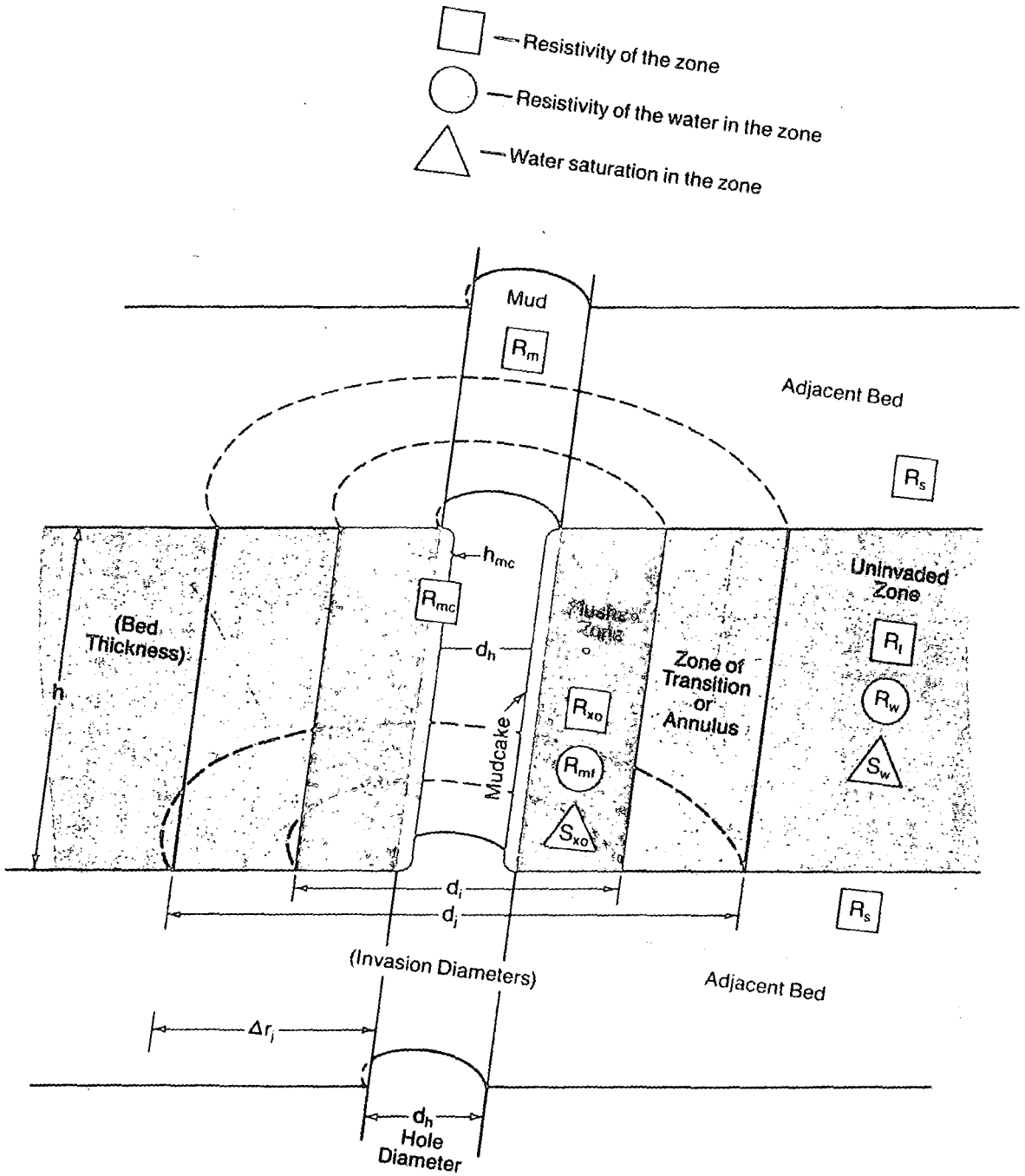

Figure S-1 Symbols used in log interpretation. (Schlumberger, 1987)

τ	Sonic interval transit time	microseconds per foot
ρ	density	grams per cubic centimetre (g/cc)
Σ	neutron capture cross section	capture units (c.u.)
τ	thermal neutron decay time	microseconds

SUBSCRIPTS

The following is a list of subscripts used in this thesis (refer to figure S-1) :

Subscripts	Explanation	Example
a	apparent (general)	R_a
b	bulk	ρ_b
clay	clay	V_{cl}
cor	corrected	τ_{cor}
c	electrochemical	E_c
cp	compaction	B_{cp}
g	gas	S_g
h	hydrocarbon	S_h
hr	residual hydrocarbon	S_{hr}
i	invaded zone (inner boundary)	d_i
int	intrinsic (as opposed to log value)	Σ_{int}
j	invaded zone (outer boundary)	d_j
k	electrokinetic	E_k
log	log values	τ_{log}
m	mud	R_m
max	maximum	ϕ_{max}
ma	matrix	τ_{ma}
mc	mud cake	R_{mc}
mf	mud filtrate	R_{mf}
min	minimum	ϕ_{min}
ni	non-invaded zone	R_{ni}
o	oil (except with resistivity)	S_o
or	residual oil	S_{or}
r	residual	S_{or}, S_{hr}
sh	shale	V_{sh}
SP	spontaneous potential	E_{sp}
SSP	static SP	E_{ssp}
w	water, formation water	S_w
xo	flushed zone	R_{xo}

DECLARATION

The work contained in this thesis has not been submitted for any other degree or qualification, and unless otherwise referenced it is the authors own work.

ACKNOWLEDGEMENTS

I wish to thank my supervisor, Eur Ing Graham M.Geary, for his guidance, advice, support and hospitality throughout the thesis.

Also I wish to thank Professor M.J.H. Sterling for his support throughout the thesis.

Also particular thanks are due to my parents, Saopha and Mom Tada Kunsuik-Mengrai for their guidance, support and encouragement throughout the thesis.

1. INTRODUCTION

Electrical well logging was introduced to the oil industry over half a century ago. Since that time, many additional and improved logging devices have been developed and put into general use.

As the science of well logging advanced, the art of interpreting the data also advanced. Today, the detailed analysis of a carefully chosen suite of wireline services provided a method of deriving or inferring accurate values for the hydrocarbon and water saturations, the porosity, the permeability index, and the lithology of the reservoir rock.

Hundreds of technical papers have been written describing the various logging methods, their application, and their interpretation. This abundance of literature is overwhelming in content and frequently unavailable to the average well log user.

This thesis therefore presents a review of these well logging methods and the equipment of the major logging companies which are available. The various openhole and casehole services offered by these companies are presented and discussed, together with the basic applications. With the huge amount of services available, the discussion is kept as brief and clear as possible. Furthermore this thesis discusses how in the future, the oil industry can affect well logging methods, and how and where the well logging techniques are developing.

It is hoped that this thesis will serve as a useful introduction for anyone interested in electrical well logging. For those who may be interested in more detailed material the references at the end of the thesis and the other well logging literature can be consulted.

2. THE OIL INDUSTRY

2.1 Introduction

Back in August 1859, a blacksmith known as Uncle Billy Smith was drilling a well near Oil Creek just outside of Titusville, Pennsylvania, U.S.A., owned by Edwin L. Drake. The Drake well bottomed out at 69 1/2 feet, not a particularly monumental depth even for 1859, but it was full of oil. Thus, the Drake well heralded the beginning of an era: the petroleum era.

Since then, from a small number of promoters in Pennsylvania, producing and marketing "rock oil" in competition with whale oil, the oil business has grown to the millions who now participate in the finding, drilling, producing, refining, and marketing of oil and gas the world over. And this is not to mention the large number of everyday citizens who own stock in petroleum and petroleum-related companies. In addition, the scientific discoveries and technological developments stimulated by the needs of the petroleum industry furnish the livelihood for thousands of other workers. And, of course, the majority of people in the world nowadays are also petroleum consumers.

At the mention of the petroleum industry, the names of Exxon, Shell, Gulf, or Mobil, to name but a few come to mind. The majority of people visualise these names being associated with the industry from the start, at the exploration stage, to the finish, with the consumers in their homes. However with a closer look, there are many more companies, governments, and people involved in the process. This chapter gives an insight into the industry, with a special attention to electrical well logging.

2.2 Operating Companies

Operating companies are the financiers of the industry and are the principle users of the services provided by drilling contractors and service companies. An operating company, often called simply an operator, is a person or company who actually has the right to drill and produce petroleum that may exist at a particular site. The operator acquires the right by buying or leasing it from the person or persons who own the land under which petroleum may exist. An operator can be a government, a department of the government of a country, or a major company, such as Exxon or Shell. Or an operator can be an "independent", a relatively small and largely

unintegrated company or individual who produces and sells oil and gas but is not engaged in the transporting, refining or marketing of it. A major oil company, on the other hand, is a large integrated company that not only produces oil and gas, but transports it from the field to the refinery and plant, refines or processes it, and sells the product to the general public and other consumers.

A major oil company usually initiates the sequence of events that leads to the drilling of oil and gas wells in foreign fields, but independent oil operators pay for most of the wells in the United States. Sometimes the operating company is also referred to as the "client" by the contractors too.

2.3 Drilling Contractors

Operating companies, both large and small, have found it more expedient to utilise the men, equipment, and skills and experience of drilling contractors to perform the actual drilling of a well. Drilling contractors include names such as Santa Fe, Sedco Forex, Reading and Bates, etc..

2.4 Service and Supply Companies

The contract for "making hole" goes to a drilling contractor, but the operating company is usually the one that awards other contracts to the service and supply companies. The service companies provide specialists at various stages to the well operation. For example, this can be a directional drilling specialist firm (Eastman Whipstock, etc.), electric well loggers (Schlumberger, Western Atlas, etc.), cementing specialists (Halliburton, Dowell Schlumberger, etc.), mud loggers (Exlog, Anadrill, etc.), or well testers (Otis, Schlumberger, etc.). The supply companies provide the operating companies with the tools needed to drill the well, for example the drilling mud and bits. These companies include names such as Baker, Baroid, Magobar, or Reed, etc..

Also, there are numerous consultant companies who can advise the operating companies on the well projects. Indeed, after all the various attendant services needed to drill a well are summed up, there could be as many as a hundred service and supply companies working at the drill site at one time or another. The coordination of all these services is supervised by the operating company, its managers, and engineers. Full cooperation and assistance of all the contractors is required in almost every instant

throughout the operation.

2.5 The Well Plan

The operator, on acquiring the right to explore, initiates the sequence of events from start to finish. The stages involved can be summarised as follow:-

a) Surface seismic survey of the area.

b) If favourable, an exploration (wild cat) well is "spud".

c) At each stage of the well, the well may be cored, is drilled, logged, cased and cemented.

d) If the recovered data look favourable, then the well is planned for production testing.

e) Further analysis of the above will lead probably to the drilling of another well or more.

f) Depending on the result of the whole project, the area may be scrapped if proved "dry", developed if productive, or put on-hold for further study or for economic reasons.

At these various stages, the operator will decide on how to plan the project and who should be the contractors in the project.

2.6 Electric Well Logging

The first electrical log was recorded in 1927 in a well in the small oil field of Pechelbronn, in Alsace, a province of eastern France. This log, a single graph of the electrical resistivity of the rock formations cut by the borehole, was recorded by the "station" method. The downhole measurement instrument (sonde) was stopped at periodic intervals in the borehole, measurements were made, and the calculated resistivity was hand-plotted on a graph. This procedure was carried on from station to station until the entire log was recorded. A portion of this first log is shown in figure 2-1.

In 1929, electrical resistivity logging was introduced on a commercial basis in Venezuela, the United States, and Russia, and soon afterwards in the Dutch East Indies. The usefulness of the resistivity measurement for correlation purposes and for identification of potential hydrocarbon bearing strata was quickly recognised by the oil industry.

In 1931, the spontaneous potential (SP) measurement (ref.: chapter 3) was

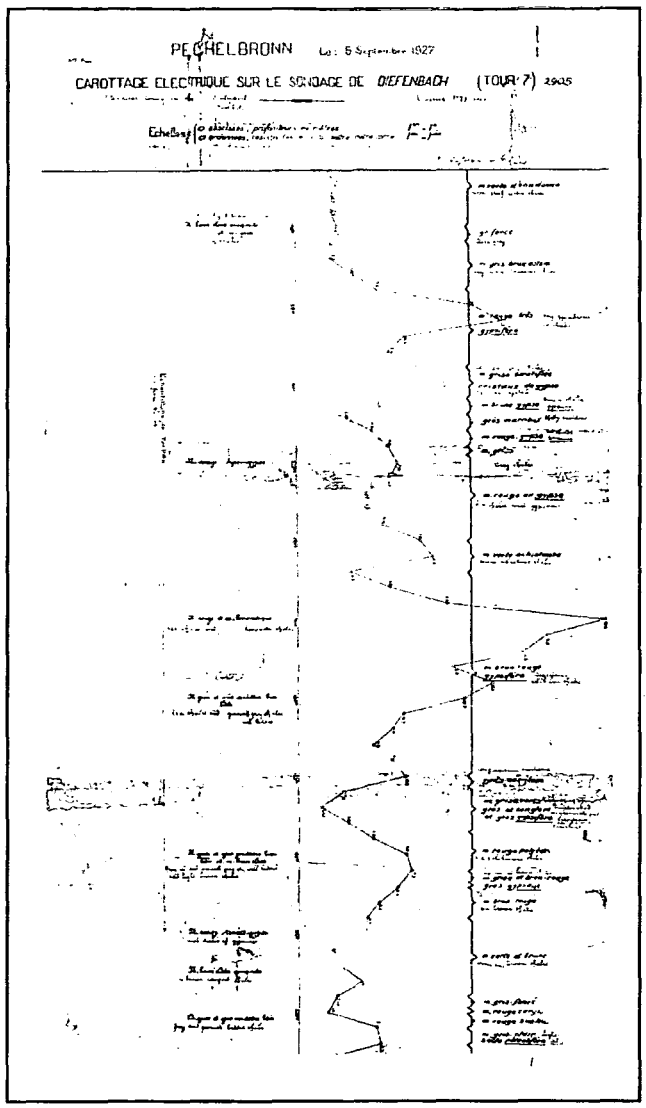

Figure 2-1. The first log: points plotted graph paper by Henri Doll. (Doll, 1943)

included with the resistivity curve on the electrical log. In the same year, the Schlumberger brothers, Marcel and Conrad, perfected a method of continuous recording and the first pen recorder was developed.

Since then many logging services have been developed and used to provide data on the formation within a borehole. Electrical well logging data is usually regarded as providing important information to the operator before he decides whether to embark on a costly production testing process.

2.7 Petroleum Geology

Wireline logs provide a continuous recording of formation parameters versus depth that can be very useful for geologic applications. These range from simple well-to-well correlations through stratigraphic features to the study of entire reservoirs.

Lithology determination from wireline logs is covered in chapter 5. This chapter gives a brief overview of the applications of wireline logs for other geological information. The three fundamental geological parameters, composition, texture, and structure, can be related in some manner to the response of well-logging sensors.

The composition of a rock can be expressed as minerals or as chemical elements. The mineral composition provides the petrophysical properties, such as hardness, density, resistivity and travel time. Some tools measure the concentration in elements, while others have a response that depends on the percentage and distribution of the minerals in the rock. Table 2-1 summarises the relationship between rock composition and logging parameters.

Texture relates to the geometrical aspects of the rock constituents such as grain size sorting, packing shape and arrangement (fabric); matrix and cement arrangement; and the grain-grain, grain-matrix, or grain-cement contacts. The petrophysical properties of the rock, such as porosity and permeability, depend primarily on texture. Table 2-2 show the relationship between rock texture and log parameters.

While texture deals with the grain-to-grain relations in a rock, sedimentary structures are related to the larger features that reflect the conditions at the time of deposition such as energy and type of current. Structures constitute an important element of the facies of a sedimentary unit and aid in defining the depositional environment. The relationship between sedimentary features and log parameters is summarised in table 2-3.

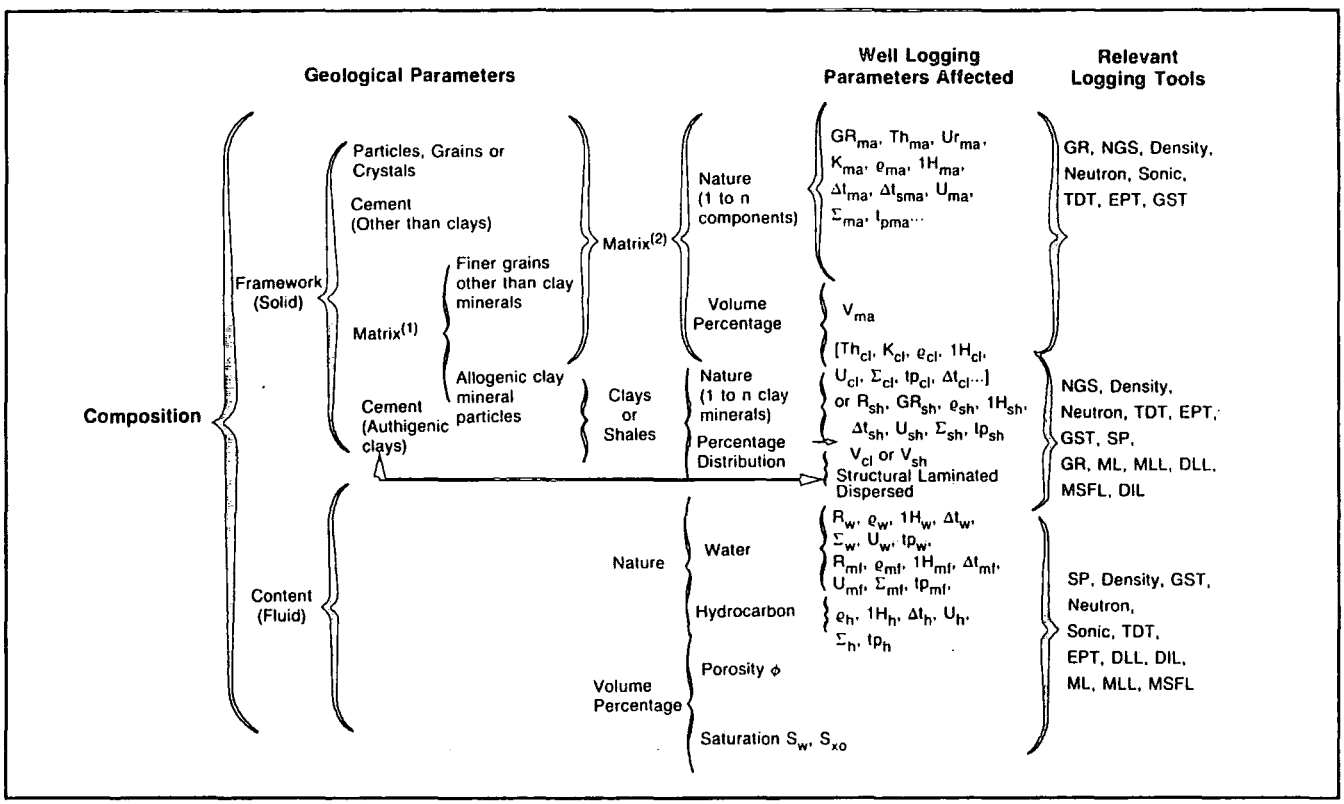

Table 2-1. Relationship between composition of a rock and well logging parameters. (Schlumberger, 1987)

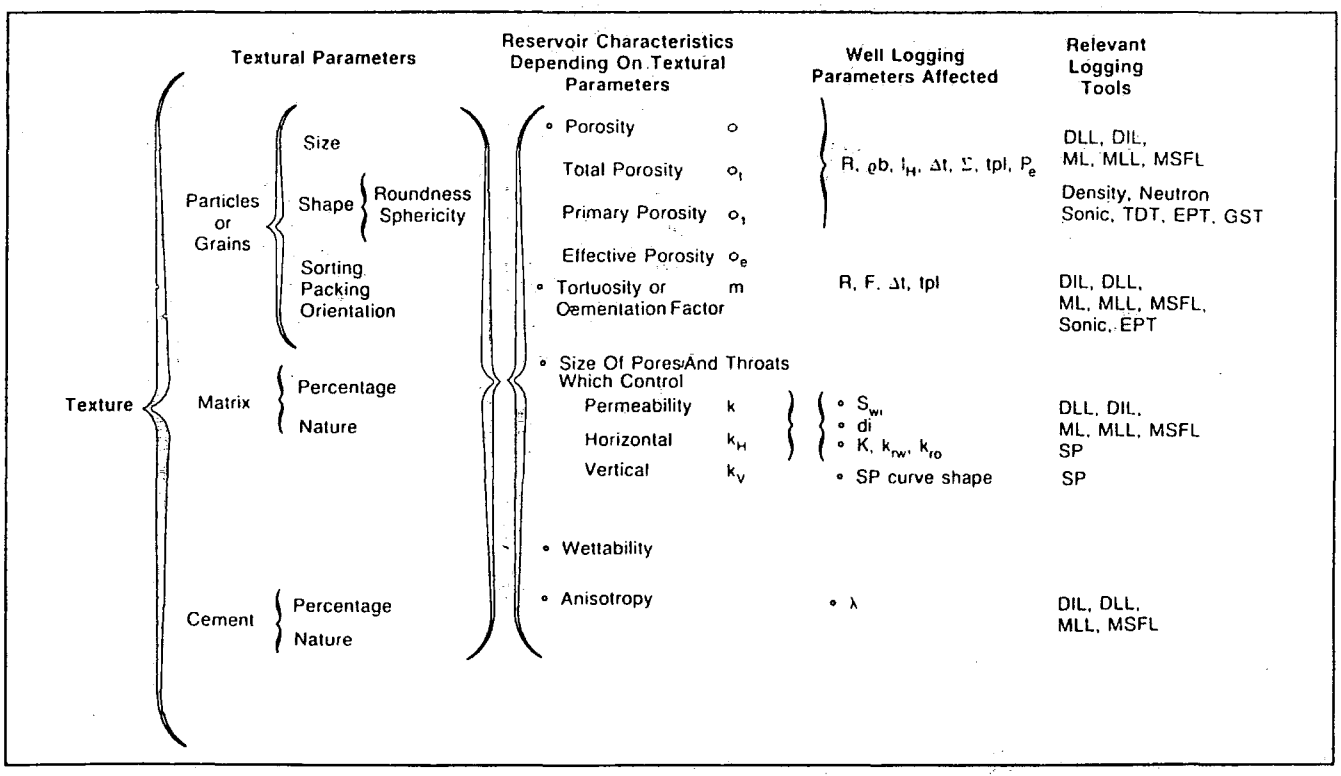

Table 2-2. Relationship between rock texture and well logging parameters. (Schlumberger, 1987)

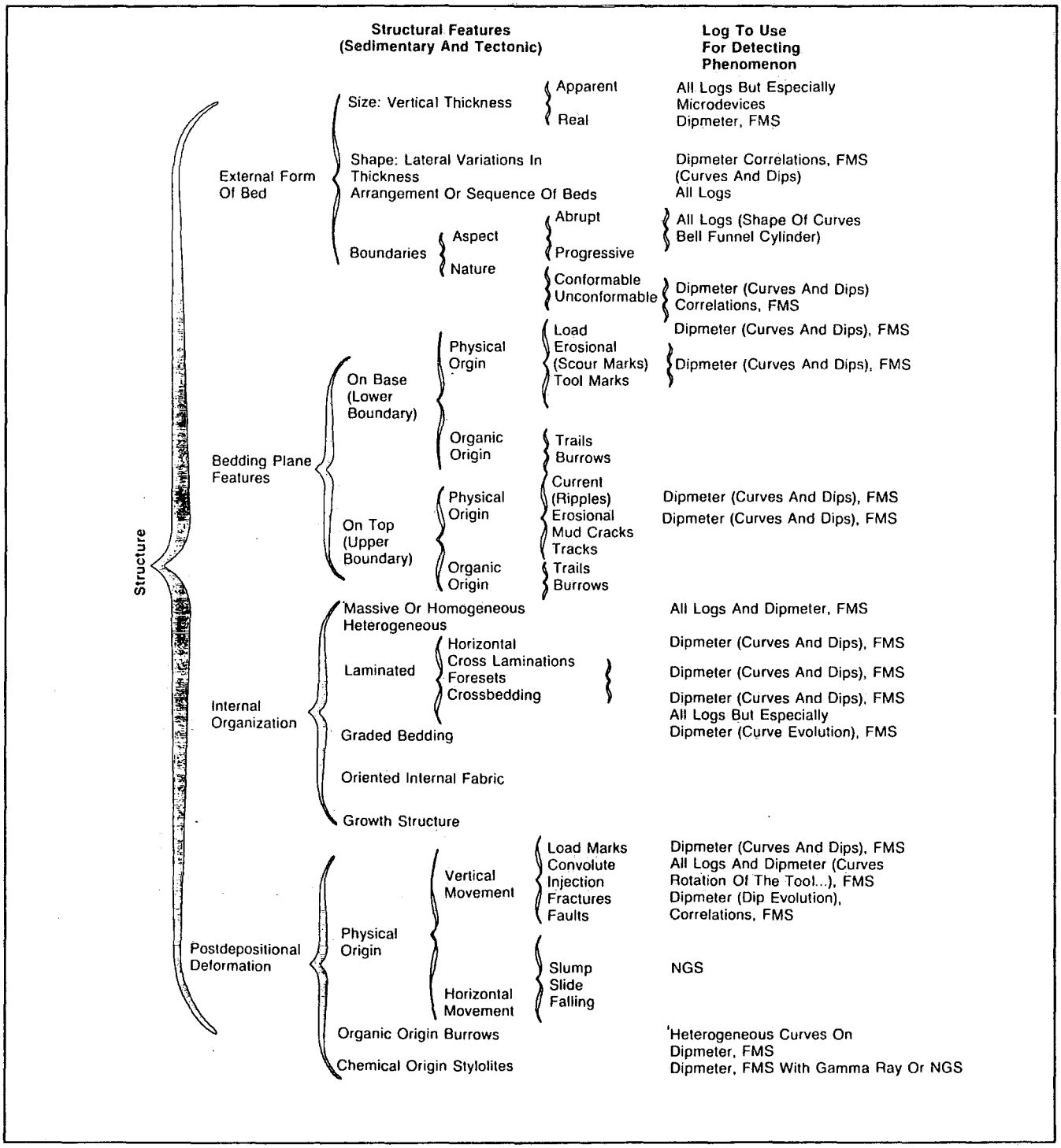

Table 2-3. Relationship between sedimentary features and well logging parameters. (Schlumberger, 1987)

2.7.1 Correlation

One of the first uses of well logs was correlation of equivalent strata from one well to the next. This is still one of their most important uses. Logs from different wells are matched for similarity or for characteristic log responses to lithological markers.

Well logs have the advantage for correlation of providing a continuous record over the entire well. There are no missing sections as can be the case with core samples. Most important, because sonde depth is recorded, there is no ambiguity as to the depth of various markers.

Well-to-well correlation studies thus permit accurate subsurface mapping and the determination of:

a) The elevations of formations present in the well relative to other wells, outcrops, or geophysical projections.
b) Whether or not the well is within a given major geological structure.
c) Whether well depth has reached a known productive horizon, and, if not, approximately how much remains to be drilled.
d) The presence or absence of faults.
e) The existence of dip, folds, unconformities; the thickening and thinning of lithologic sections; or lateral changes of sedimentation or lithology.

Any continuously recorded log has some correlation potential. For the best correlation, however, the log should respond to some property of the stratum that does not vary too much from well to well.

The logs most frequently used for correlation are the resistivity, SP and gamma ray. The basic logs used in the majority of log-correlation studies are listed in table 2-4 with their various uses and advantages. Tables 2-1 to 2-4 are those produced for Schlumberger tools but obviously they also apply to tools of other companies of the same nature and function.

In general, correlation features from computed logs vary from very good to indifferent. Examples of the parameters which have good correlation features are the apparent-matrix-density (ρ_{ma}), the shale-fraction (V_{Sh}), and lithology analysis.

2.8 The Field Operation

Electrical well logging is sometimes referred to as wireline electrical logging

Log	Correlates On	Conditions For Best Use	Uses Or Advantages
SP	Permeable beds vs. shale beds	Uncased hole Good contrast between R_{mf} and R_w Low-to-moderate formation resistivity. Fresh mud (but still useful in saline mud).	Displays easily read shale-sand profiles Much used (usually with resistivity for correlation. Not affected by washed-out holes or deep or variable invasion
Gamma Ray	Radioactivity associated with shaliness. Radioactive beds.	Moderate hole size with no large washed-out zones.	Insensitive to drilling fluid; thus can be used in oil- or salt-based muds and in air- or gas-filled holes. Can be used in cased hole.
Short-Spacing Resistivity (SN, LL8, SFL)	Invaded, porous beds. Deflection depends on formation factor, water resistivity, and shaliness. Dense strata (low water content and nonconductive matrix).	Uncased hole. Fresh mud. Invaded formations, not too resistive.	Much used (usually with SP or gamma ray) for correlation.
Amplified Short-Spacing Resistivity	Same as above.	Same as above.	Useful for correlation in shales or other low-resistivity sections.
Deep Laterolog	Same as above.	Uncased hole. Fresh to salt mud. High R_t/R_w ratio.	Useful for salt muds, resistive formations.
Induction Log	Variations of water content (and salinity) in beds with nonconductive matrix. (Porous-zone response varies with formation porosity and pore-fluid conductivity.)	Uncased hole. Fresh mud. Formation resistivity below 100 ohm-m.	The induction conductivity curve is useful for correlation in shales or other low-resistivity sections.
Sonic	Δt (dependent on lithology and porosity).	Liquid-filled gas-free holes.	Good porosity correlation, useful in low resistivities. Provides Δt parameter measurement for identification of lithological markers.
Neutron	Hydrogen content of formation. Large shale response.	Depends on tool type.	Good porosity correlation. Good in combination with other logs for gas detection. Provides ϕ_N parameter measurement for identification of lithological markers. Useful in cased holes. (Often run with gamma ray.)
Density	Formation density (dependent on lithology and porosity).	Uncased hole, with little mudcake and no hole-wall rugosity.	Chiefly useful for identification of lithological markers.
Caliper	Hole-size variations (washouts, noncircular boreholes, fracturing).	Uncased hole.	Seldom correlatable by itself, but often helps resolve ambiguities on other logs.

Table 2-4. Basic well logs used for correlation. (Schlumberger, 1987)

or more generally as simply logging. It is carried out from a logging truck when on land (figure 2-2) or a mounted unit when offshore. In either cases, it is sometimes referred to as a "mobile laboratory". Figure 2-3 shows a typical Schlumberger Cyber Service Unit (CSU, 1987). Similarly companies such as Gearhart uses the Direct Digital Logging Unit (DDL, 1985) and Western Atlas uses the Computer Logging Service Unit (CLS, 1985). The truck carries the downhole measurement instruments, the electrical cable and winch needed to lower the instruments into the borehole, the surface instrumentation needed to power the downhole instruments and to receive their signals, and the equipment needed to make a permanent recording of the "log".

The downhole measurement instruments are usually composed of two components. One component contains the sensors used in making the measurement, called the "sonde". The type of sensor depends of course upon the nature of the measurement. Resistivity sensors use electrodes or coils; acoustic sensors use tranducers; radioactivity sensors use detectors sensitive to radioactivity; etc.. The sonde housing may be constructed of steel and/or fiberglass.

The other component of the downhole tool is the cartridge. The cartridge contains the electronics that power the sensors, process the resulting measurement signals and transmit the signals up the cable to the truck. The cartridge may be a separate component screwed to the sonde to form the total tool or it may be combined with the sensors into a single tool. That depends, of course, upon how much space the sensors and electronics require and the sensor requirements. The cartridge housing is usually made of steel.

Today, most logging tools are readily combinable. In other words the sondes and cartridges of several tools can be connected to form one tool and thereby make many measurements and logs on a single descent into and ascent from the borehole.

The downhole tool (or tools) is attached to an electrical cable that is used to lower the tool into and remove it from the well. Most cable used in openhole logging today contains seven insulated copper conductors. The cable is wrapped with a steel armour to give it the strength to support the tool weight and provide some strength to pull on the tool in case it becomes stuck in the borehole. The cable and tools are run in and out of the borehole by means of a unit-mounted winch.

Well depths are measured with a calibrated measuring wheel system. Logs are normally recorded during the ascent from the well to assure a taut cable and better

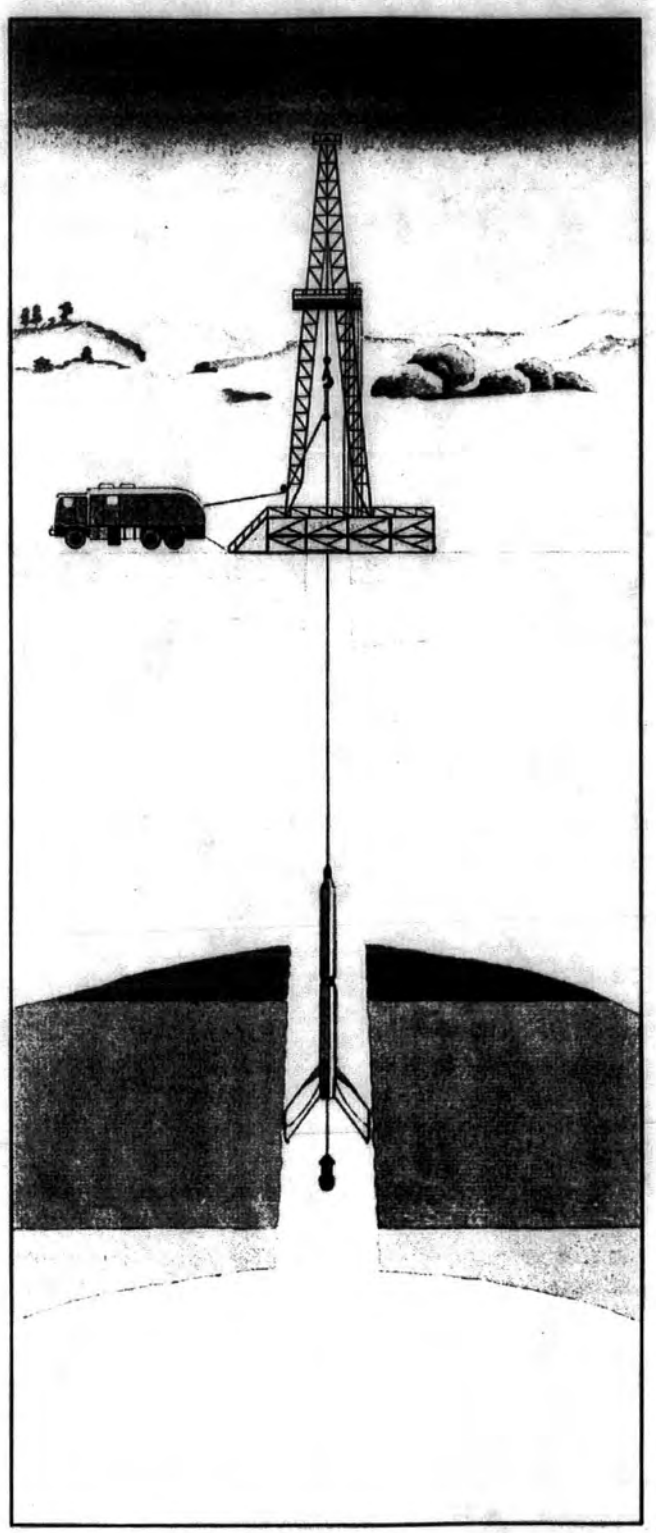

Figure 2-2. Wireline logging operation.

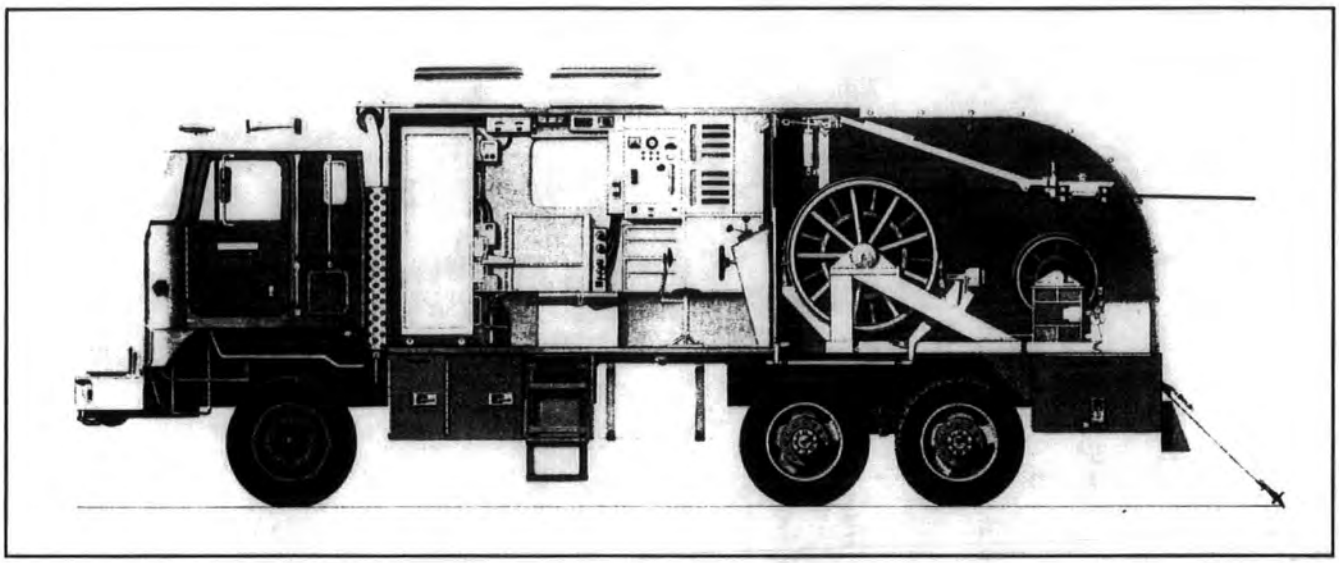

Figure2-3. A typical CSU wellsite mobile laboratory. The main winch contains up to 30000 feet of seven-conductor logging cable; the optional small winch at the rear contains 24000 feet of slim monoconductor cable for servicing producing wells under pressure. Data acquisition and computer equipment are inside the logging cab. For offshore-remote locations the cab and winch assemblies are mounted on a skid. (CSU, Schlumberger, 1987)

depth control.

Signal transmission over the cable may be in analog or digital form; modern trends favour digital. The cable is also used, of course, to transmit the electrical power from the surface to the downhole tools.

The surface instrumentation (figure 2-4) provides the electrical power to the downhole tools. More importantly, the surface instrumentation receives the signals from the downhole tools, processes and/or analyses those signals, and responds accordingly. The desired signals are output to magnetic tape in digital form and to a cathode-ray tube and photographic film in analytical form.

The photographic film is processed on the unit, and paper prints are made from the film. This continuous recording of the downhole measurement signals is referred to as the log.

2.9 Log Data Acquisition

Wireline technology is being changed by the rapid advancements in digital electronics and data-handling methods. These new concepts have changed the thinking about existing logging techniques and remoulded ideas about the direction of future developments. Affected are the sensors, the downhole electronics, the cable, the cable telemetry and the signal processing at the surface.

Basic logging measurements may contain large amounts of information. In the past some of this data was not recorded because of the lack of high data-rate sensors and electronics downhole, the inability to transmit the data up the cable and the inability to record it in the logging unit. Similarly those limitations have prevented or delayed the introduction of some new logging measurements and tools. With digital telemetry there has been a tremendous increase in the data rate that can be handled by the logging cable. Digital recording techniques within the logging unit provide a substantial increase in recording capability. The use of digitised signals also facilitates the transmission of log signals by radio, satellite, or telephone line to computing centres, base offices, or the operator's office.

In table 2-5, the data rate for one of the older tool systems, the induction-sonic combination, is contrasted with the data-rate transmission requirements for some of the newer tools. It illustrates the tremendous increases in the data rate that can now be handled by the newer downhole sensors, by the logging cable, and by the

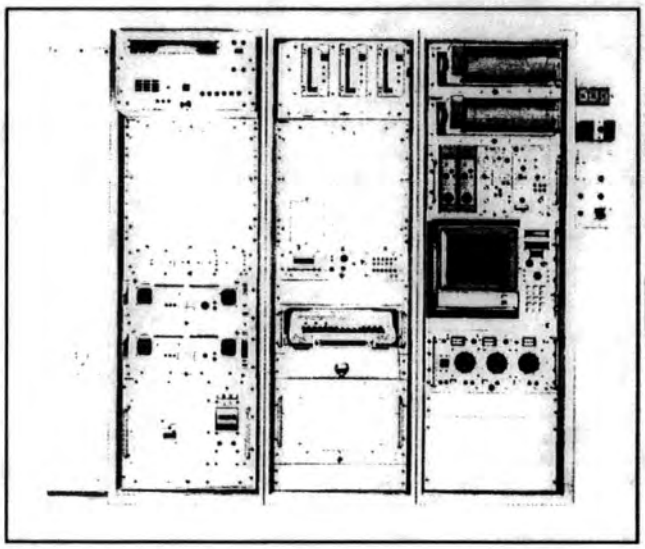

Figure 2-4. The CSU is a computer-based integrated data acquisition and processing system. The main elements are a video data display and optical film units to record data (right), the keyboard/ printer unit below three cartridge tape drives, and twin DEC 1134 computers each having 2-megabyte memory and at the top a dual hard-disk drive with 42-megabyte capacity and a backup 48-megaleyte cartridge tape unit. (CSU, Schlumberger, 1987)

surface instrumentation as a result of digital techniques.

Tool	Data	Data Rate
Induction-Sonic		200 bits/borehole ft
HDT	10 dip channels	25000 bits/borehole ft
Array Sonic	Full Waveform	60000 bits/borehole ft
Inelastic Spectroscopy	Energy Spectrum	20000 bits/second
Well Seismic Tool	5-Second Wavetrain	80000 bits/second

Table 2-5. Data rate transmission requirements of some well logging tools. (CSU, Schlumberger, 1987)

Signal processing can be performed on at least three points: downhole in the tool, uphole in the unit, and at a central computing centre. The point of processing depends on where the desired results can most efficiently be produced, where the extracted information is first needed, where the background expertise exists, or where technological considerations dictate.

2.10 A Well Program

The oil industry, in terms of the discovery process, can generally be split into two main stages: one is known as exploration and the other as development.

The exploration stage applies to a well or an area whose geologic information is relatively unknown. The wells spud in such area are often termed "wildcats". The only information prior to drilling, are surface data collected from satellite and surface seismic. Generally when a wildcat is drilled, there is plenty of coring, and in terms of electrical well-logging, all the logging services available are used. The full suite of logging services generally include the following:- (Refer to later text for explanation of these terms)

a) Resistivity logs (see chapter 4).
b) Porosity logs (see chapter 5).
c) Dipmeter logs (see chapter 6).
d) Pressure and fluid sampling (see chapter 7).
e) Side-wall core sampling (see chapter 7).
f) Borehole seismic (see chapter 9), taken either before or after the final stage of casing depending on the prospect of the well.

If the data gathered look promising the casing is then run and a testing program is drawn up. The possible logging services might include:-

g) Perforations (see chapter 10).

h) Production logs (see chapter 11).

Being an exploration well, the operator is very much interested in obtaining as much information as possible from downhole regardless of the prospect of the well. The data obtained with the first exploration wells will enhance his understanding of the area, and hence influence his decision on where to drill the next well in the area, if at all.

When a number of exploration wells have been drilled, logged, and tested, and if the operator decides the area has good prospects he will decide to develop the area (or reservoir). The program now enters the development stages. All over the area, there will be designated positions for wells to be drilled. Offshore, platforms will be planned. These will have anywhere from one to fifty well slots such as in the platforms in the North Sea and the Gulf of Mexico. Economic factors will dictate the size of the platform to be constructed.

The electrical well-logging program for each new development could be the same as the exploration stage depending on how well the operator feels he knows his area. At the initial stages all logs will probably be required, and once the area is better understood and if the geological structure encountered is not too complex, the logging program could be reduced to:-

a) Resistivity logs.

b) Porosity logs.

c) Pressure sampling (if desired).

d) Perforations.

e) Production logs.

The main reasons to log development wells are:-

a) To find the pay zones.

b) To establish well production.

c) To monitor the well production performance.

From time to time, during the life of a development well, further logs may be needed to determine the well performance. Based on the results, old pay zones may

need to be plugged off due to water influx (figure 2-5), and when this is undertaken the well enters a "work-over" program. This program generally requires a change-over of the completion string (figure 2-6), reperforations, and further production logging once the well is back on production. These logs are to determine the efficiency of the work-over program.

2.11 The Market for the Electric Well Logging Companies

There are numerous electric well logging companies operating in the world. Some are able to provide a full range of services, while others only specialise or can offer only one or two services. This share of the world market is divided as follow:-

a) Gearhart Industries - 4.5 %
b) Schlumberger Wireline (Schlumberger Ltd.) - 82.5 %
c) Welex (Halliburton Ltd.) - 1.6 %
d) Western Atlas (Atlas Wireline Services) - 5.8 %
e) Others - 6.1 %

This thesis presents the services on offer by the major logging companies, and evaluates where possible their advantages and disadvantages. It also gives an insight to the future of the industry.

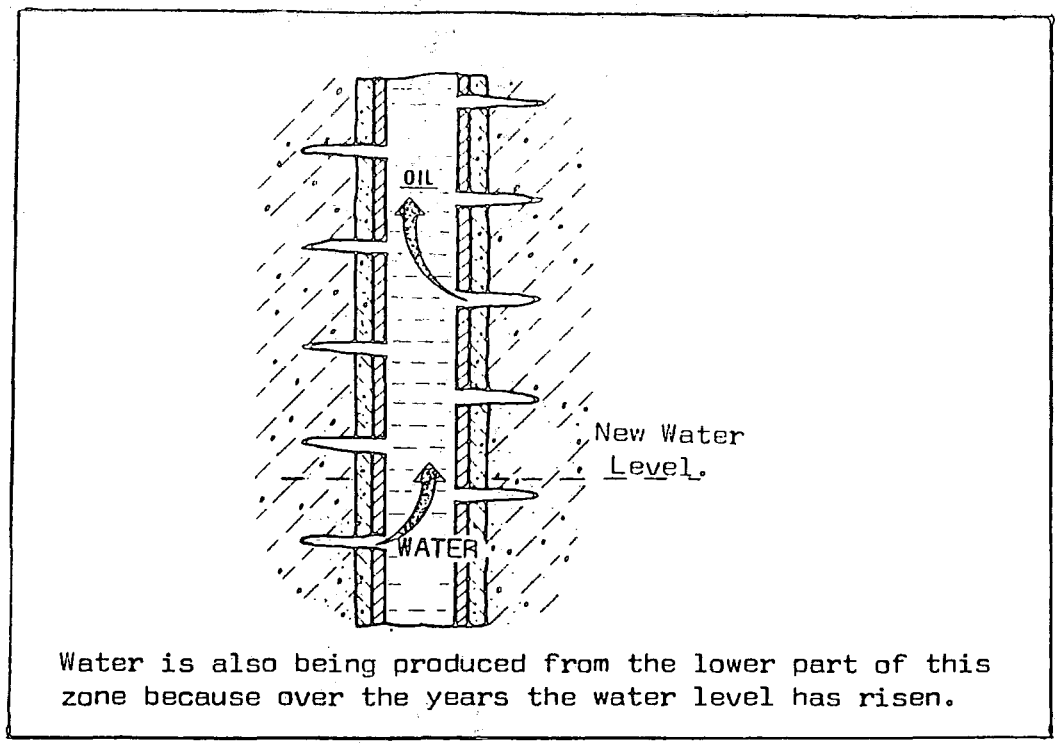

Figure 2-5. Water influx from older zones.

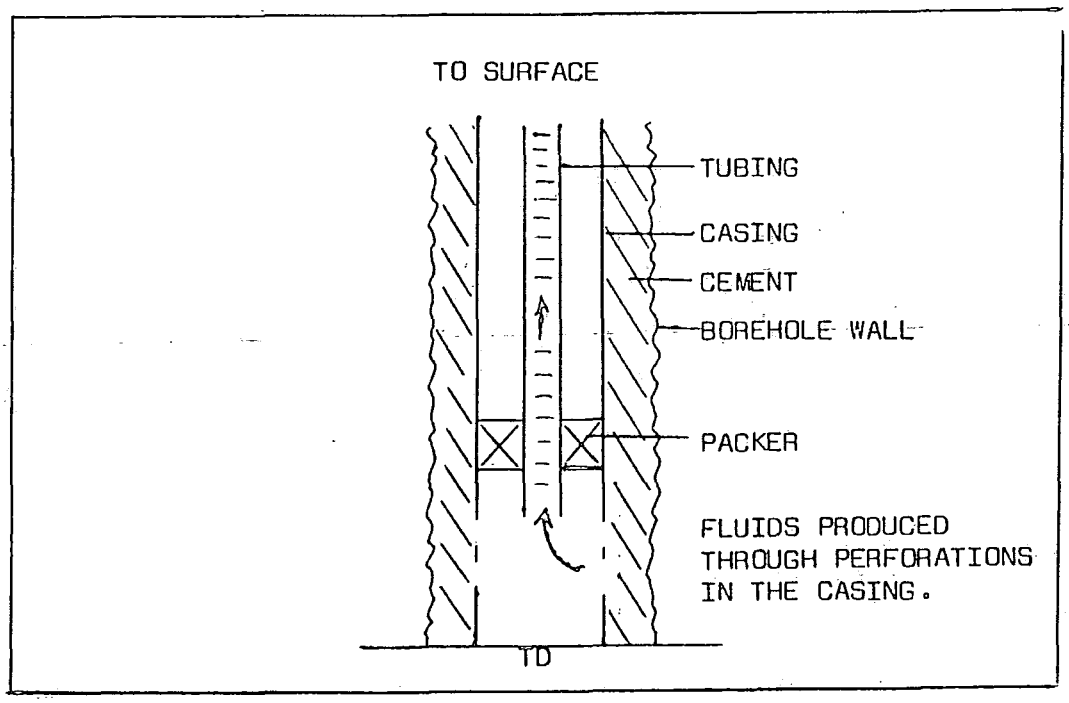

Figure 2-6. A completion string.

3. SPONTANEOUS POTENTIAL AND NATURAL GAMMA RAY LOGS.

The spontaneous potential (SP) curve and the natural gamma ray (GR) log are recordings of naturally occuring physical phenomena in in-situ rocks. The SP curve records the electrical potential (voltage) produced by the interaction of formation connate water, conductive drilling fluid, and certain ion-selective rocks (shale). The GR log indicates the natural radioactivity of the formations. Nearly all rocks exhibit some natural radioactivity and the amount depends on the concentration of potassium, thorium, and uranium. There are two types of GR logs. One, the standard GR log, measures only the total radioactivity. The other, the natural gamma ray spectrometry log, measures the total radioactivity and concentrations of potassium, thorium, and uranium producing the radioactivity.

Although relatively simple in concept, the SP and GR logs are quite useful and informative. Among their uses are the following:-

a) Differentiate potentially porous and permeable reservoir rocks (sandstone, limestone, dolomite) from nonpermeable clays and shales.

b) Define bed boundaries and permit correlation of beds.

c) Give a qualitative indication of bed shaliness.

d) Aid in lithology (mineral) identification.

e) In the case of the SP curve, permit the determination of formation water resistivity, R_W.

f) In the case of the GR and natural gamma ray spectrometry logs, detect and evaluate deposits of radioactive minerals.

g) In the case of the natural gamma ray spectrometry log, define the concentrations of potassium, thorium and uranium.

3.1 The Spontaneous Potential (SP) Curve

The SP curve is a recording versus depth of the difference between the electrical potential of a movable electrode in the borehole and the electrical potential of a fixed surface electrode. The unit of the SP is usually measured is millivolts (mV), and the order of magnitude is in the range of 0-100 mV. Generally, it is the difference of the SP values of one formation to the next which is of particular interest.

Opposite shales the SP curve usually defines a more-or-less straight line on the log, called the shale baseline; in thick beds, these excursions (deflections) tend to reach an essentially constant deflection defining a sand line. The deflection may be either to the left (negative) or to the right (positive), depending primarily on the relative salinities of the formation water and of the mud filtrate. If the formation water salinity is greater than the mud filtrate salinity, the deflection is to the left. For the reversed salinity contrast, the deflection is to the right.

The position of the shale baseline on the log has no useful meaning for interpretation purposes. The SP sensitivity scale is chosen and the shale baseline position is set by the engineer running the log so that the curve deflections remain in the SP track.

An SP curve cannot be recorded in holes filled with nonconductive muds because such muds do not provide electrical continuity between the SP electrode and the formation. Furthermore if the resistivities of the mud filtrate and the formation water are about equal the SP deflections will be small and the curve will be rather featureless.

3.1.1 Origin of the SP

The deflections on the SP curve result from electric currents flowing in the mud in the borehole. These SP currents are caused by electromotive forces in the formations, which are of electrochemical and electrokinetic origins. Usually there are three components which constitute an SP log. These are:-

a) Electrochemical component.

b) Electrokinetic component.

c) Static component.

3.1.1.1 Electrochemical Component of the SP.

Mounce and Rust (1944) used a simple experiment to prove that waters of different salinities, together with shale and a permeable inert membrane between the two fluids, generate an electromotive force and current flow in the cell (figure 3-1). The current flows from the fresh to the salty water and through the shale. Removal of the shale stops the current flow. Interchanging the two liquids reverses the direction of the current flow.

The cell in figure 3-1 proves very similar to conditions existing in the borehole, where the drilling mud salinity is different from the formation water salinity. The measured SP is the voltage observed in the borehole caused by the potential drop as the currents flow through the mud. Generally, the potential drop is larger in the borehole than in the shale or permeable formations.

Assuming the solutions contain only NaC1 and the mud activity is limited to the free fluid within it, then the following simplified analysis applies. This discussion is based on fresh mud and salty formation water (figure 3-2). The shale, due to its predominant clay content, acts as cationic membrane. That is, it is permeable to cations (Na^+), but not to anions ($C1^-$) due to an apparently high negative charge on the clay lattice. The sodium ions (Na^+) can then move through the shale from the high concentration salt water to the lower concentration fresh water of the mud. This movement of cations generates a membrane potential.

At the salt water (formation water) and the fresh water (mud filtrate) contact, the Cl^- ions have greater mobility than the Na^+ ions and thus move more rapidly. This rapid movement generates a negative potential across the "liquid junction".

In the mud column opposite the shale, a positive potential is generated by the Na^+ ions while at the junction between the formation water and the mud filtrate a negative potential is developed. These spontaneous potential differences cause current flow in the mud column.

The magnitude of this electrochemical potential, E_c, is

$$E_c = -K \log \frac{a_w}{a_{mf}} = -K \log \frac{R_{mf}}{R_w} \qquad (3\text{-}1)$$

(Wyllie, M.R.J., 1949)

where

a_w and a_{mf} are the chemical activities of the two solutions (formation water and mud filtrate) at formation temperature;

K is a coefficient proportional to the absolute temperature and for NaC1 formation water and mud filtrate, is equal to 71 at 25°C (77°F).

The chemical activities are related to the salinity of the solutions and thus to the relative resistivities.

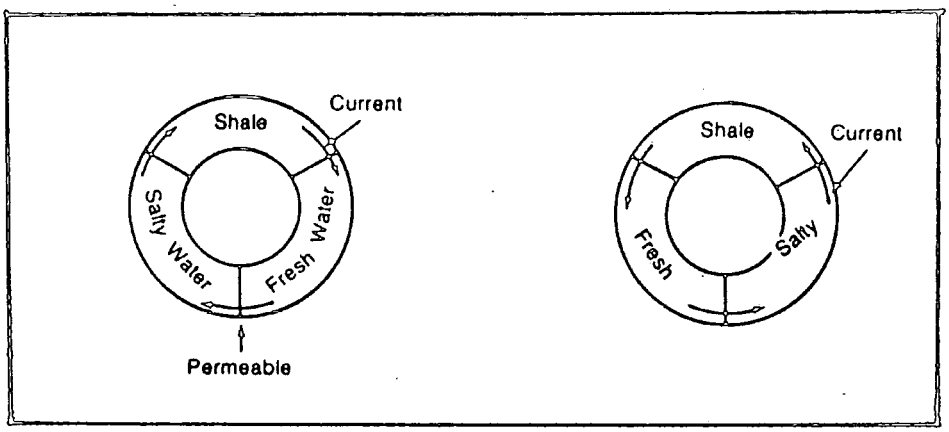

Figure 3-1. Electrochemical component of the SP.

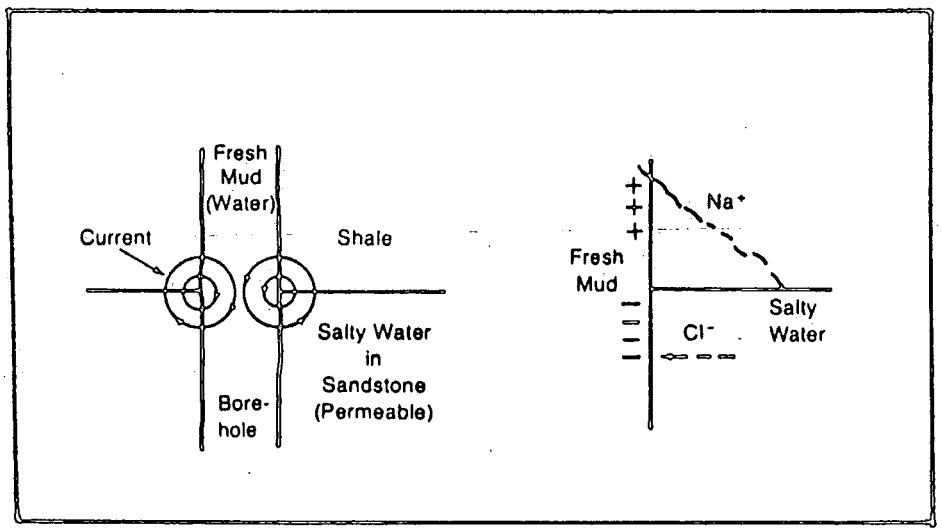

Figure 3-2. Fresh mud and salty formation water effects.

3.1.1.2 Electrokinetic Component of the SP

An electrokinetic potential, E_k (also known as a streaming potential or electrofiltration potential), is produced when an electrolyte flows through a permeable, non-metallic, porous medium (Wyllie, M.R.J., 1956). The magnitude of the electrokinetic potential is determined by several factors, among which are the differential pressure producing the flow and the resistivity of the electrolyte.

In the borehole an electrokinetic emf, E_{kmc}, is produced by the flow of mud filtrate through the mudcake deposit on the borehole wall opposite permeable formations. The mudcake acts as a permeable membrane through which the mudfiltrate can flow (figure 3-3). It flows because of the differential pressure between the mudcolumn and the formation. In practice little or no electrokinetic emf is actually generated across the permeable formation itself. This is because practically all the differential pressure between the borehole and undisturbed virgin formation is expended across the less permeable mudcake. Any remaining differential pressure across the formation is normally not great enough to produce any appreciable electrokinetic emf.

An electrokinetic emf, E_{kmc}, may however be produced across the shale since it may have sufficient permeability to permit a tiny amount of filtration flow from the mud.

It is also possible for electrokinetic effects to become more important in cases of unusually large pressure differentials (e.g., in depleted formations of low pressure or when very heavy drilling muds are used). In these cases the electrokinetic emf's may be quite significant and the mudcake and shale electrokinetic effects may not cancel each other.

Important electrokinetic effects may also be seen in very low permeability formations (less than a few millidarcies) in which an appreciable part of the pressure differential is applied across the formation itself. If formation permeability is so low that little or no mudcake is formed most of the pressure differential between the formation pore pressure and hydrostatic head of the mud column is applied to the formation.

These infrequent effects are difficult to detect but conditions favouring their existence should alert us to the possibility of a large electrokinetic potential. When

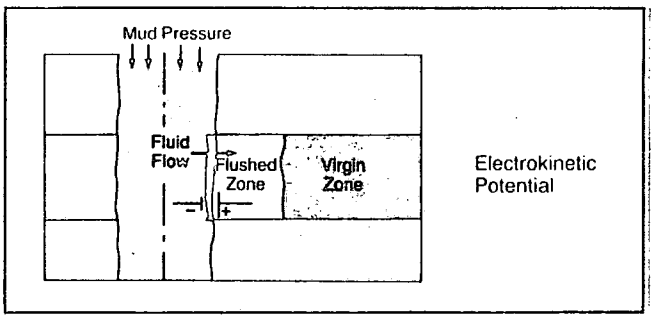

Figure 3-3. Electrokinetic component of the SP.

a significant electrokinetic potential exists the SP deflection cannot be used to calculate a reliable value of formation water resistivity, R_w.

3.1.1.3 Static SP

The Static SP (SSP) refers to the maximum SP that can be obtained given a shale and two waters of different salinity. It is essentially the SP that would be obtained if no current flowed. The SSP has no bed boundary effects. Since current flows and the actual SP is the measurement of the potential changes in the wellbore, there are variations between the idealised SSP and the actual SP (figure 3-4). The bed boundaries of the actual SP are the inflection points where the greatest potential drop occurs. If the currents could be prevented from flowing by means such as the insulating plugs schematically indicated in the upper part of figure 3-4, the potential differential differences observed in the mud would equal the total emf. The SP curve recorded in such an idealised condition is called the static SP curve. The static SP or SSP is the SP deflection opposite a thick clean formation. The deflection is measured from the shale baseline and its magnitude is

$$SSP = -K \log \frac{a_w}{a_{mf}} \qquad (3\text{-}2)$$

(Wyllie, M.R.J. 1949)

Fortunately because the borehole presents a much smaller cross-sectional area to current flow relative to the formations, most of the SP voltage drop does occur in the borehole provided formation resistivities are low to moderate (up to 20 Ωm) and the beds are moderately thick (> 10 ft). Therefore the recorded SP deflection does approach the static SP value in most thick permeable beds.

3.2 The Gamma Ray (GR) log

The GR log is a measurement of the natural radioactivity of the formations. In sedimentary formations the log normally reflects the shale content of the formations. This is because the radioactive element tend to concentrate in clays and shales. Clean formations usually have a very low level of radioactivity, unless a radioactive contaminant such as volcanic ash or granite wash is present or the formation contains dissolved radioactive salts.

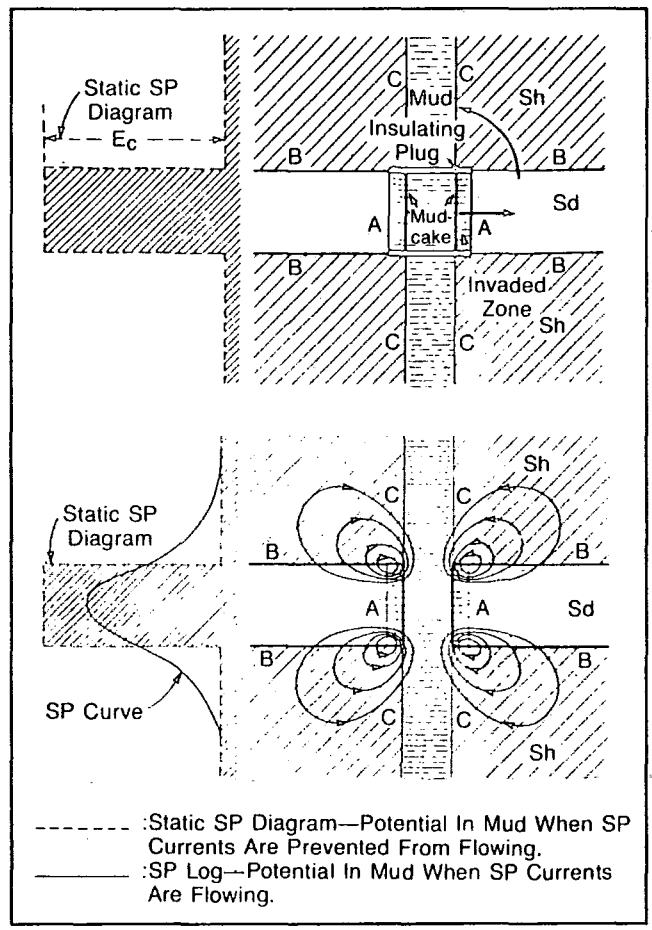

Figure 3-4. Schematic representation of potential and current distribution in and around a permeable bed. (Schlumberger, Schlumberger and Leonardon, 1934)

The GR log can be recorded in cased wells which makes it very useful as a correlation curve in completion and workover operations. It is frequently used to complement the SP log and as a substitute for the SP curve in wells drilled with salt mud, air, or oil-based muds. In each case it is useful for location of shales and nonshaly beds and, most importantly for general correlation.

3.2.1 Properties of Gamma Rays.

Gamma rays are bursts of high-energy electromagnetic waves that are emitted spontaneously by some radioactive elements. Nearly all the gamma radiation encountered in the earth is emitted by the radioactive potassium isotope of atomic weight 40 (K^{40}) and by the radioactive elements of the uranium and thorium series.

Each of these elements emits gamma rays the number and energies of which are distinctive of each element. Figure 3-5 shows the energies of the emitted gamma rays : potassium (K^{40}) emits gamma rays of a single energy at 1.46 MeV, whereas the uranium and thorium series emit gamma rays of various energies.

In passing through matter, gamma rays experience successive Compton Scattering collisions with atoms of the formation material, losing energy with each collision. After the gamma ray has lost enough energy, it is absorbed, by means of the photoelectric effect, by an atom of the formation. Thus, natural gamma rays are gradually absorbed and their energies degraded (reduced) as they pass through the formation. The rate of absorption varies with formation density. Two formations having the same amount of radioactive material per unit volume, but having different densities, will show different radioactivity levels; the less dense formations will appear to be slightly more radioactive. The GR log response, after appropriate corrections for borehole etc., is proportional to the weight concentrations of the radioactive material in the formation:

$$GR = \frac{\Sigma \rho_i V_i A_i}{\rho_b} \qquad (3\text{-}3)$$

(Blanchard, A.,and Dewar, J.T., 1953)

where

ρ_i are the densities of the radioactive minerals,

V_i are the bulk volume factors of the minerals,

A_i are proportionality factors corresponding to the radioactivity of the mineral, and

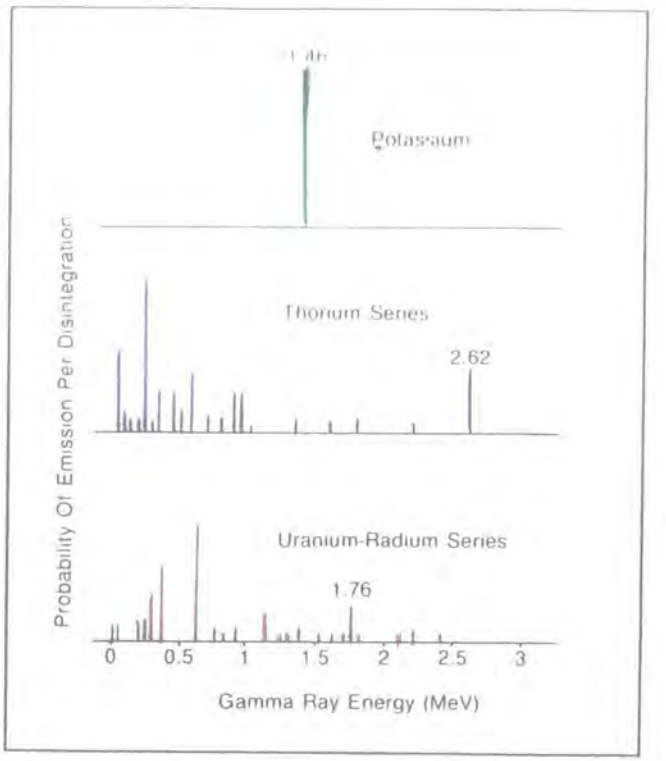

Figure 3-5. Gamma ray emission spectra of radioactive minerals. (Schlumberger, 1985)

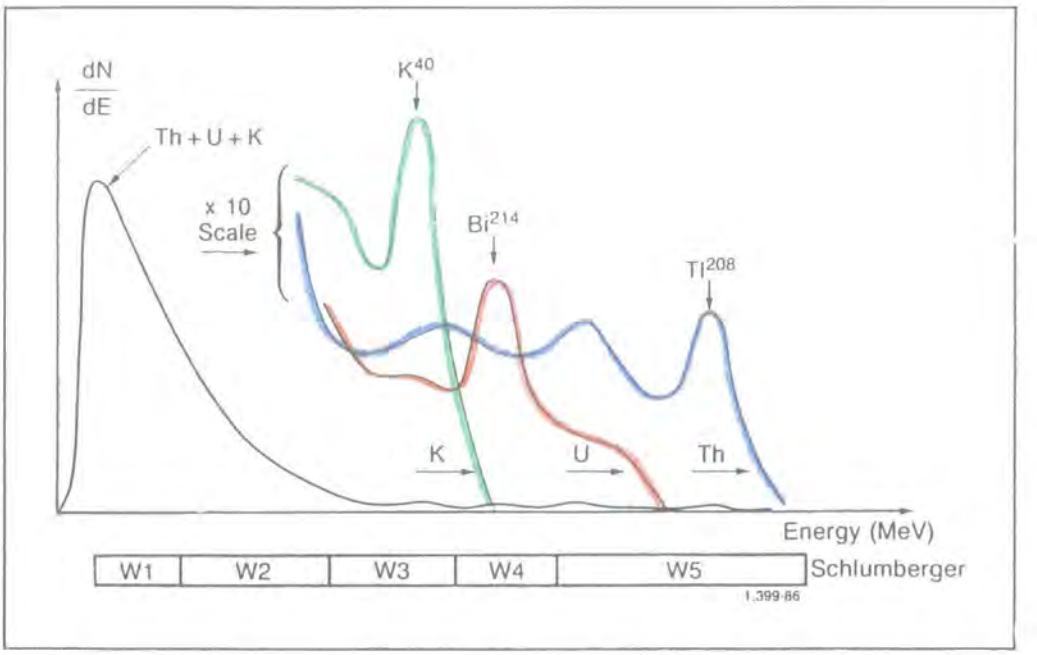

Figure 3-6. Potassium, thorium, and uranium response curves (NaI crystal detector). (Schlumberger, 1985)

ρ_b is the bulk density of the formation.

In sedimentary formations, the depth of investigation of the GR log is about 1 foot.

3.2.2 Equipment

The GR sonde contains a detector to measure the gamma radiation originating in the volume of formation near the sonde. In the industry, scintillation counters are now generally used for this measurement. They are much more efficient than the Geiger-Muller counters used in the past. Because of its higher efficiency a scintillation counter need only be a few inches in length; therefore, good formation detail is obtained.

The primary calibration standard for GR tools is the American Petroleum Institute (API) test facility in Houston. A field calibration standard is used to normalise each tool to the API standard and the logs are calibrated in API units. The radioactivities in sedimentary formations generally range from a few API units in anhydrite or salt to 200 or more in shales. (A.P.I., 1959)

3.2.3 The Natural Gamma Ray Spectrometry Log

Like the GR log, the natural gamma ray spectrometry log measures the natural radioactivity of the formation. Unlike the GR log which measures only the total radioactivity, this log measures both the number of gamma rays and the energy level of each and permits the determination of the concentrations of radioactive potassium, thorium, and uranium in the formation rocks.

Schlumberger have developed the NGS natural gamma ray spectrometry tool for this purpose, Gearhart have developed the SGR spectral gamma ray tool and Western Atlas the SPL spectral log tool (see table 3-1).

Company	Tool	Max.Temp. (°F)	Max.Pressure (kpsi)
Gearhart	SGR	400	20
Schlumberger	NGS	350	20
Western Atlas	SPL	400	20

Table 3-1 GR Tools' Ratings

3.2.3.1 Physical Principle.

Most of the gamma ray radiation in the earth originates from the decay of three radioactive isotopes: potassium 40 (K^{40}), with a half-life of 1.3 X 10^9 years; uranium 238 (U^{238}), with a half-life of 4.4 X 10^9 years; and thorium 232 (Th^{232}), with a half-life of 1.4 X 10^{10} years.

Potassium 40 decays directly to stable argon 40 with the emission of a 1.46 MeV gamma ray. However uranium 238 and thorium 232 decay sequentially through a long sequence of various daughter isotopes before arriving at stable lead isotopes. As a result, gamma rays of many different energies are emitted and fairly complex energy spectra are obtained, as figure 3-6 shows. The characteristic peaks in the thorium series at 2.62 MeV and the uranium series at 176 MeV are caused by the decay of thallium 208 and bismuth 214, respectively.

It is generally assumed the formations are in secular equilibrium; that is, the daughter isotopes decay at the same rate as they are produced from the parent isotope. This means that the relative proportions of parent and daughter elements in a particular series remain fairly constant; so by looking at the gamma ray population in a particular part of the spectrum it is possible to infer the population at any other point. In this way the amount of parent isotope present can be determined.

Once the parent isotope population is known the amount of non radioactive isotope can also be found. The ratio of potassium 40 to total potassium is very stable and constant on the earth while apart from thorium 232, the thorium isotopes are very rare and so can be neglected. The relative proportions of the uranium isotopes depend somewhat on their environment, and there is also a gradual change because of their different half-lives; at present, the ratio of uranium 238 to uranium 235 is about 137.

3.2.3.2 Measurement Principle

The NGS tool of Schlumberger uses a sodium iodide scintillation detector contained in a pressure housing which, during logging, is held against the borehole wall by a "bow spring" to enable better contact between the tool and the borehole wall.

Gamma rays emitted by the formation rarely reach the detector directly. Instead they are scattered and lose energy through three possible interactions with the formation; the photoelectric effect, Compton Scattering, and pair production. Because of these interactions and the response of the sodium iodide scintillation

detector, the original spectra of figure 3-5 are degraded to the rather "smeared" spectra shown in figure 3-6.

The high-energy part of the detected spectrum is divided in three energy windows, W1, W2, and W3; each covering a characteristic peak of the three radioactivity series (figure 3-6). Knowing the response of the tool and the number of counts in each window it is possible to determine the amounts of thorium 232, uranium 238, and potassium 40 in the formation. There are relatively few counts in the high-energy range where peak discrimination is best; therefore, measurements are subject to large statistical variations even at low logging speeds. By including a contribution from the high-count rate, low energy part of the spectrum (windows W4 and W5), these high statistical variations in the high-energy windows can be reduced by a factor of 1.5 to 2. The variation further reduced by a factor of 1.5 to 2 by using a filtering technique that compares the counts at a particular depth with the previous values in such a way that spurious changes are eliminated while the effects of formation changes are retained. Normally only the final filtered data are presented on film but the unfiltered raw data are always recorded on tape.

The SGR tool of Gearhart uses a sodium activated caesium iodide, Cs I (Na), crystal detector. The detector receives and divides the data into 256 channels of energy of incident gamma ray which are sent uphole. Unlike the Schlumberger method, the computation is based upon the three energy windows, which are as follows:-

a) 2.30 - 2.80 MeV : Thorium window
b) 1.58 - 1.98 MeV : Uranium window
c) 1.37 - 1.57 MeV : Potassium window

This is as shown in figure 3-7. The tool is calibrated to reproduce the shale as calculated in figure 3-7. Figure 3-8 shows a gamma ray spectrum generated during a field calibration procedure. This spectrum may be used to quality control the tool response during the logging operations or may be used to examine zones of interesting or unusual response.

However due to the statistical variations the raw data can be post-processed using an optional five-window algorithm to improve the computation of elemental concentrations. Also an adaptive filtering procedure which uses the gross gamma ray as reference to allow flexibility in the operation can be applied. The gross GR is an

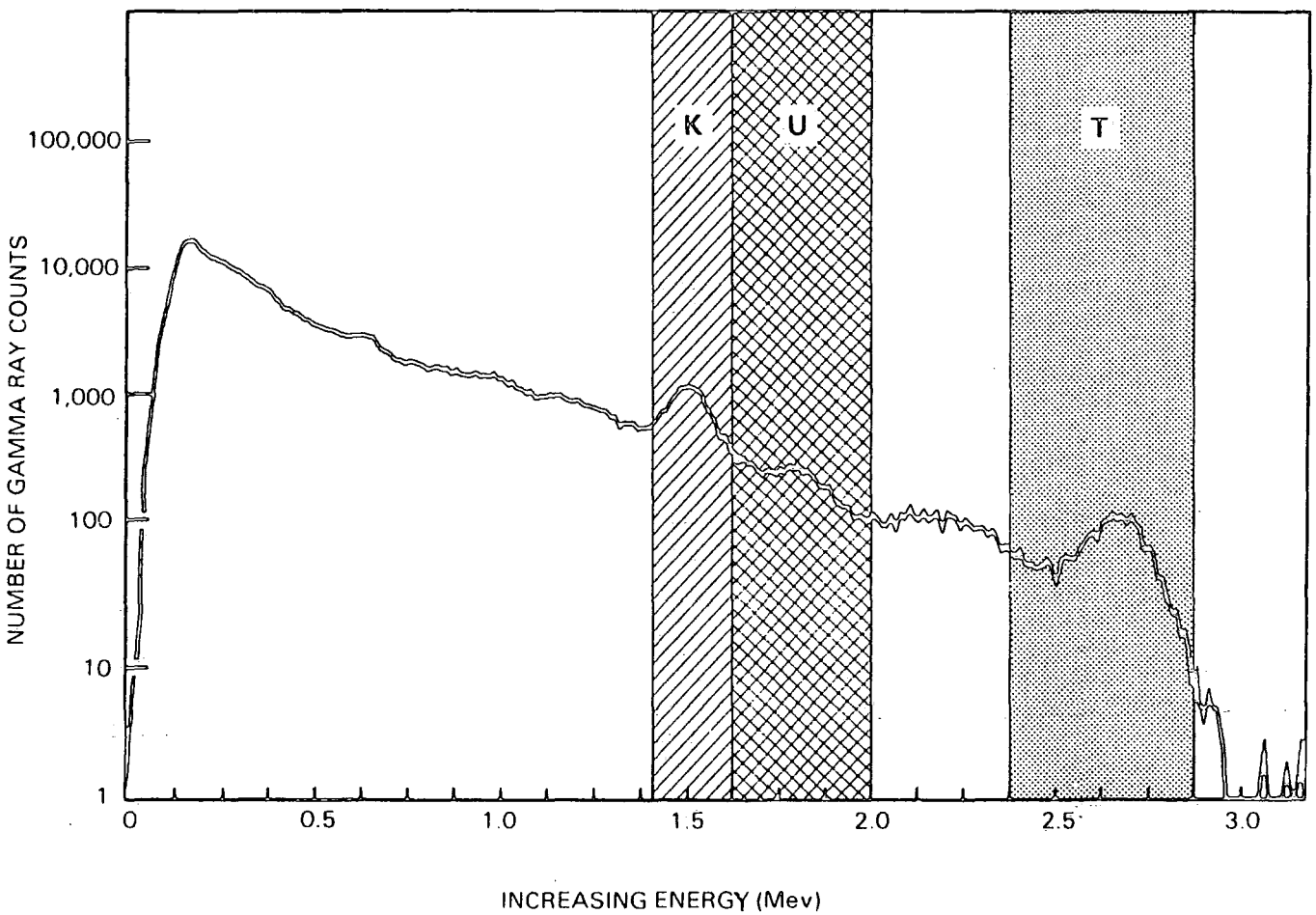

Figure 3-7. Typical gamma ray spectrum of a simulated shale formation. This shows the profile when all three elements are present in the formation. (Gearhart, 1986)

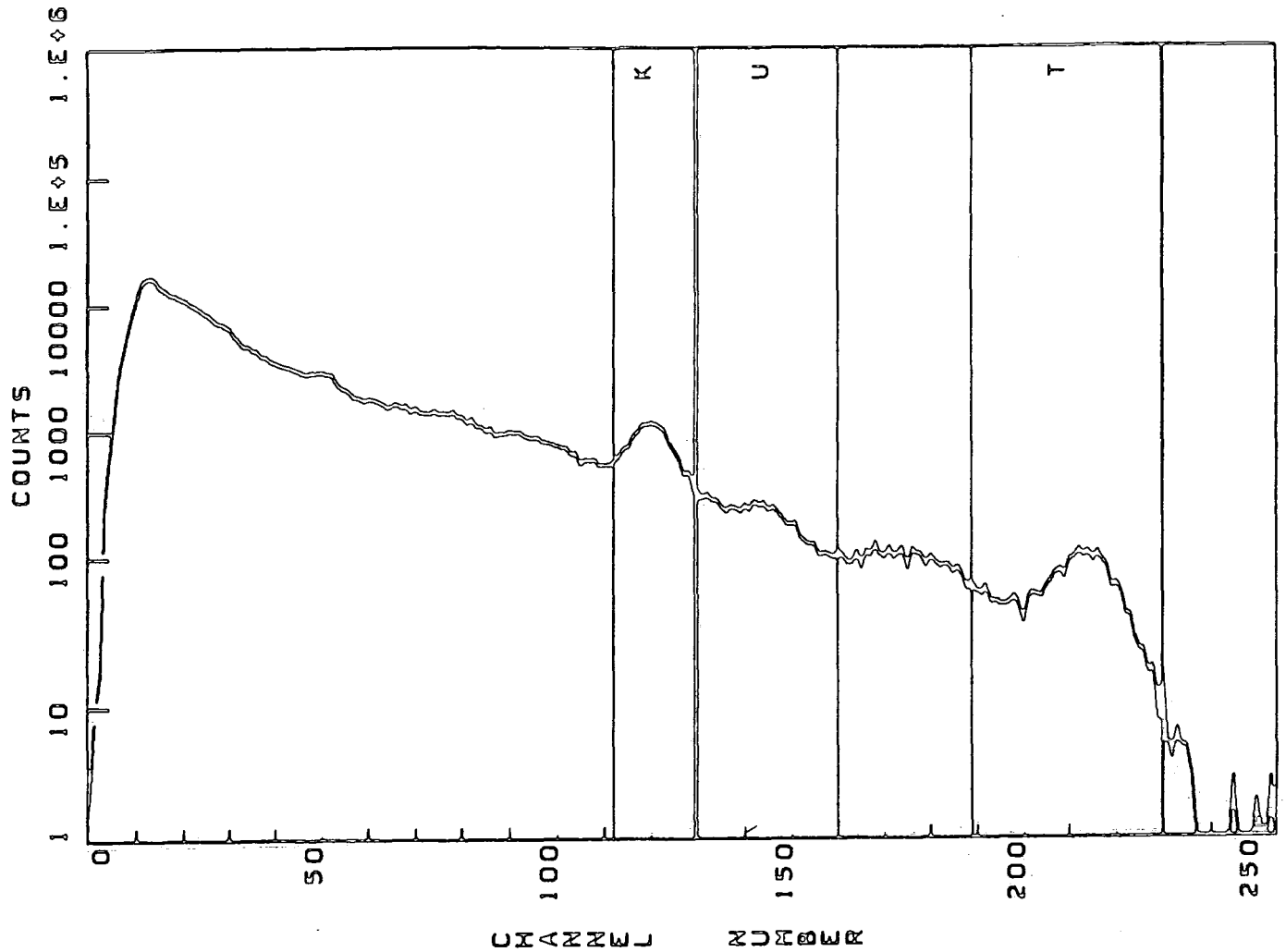

Figure 3-8. A gamma ray spectrum generated during a field calibration procedure. (Gearhart, 1986)

active part of this filter and gives a comparison of the transient response to the formation under investigation by using the assumption that gross gamma response is a superposition of the individual potassium, uranium and thorium activities. The constant gross gamma ray reflects very little statistical variation in the reading, therefore the abnormally large variations in the uranium-free gamma ray must be due to statistical noise. Under constant or slowly changing conditions the filter is applied to reduce statistical noise but under rapidly changing conditions this filtering technique allows the signal to follow these transient responses as rapidly as possible.

The gamma ray tool is generally used in combination with other tools. It is useful because its data can give a first hand indication of the shaliness and cleanliness of the formation and furthermore, it can be used for correlation with other suites of logs. The tool concept is relatively simple and all the logging companies provide this service.

Generally gamma ray data are treated as supporting data for use in log interpretation. However when the more detailed spectral gamma ray log is used the data obtained can give a better determination of the clay content within the formations in a well. Since the primary interest to an operator is the clean zone and since the gamma ray responds more to the clay zone the data obtained becomes of secondary importance.

The tool performance relies heavily on the natural radioactivity of the formation. When the amount of radiation is low statistical variation is an important factor in the accuracy of the data. Generally an operator is interested in the qualitative more than the quantitative nature of the data. This is also true even when the spectral gamma ray log is used.

4. RESISTIVITY

Ohm's law describes the behaviour of electrical current flow through a substance.

$$r = \frac{E}{i} \qquad (4\text{-}1)$$

where r = resistance, ohm

E = electromotive force, volts

i = current, amperes.

The electrical resistivity of a substance is its ability to impede the flow of electrical current through the substance.

$$R = r\frac{A}{L} \qquad (4\text{-}2)$$

where R = resistivity, ohm-m^2 /m

r = resistance, ohms

A = cross-sectional area, m^2

L = length of material, m

In practice (well logging), the resistance of a certain volume is measured. The volume of formation measured is a function of the configuration of the instrument, which is a constant, therefore, the measurement is expressed in terms of resistivity. The unit used is ohm-m^2 /m, usually written as ohm-m. Electrical conductivity is the reciprocal of resistivity and is usually expressed in millimhos per meter (mmho/m).

Most formations logged for potential oil and gas saturation are made up of rocks which, when dry, will not conduct an electrical current; i.e., the rock matrix has zero conductivity or infinitely high resistivity. An electrical current will flow only through the interstitial water saturating the pore structure of the formation, and then only if the interstitial water contains dissolved salts. These salts dissociate into positively charged cations (Na^+, Ca^{++},...) and negatively charged anions (Cl^-, SO_4^{--},...). Under the influence of an electrical field these ions move, carrying an electrical current through the solution. Other things being equal, the greater the salt concentration, the lower the resistivity of the formation and, hence, the greater the amount of formation water, the lower the resistivity.

Resistivity is of particular importance because it is the one measurement for which tools having a deep depth of investigation (up to several feet beyond the borehole) exist. Resistivity measurements are essential for saturation determinations particularly saturation determinations in the virgin, "noninvaded" portion of the reservoir. Resistivity measurements are employed, singly and in combination, to determine formation resistivity in the noninvaded formation (called true resistivity, R_t) and resistivity close to the borehole (called flushed-zone resistivity, R_{xo}), where mud filtrate has largely replaced the original pore fluids. Resistivity measurements, along with porosity and water resistivity, are used to obtain values of water saturation. Saturation values from both shallow and deep resistivity measurements can be compared to evaluate the producibility of the formation.

4.1 Formation Factor and Porosity

It has been established experimentally that the resistivity of a clean, water-bearing formation (i.e., one containing no appreciable amount of clay and no hydrocarbons) is proportional to the resistivity of the brine with which it is fully saturated. The constant of proportionality is called the formation resistivity factor, or simply the formation factor, F. Thus, if R_o is the resistivity of a nonshaly formation rock 100% saturated with brine of resistivity R_w, then

$$F = R_o / R_w \qquad (4\text{-}3) \quad \text{(Archie)}$$

for a given porosity, the ratio R_o / R_w remains nearly constant for all values of R_w below about 1 ohm-m. For fresher, more resistive waters, the value of F may decrease as R_w increases. This phenomenon is attributed to a greater proportionate influence of surface conductance of the rock matrix.

For a given saturating brine water, the greater the porosity of a formation, the lower the resistivity R_o of the formation, and the lower the formation factor F (from equation 4-3). Therefore, the formation factor is inversely related to porosity. It is also a function of pore structure and pore-size distribution.

Gustave E. Archie, an early pioneer in the development of formation evaluation techniques proposed, based on observations, a formula relating porosity,

ϕ, and formation factor, F; the relationship is

$$F = a/\phi^m \qquad (4\text{-}4) \quad \text{(Archie)}$$

where m is the cementation factor or exponent. The cementation exponent and the constant a are determined empirically.

Over the years, experience has generated general acceptance of the following formation factor-porosity relationships (dependent on lithology or pore structure):-

$$F = 0.62/\phi^{2.15} \quad \text{for sands,} \qquad (4\text{-}5) \quad \text{(Humble)}$$

and

$$F = 1/\phi^2 \qquad (4\text{-}6) \quad \text{(Archie)}$$

for compacted formations. The first relationship is popularly referred to as the Humble formula; the second, as the Archie formation factor relationship.

To eliminate the fractional cementation exponent, the Humble formula is sometimes simplified to

$$F = 0.81/\phi^2 \qquad (4\text{-}7) \quad \text{(Humble)}$$

Within their normal range of application, these two ways of expressing the Humble formula yield quite similar results.

4.2 Water Saturation

Neither oil nor gas conducts electrical current, both are excellent insulators. Indeed oil is widely used as an insulator in some electrical equipment. Thus in a formation containing oil or gas the resistivity is a function not only of F and R_w but also of the fraction of the pore volume occupied by formation water S_w. $(1\text{-}S_w)$ is therefore the fraction of the pore volume occupied by hydrocarbons.

Archie determined experimentally that the water saturation of a clean formation can be expressed in terms of its true resistivity as

$$S_w^n = F R_w / R_t \qquad (4\text{-}8) \quad \text{(Archie)}$$

Although laboratory measurements do show some variation in the value of n most formation samples yield a saturation exponent of about 2. Therefore in log interpretation practice n is taken equal to 2 unless it is known to be otherwise.

Accepting $n = 2$, equation 4-7 may be written as

$$S_w^2 = F R_w / R_t \qquad (4\text{-}9) \quad \text{(Archie)}$$

This equation is often popularly referred to as the Archie water saturation equation. It is the fundamental to most electrical log interpretation techniques.

In equation 4-3 FR_w is equal to R_o the resistivity of the formation when 100% saturated with water of resistivity R_w.

The water saturation equation, equation 4-9, may then be written :

$$S_w = \sqrt{R_o/R_t} \qquad (4\text{-}10) \quad \text{(Archie)}$$

Early quantitative electric log interpretation used this formula. It simply involved the comparison of R_t , recorded in a potential hydrocarbon-bearing reservoir rock, to R_o, recorded in a known 100% water bearing rock. Its use assumes that the two beds have similar porosities and formation factors and contain formation waters of similar salinity. The most appropriate application of equation 4-8 is therefore a thick reservoir of constant porosity, which has a water column at its base and an oil column at its top.

The ratio R_t/R_o is called the resistivity index. A resistivity index of unity implies 100% water saturation; a resistivity index of 4 corresponds to 50% water saturation; an index to 10, to 31.6 % water saturation; an index of 100, to 10% water saturation (see chart 4-1).

The water (mud filtrate) saturation, S_{xo}, of the flushed zone can also be expressed by the Archie formula as:

$$S_{xo} = \sqrt{F R_{mf} / R_{xo}} \qquad (4\text{-}11) \quad \text{(Archie)}$$

where R_{mf} is the resistivity of the mud filtrate and R_{xo} is the resistivity of the flushed zone. S_{xo} is equal to $(1\text{-}S_{hr})$, S_{hr} being the residual hydrocarbon saturation

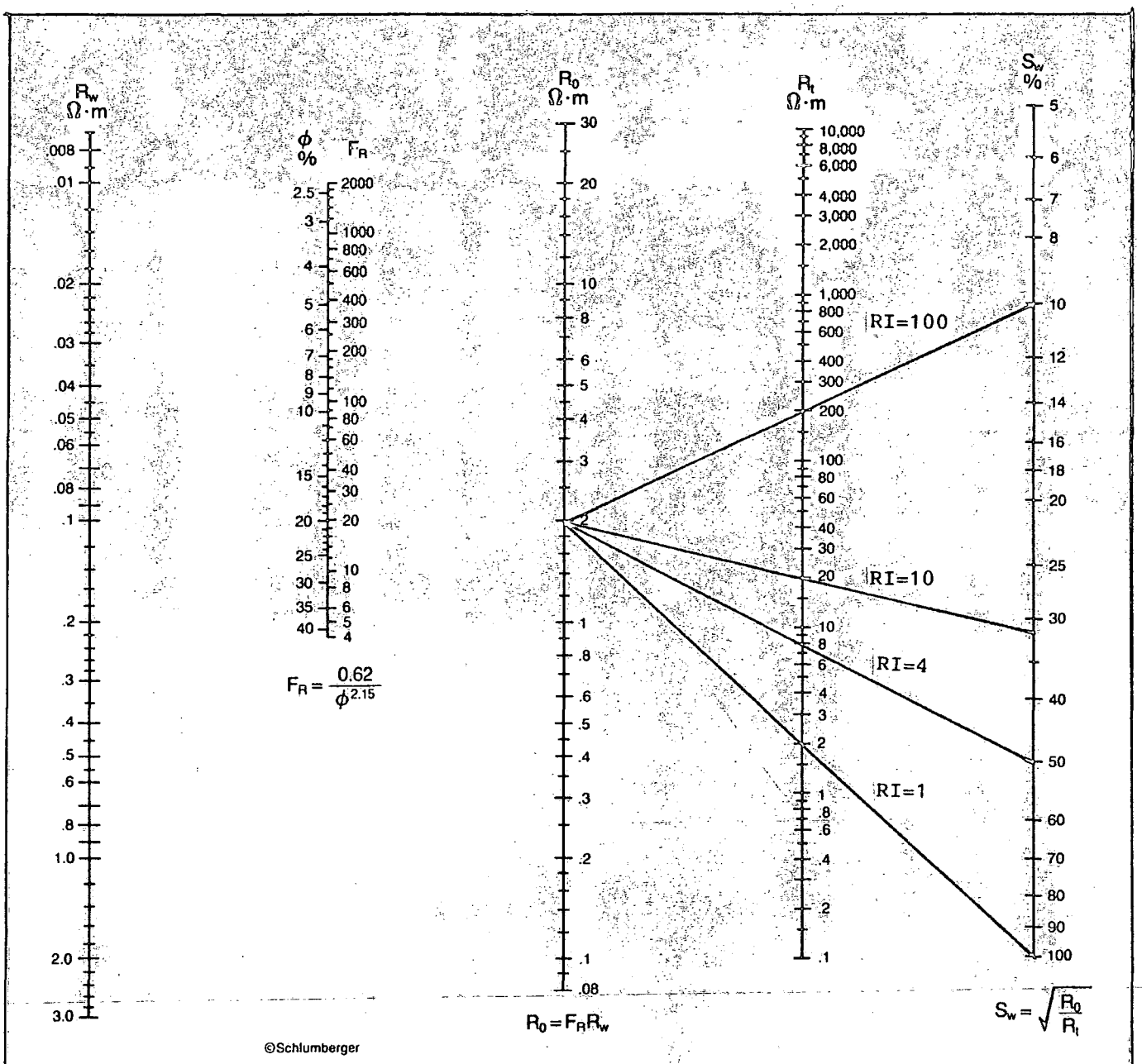

This nomograph solves the Archie water saturation equation $S_w = \sqrt{\frac{R_0}{R_t}} = \sqrt{\frac{F_R R_w}{R_t}}$. It should be used in clean (nonshaly) formations only. If R_0 (resistivity when 100% water saturated) is known, a straight line from the known R_0 value through the measured R_t value gives water saturation, S_w. If R_0 is not known, it may be determined by connecting the formation water resistivity, R_w, with the formation resistivity factor, F_R, or porosity, ϕ.

EXAMPLE: R_w = 0.05 Ω·m at formation temperature
ϕ = 20% (F_R = 20)
R_t = 10 Ω·m
Thus, S_w = 31.6%

Chart 4-1. Saturation Determination. (Schlumberger, 1987)

in the "flushed" zone. S_{hr} depends to some extent on the hydrocarbon viscosity; it generally increases as the viscosity increases.

The comparison of the water saturations obtained in the flushed zone (equation 4-11) and in the noninvaded zone (equation 4-10) determines the bulk-volume fraction of oil displaced by the invasion process. (Since $S_h = (1-S_w)$ and $S_{hr} = (1-S_{xo})$, the bulk volume of "moved oil" is $\phi\,(S_{xo}-S_w)$.) The ability of the mud filtrate to displace or move oil in the invasion process implies that the formation exhibits relative permeability to oil; conversely, oil production can be expected when the reservoir is put on production.

4.3 Resistivity Logging.

Evaluating a reservoir for its water and hydrocarbon saturation involves measurement of the saturating formation water resistivity, R_w ; the formation factor, F, or porosity, ϕ ; and the true formation resistivity, R_t. Flushed zone resistivity, R_{xo}, is also of interest because it can be used to obtain S_w when porosity is unknown to indicate hydrocarbon moveability and where invasion is deep to obtain a better value of R_t.

The resistivity parameter of greatest interest is R_t because of its relationship to hydrocarbon saturation in the noninvaded, virgin formation. Determination of R_t is therefore of paramount importance. In determining R_t and R_{xo} from resistivity logs several perturbing factors affecting the log readings must be taken into account. These are :-

a) the borehole, filled with fluid,

b) the adjacent formations and

c) the influence of R_{xo} (invasion) on the R_t measurement and vice versa.

The effect of the first two factors can be mininised by using logging tools designed to minimise borehole effect and to provide good vertical definition. The third is resolved by using several resistivity devices having different depths of investigation.

When $R_{xo} > R_t$ and formation resistivities are low to moderate the dual induction log is recommended for R_t determination. This survey, consisting of a deep induction log, a medium induction log, and a shallow investigating resistivity log, will furnish good values of R_t for beds thicker than 4 or 5 ft if invasion is not too

deep. Adding a microresistivity log to the suite will permit a better evaluation of R_{xo}, and thus R_t, in more deeply invaded formations.

When $R_{xo} < R_t$ and formation resistivity is high the dual laterolog is recommended for R_t determination. The log provides a deep laterolog and a shallow laterolog. Adding a microresistivity log to the suite will permit a better evaluation of R_{xo} and R_t.

Interpretation charts are available to correct for borehole, adjacent formation, and invasion effects.

4.3.1 Resistivity Logs

During the first quarter-century of well-logging, the only resistivity logs available were the conventional electrical surveys. Thousands of them were run each year in holes drilled all over the world. Since then more sophisticated resistivity logging methods have been developed to measure the resistivity of the flushed zone, R_{xo}, and the true resistivity of the uninvaded virgin zone, R_t.

Today the very first log run in the hole is still the resistivity log. This log can give a very good firsthand indication of the potential of the well. Furthermore, when used inconjunction with other logs it can lead to the determination of the water saturation, S_w, as described earlier. Although there are many uses from resistivity logs (refer to section 4-3), the methods of obtaining them nowadays use primarily three main logging principles. These are focusing electrode principle, induction principle, and microresistivity principle.

4.3.2 Focusing Electrode Logs (Figure 4-1)

Current is passed through the formation by means of current electrodes, and voltages are measured between measure electrodes. These measured voltages provide the resistivity determination for each device.

In a homogeneous, isotropic formation of infinite extent, the equipotential surfaces surrounding a single current-emitting electrode (A) are spheres. The voltage between an electrode (M) situated on one of these spheres and one at infinity is proportional to the resistivity of the homogenous formation. The measured voltage can be scaled in resistivity units.

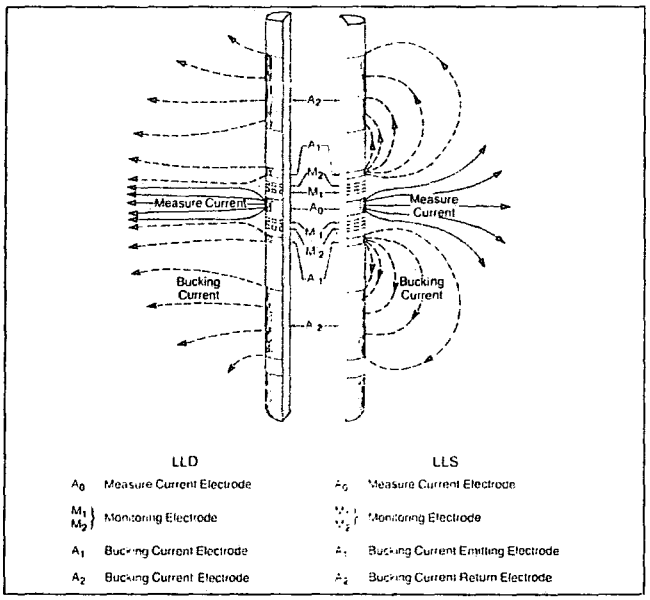

Figure 4-1. Schematic of the Dual Laterolog. (Doll, 1951)

The responses of conventional electrical logging systems can be greatly affected by the borehole and adjacent formations. These influences are minimized by a family of resistivity tools that uses focusing currents to control the path taken by the measured current. The currents are emitted from special electrodes on the sonde.

The focusing electrode tools include the laterolog and spherically focused devices. These tools are much superior to the older electrical survey devices for large R_t/R_m values (salt muds and/or highly resistive formations) and for large resistivity contrasts with adjacent beds (R_t/R_s or R_s/R_t). They are also better for resolution of thin to moderately thick beds. Focusing electrode systems are available with deep, medium, and shallow depths of investigation. Devices using this principle have as quantitative applications the determination of R_t and R_{xo}.

The objective of any deep-reading resistivity device is to measure the true formation resistivity, R_t. Deep-reading resistivity tools were designed so that, as much as possible, their response is determined by the resistivity of the virgin formation beyond the invaded zone. Unfortunately no single measurement has yet succeeded in entirely eliminating the effects of the invaded zone.

A solution is to measure the resistivity with several arrays having different depths of investigation. Measurements responding to three appropriately chosen depths of investigation usually approximate the invasion profile well enough to determine R_t.

For best interpretation accuracy such a combination system should have certain desirable features:-

a) Borehole effects should be small and/or correctable.

b) Vertical resolutions of the devices should be similar.

c) Radial investigations should be well distributed: i.e., one reading as deep as practical, one reading very shallow, and the third reading in between.

This resulted in the development of the laterolog-microresistivity tool with simultaneous recordings. The microresistivity tool is covered by section 4-4. The laterolog tool has a small current electrode positioned between two long guard electrodes. An auxiliary current of the same polarity is applied to the guard electrodes. The guard electrode current is automatically and continuously adjusted

to maintain a zero potential difference between the centre electrode and guard electrodes. This forces the current emanating from the current electrode to flow into the formation. A drop in potential is caused by the flow of the current through the surrounding formation to a remote current return electrode. This potential difference is related to the resistivity of the formation.

Invasion can be a major influence on the laterolog. Experience shows that the use of salt base muds generally results in only limited invasion which does not normally hamper the laterolog in the determination of true resistivity. If the muds are less saline (more resistive) than the formation water, the laterolog tends to be overly influenced by the invaded zone. This holds true unless the resistivity of the virgin zone is considerably higher than the invaded zone. Borehole size and bed thickness do affect the laterolog response, but normally the readings are accepted as true resistivity and used directly in the Archie equation. The laterolog is normally used in high resistivity, low porosity formations in the presence of saline drilling fluids.

The laterolog has good vertical resolution and will obtain good values of resistivity in beds thicker than 2 feet. Generally, the peak value of the curve represents the resistivity of thinner beds while in a very thick bed an average in the zone is often used.

Normally in a dual laterolog tool, the deep laterolog measurement is achieved by using very long guarded electrodes, and the shallow laterolog is achieved by using a type of focusing called "pseudolaterolog" in which the focusing current is returned to the nearby electrodes instead of to a remote electrode. This causes the measure current to diverge more quickly once it has entered the formation, thus producing a relatively shallow depth of investigation (see figure 4-1).

4.3.3 Induction Logging

The induction logging tool was originally developed to measure formation resistivity in boreholes containing oil-base muds and in air-drilled boreholes. Electrode devices did not work in these nonconductive muds, and attempts to use wall-scratcher electrodes were unsatisfactory.

Experience soon demonstrated that the induction log had many advantages

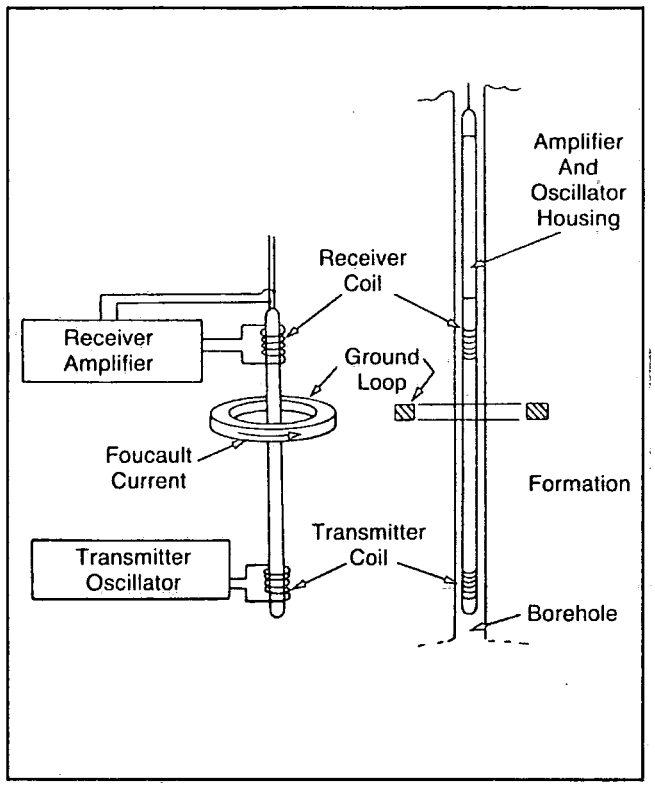

Figure 4-2. Basic two-coil induction log system. (Doll, 1949)

over the conventional electrical survey log when used for logging wells drilled with water-base muds.

Today's induction tools have many transmitter and receiver coils. However, the principle can be understood by considering a sonde with only one transmitter coil and one receiver coil (see figure 4-2).

A high-frequency alternating current of constant intensity is sent through a transmitter coil. A typical frequency value of 20 kHz is generally used. This is an empirical value which has been found to be most useful. The alternating magnetic field created induces currents in the formation surrounding the borehole. These currents flow in circular ground loops coaxial with the transmitter coil and create, in turn, a magnetic field that induces a voltage in the receiver coil.

Because the alternating current in the transmitter coil is of constant frequency and amplitude, the ground loop currents are directly proportional to the formation conductivity. The voltage induced in the receiver coil is proportional to the ground loop currents and, therefore, to the conductivity of the formation.

There is also a direct coupling between the transmitter and receiver coils. The signal originating from this coupling is eliminated by using "bucking" coils.

If the model is simplified (sonde centred and formation homogeneous and isotropic), the tool response can be calculated as the sum of the elementary signals created by all formation loops coaxial with the sonde. This neglects the mutual and self-inductance of the ground loops. Each elementary signal is proportional to the loop conductivity and to a geometrical factor that is a function of the loop position with reference to the transmitter and receiver coils. Therefore,

$$E = K \Sigma g_i c_i, \qquad (4\text{-}12)\ \text{(Doll, 1949)}$$

where E is the induced electromotive force,

K is the sonde constant,

g_i is the geometrical factor for that particular loop,

c_i is the conductivity of that loop,

and $\Sigma g_i = 1.$

The geometrical factor, g_i, corresponding to a medium is defined as the proportion of the total conductivity signal contributed by the given medium. The

formation can be split into cylinders coaxial with the sonde (tool being centralised). These correspond to the mud column, invaded zone, virgin zone, and shoulder beds. The total signal can be expressed by

$$C_I = G_m C_m + G_{xo} C_{xo} + G_t C_t + G_s C_s \quad (4\text{-}13)$$

(Doll, 1949)

where $G_m + G_{xo} + G_t + G_s = 1$,

G is the geometrical factor for a defined region, and

subscripts m, xo, t and s correspond to mud column, invaded zone, virgin zone and shoulder beds respectively.

Thus, a volume of space defined only by its geometry relative to the sonde has a fixed and computable geometrical factor G (see figure 4-3). This permits the construction of mathematically sound correction charts to account for the effects of borehole mud, invaded zone, and adjacent beds on the R_t measurement, providing symmetry of resolution exists.

Because induction tools are designed to evaluate R_t all the corresponding geometrical factors are minimised using a focused signal. Even though the two-coil system does not represent the tool used today it can be considered the building block from which today's multicoil sonde was built. The responses of a multicoil sonde is obtained by breaking it down into all possible two-coil combinations of transmitter-receiver pairs. The responses of all coil pairs are added with due regard to the algebraic sign of their contributions and their relative positions.

Multicoil sondes, or focused sondes, offer certain advantages. Vertical resolution is improved by suppressing the response from the shoulder formations and depth of investigation is improved by suppressing the response from the mud column and the formation close to the hole.

In very conductive formations the induced secondary currents in the ground loops are large and their magnetic fields are important. The magnetic field of these ground loops induce additional emf's (electrical voltages) in other ground loops. These induced emf's are out of phase with those induced by the transmitter coil of the induction tool. This interaction between the ground loops causes a reduction of the conductivity signal recorded on the induction logs which is called "skin effect".

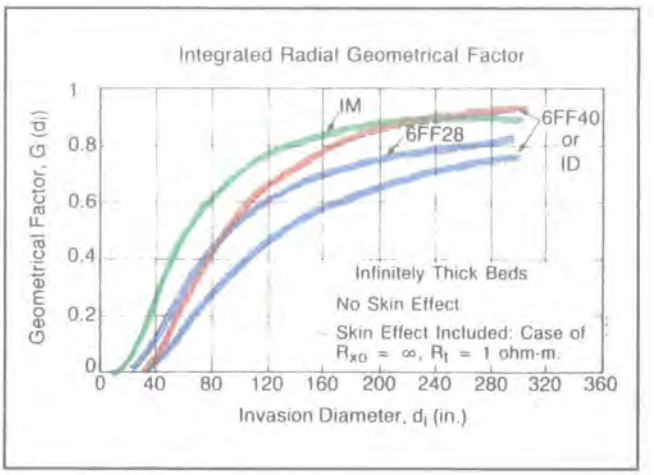

Figure 4-3. Geometrical Factors. Red curve includes skin effect, under conditions shown, for 6FF40 or the deep induction (ID) devices. (Moran and Kunz, 1962)

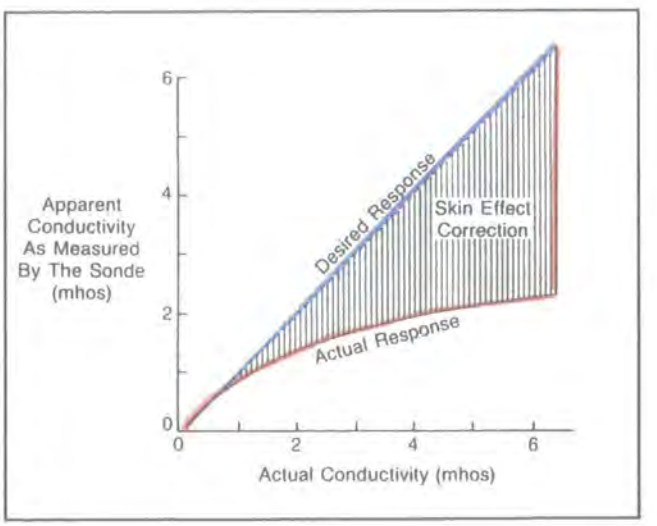

Figure 4-4. Actual response of an induction log compared to the desired response. (Moran and Kunz, 1962)

It is a predictable phenomenon. Figure 4-4 shows the response of the tool compared to the actual formation conductivity of the formation. Skin effect becomes significant when formation conductivity exceeds 1000 mmho/m.

The induction tool works best when the borehole fluid is an insulator, even air or gas. The tool also works well when the borehole contains conductive mud unless the mud is too salty, the formations are too resistive, or the borehole diameter is too large.

4.3.4 Induction versus Laterolog Measurements

Nearly all resistivity measurements are now made with focused devices. The induction log is generally recommended in holes drilled with only moderately conductive drilling muds, non-conductive muds (e.g., oil-based muds), and is empty or air-drilled holes. The laterolog is generally recommended in holes drilled with very conductive drilling muds (i.e., salt muds).

The induction tool, being a conductivity-sensitive device is most accurate in low-to medium-resistivity formations. The laterolog tool, being a resistivity device is most accurate in medium- to high-resistivity formations. There is an overlap in the areas of applicability (refer to figure 4-5). Thus, when R_{xo} is greater than R_t, the induction tool is preferred for R_t determination and the laterolog tool is preferred where R_{xo} is less than R_t.

Induction logs provide acceptable thin-bed resolution which make reliable formation evaluation possible in beds down to 5 foot thick. The laterolog devices exhibit even better thin bed resolution. Except for beds with extremely high resistivity reliable formation is possible in beds as thin as 3 feet.

The path taken by the measure current of the laterolog constitutes a "series circuit" through the drilling mud, mud cake, flushed and invaded zones and the noninvaded formation. Thus, from the analogy of electric circuits, the greatest

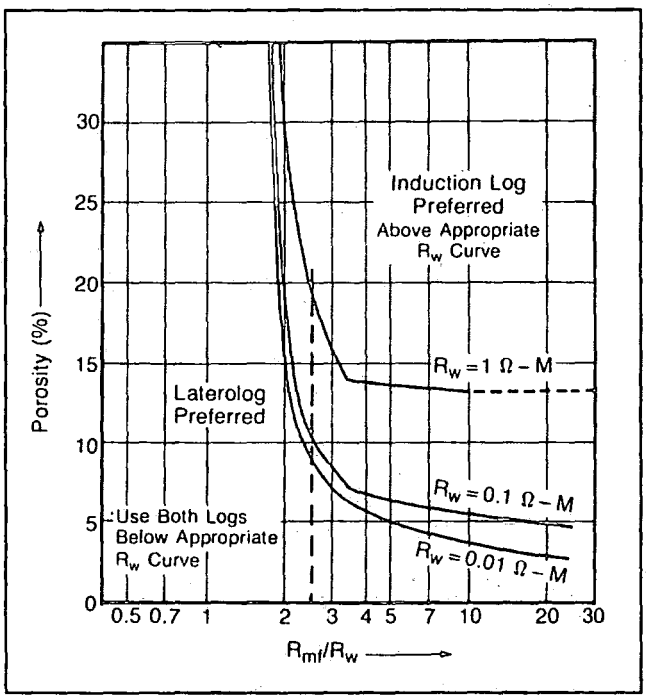

Figure 4-5. Preferred ranges of application of induction logs and laterologs for usual cases. (Schlumberger, 1986)

voltage drop will appear across those sections having the highest resistance. Note that in contrast, the induction log which measures conductivity sees the different zones as constituting a parallel circuit of resistors.

There are a variety of laterolog and induction tools on offer from the logging companies. These tools are listed in table 4-1.

Tool Type	Company	Tool	Max.Temp.(°F)	Max. Pressure (Kpsi)
Laterolog	Gearhart	DLL	350	20
	Schlumberger	DLT	350	20
	Western Atlas	DL	350	20
Induction	Gearhart	IEL	350	18.5
		DIL	350	20
		HRI	350	20
	Schlumberger	ISF	350	20
		DIL	350	20
		PHASOR	350	20
	Western Atlas	IEL	350	18
		DIFL	350	18

Table 4-1 Resistivity Tools' Ratings.

In the laterolog family Gearhart, Schlumberger and Western Atlas all have a tool of the same name, the Dual Laterolog tool. In the induction family, Gearhart has the Induction Electric Log (IEL) tool and the Dual Induction Laterolog (DIL) tool; Schlumberger has the Induction Spherically Focused (ISF) tool and the Dual Induction Log (DIL) tool; and Western Atlas has the Induction Electrolog (IEL) tool and the Dual Induction-Focused Log (DIFL) tool. Despite the difference in names, the basic principle behind each family of resistivity tool, whether it is a laterolog or induction device, still applies throughout. As technology advances the hardware improves and hence more and better data are obtainable.

One such an example is the introduction of the Phasor Dual Induction (PHASOR) tool by Schlumberger. The PHASOR tool employs a digital transmis-

sion and processing system. It also can be operated at frequencies of 10 and 40 kHz, as well as at 20 kHz (the operating frequency of most previous induction devices). The lower frequency reduces skin effect in very low resistivity formations and the higher frequency provides more accurate measurements in high resistivity formations through better signal-to-noise ratio and better sonde error stability. However, except for these special situations most logs are run at 20 kHz. In addition to in-phase resistivity (or conductivity) measurements the PHASOR tool measures the out-of-phase quadrature or X-signal. The availability of the X-signal improves the accuracy to the skin-effect correction, the thin-bed response and the overall presented data. The PHASOR logs are completely corrected for shoulder bed effect, have vertical response functions that are constant with formation conductivity changes and have more nearly linear radial responses. Also the effective depth of investigation of the PHASOR tool is slightly greater and the resolution in deeply invaded formations is significantly improved.

Similarly, in response to the PHASOR tool, Gearhart has the High Resolution Induction (HRI) tool. The benefits are similar to those of the PHASOR tool. The tool principle also seems to be the same.

All the logging companies are interested to provide the best tools to monitor the true resistivity of the formation. This is because resistivity is one of the most important parameters necessary to determine the existence of hydrocarbons. In the laterolog devices all the companies use a similar known principle to build their tools and no doubt the data obtained are probably similar too. Similarly, the principle behind the induction devices is all the same too and here again the data obtained are probably similar too.

The trend towards "High Resolution Logging" (see chapter 13) will favour the introduction of both the Gearhart HRI and Schlumberger PHASOR tools. In the meantime, Western Atlas still has no such tool on the market. The tools have reduced vertical resolution to 2 feet, depth of investigation to greater than 55 inches, reduced residue sonde error (up to +/- 0.5 mmho), and enhanced skin effect correction to allow accurate measurements below 0.5 ohm-m.

4.4 Microresistivity Devices

Microresistivity devices are used to measure the resistivity of the "flushed

zone", R_{xo}, and to delineate permeable beds by detecting the presence of mudcake.

Measurements of R_{xo} are important for several seasons. When invasion is moderate to deep a knowledge of R_{xo} allows the deep resistivity measurement to be corrected to true formation resistivity. Also, some methods for computing saturation require the R_{xo}/R_t ratio. In the clean formations a value of F can be computed from R_{xo} and R_{mf} if S_{xo} is known or can be estimated.

To measure R_{xo} the tool must have a very shallow depth of investigation because the flushed zone may extend only a few inches beyond the borehole wall. Since the reading should not be affected by the borehole a sidewall-pad tool is used. The pad carrying short-spaced electrode devices is pressed against the formation and reduces the short-circuiting effect of the mud. Currents from the electrodes on the pad must pass through the mudcake to reach the flushed zone (see figures 4-6 to 4-8).

Microresistivity readings are affected by mudcake; the effect depends on mudcake resistivity, R_{mc}, and thickness, h_{mc}. Moreover, mudcake can be anisotropic with mudcake resistivity parallel to the borehole wall less than that across the mudcake. Mudcake anisotropy increases the mudcake effect on microresistivity readings so that the effective, or electrical, mudcake thickness is greater than that indicated by the caliper. Hence, the resistivity reading of the flushed zone can seem higher by up to 0.5 ohm-m. During interpretation this must be taken into account and corrected before use.

4.4.1 Microlog

With the microlog tool (figure 4-6), two short-spaced devices with different depths of investigation provide resistivity measurements of a very small volume of mudcake and formation immediately adjoining the borehole. Comparison of the two curves readily identifies mudcake which indicates invaded and therefore permeable formations.

4.4.1.1 Principle

The rubber microlog pad is pressed against the borehole wall by arms and springs. The face of the pad has three small in-line electrodes spaced 1 inch apart. With these electrodes a 1- by 1-inch microinverse ($R_{1"x1"}$) and a 2-inch micronormal

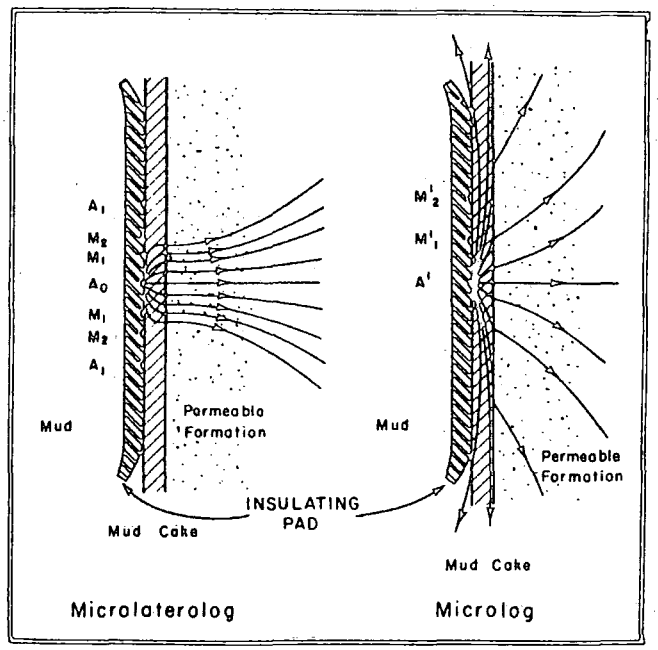

Figure 4-6. Comparative distribution of current lines of Microlaterolog and Microlog. (Doll, 1950)

($R_{2"}$) measurement are recorded simultaneously.

As drilling fluid filters into the permeable formations mud solids accumulate on the borehole wall and form a mudcake. Usually, the resistivity of the mudcake is slightly greater than the resistivity of the mud and considerably lower than the resistivity of the invaded zone near the borehole.

The 2-inch micronormal device has a greater depth of investigation than the microinverse. It is therefore less influenced by the mudcake and reads a higher resistivity, which produces "positive" curve separation. In the presence of low-resistivity mudcake both device measure moderate resistivities usually ranging from 2 to 10 times R_m.

In impervious formations the two curves read similarly or exhibit some "negative" separation and the resistivities are usually much greater than in permeable formations.

4.4.1.2 Equipment

Tool Type	Company	Tool	Max. Temp. (°F)	Max.Pressure(kpsi)
Microlog	Gearhart	MEL	350	18.5
	Schlumberger	MLT	350	20
	Western Atlas	ML	350	18
Micro-laterlog	Gearhart	MLL	350	18.5
	Schlumberger	MLL	350	20
	Western Atlas	MLA	350	20
Proximity Log	Schlumberger	MPT	350	20
	Western Atlas	PLM	350	20
MicroSFL	Gearhart	MSF	350	20
	Schlumberger	MSFL	350	20

Table 4-2 Microresistivity Tools' Ratings.

For the microlog family Gearhart has the MicroElectric Log (MEL) tool, Schlumberger has the Microlog (MLT) tool and Western has the Minilog (ML) tool (see table 4-2). All the tools have a depth of investigation of approximately 4 inches for micronormal output and approximately 5 inches for microinverse output. The Microlog tool is primarily designed for use in fresh muds where $R_{xo}/R_{mc} < 15$ and

porosity > 15%。

4.4.2 Microlaterolog

The microlaterolog was designed to determine R_{xo} accurately for higher values of R_{xo}/R_{mc} where the microlog interpretation lacks resolution.

4.4.2.1 Principle

The microlaterolog pad is shown in figure 4-7. The principle of micro-laterolog is much the same as that of the laterolog but on a smaller scale. The resulting lines are shown on the figure. Figure 4-6 compares qualitatively the current-line distributions of the microlaterolog and the microlog devices when the corresponding pad is applied against a permeable formation. The greater the value of R_{xo}/R_{mc}, the greater the tendency for the microlog current, i_o, to escape through the mudcake to the mud in the borehole. Consequently for high R_{xo}/R_{mc} values, microlog readings respond very little to variations of R_{xo}. On the contrary, all the microlaterolog current flows into the permeable formation and the microlaterolog reading depends mostly on the value of R_{xo}.

4.4.2.2 Equipment

For the microlaterolog family, Gearhart has the MicroLaterolog (MLL) tool, Schlumberger has the MicroLaterolog (MLL) tool and Western Atlas has the MicroLaterolog (MLA) tool (table 4-2). These tools are designed primarily for use in salt muds. Their depth of investigation is still approximately 4 inches.

4.4.3 Proximity Log

The proximity log is designed as the freshwater mud equivalent of the microlaterolog. The tool principle is still similar to the microlaterolog.

4.4.3.1 Equipment

For the proximity log family, Schlumberger has the MicroProximity Log (MPT)tool and Western Atlas has the Proximity Minilog (PLM) tool (table 4-2) . The tools have stronger focusing and the ability to read deeper into the formation. Gearhart has no such service on offer.

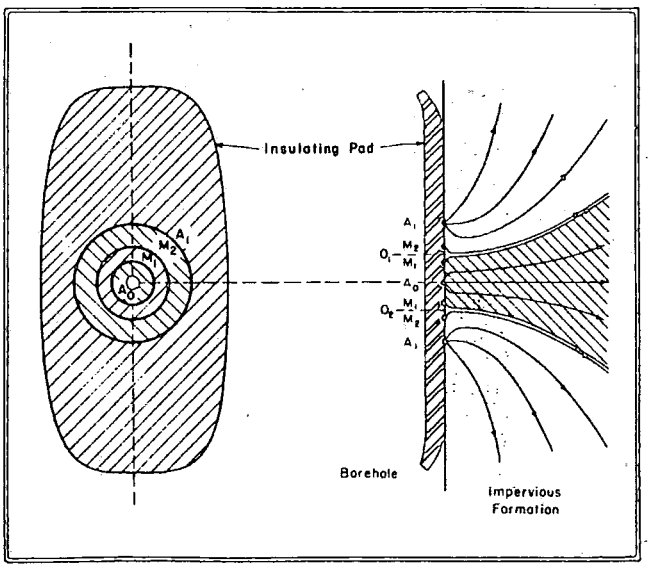

Figure 4-7. Microlaterolog pad showing electrodes (left) and schematic current lines (right). (Doll, 1953)

4.4.4 MicroSFL

The MicroSFL is a pad-mounted spherically focused logging device which is replacing the microlaterolog and proximity log tools. It has a distinct advantage over the other R_{xo} devices in that it has a much improved response to shallow R_{xo} zones in the presence of mudcake. The chief limitation of the microlaterolog measurement is its sensitivity to mudcakes. When mudcake thickness exceeds 3/8 inch the log readings are severely influenced at high R_{xo} /R_{mc} contrasts. The proximity log, on the other hand, is relatively insensitive to mudcakes but it requires an invaded zone with an investigation diameter of about 4 inches in order to provide direct approximations of R_{xo}.

The solution was found in an adaptation of the principle of spherical focusing in a sidewall-pad device. By careful selection of electrode spacings and bucking-current controls the microSFL measurement was designed for minimum mudcake effect without an undue increase in the depth of investigation. Figure 4-8 illustrates schematically the electrode arrangement (right) and the current patterns (left) of the microSFL tool.

The principle is much the same as the laterolog. By forcing the measure current to flow directly into the formation the effect of mudcake resistivity on tool response is minimised yet the tool still has a very shallow depth of investigation.

Synthetic microlog curves can be computed from microSFL parameters.Since the measure current sees mostly the flushed zone and the bucking current sees primarily the mudcake, it is possible to derive mathematically micronormal and microinverse curves.

4.4.4.1 Equipment

For the microSFL family, only Gearhart who offers the MicroSpherically Focused Log (MSF) tool, and Schlumberger who offers the MicroSpherically Focused Log (MSFL) tool, are providing this service while Western Atlas has no such service on offer (see table 4-2).

There are a large variety of microresistivity devices, and the choice is governed by the borehole condition and mud type used. However, the trend today is towards the microSFL tool because it has a much improved response to shallow R_{xo} zones in the presence of mudcake. This is obtained by the principle of spherical

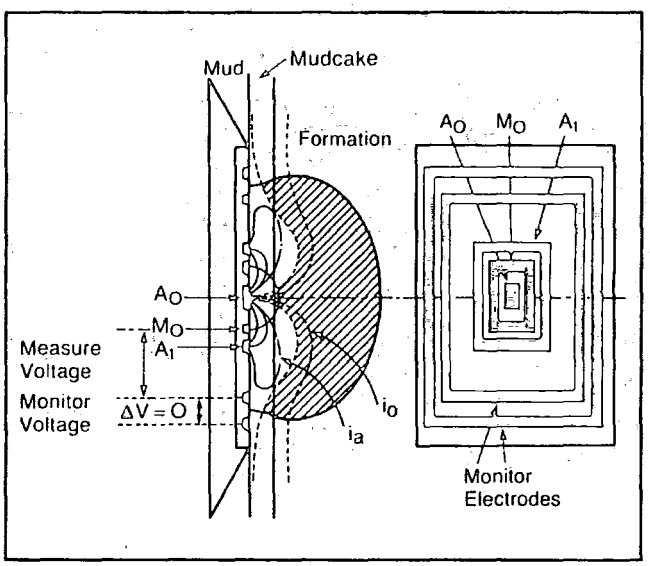

Figure 4-8. Electrode arrangement of MicroSFL device (right) and current distribution (left). (Schlumberger, 1984)

focusing used on the current and bucking current. Gearhart and Schlumberger are the only two companies who provide this service, and therefore are more likely to be favoured by an operator who wishes to know more information from the flushed zone.

5. POROSITY

Porosity is the pore volume per unit volume of formation; it is the fraction of the total volume of a sample that is occupied by pores or voids. The symbol for porosity is "ϕ". A dense, uniform substance, such as a piece of glass, has a porosity approaching zero; a sponge, on the other hand, has a very high porosity.

Porosity of subsurface formations can vary widely. Dense carbonates (limestones and dolomites) and evaporites (salt, anhydrite, gypsum, sylvite, etc.) may show practically zero porosity; well-consolidated sandstones may have 30 %,or more, porosity. Shales or clays may contain over 40 % water filled porosity, but the individual pores are usually so small the rock is impervious to the flow of fluids.

Porosities are classified according to the physical arrangement of the material that surrounds the pores and to the distribution and shape of the pores. In a clean sand the rock matrix is made up of individual sand grains more or less spherical in shape packed together in some manner where the pores exist between the grains. Such porosity is called intergranular, sucrosic or matrix porosity. Generally it has existed in the formations since the time they were deposited. For this reason it is also referred to as primary porosity.

Depending on how they were actually deposited limestones and dolomite may also exhibit intergranular porosity. They may also have second porosity in the form of vugs or small caves. Secondary porosity is caused by the action of the formation waters or tectonic forces on the rock matrix after deposition. For instance slightly acidic percolating waters may create and enlarge the pore spaces while moving through the interconnecting channels in the limestone formations and shells of small crustaceans trapped therein may be dissolved and form vugs. Conversely, percolating waters rich in minerals may form deposits that partially seal off some of the pores or channels in a formation thereby reducing its porosity and/or altering the pore geometry. Waters rich in magnesium salts can seep through calcite with a gradual replacement of calcium by magnesium. Since the replacement is atom for atom, mole for mole, and the volume of one mole of dolomite is 12 % less than that of calcite the result is a reduced matrix volume and a corresonding increase in pore volume.

Stresses in the formation may also occur and cause networks of cracks, fissures, or fractures, which add to the pore volume. In general however, the actual

volume of the fractures is usually relatively small. They do not normally increase the porosity of the rock significantly although they may significantly increase its permeability.

Porosity can be obtained from a sonic log, a density log, or a neutron log provided the lithology of the formation is known. Where τ, τ_f and τ_{ma} are the transit times in the log, pore fluid and rock matrix, respectively. The neutron and density logs respond to total porosity which is the sum of the primary (intergranular or intercrystalline) porosity and the secondary (vugs, fissures, fractures) porosity. The sonic logs however tend to respond only to evenly distributed primary porosity. If lithology is not known or if mixtures of known minerals exist, a combination of two or more porosity and lithology-sensitive logs can be used to define the lithology and to provide an accurate value of porosity.

The porosity logs are also somewhat sensitive to the nature of the saturating fluid(s) within the pores investigated by the tool. A combination of two porosity logs can sometimes detect the presence of gas or light oil in the formation.

The sonic tool measures the interval transit time, τ, or the time in microseconds for an acoustic wave to travel through 1 foot (or 1 metre) of formation along a path parallel to the borehole.

Porosity can be derived from the interval transit time using an empirical weighted-average or time-average relationship,

$$\text{porosity, } \phi = \frac{\tau - \tau_{ma}}{\tau_f - \tau_{ma}} \quad \text{(5-1)} \quad \text{(Wyllie, Gregory, and Gardner, 1956)}$$

where τ, τ_f and τ_{ma} are the transit times in the log, pore fluid and rock matrix, respectively. This time average relationship is good for clean, compacted formations of intergranular porosity containing liquids.

Another empirical relationship for porosity from the interval transit time is

$$\text{porosity, } \phi = \frac{C(\tau - \tau_{ma})}{\tau} \quad \text{(5-2)} \quad \text{(Wyllie, Gregory, and Gardner, 1958)}$$

where $C = 0.67$. This empirical relationship is restricted to the same conditions as the time average relationship except that it can be used in noncompacted

as well as compacted formation.

The density tool responds to the electron density of the material in the formation. For common formation materials the electron density is proportional to actual density.

Porosity is derived from the bulk density of clean liquid-filled formation when the matrix density, ρ_{ma}, and the density of the saturating fluids, ρ_f, are known:

$$\text{porosity, } \phi = \frac{\rho_{ma} - \rho_b}{\rho_{ma} - \rho_f} \qquad (5\text{-}3)$$

(Alger, Rayner, Hoyle, and Texier, 1963)

The presence of shale or gas in the formation complicates the response but this can be resolved using an appropriate combination of porosity logs.

The neutron log responds chiefly to the presence of hydrogen atoms. If the pore space in the formation is liquid-filled the response is basically a measure of porosity. The log is usually scaled in porosity units on the basis of a limestone matrix. Corrections must be made if the formation lithology differs from that which the tool is calibrated. Again, shale and gas affect the porosity readings and must be accounted for.

Porosity can be derived from the log porosity of clean liquid-filled formation when the matrix porosity, ϕ_{ma}, and hydrogen index of the fluid saturating the pores, ϕ_f, are known:

$$\text{porosity, } \phi = \frac{\phi_{ma} - \phi_N}{\phi_{ma} - \phi_f} \qquad (5\text{-}4)$$

(Alger, Locke, Nagel, and Sherman, 1987)

Similarly, the presence of shale or gas in the formation complicates the response, but this can be resolved using an appropriate combination of porosity logs.

Rock porosity can be obtained from the sonic log, the density log, or the neutron log. For all these devices the tool response is affected by the formation porosity, fluid, and matrix. If the fluid and matrix effects are known or can be determined the tool response is affected by the formation porosity, fluid, and matrix.

All three logging techniques respond to the characteristics of the rock immediately adjacent to the borehole. Their depth of investigation is very shallow (only a few inches or less) and therefore generally within the flushed zone.

The measurements of the sonic, density and neutron logs respond not only to porosity (ϕ) but also to the formation lithology, to the fluid in the pores and in some instances to the geometry of the pore structure. When the lithology and therefore the matrix parameters (τ_{ma}, ϕ_{ma}) are known, correct porosity values can be derived from these logs, appropriately corrected for environmental effects, in clean water-filled formations. Under these conditions a single log either the neutron or the density or, if there is no secondary porosity, the sonic can be used to determine porosity.

Accurate porosity determination is more difficult when the matrix lithology is unknown or consists of two or more minerals in unknown proportions. Determination is further complicated when the response of the pore fluids in the portion of the formation investigated by the tool differs appreciably from that of water. In particular light hydrocarbon (gas) can significantly influence the response of all three porosity logs.

5.1 Sonic Logs

In its simplest form, a sonic tool consists of a transmitter that emits a sound pulse and a receiver that picks up and records the pulse as it passes the receiver. The sonic log is simply a recording versus depth of the time required for a sound wave to transverse 1 ft of formation. Known as the interval transit time, τ, or slowness, is the reciprocal of the velocity of the sound wave. The interval transit time for a given formation depends upon its lithology and porosity. This dependence upon porosity when the lithology is known makes the sonic log very useful as a porosity log. Integrated sonic transit times are also helpful in interpreting seismic records. The sonic log can be run simultaneously with many other services.

5.1.1 Principle

The propagation of sound in a borehole is a complex phenomenon. It is governed by the mechanical properties of several separate acoustical domains. These include the formation, the borehole fluid column, and the logging tool itself.

The sound emanating from the transmitter impinges on the borehole wall. This

establishes compressional and shear waves within the formation, surface waves along the borehole wall and guided waves within the fluid column.

In the case of well logging the borehole wall, formation bedding, borehole "rugosity" and fractures can all represent significant acoustic discontinuities. Therefore,the phenomena of wave refraction, reflection, and conversion lead to the presence of many acoustic waves in the borehole when a sonic log is being run. Therefore many acoustic energy arrivals are seen by the receivers of a sonic logging tool. The more usual energy arrivals are seen by the receivers of a sonic logging tool. The more usual energy arrivals are shown in the acoustic waveforms displays of figure 5-1. This is a case where waveforms were recorded with an array of eight receivers located 8 to 11 1/2 feet from the transmitter. The various wave packets have been labelled. Although the wave packets are not totally separated in time at this spacing, the distinct changes corresponding to the onset of the formation compressional and shear arrivals and the Stoneley arrival can be observed.

The first arrival or compressional wave is one that has travelled from the transmitter to the formation as a fluid pressure wave, has been refracted at the borehole wall, has travelled within the formation at the compressional wave velocity of the formation as a fluid pressure wave and then has travelled back to the receiver as a fluid pressure wave.

The shear wave is one that has travelled from the transmitter to the formation as a fluid pressure wave, has travelled within the formation at the shear wave velocity of the formation, and has travelled back to the receiver as a fluid pressure wave.

The mud wave (not strongly evident in the figure 5-1) is one that has travelled directly from transmitter to receiver in the mud column at the compressional wave velocity of the borehole fluid.

The Stoneley wave is one of large amplitude that has travelled from transmitter to receiver with a velocity less than that of the compressional waves in the borehole fluid.

The velocity of the Stoneley wave is dependent upon the frequency of the sound pulse, hole diameter, formation shear velocity, densities of the formation and fluid compressional wave velocity.

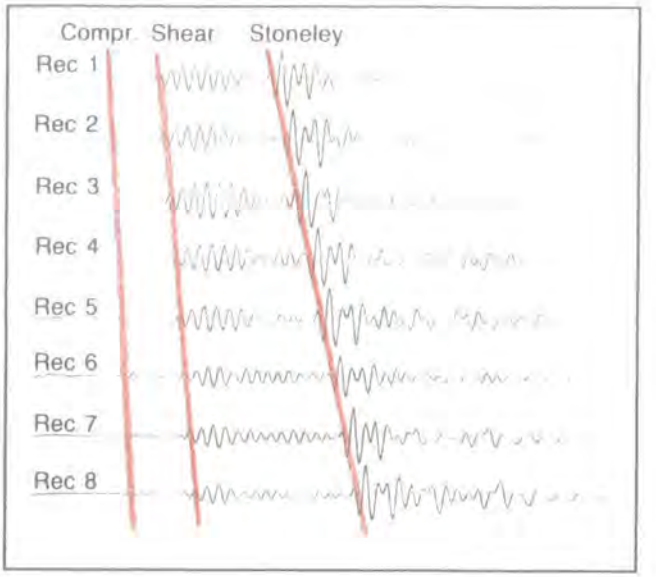

Figure 5-1. Example waveforms from the eight-receiver Array Sonic tool. (Morris, Little, and Letton, 1984)

	v_{ma} (ft/sec)	$\triangle t_{ma}$ (μsec/ft)	$\triangle t_{ma}$ (μsec/ft) (commonly used)
Sandstones	18,000-19,500	55.5-51.0	55.5 or 51.0
Limestones	21,000-23,000	47.6-43.5	47.5
Dolomites	23,000	43.5	43.5
Anhydrite	20,000	50.0	50.0
Salt	15,000	66.7	67.0
Casing (iron)	17,500	57.0	57.0

Table 5-1. Range of sonic velocity and transit time values. (Kokesh , Schwartz, Wall and Morris, 1965)

The ranges of values of sonic velocity and transit time for common rock matrix materials and casing are listed in table 5-1. The values listed are for non-porous substances. Porosity decreases the velocity of sound through the rock material and correspondingly increases the interval transit time.

5.1.2 Equipment

In Schlumberger, there are currently three sonic tools in use: the BHC borehole compensated sonic tool, the LSS long-spaced sonic tool, and the Array-Sonic tool. Although the entire sonic waveform can now be recorded with any of these tools only the Array-Sonic tool has been designed to provide full-waveform recording as a standard feature.

Nearly all BHC logs recorded in the past provide only a measurement of formation compressional interval transit time, accomplished through first motion detection at the receiver. In other words the receiver triggers on the first arrival of compressional energy.

As shown in figure 5-2 the BHC system uses one transmitter above and one below two pairs of sonic receivers. This sonde substantially reduces the spurious effects of hole-size changes and errors from sonde tilt. When one of the transmitters is pulsed the time elapsed between detection of the first arrival at the two corresponding receivers is measured.

The speed of sound in the sonic sonde and in the drilling mud is less than that in the formation. Accordingly the first arrivals of sound energy at the receivers correspond to sound-travel paths in the formation near the borehole wall.

The BHC tool transmitters are pulsed alternately and values are read on alternate pairs of receivers. The values from the two sets of receivers are averaged automatically by a computer at the surface for borehole compensation. The computer also integrates the transit time readings to obtain total travel time.

Sometimes the first arrival although strong enough to trigger the receiver nearer the transmitter may be too weak by the time it reaches the far receiver to trigger it. Instead the far receiver may be triggered by a different, later arrival on the sonic wave train and the travel time measured on this pulse cycle will then be too large. When this occurs, the sonic curve shows a very abrupt and large excursion towards a higher value; this is known as cycle skipping. Such skipping is more likely to occur

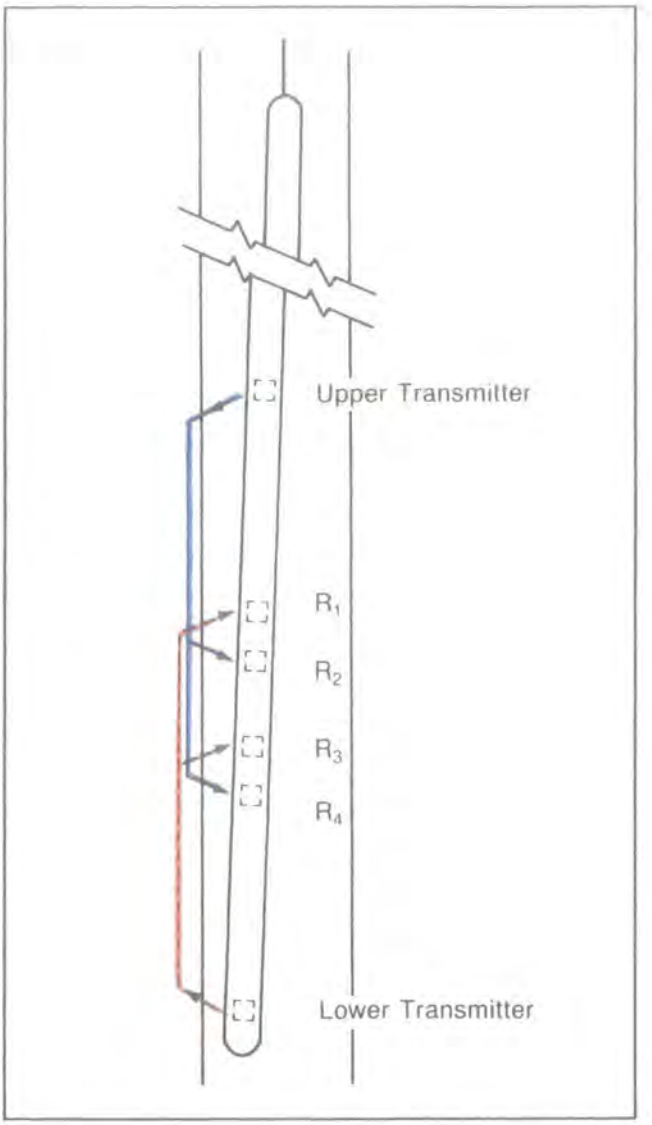

Figure 5-2. Schematic of BHC sonde, showing ray paths for the two transmitter-receiver sets. Averaging the two Δt measurements cancel errors from sonde tilt and hole-size changes. (Kokesh, Schwartz, Well, and Morris, 1965)

when the signal is strongly attenuated by unconsolidated formations, formation fractures, gas saturation, aerated muds, or "rugose" or enlarged borehole sections.

In early studies of velocity logging the rock surrounding the wellbore was regarded as an infinite homogeneous medium for the propagation of sound waves. It is now apparent that in some shales a lateral velocity gradient exists. Sound waves travel at lower speeds near the borehole; at some greater distance from the borehole they propagate at the true speed of sound in the shale. Similar variations may exist in the radial velocity profile in some unconsolidated cracks and in permafrost.

In large-diameter boreholes it is possible to have a mud wave arrival at the near receiver before the formation signal. This problem is particularly prevalent at shallower depths where sonic logs are often run for seismic purposes.

In all these cases a sonic tool with long spacing is required to provide a correct measurement of the velocity in the nonaltered zone. When the receivers are far enough from the transmitter the first arrival is not the refracted ray travelling just inside the borehole wall but a wave penetrating beyond the borehole into the faster nonaltered zone.

LSS sonic tools, with transmitter-receiver spacings of 8 feet and 10 feet or 10 feet and 12 feet, are available. They measure the interval transit time of the formation at a much greater depth into the formation that the usual BHC sonic tool. This tool is more likely to yield a measurement free from the effects of formation alteration, relaxation damage (from drilling process), and enlarged borehole. These more accurate measurements are always desirable when the sonic data are to be used to calibrate seismic results (see chapter 9). Figure 5-3 compares the transit time recorded with an LSS tool to that from a standard spacing tool in a formation with alteration.

Using the standard BHC system for borehole compensation with an LSS sonde would make the tool excessively long. An alternate solution called "depth-derived" borehole compensation is used.

The LSS sonde has two transmitters and two receivers arranged as shown in figure 5-3. Readings are taken at two different depth positions of the sonde: once when the two receivers straddle the measure point depth and once when the two transmitters straddle the measure point depth.

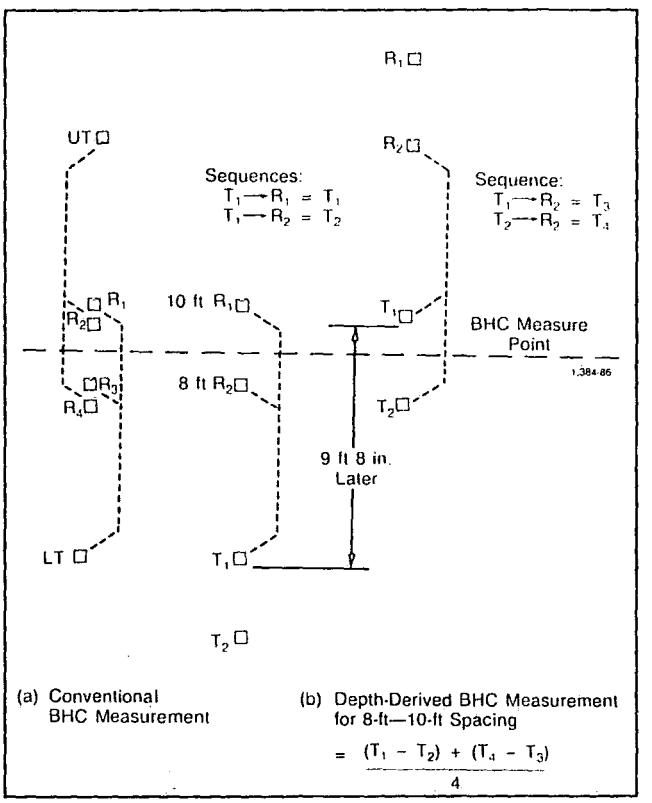

Figure 5-3. Depth-derived compensation for long-spaced sonic tool. (Kokesh, Schwartz, Wall, and Morris, 1965)

First reading $= T_1 \text{----}> R_1 - T_1 \text{----}> R_2$ (5-4)

Second reading $= T_1 \text{----}> R_2 - T_1 \text{----}> R_2$ (5-5)

The first reading is memorised until the sonde has reached the position to make the second reading, then both are averaged to obtain the borehole compensated measurement.

$$\tau = \frac{\text{memorised first } \tau \text{ reading} + \text{second } \tau \text{ reading}}{2 \times \text{Span}} \quad (5\text{-}6)$$

(Schlumberger, 1987)

where span is the distance (2ft) between a pair of receivers.

Assuming the two sonde position depths are accurate the depth-derived borehole compensated system is equivalent to the standard BHC system. Use of the upper transmitter and receiver yields an 8 feet - 10 feet sonic τ measurement and use of the lower transmitter and receiver yield a 10 feet - 12 feet τ sonic measurement.

The Array-Sonic service provides all measurements of the BHC and LSS logs and in addition provides several other features. The tool contains two broadband (5 to 18 kHz) piezoelectric transmitters spaced 2 feet apart. Two piezoelectric receivers are located 3 feet and 5 feet from the upper transmitter. These two receivers have a dual role. In open hole they are used in conjunction with the two transmitters to make standard short-spaced 3 feet - 5 feet and 5 feet - 7 feet depth derived borehole compensated logs. In cased wells they are used to make standard 3- foot Cement Bond logs (CBL) and 5- foot Variable Density logs (VDL).

The Array-Sonic tool (figure 5-4) also contains an array of eight wideband piezoelectric receivers. The receivers are spaced 6 inches apart with the closest receiver 8 ft from the upper transmitter. Two of these receivers, 1 and 5, spaced 2 feet apart can be used for making standard long spaced 8 feet - 10 feet and 10 feet- 12 feet depth-derived borehole compensated logs. Measurement hardware also exists, consisting of a closely spaced transmitter-receiver pair, to make a continuous mud log. Borehole fluid is drawn through this measurement section as the tool is moved during logging.

The eight-array receiver outputs and the two from the sonic sonde are

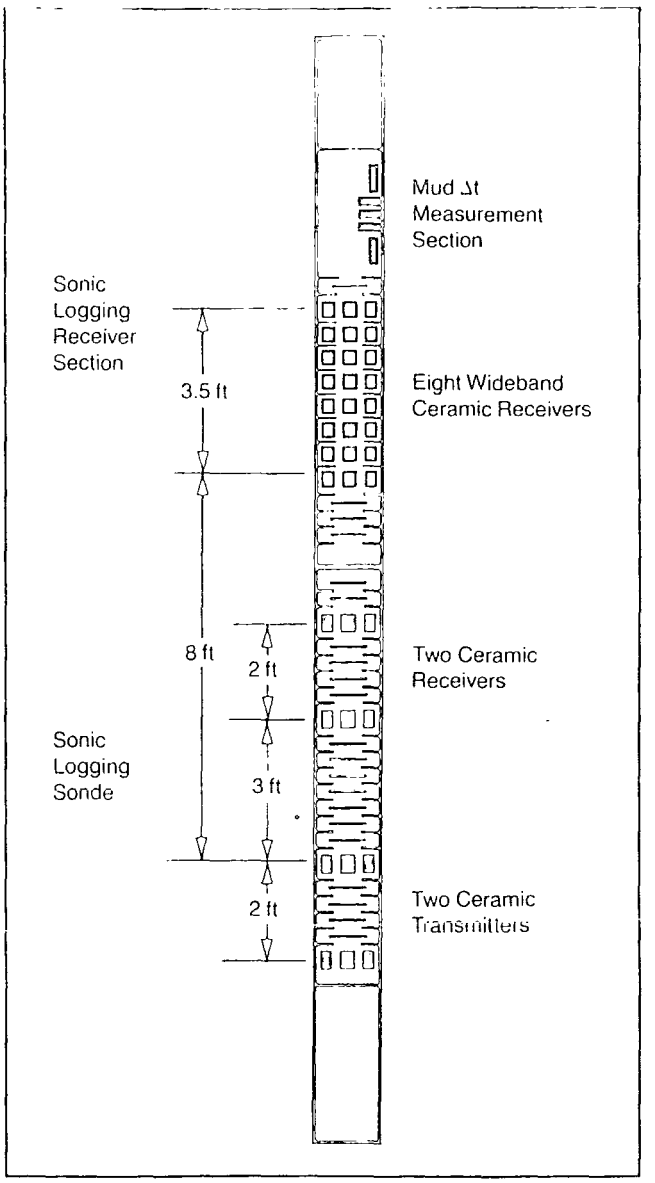

Figure 5-4 . Multipurpose sonic sonde configuration. (Schlumberger, 1987)

multiplexed with the mud receiver output and an example of a set of waveforms digitised from the eight-receiver array is shown in figure 5-1

The array waveforms are processed at the wellsite with the CSU surface instrumentation and array processor or at the computing centre using a true fullwaveform technique.

Rather than recording just the compressional wave component a waveform processing technique is used to find and analyse all propagating waves in the composite waveform. This slowness-time coherence technique (STC) uses a semblance algorithm similar to that employed in seismic processing to detect arrivals that are coherent across the array of receiver waveforms and to estimate their interval transit time.

Applying this semblance algorithm to the waveforms of figure 5-1 produces the coherence map shown in figure 5-5. Regions of large coherence correspond to the compressional, shear, and Stoneley arrivals. The apex of each region defines the slowness of that wave. This process is repeated for each set of array waveforms acquired by the tool while moving up the hole and is used to produce a log. A typical log determined in this fashion is shown in figure 5-6. Compressional transit time, τ_c, shear transit time, τ_s, and Stoneley transit time, τ_{st}, are presented. In a slow formation the tool obtains real-time measurements of compressional, Stoneley, and mud wave velocities. Shear wave values are then derived from these velocities.

Because of the number of receivers, the full wavetrain recording, and digital transmission, the Array-Sonic can provide a large amount of acoustic information. Among these data are:

a) 3 foot - 5 foot τ_c

b) 5 foot - 7 foot τ_c

c) 8 foot - 10 foot τ_c

d) 10 foot - 12 foot τ_c

e) τ_c (wavetrain derived compressional transit time).

f) τ_s (wavetrain derived shear transit time).

g) τ_{st} (wavetrain derived Stoneley transit time).

h) 6-inch τ_c (first motion compressional transit time).

i) Mud transit time.

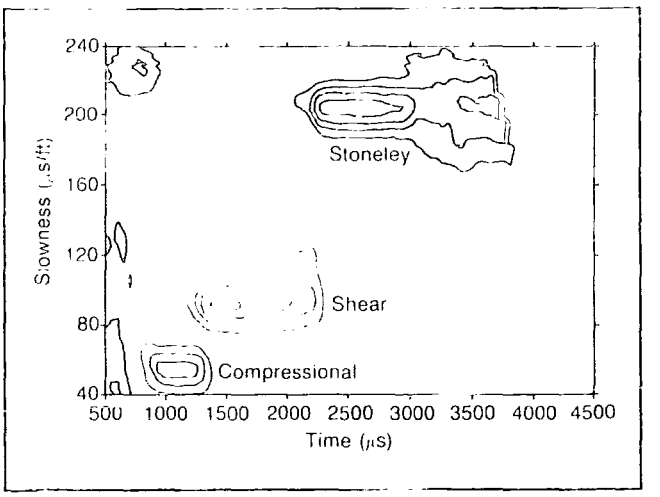

Figure 5-5. Contour plot of the STC coherence function. (Morris, Little, and Letton, 1984)

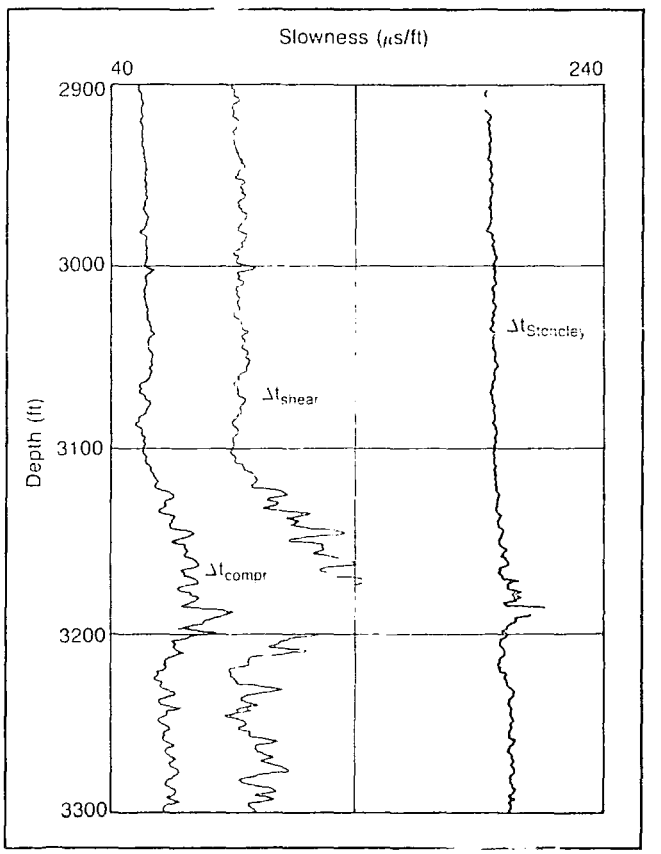

Figure 5-6. Log of classified component slownesses. (Morris, Little, and Letton, 1984)

j) Amplitude logging.

k) Energy analysis.

l) Frequency analysis.

m) τ_c , τ_s and τ_{st} through casing.

n) CBL-VDL data through casing.

The velocity of the sound wave from which the porosity is derived is determined from the first-motion compression transit time. The derived velocity of the sound wave from any of the transmitter-receiver spacing is the same if the borehole is good. However if the borehole is rugose then the velocity derived from the longer transmitter-receiver spacing is generally more accurate. The 6-inch τ_c is used in the case where a finer vertical resolution of sonic data is needed.

The mechanical properties of the rock can be derived from the wavetrain-derived compressional and shear transit times. The mechanical properties are useful when making a "sanding" analysis of the rock. A sanding analysis is most advantageous when a well is to be perforated because it enables the client to know how much drawdown pressure can applied to produce from the reservoir. If the differential drawdown pressure is too high the reservoir will collapse and sanding will occur. However if the drawdown pressure is too low the well is not being produced at its optimum pressure.

The wavetrain-derived Stoneley transit time enables the determination of the permeability and the extent of fracture of a reservoir. This can be of particular importance in carbonate reservoirs and in low porosity rocks. More detailed analysis of the wave amplitude, energy and frequency also enhance the above. For example when examining Stoneley waves the loss of energy can be correlated with permeability through fractures.

In cased hole applications, the Array-Sonic tool can be used to determine the cement bonding between the casing to the formation. Furthermore studying the wavetrains which can be recorded through casing can still give a reasonable determination of τ_c, τ_s and τ_{st}.

Company	Tool	Max. Temp. (°F)	Max. Pressure (kpsi)
Gearhart	BCS	350	18.5
Schlumberger	BHC	350	20
	LSS	350	20
	SDT	350	20
Western Atlas	AC	300	20
	ACL	300	20
	CAC	350	20

Table 5-2. Sonic Tools' Ratings.

Gearhart has the Borehole Compensated Sonic (BCS) tool and Western Atlas has the Acoustilog (AC) tool. Both work on the same principle as the Schlumberger BHC tool. Also Western Atlas has the Long-Spaced Acoustilog (ACL) tool which is similar to Schlumberger LSS tool. Since the primary interest is to find the sonic travel time through the formation it is noticeable that all the logging companies use similar principle of two pairs of transmitters and receivers to achieve a borehole compensated sonic travel time.

Furthermore Western Atlas has come up with the newer Circumferential Acoustilog (CAC) tool. However although it is an acoustic tool it has been designed to compliment their existing tool to detect and evaluate natural formation fracture systems using circumferentially propagated acoustic waves. Chapter 6 explains formation fracture systems, their identifications and applications using sonic tools and other available tools.

From the available data Schlumberger seems to have the edge with their newer Array-Sonic tool. This is because with one trip into the hole it is able to acquire a large amount of data for possible further analysis. The trend towards fracture detection calls more detailed analysis of the acoustic data and this is provided by means of recording the acoustic waveforms for further analysis. Furthermore the operator is now more interested in obtaining a better thin bed resolution (see chapter 13) with the data and presently it seems that

Schlumberger is the only company who can provide this sonic data by means of recording 6-inch first-motion compressional transit Time.

The importance of acoustic data is slowly being accepted and hence the operator will seek the service of newer tools such as the Schlumberger Array-Sonic tool and the Western Atlas Circumferential Acoustilog tool.

5.1.3 Porosity Determination from Sonic Data.

5.1.3.1 Measurements in Consolidated & Compacted Sandstones

After numerous laboratory determinations M.R.J. Wyllie proposed for clean and consolidated formations with uniformly distributed small pores a linear time-average of weighted-average relationship between porosity and transit time:

$$\tau_{LOG} = \phi\,\tau_f + (1-\phi)\,\tau_{ma} \qquad (5\text{-}7a)$$

or

$$\phi = \frac{\tau_{LOG} - \tau_{ma}}{\tau_f - \tau_{ma}} \qquad (5\text{-}7b)$$

(Wyllie, Gregory, and Gardner, 1956)

where

τ_{LOG} is the reading on the sonic log in μs/ft,

τ_{ma} is the transit time of the matrix material,

and

τ_f is the transit time of the saturating fluid (about 189 μs/ft for freshwater mud systems).

Generally consolidated and compacted sandstones have porosities from 15 to 25 %. In such formations the response of the sonic log seems to be relatively independent of the exact contents of the pores: water, oil, gas, or even disseminated shale. However in some higher porosity sandstones (30 % or greater) that have very low water saturation (high hydrocarbon saturation) and very shallow invasion the values may be somewhat greater than those in the same formation when water saturated.

If any shale laminae exists within the sandstone the apparent sonic porosity values are usually increased by an amount proportional to the bulk volume fraction of laminae. The readings are increased because τ_{sh} is generally greater than τ_{ma} of the

sandstone matrix.

5.1.3.2 Measurements in Carbonates

In carbonates having intergranular porosity the time average formula still applies but sometimes pore structure and pore size distribution are quite different from that of sandstones. There is often some secondary porosity consisting of vugs and/or fractures with much larger dimensions than the pores of the primary porosity.

In vuggy formation the velocity of sound seems to depend mostly on the primary intergranular porosity and the porosity derived from the sonic reading through the time-average formula (ϕ_{sv}) will tend to be too low by an amount approaching the secondary porosity. Thus if the total porosity (ϕ_t) of a formation exhibiting primary and secondary porosity (ϕ_2) is available (from a neutron and/or density log for example) the amount of secondary porosity can be estimated:

$$\phi_2 = \phi_t - \phi_{sv} \qquad (5\text{-}8)$$

(Wyllie, Gregory, and Gardner, 1958)

5.1.3.3 Measurements in Uncompacted Sands

Direct application of the time-average equation gives values of porosity that are too high in unconsolidated and insufficiently compacted sands. Uncompacted sands are most prevalent in the geologically younger formations particularly at shallow depths. However, even at deeper depths these younger sands are often uncompacted when the overburden-to-formation fluid pressure differentials are less than about 4000 to 5000 psi. Such lack of compression may be indicated when adjacent shales exhibit values greater than 100 μs/ft.

When the formations are not sufficiently compacted the observed values are greater than those that correspond to the porosity according to the time-average formula but the ϕ versus τ relationship is still approximately linear. In these cases an empirical correction factor, C_p , is applied to equation 5-7b to give a corrected porosity, $\phi_{sv\,cor}$:

$$\phi_{sv\ cor} = \frac{\tau - \tau_{ma}}{\tau_f - \tau_{ma}} \cdot \frac{1}{C_p} \qquad (5\text{-}9)$$

(Wyllie, Gregory, and Gardner, 1958)

The value of C_p can be determined in a number of ways: the R_o method, the density-sonic crossplot method, the neutron method and a method based on field observations.

The R_o method compares the sonic and induction or laterolog values in a clean water sand. The value of R_o found from the resistivity is divided by R_w to obtain F. Then ϕ is found from F and compared with ϕ_{sv} from equation 5-7b. The value of C_p is equal to ϕ_{sv}/ϕ.

From a plot of density (in ordinate) and sonic transit time (in abscissae), the clean sand line is the line drawn from the matrix point through the points lying towards the upper left portion. For any given porosity value on this clean sand line there will be a value of τ. If a sand is known to be clean and liquid filled then $C_p = \phi_{sv}/\phi_d$.

The previous two methods require clean sand. The neutron method compares ϕ_n and ϕ_{sv}. The difference between ϕ_n and ϕ_{sv} in water-filled sands are due to lack of compaction. For such sands, $C_p = \phi_{sv}/\phi_n$.

From field observations the empirical transform can be approximated over the range of normally encountered porosities by the following equation:

$$\phi_{sv} = \frac{C\,(\phi_{LOG} - \phi_{ma})}{\phi_{LOG}} \qquad (5\text{-}10)$$

(Wyllie, Gregory, and Gardner, 1958)

The value of the constant C has a range of 0.625 to 0.7. 0.67 is more appropriate. For the case of a gas-saturated reservoir rock C becomes 0.6. It should be used when the rock investigated by the sonic tool contains an appreciable amount of hydrocarbon in the gassy (vapour) phase. Because of the very shallow depth of investigation the condition normally exists only in higher porosity sandstones (greater than 30 %).

5.1.4 Shear-Wave Interpretation

All the preceeding discussion has concerned compressional transit time interpretation. With the newer Array-Sonic tool and full waveform recording it is now possible to obtain shear-wave transit time measurements on a more routine basis.

Application of the shear wave information evaluation is now beginning to be explored. The shear-wave velocity data will be useful in calculating rock elastic or inelastic properties and as an adjunct to shear seismic data.

5.2 Density Logs

Density logs are primarily used as porosity logs. Other uses include identification of minerals in evaporite deposit, detection of gas, determination of hydrocarbon density, evaluation of shaly sands and complex lithologies, determinations of oil-shale yield, calculation of overburden pressure and rock mechanical properties.

5.2.1 Principle

A radioactive source, applied to the borehole wall in a shielded sidewall skid emits medium-energy gamma rays into the formations. These gamma rays may be thought of as high velocity particles that collide with the electrons in the formation at each collision and then continues with diminished energy. This type of interaction is known as Compton Scattering. The scattered gamma rays reaching the detector at a fixed distance from the source are counted as an indication of formation density.

The number of Compton Scattering collisions is related directly to the number of electrons in the formation. Consequently, the response of the density tool is determined essentially by the electrons per cubic centimetre of the formation. Electron density is related to the true bulk density, ρ_b , which in turn depends on the density of the rock matrix material, the formation porosity, and the identity of the fluids filling the pores(see equations 5-11a and 5-11b).

5.2.2 Equipment

Generally the density tool composes of a skid mounted source and a detector. To minimise the influence of the mud column the Schlumberger skid mounted source and detector are shielded. The openings of the shield are applied against the wall of the borehole by an eccentering arm. The force exerted by the arm and the plough-shaped design of the skid allow it to cut through soft mudcakes. Any mudcake or mud remaining between the tool and the formation is "seen" as part of the formation and must be accounted for.

A correction is needed when the contact between the skid and the formation is not perfect (mudcake or irregularities in the borehole wall). In unfavourable cases the correction can be fairly large. If only one detector is used the correction is not easy to determine because it depends on the thickness, the weight, and even the composition of the mudcake or mud interposed between the skid and the formations.

In Schlumberger, during the earlier stage there was the FDC compensated formation density tool. It uses two detectors of differing spacing and depth of investigation as shown on figure 5-7. The chart of figure 5-8 is a plot of long-spacing versus short-spacing count rates. Points for a given value of ρ_b and various mudcake conditions fall on or very close to an average curve. Using these average curves it is possible to enter the chart with the two count rates and determine the corrected ρ_b from the plot without any explicit measurement of the mudcake density or thickness. This measurement technique is referred to as ''spine and ribs''.

The correction is made automatically and the corrected ρ_b curve and $\Delta\rho$ (the correction made) are recorded directly on the log. The distance between the face of the skid and the extremity of the eccentering arm is recorded as a caliper log which helps to assess the quality of contact between the skid and the formation.

Nowadays the LDT Litho-Density tool which is an improved and expanded version of the FDC tool is more commonly used. In addition to the bulk density measurement the tool also measures the photoelectric absorption index of the formation, Pe. Photoelectric absorption can be related to lithology; whereas the ρ_b measurement responds primarily to porosity and secondarily to rock matrix and pore fluid, the Pe measurement responds primarily to rock matrix (lithology) and secondarily to porosity and pore fluid.

In the LDT tool, gamma rays, emitted by the source at an energy of 662 keV are scattered by the formation and lose energy until absorbed through photoelectric effect. At a finite distance from the source such as the far detector the energy spectrum might look as illustrated in figure 5-9. The number of gamma rays in the higher energy region (region of Compton Scattering) is inversely related only to the electron density of the formation (i.e., an increase in the formation density increases the number of gamma rays). The number of gamma rays in the lower energy region (region of photoelectric effect) is inversely related to both the electron density and the phoelectric

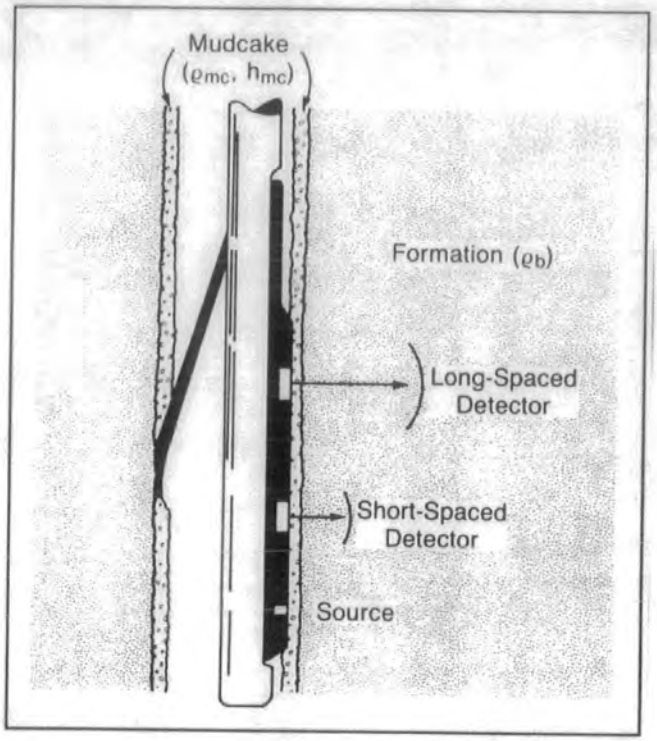

Figure 5-7. Schematic drawing of the dual spacing Litho-Density Logging Device (LDL). (Wahl, Tittmann, and Johnstone, 1964)

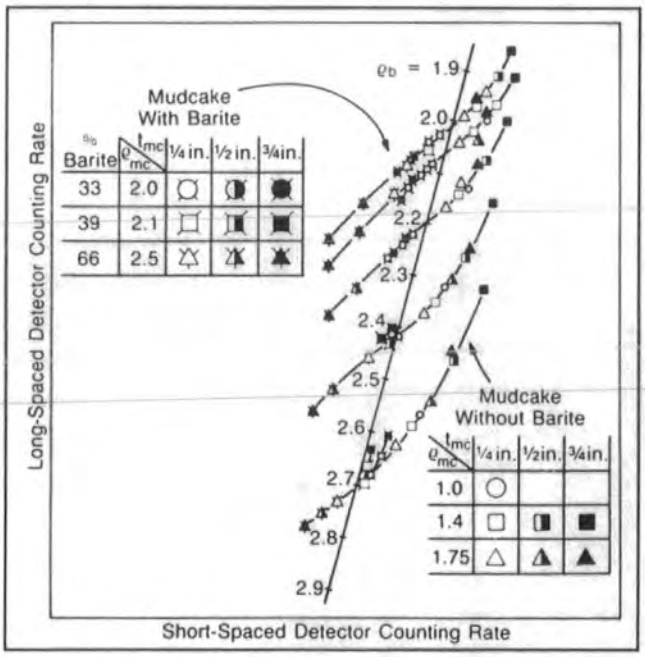

Figure 5-8. "Spine-and-ribs" plot , showing response of LDL counting rates to mudcake. (Wahl, Tittmann, and Johnstone, 1964)

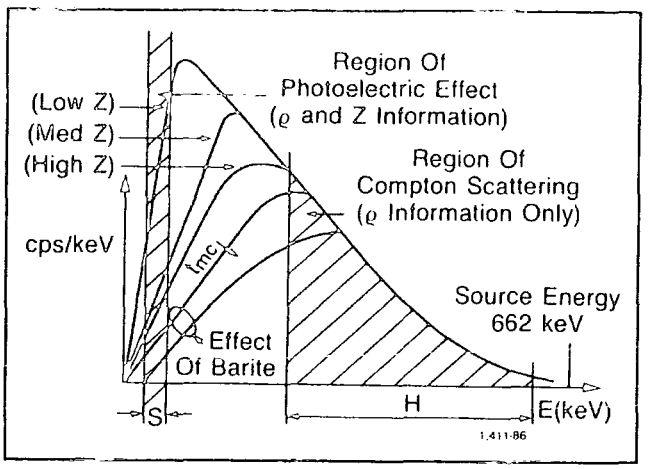

Figure 5-9. Variation in spectrum for formation with constant density but different Z. (Tittmann and Wahl, 1965)

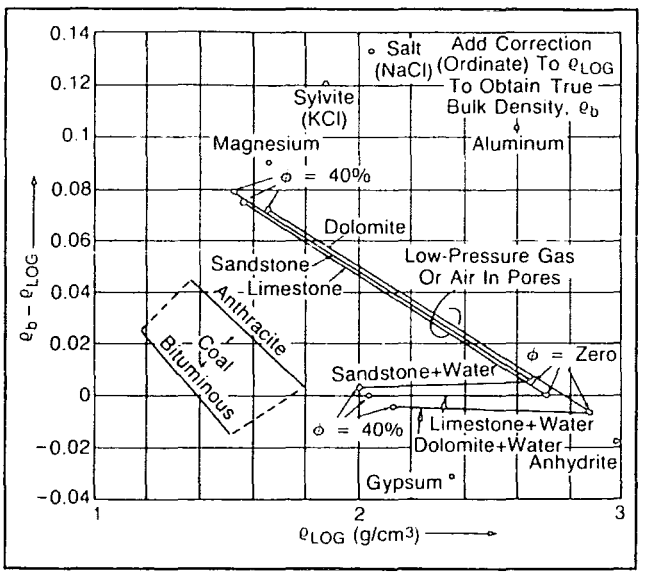

Figure 5-10. Correction meeded to get true bulk density from log density. (Kokesh, Schwartz, Wall, and Morris, 1965)

absorption. By comparing the counts in these two regions the photoelectric absorption index can be determined.

The gamma ray spectrum at the near detector is used only to correct the density measurement from the far detector for the effects of mudcake and borehole rugosity.

The primary calibration standard for the FDC tool are laboratory freshwater-filled limestone formations of high purity and known densities. The secondary (shop calibration) standards are large aluminium and sulphur blocks into which the sonde is inserted. These blocks are of carefully designed geometry and composition and their characteristics have been related to the limestone formations. With the blocks two different thicknesses of artificial mudcakes are used to check the automatic mudcake correction. Finally, at the wellsite a radioactive test jig is used to produce a signal of known intensity to verify the detection system.

As mentioned earlier, the density log responds to the electron density of the formations. For a substance consisting of a single element, the electron density index, Pe, is related to the bulk density, ρ_b :

$$Pe = \rho_b \frac{2Z}{A} \quad , \qquad (5\text{-}11a)$$

(Tittman and Wahl, 1965)

where

ρ_b is the actual bulk density,

Z is the atomic number (number of electrons per atom),

and

A is the atomic weight (ρ_b/A is proportional to the number of atoms per cubic centimetre of the substance).

For a molecular substance, the electron density index is related to the bulk density :

$$Pe = \rho_b 2 \frac{\Sigma Z}{\text{Mol.Wt.}} \qquad (5\text{-}11b)$$

(Tittman and Wahl, 1965)

where

ΣZ's is the sum of the atomic numbers of atoms making up the molecule (equal to number of electrons per molecule) and Mol. Wt. is the molecular weight.

For most formation substances, the bracketed quantities in equations 5-11a and 5-11b are very close to unity (column 4 of tables 5-3 and 5-4). When the density tool is calibrated in freshwater-filled limestone formations the apparent bulk density, ρ_a, as read by the tool is related to the electron density index, Pe, by:

$$\rho_a = 1.0704\ Pe - 0.1883 \quad (5\text{-}12)$$

(Alger, Raymer, Hoyle, and Tixier, 1963)

For liquid-filled sandstones, limestones, and dolomites the tool reading, ρ_a, is practically identical to actual bulk density, ρ_b. For a few substances such as sylvite, rock salt, gypsum, anhydrite, coal, and gas-bearing formations, the corrections shown in figure 5-10 are needed to obtain bulk density values from the density log readings.

Similarly to Schlumberger, Western Atlas has the Compensated Densilog tool and Gearhart has the Compensated Density (CDL) tool. Using the same principle of evaluating the electron density of the formation to obtain the density of the formation all the companies use the method of two detectors to compensate for borehole corrections.

Recently Western Atlas has developed the Compensated Z-Densilog tool in response to the Schlumberger's Litho-Density tool. From the data available both tools use scintillation detectors for increased count rates for measuring gamma ray energy spectra to determine Pe and density. It is noticeable that both tools have been designed to provide a more comprehensive evaluation in complex lithologies.

Element	A	Z	$2\frac{Z}{A}$
H	1.008	1	1.9841
C	12.011	6	0.9991
O	16.000	8	1.0000
Na	22.990	11	0.9569
Mg	24.320	12	0.9868
Al	26.980	13	0.9637
Si	28.090	14	0.9968
S	32.070	16	0.9978
Cl	35.460	17	0.9588
K	39.100	19	0.9719
Ca	40.080	20	0.9980

Table 5-3 . Common atomic numbers and weights. (Edmundson and Raymer, 1979)

Compound	Formula	Actual Density ϱ_b	$\frac{2\Sigma Z's}{\text{Mol. Wt.}}$	ϱ_e	ϱ_a (as seen by tool)
Quartz	SiO_2	2.654	0.9985	2.650	2.648
Calcite	$CaCO_3$	2.710	0.9991	2.708	2.710
Dolomite	$CaCO_3MgCO_3$	2.870	0.9977	2.863	2.876
Anhydrite	$CaSO_4$	2.960	0.9990	2.957	2.977
Sylvite	KCl	1.984	0.9657	1.916	1.863
Halite	NaCl	2.165	0.9581	2.074	2.032
Gypsum	$CaSO_42H_2O$	2.320	1.0222	2.372	2.351
Anthracite Coal		{1.400 / 1.800}	1.0300	{1.442 / 1.852}	{1.355 / 1.796}
Bituminous Coal		{1.200 / 1.500}	1.0600	{1.272 / 1.590}	{1.173 / 1.514}
Fresh Water	H_2O	1.000	1.1101	1.110	1.000
Salt Water	200,000 ppm	1.146	1.0797	1.237	1.135
Oil	$n(CH_2)$	0.850	1.1407	0.970	0.850
Methane	CH_4	ϱ_{meth}	1.2470	1.247 ϱ_{meth}	1.335 ϱ_{meth}—0.188
Gas	$C_{1.1}H_{4.2}$	ϱ_g	1.238	1.238 ϱ_g	1.325 ϱ_g—0.188

Table 5-4. Common Density values. (Edmundson and Raymer , 1979)

Company	Tool	Max. Temp. (°F)	Max.Pressure (kpsi)
Gearhart	CDL	350	20
Schlumberger	FDC	350	20
	LDL	350	20
Western Atlas	CDL	300	20
	CZD	350	20

Table 5-5 Density Tools' Ratings

5.2.3 Porosity Determination from Density Log

For a clean formation of known matrix density, ρ_{ma}, having a porosity, ϕ that contains a fluid of average density, ρ_f, the formation bulk density, ρ_b, will be :

$$\rho_b = \phi \rho_f + (1-\phi) \rho_{ma} \qquad (5\text{-}13)$$

(Alger, Raymer, Hoyle, and Tixier, 1963)

For usual pore fluids (except gas and light hydrocarbons) and for common reservoir matrix minerals the difference between the apparent density, ρ_a, read by the density log, and the bulk density, ρ_b, is so trivial that it is disregarded. Solving for ϕ,

$$\phi = \frac{\rho_{ma} - \rho_b}{\rho_{ma} - \rho_f} \qquad (5.14)$$

(Alger, Raymer, Hoyle, and Tixier, 1963)

where $\rho_b = \rho_a$ (with exceptions noted).

Common values of ρ_{ma} are given in table 5-4

5.2.4 Photoelectric Absorption

In nuclear experiments cross section is defined as a measure of the probability that a nuclear reaction will take place, under specified conditions, between two

particles or a particle and another target. It is usually expressed in terms of the effective area a single target presents to the incoming particle. Table 5-6 lists the photoelectric absorption cross section, given in barns per atom, for several elements at the incident gamma ray energy level. The atomic number, Z, for each of these elements is also listed. The photoelectric cross section index, Pe, in barns per electron is related to Z by :

$$Pe = \frac{Z^{3.6}}{10} \qquad (5\text{-}15)$$

(Gardner and Dumanoir, 1980)

For a molecule made up of several atoms a photoelectric absorption cross section index, Pe, may be determined based upon atomic fractions. Thus,

$$Pe = \Sigma \frac{A_i Z_i P_i}{A_i Z_i} \qquad (5\text{-}16)$$

(Gardner and Dumanoir, 1980)

where A_i is the number of each atom in the molecule.

Table 5-7 gives the Pe value for several reservoir rocks, minerals, and fluid commonly encountered in the oil field. From this list it is not readily apparent that the cross section is relatively independent of porosity and the satuarating fluid. To verify this relative independence, the photoelectric absorption cross section index is expressed in volumetric terms rather than in electron terms.

By definition :

$$U = Pe\ \rho_e \qquad (5\text{-}17)$$

(Gardner and Dumanoir, 1980)

Since Pe has the units of barns per electron and ρ_e the units of electrons per cubic centimetre, U has the units of barns per cubic centimetre. This parameter permits the cross section of the various volumetric components of a formation to be added in a simple weighted average manner. Thus,

$$U = \phi\ U_f + (1-\phi)\ U_{ma} \qquad (5\text{-}18)$$

(Bardner and Dumanoir, 1980)

Element	Photoelectric Cross Section	Atomic Number Z_e
Hydrogen	0.00025	1
Carbon	0.15898	6
Oxygen	0.44784	8
Sodium	1.4093	11
Magnesium	1.9277	12
Aluminum	2.5715	13
Silicon	3.3579	14
Sulfur	5.4304	16
Chlorine	6.7549	17
Potassium	10.0810	19
Calcium	12.1260	20
Titanium	17.0890	22
Iron	31.1860	26
Copper	46.2000	29
Strontium	122.2400	38
Zirconium	147.0300	40
Barium	493.7200	56

Table 5-6. Common photoelectric cross-section. (Gardner and Dumanoir, 1980)

Name	Formula	Molecular Weight	P_e	ϱ_b	ϱ_a	U
Minerals						
Anhydrite	$CaSO_3$	136.146	5.055	2.960	2.957	14.95
Barite	$BaSO_4$	233.366	266.800	4.500	4.011	1070.00
Calcite	$CaCO_3$	100.090	5.084	2.710	2.708	13.77
Carnallite	$KCl\text{-}MgCl_2\text{-}6H_2O$	277.880	4.089	1.610	1.645	6.73
Celestite	$SrSO_4$	183.696	55.130	3.960	3.708	204.00
Corundum	Al_2O_3	101.900	1.552	3.970	3.894	6.04
Dolomite	$CaCO_3Mg CO_3$	184.420	3.142	2.870	2.864	9.00
Gypsum	$CaSO_4\text{-}2H_2O$	172.180	3.420	2.320	2.372	8.11
Halite	NaCl	58.450	4.650	2.165	2.074	9.65
Hematite	Fe_2O_3	159.700	21.480	5.210	4.987	107.00
Ilmenite	$FeO\text{-}TiO_2$	151.750	16.630	4.700	4.460	74.20
Magnesite	$MgCO_3$	84.330	0.829	3.037	3.025	2.51
Magnetite	Fe_3O_4	231.550	22.080	5.180	4.922	109.00
Marcasite	FeS_2	119.980	16.970	4.870	4.708	79.90
Pyrite	FeS_2	119.980	16.970	5.000	4.834	82.00
Quartz	SiO_2	60.090	1.806	2.654	2.650	4.79
Rutile	TiO_2	79.900	10.080	4.260	4.052	40.80
Sylvite	KCl	74.557	8.510	1.984	1.916	16.30
Zircon	$ZrSiO_4$	183.310	69.100	4.560	4.279	296.00
Liquids						
Water	H_2O	18.016	0.358	1.000	1.110	0.40
Salt Water	(120,000 ppm)		0.807	1.086	1.185	0.96
Oil	$CH_{1.6}$		0.119	0.850	0.948	0.11
	CH_2		0.125	0.850	0.970	0.12
Miscellaneous						
Clean Sandstone			1.745	2.308	2.330	4.07
Dirty Sandstone			2.700	2.394	2.414	6.52
Average Shale			3.420	2.650	2.645	9.05
Anthracite Coal	C:H:O - 93:3:4		0.161	1.700	1.749	0.28
Bituminous Coal	C:H:O - 82:5:13		0.180	1.400	1.468	0.26

Table 5-7. Common reservoir rocks and some of their relative parameters. (Edmundson and Raymer, 1979)

where U, U_f, and U_{ma} are the photoelectric absorption cross sections of the mixture, pore fluid, and matrix respectively; all are expressed in barns per cubic centimetre.

5.2.5 Tool Response

The Litho-Density tool skid and detector system have been designed so that greater counting rates are obtained than with the FDC tool and result in lower statistical variations and better repeatability of the measurements. The geometry of the skid has also been altered so that the density reading has a greater vertical resolution than that of the FDC measurement. The Pe measurement exhibits even better vertical resolution. This has applications in identifying fractures and laminar formations. The above is also applicable to the Compensated Z-Densilog tool developed by Western Atlas.

All logging companies have tools to provide information on the bulk density of the formation. They are all using the same basic principle to obtain the density data. Both Schlumberger and Western Atlas are able to provide data for lithology determination by using the photoelectric absorption index. Gearhart presently is unable to offer this additional service.

Both the Schlumberger Litho-Density tool and the Western Atlas Compensated Z-Densilog tool work with higher measured count rates and hence the count variation due to statistics are decreased. This leads to both better accuracy and better data repeatability. Both tools claim to have an accuracy of +/- 0.01 g/cm^3 for bulk density and +/- 0.20 barns/electron for photoelectric index. These are vast improvement on earlier generation of tools whose accuracy was in the order of +/- 0.05 g/cm^3 for bulk density and no measurement of photoelectric index was possible. Being dependent on count statistics, the tool performance will be heavily influenced by the hole condition of the wellbore during the time of measurement.

Given the choice an operator will tend to choose either the Schlumberger Litho-Density tool or the Compensated Z-Densilog tool because they have better accuracy and are able to offer more information on the wellbore.

5.3 Neutron Logs

Neutron logs are used principally for delineation of porous formations and determination of their porosity. They respond primarily to the amount of hydrogen in the formation. Thus, in clean formations where pores are filled with water or oil the neutron log reflects the amount of liquid-filled porosity.

Gas zones can often be identified by comparing the neutron log with another porosity log or a core analysis. A combination of the neutron log with one or more other porosity logs yields more accurate porosity values and lithology identification.

5.3.1 Principle

Neutrons are electrically neutral particles each having a mass almost identical to the mass of a hydrogen atom. High-energy (fast) neutrons are continuously emitted from a radioactive source in the sonde. These neutrons collide with nuclei of the formation materials in what may be thought of as elastic "billard-ball" collisions. With each collision the neutron loses some of its energy.

The amount of energy lost per collision depends on the relative mass of the nucleus with which the neutron collides. The greater energy loss occurs when the neutron strikes a nucleus of practically equal mass i.e., a hydrogen nucleus. Collisions with heavy nuclei do not slow the neutron very much. Thus the slowing of neutrons depends largely on the amount of hydrogen in the formation.

Within a few seconds the neutrons have been slowed by successive collisions to thermal velocities corresponding to energies of around 0.025 eV. They then diffuse randomly without losing more energy until they are captured by the nuclei of atoms such as chlorine, hydrogen, or silicon.

The capturing nucleus becomes intensely excited and emits a high energy gamma ray of capture. Depending on the type of neutron tool either these capture gamma rays or the neutrons themselves are counted by a detector in the sonde.

When the hydrogen concentration of the material surrounding the neutron source is large, most of the neutrons are slowed and captured within a short distance of the source. On the contrary, if the hydrogen concentration is small, the neutrons travel farther from the source before being captured. Accordingly, the counting rate at the detector increases for decreased hydrogen concentration, and vice versa.

5.3.2 Equipment

The most common neutron porosity tool used in Schlumberger is the compensated neutron CNT tool. With the advance in technology this CNT has been improved to give a dual porosity log. Both current tools use the americium-beryllium (Am-Be) sources to provide neutrons with initial energies of several million electron volts.

The CNT is a mandrel-type tool especially designed for combination with any of several other tools to provide a simultaneous neutron log. The earlier CNT is a dual-spacing, thermal neutron-detection instrument. The ratio of counting rates from the two detectors is processed by the surface equipment to produce a linearly scaled recording of neutron porosity index. A 16-curie source and longer source-to-detector spacings give the CNT a greater depth of investigation than the older generation of porosity tools such as the SNP sidewall neutron porosity tool. The effect of borehole parameters is greatly reduced by taking the ratio of two counts each of which is similarly affected by these parameters. The CNT can be run in liquid-filled holes, either cased or uncased, but cannot be used in gas-filled holes.

Since thermal neutrons are measured in the CNL tool the response is affected by elements having a high thermal neutron capture cross section. The tool is sensitive to shale in the formation since shale usually contain small amounts of boron and other rare earth elements having a particularly high thermal neutron capture cross section. If excessive this effect can mask the tool response to gas in shaly formations.

To improve the response to gas and to enhance interpretation in the presence of thermal neutron absorbers the Dual Porosity tool incorporates two epithermal neutron detectors in addition to the two thermal neutron detectors (figure 5-11). Two separate porosity measurements are obtained, one from each pair of detectors. In clean formations the measured porosities generally agree. In shaly formations containing a large number of thermal neutron absorbers the porosity measured by the epithermal

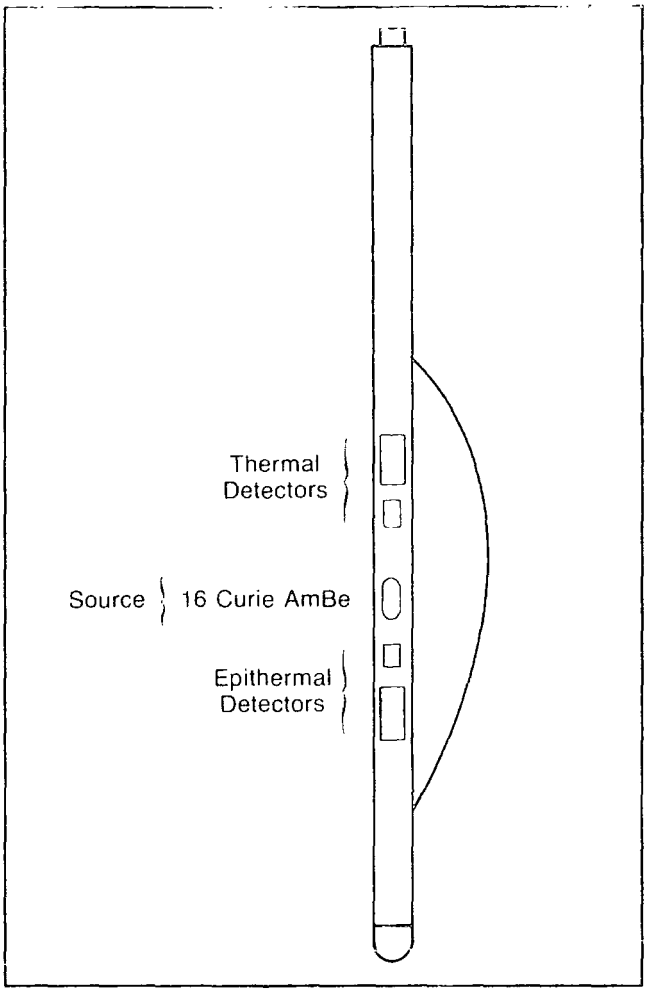

Figure 5-11. CNT-G tool configuration. (Scott, Flaum and Sherman, 1982)

detectors reads lower and agrees more closely with density-derived porosity. A comparison of the two porosity measurements indicates the shale or clay content or the formation fluid salinity.

At a given source-detector spacing epithermal neutron count rate is approximately an order of magnitude less than that for thermal neutrons. Therefore, to have reasonable epithermal neutron count rates the epithermal detectors have been placed nearer to the neutron source than the thermal neutron detectors. The thermal neutron-detector configuration duplicated that of the standard CNL tool.

Since the two pairs of detectors are placed at different spacings and neutrons are detected at different energy levels the environmental effects can be expected to be significantly different on the two neutron measurements.

If the ratio processing used on the thermal neutron measurement is used for the epithermal measurement the computed porosity is quite sensitive to borehole effects. As a result of a detailed study of detector response to many environmental variables an epithermal neutron processing technique has been developed that uses individual detector count rates. The method, which is analogous to the spine-and-ribs analysis developed for the density tools, greatly reduces borehole effects on the epithermal neutron porosity measurement. The epithermal count rates can also be used to determine neutron porosity in air-filled boreholes.

The combined epithermal and thermal neutron Dual Porosity measurements provide improved porosity determination. Since the epithermal measurements are relatively free of neutron absorber effects it yields improved gas detection in shaly reservoirs (figure 5-12). A comparison of the two neutron responses also provides information on the presence of materials with significant thermal neutron capture cross section.

5.3.2.1 Calibration

The primary calibration standard for CNL tools is a series of water-filled laboratory formations. The porosities of these controlled formations are known within +/- 0.5 porosity units. The secondary (shop) standard is a water-filled calibrating tank. A wellsite check is made by using a fixture that produces the count rate ratio obtained in the tank.

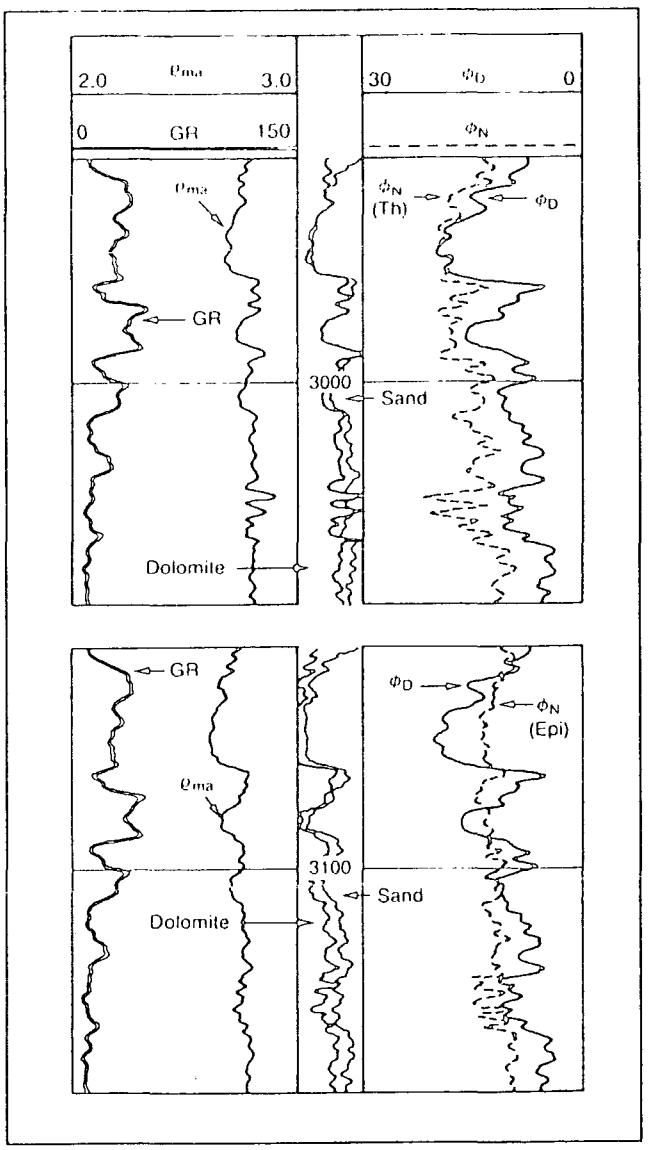

Figure 5-12. Thermal / epithermal neutron log comparison in a gas zone. (Scott, Flaum and Sherman, 1982)

5.3.2.2 Investigation Characteristics

The typical vertical resolution of the CNL tool is 2 feet. However, a new method of processing the count rates of the CNL tool is now available that increases the vertical resolution to 1 foot by exploiting the better vertical resolution of the near detector (see chapter 13).

The radial investigation depends on the porosity of the formation. Very roughly at zero porosity the depth of investigation is about 1 foot. At higher porosity in liquid-filled holes the depth of investigation is less because neutrons are slowed and captured closer to the borehole. For average conditions the depth of investigation for CNL tool is about 10 inches in a high-porosity rock. The CNL tool samples a somewhat larger volume of formation than the density tool.

5.3.3 Equipment (Others)

Company	Tool	Max.Temp. (°F)	Max.Pressure (kpsi)
Gearhart	CNL	350	20
Gearhart	SNL	350	20
Schlumberger	CNL(H)	400	20
Schlumberger	CNL(G)	400	20
Western Atlas	CN	400	20
Western Atlas	SWN	400	20

Table 5-8. Neutron Tools' Ratings

Similar both in principle and design to the Schlumberger Compensated Neutron tool, Gearhart has the Compensated Neutron CNS tool and Western Atlas has the Compensated Neutron CN tool. Both Tools provide the same information on the porosity of the formation.

Furthermore Gearhart also has the Sidewall Neutron SNL tool and Western Atlas has the Sidewall Epithermal Neutrol SWN tool which work at the epithermal level to provide additional information on the porosity data. Both tools are similar to the Schlumberger Dual Porosity tool.

All the logging companies claim to be able to measure to a resolution of 1 porosity unit (1%). However the accuracy of the tools are not quoted because the tool measurement is heavily dependent on the hole condition of the wellbore. Generally an operator uses the repeatability of the data and the tool calibration tolerance to control the accuracy of the measurement obtained.

Generally if a typical re servoir porosity is 22 porosity units and if the measurement drifts by 1 porosity unit there is a change of 4-5% in the recorded data. The neutron tool being dependent on count rates provides data which should be used with the knowledge that there are errors involved. The operator will need to watch for repeatability of the data obtained and to crosscheck the data to the porosity obtained from other logs. In practice the porosity data obtained from the neutron tool is used with the porosity data obtained from the density tool to determine the porosity used for interpretation, and the porosity data obtained from the sonic tool is used to compliment the result where necessary, such as in the case of rugose hole.

6. DETERMINATION OF PHYSICAL GEOLOGICAL STRUCTURE

6.1 Introduction

As technology advances it is likely that dipmeter data will be a valuable supplement and used more and more to evaluate the entire reservoir. The structural-dip angle from dipmeter logs is a valuable additional piece of information for well-to-well correlation since it can be used to predict expected changes in elevations of strata from one well to the next (figure 6.1). This facilitates identification of corresponding beds and helps in the analysis of structural and stratigraphic anomalies such as faults and unconformities.

Dipmeter results are usually presented in "arrow" plots ("tadpole" plots, as they are sometimes called) as illustrated in figure 6-2,-3 and -4. The stem on each plotting symbol indicates the direction of the dip. The displacement of the symbol from the left edge of the plot represents magnitude of dip angle. Vertically, the symbols are plotted versus depth.

It is common practice to identify various characteristic patterns on the plots by colouring them. In the jargon of the dipmeter interpreter the various patterns are called by the colour names. Figure 6-2 illustrates the red, blue, and green patterns.

In a red pattern successive dips increase progressively with depth and keep about the same azimuth. As indicated in the figure red patterns may be associated with faults, channels, bars, reefs, or unconformities. Figure 6-3 illustrates red patterns seen over a bar or reef, or in a channel or trough.

In a blue pattern successive dips with about the same azimuth decrease progressively with depth. Blue patterns may be associated with faults, current bedding, or unconformities. Figure 6-4 illustrates schematically how crossbedding might show up as a blue pattern on a short-interval dipmeter arrow plot. The foreset current bedding shows larger dips at the top of each bed decreasing in a rather regular pattern toward the bottom of the bed.

A green pattern shown on figure 6-2, corresponds to structural dip. It is consistent in azimuth and dip magnitude and is more prominent if structural dip is large.

To explore for a stratigraphic trap it is necessary to know its type, internal

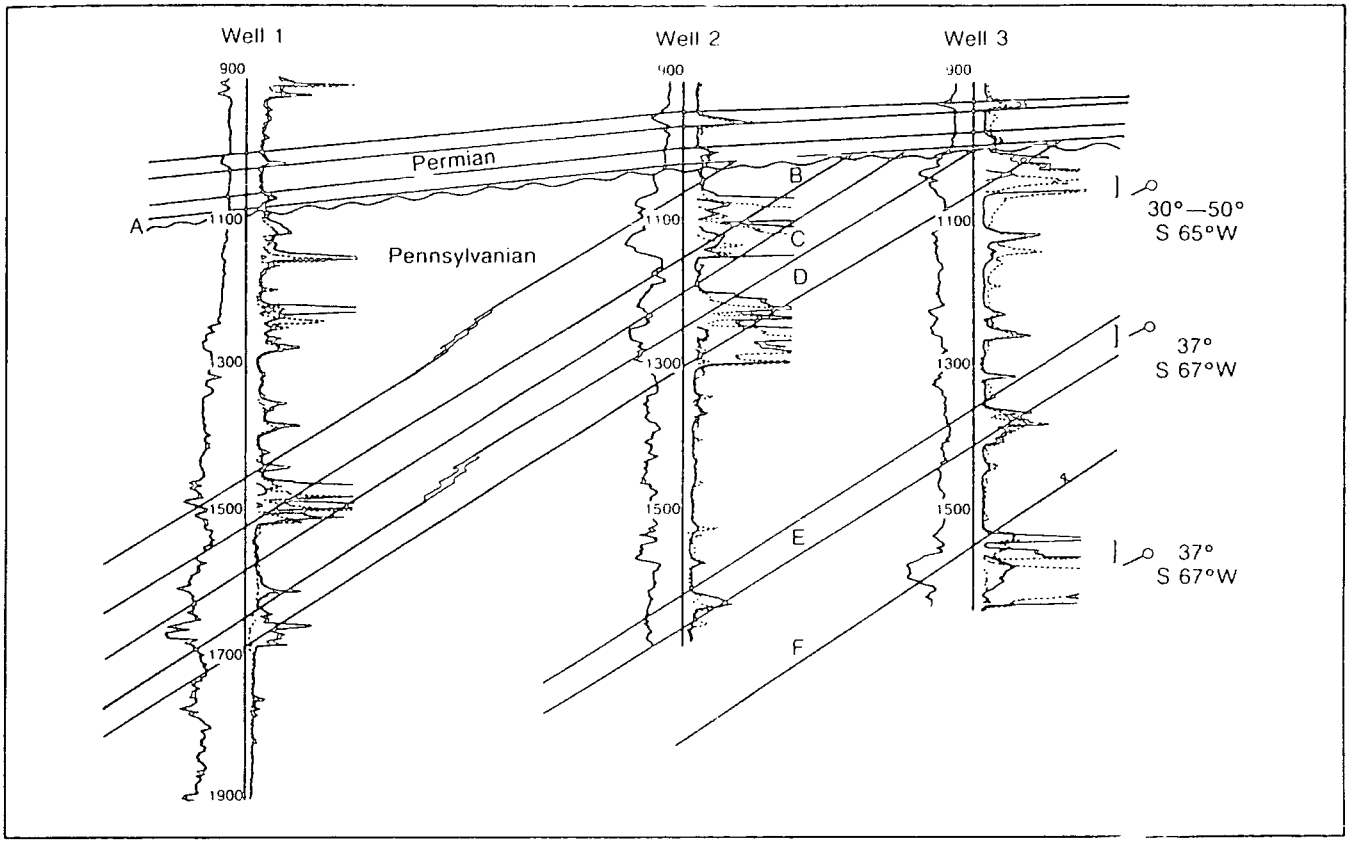

Figure 6-1. Cross section in which correlation was not readily apparent from electric logs alone. Correlation was resolved by the dipmeter run on Well 3. (Schlumberger, 1986)

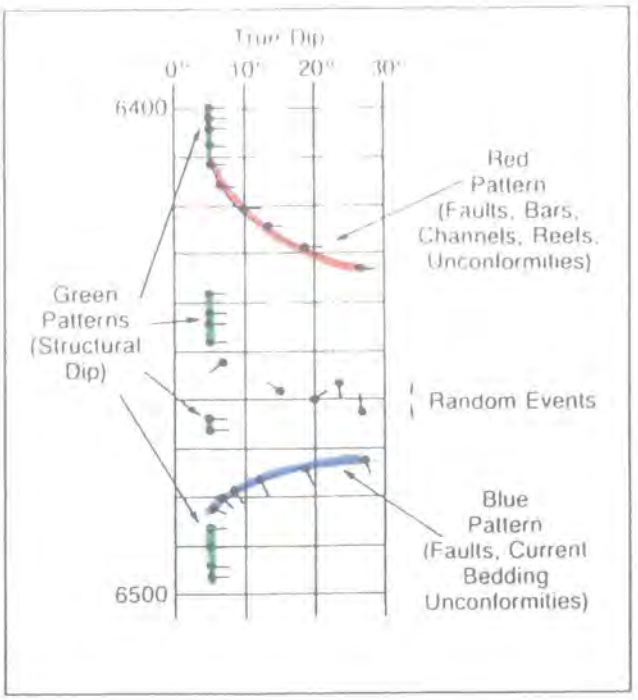

Figure 6-2. Dip patterns and the geologic anomalies commonly associated with them. (Schumberger, 1986)

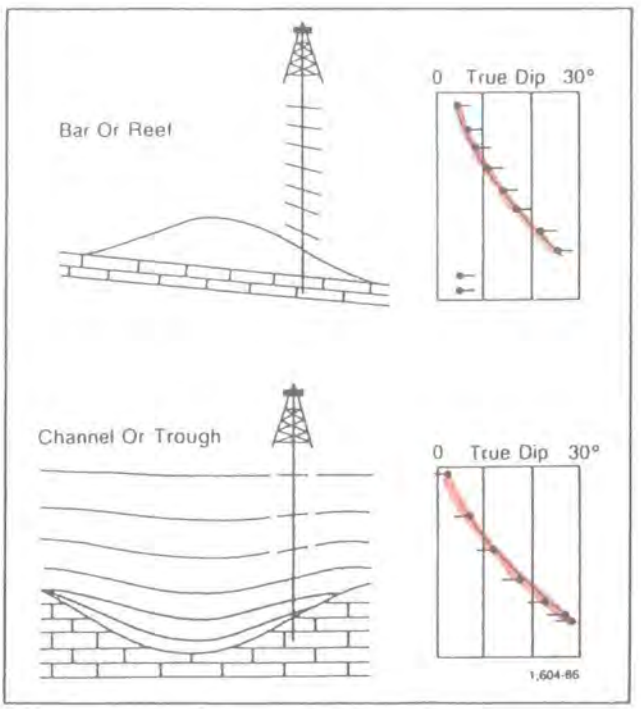

Figure 6-3. Red patterns above a bar or reef or in a channel or trough. (Schumberger, 1986)

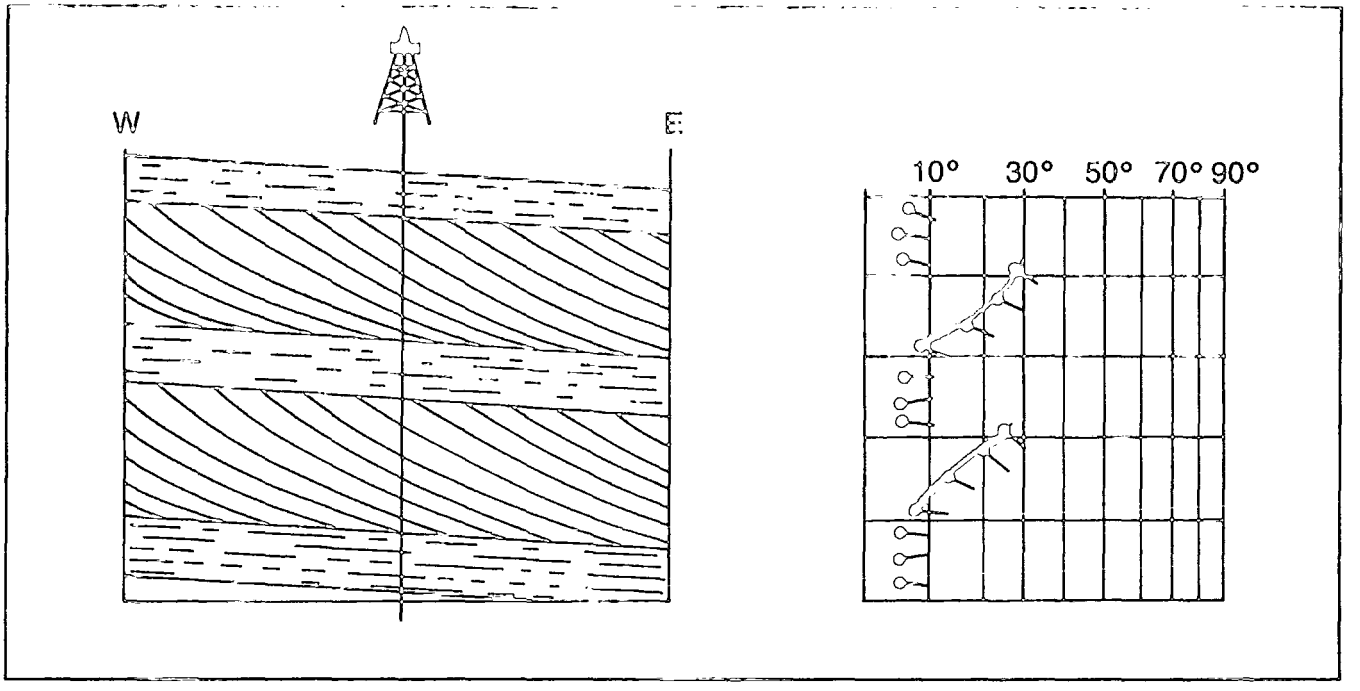

Figure 6-4. Blue pattern resulting from foreset current bedding. (Schumberger, 1986)

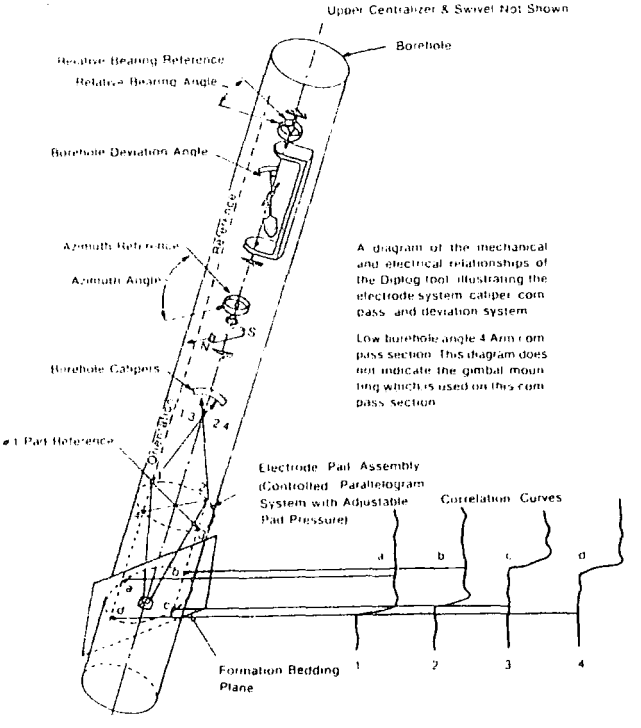

Figure 6-5. Principle of dip measuring system. (Allaud and Ringot, 1969)

crossbedding, direction of sand transport, and probable shape. The dipmeter provides data on the pattern of internal structures, direction of transport and in some instances the direction of thickening of the depositional body.

6.2 Equipment

All dipmeter tools work with four pad-type arms. Four microresistivity (or microconductivity) curves spaced at 90°intervals around the borehole are recorded. Although three curves are enough to define a dipping plane (figure 6-5) the fourth curve provides valuable redundancy in the dip computation particularly in rugose, irregular, or deviated borehole in which one pad may not make good contact with the formation.

Opposite pairs of pads are independently linked to provide a dual caliper measurement of borehole diameter. One of the pads normally contains an additional electrode, vertically displaced from the dipmeter microresistivity measurement electrode. Data from this electrode permit the dipmeter data to be automatically corrected for variations in sonde velocity.

A flux-gate compass and pair of pendulums permit the subsurface orientation of the dipmeter tool to be known. Thus, not only is the dip of subsurface beds calculated but the direction of dip is also determined. Borehole deviation and direction are determined.

Gearhart have a Four Electroded Dipmeter (FED) tool. The tool works on the principles described above. However, it does not have an extra electrode to correct for sonde velocity. In the case of a sticky, tight or rugose hole there could be an error in the data evaluation.

Schlumberger original dipmeter tool was the High Resolution Dipmeter (HDT) tool and nowadays it has been replaced by the Dual Dipmeter or the Stratigraphic High Resolution Dipmeter (SHDT) tool. The HDT works on the principles described previously in the introduction of this section. The SHDT works on the same microresistivity principle, and was designed and enhanced to overcome some of the limitations of the HDT:-

a) The sonde has been designed to maintain pad contact even in a deviated elliptical hole thereby avoiding a "floating" pad and less reliable(three-

pad) dip computation.

b) The inclinometry system has been built with no moving parts to eliminate all frictional and inertia effects that can cause inaccurate measurements and slow response times. The system has an accuracy of +/- 0.2° for tool deviation and +/- 2° for azimuth.

c) The (EMEX) survey current is automatically controlled at the optimum magnitude, thereby enabling quality dip resistivity curves to be obtained over intervals with both high- and low-resistivity formations.

d) Each of the four pads has two "side-by-side" electrodes spaced 3 cm apart (not one).This feature, together with a high data-sampling rate (0.1 inch), leads to the acquisition of more dip formation (eight microresistivity dip curves).

e) Tool-speed variation corrections can be made to the dip curves using data from two additional electrodes and a solid-state accelerometer.

With the huge amount of data acquired and the computer technology now available the SHDT presents a whole new dimension to dipmeter logging and interpretation. The cost of the SHDT to the operator is more than the HDT, but the benefits, as mentioned above, ensure that the operator has a much better quality data. Figure 6-6 is a field presentation of a SHDT log. Three different types of dip processing are available from SHDT data. Two types search for pad-to-pad correlations in order to compute the dip of features crossing the entire borehole. The other computer displacement is from side-by-side correlations on the same pad in order to detect small events that do not necessarily have a wide extension.

If a good correlation cannot be made the heterogeneous nature of the formation is clearly confirmed. Under certain conditions (deviated holes, for instance), the character of the dip curves may differ significantly from pad to pad, yet exhibit similarity from button to button (figure 6-7). In such cases formation dip can be determined from side-by-side correlations (figure 6-8) if they are available from two adjacent pads (figure 6-9). Figure 6-10 further illustrates the large number of small details that can be correlated between the two buttons of the same pad. This leads to better understanding of the sedimentary features and of the environment of depostition and consequently to a better definition of the facies. A short correlation interval

(1 foot or less) is normally used in the side-by-side correlation in order to recognise this fine stratigraphic detail. Side-by-side correlation is also most efficient in the detection of high dip.

Before computing displacements between curves for dip determination the data are processed for speed correction. This speed correction is achieved in two stages. First the eight microresistivity dip curves and the two microresistivity speed curves are depth-shifted and reinterpolated using the accelerometer data. Second the two speed curves are used during the dip computation stage to remove any remaining speed fluctuation.

For the different dip results there are numerous combinations of presentations. The presentation used depends on the purpose of the dipmeter results and on personal preference. One presentation, using a 22-inch wide display, is shown in figure 6-11. From the left to the right are:

a) Borehole depth, drift, and azimuth.

b) Two calipers and a GR curve.

c) Arrow plots corresponding to the two interval-correlation methods of dip computation: a triangular tadpole for the Mean Square Dip (MSD) pad-to-pad correlations and a circular tadpole for the Continuous Side-by-Side Dip (CSB) results.

d) The eight microresistivity curves with dip curve 1 repeated and the correlations found by the feature-correlation (LOCDIP) technique. LOCDIP is the name given to a feature-correlation interpretation technique used by Schlumberger.

e) STRATIM - a wrap-around image of the borehole based on interpolation between the eight microresistivity curves and the correlation links provided by the LOCDIP program.

f) Arrow plot corresponding to the feature-correlation method; a square tadpole is used.

Western Atlas offers the High Resolution 4-Arm Diplog (DIP) tool. It seems to be cross between the HDT and SHDT. It uses accelerometers to measure inclinometry data, and to correct for sonde velocity. The accuracy is +/- 1.2° for azimuth, and +/- 0.8° for deviation.

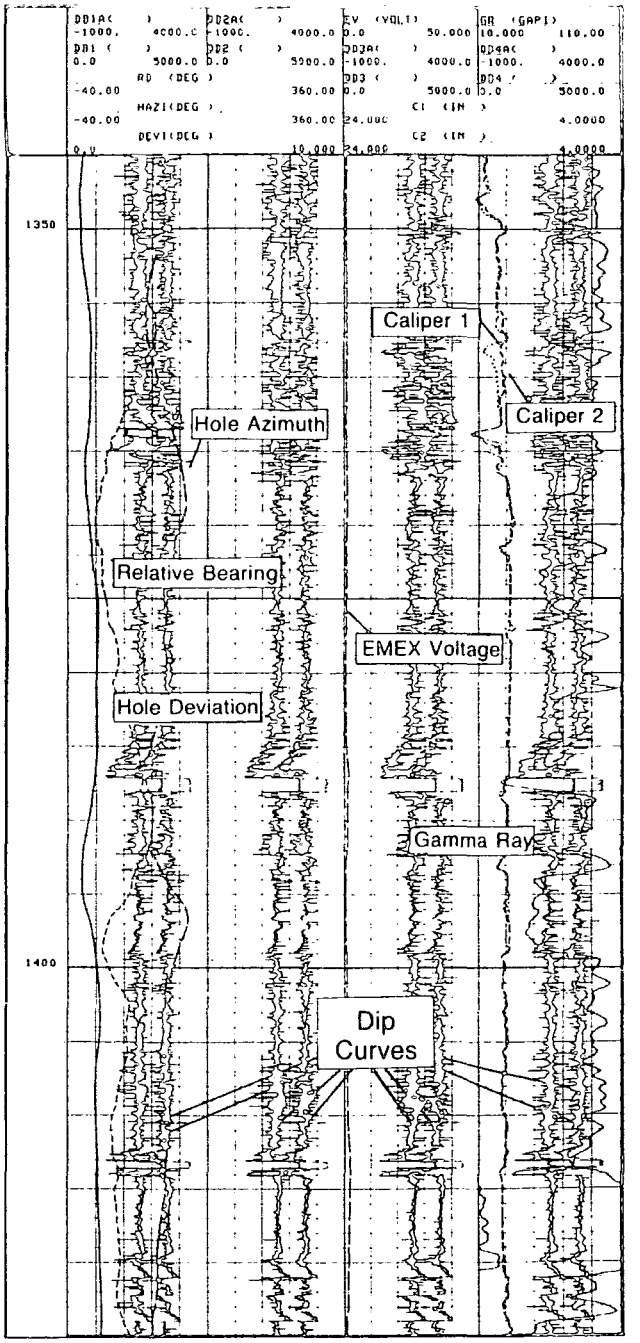

Figure 6-6. Field presentation of Dual Dipmeter (SHDT) log. (Schlumberger, 1985)

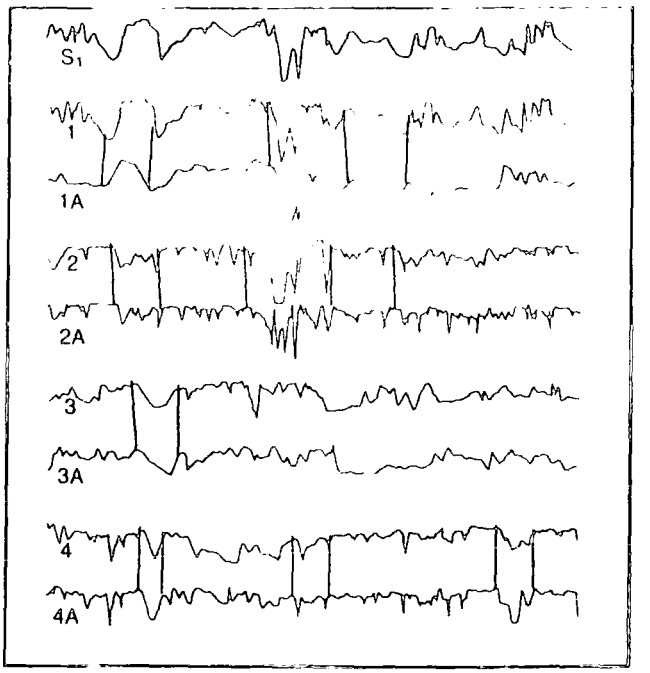

Figure 6-7. Curve shape differs from pad to pad but not from button to button. (Schlumberger, 1986)

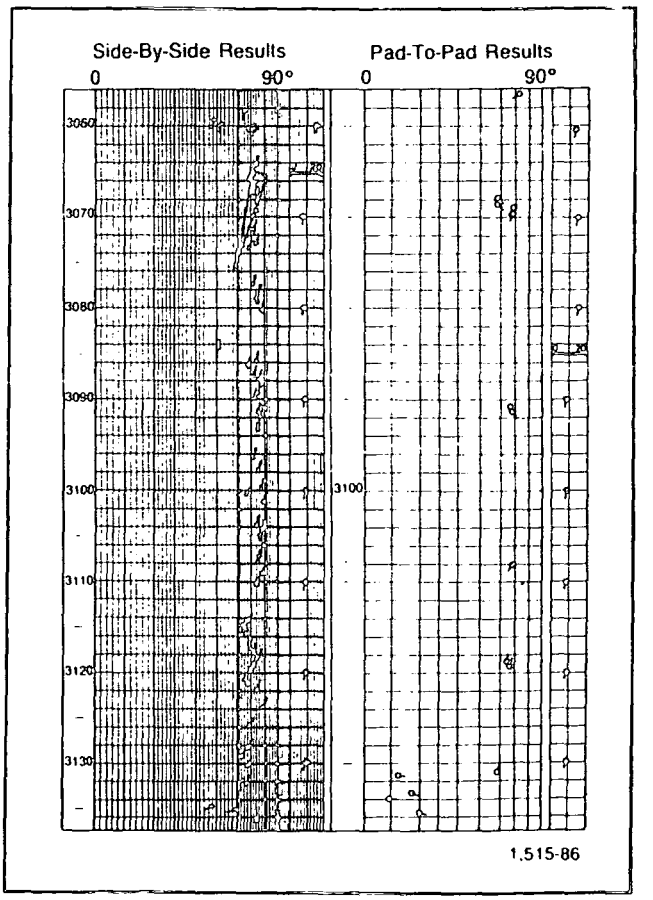

Figure 6-8. High apparent dips on pad-to-pad results are confirmed by side-by-side results. (Schlumberger, 1986)

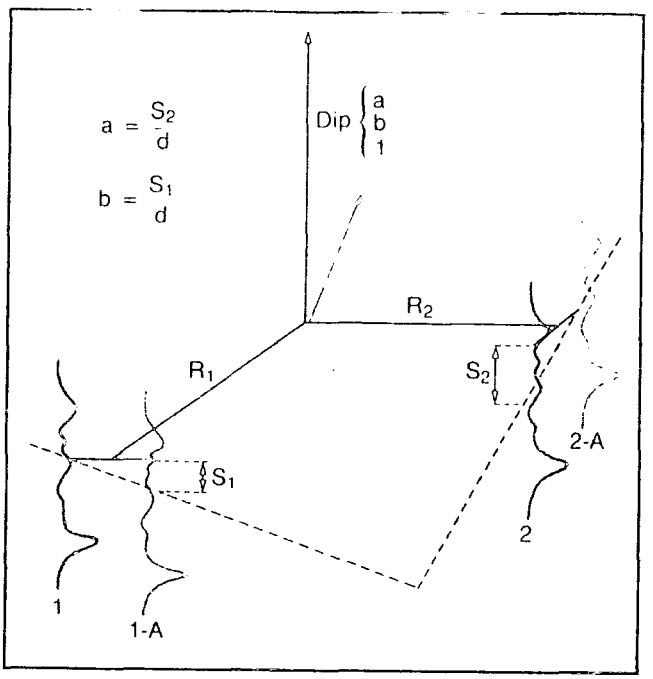

Figure 6-9. Dip computation method from side-by-side data only. (Schlumberger, 1986)

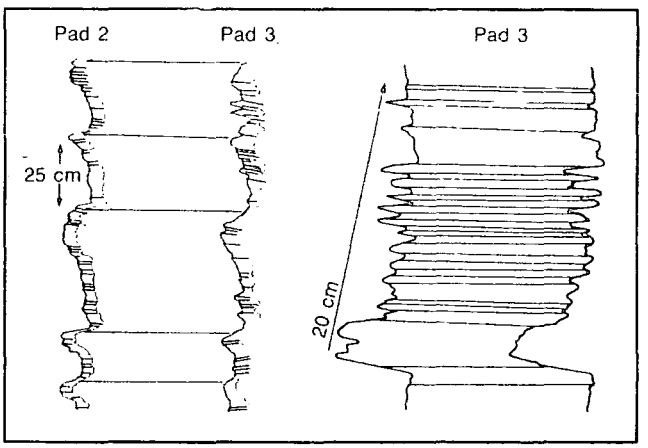

Figure 6-10. Side-by-side and pad-to-pad correlation (left) ; detail of side-by-side correlations (right). (Schlumberger, 1986)

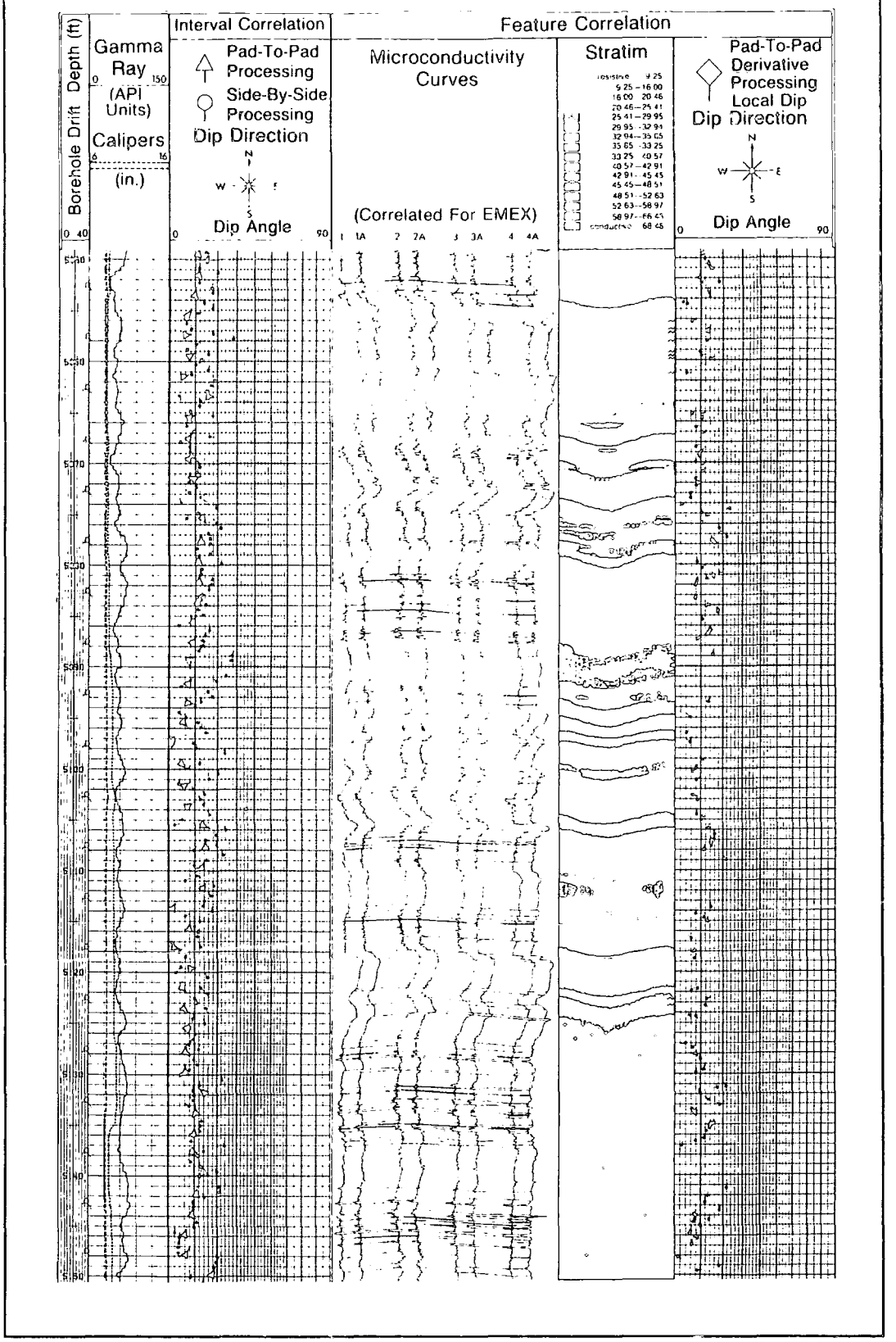

Figure 6-11. Presentation of Dual Dipmeter (SHDT) data processing results. (Schlumberger, 1985)

Table 6-1 shows temperature and pressure ratings of the dipmeter tools.

Company	Tool	Max. Temp.	Max.Pressure	Accuracy	
		(°F)	(kpsi.)	Azimuth	Deviation
Gearhart	FED	350	18.5	+/-3°	+/-0.5°
Schlumberger	FMS	350	20	+/-2°	+/-0.2°
	HDT	350	20	+/-3°	+/-0.5°
	SHDT	350	20	+/-2°	+/-0.2°
Western Atas	DIP	375	20	+/-1.2°	+/-0.8°

Table 6-1 Dipmeter Tools' Ratings.

With the improvement in technology Schlumberger has extended their dipmeter technology and using the same measurement concept has developed the Formation MicroScanner (FMS) tool. The FMS obtains two-dimensional, high resolution imagery of microresistivity variations around the borehole wall.

The FMS has four articulated pads that contains two sets of electrodes. One set provides the standard SHDT measurement and the other set provides the borehole imaging.

Figure 6-12 show the pad configuration for one of the imaging arrays, which are located on adjacent pads 90° apart. Each array has 27 electrodes with a lateral span of 2.8 inches. The two arrays cover approximately 20 % of an 8.5-inches borehole.

The FMS service provides the geologist with formation details that were previously available only from full-hole cores. These are obtainable by coring with the drillstring. The method is lengthy and expensive. For example, coring a 90feet core could take anywhere from 2 to 24 hours. Hence, it is not practical to core the whole wellbore but just the zone of interest. These features or heterogeneities may identify :-

a) Bedding deposited under a variety of flow regimes, such as trough and tabular crossbeds, ripples, very thin beds, and graded beds.
b) Bedding subject to postdepositional distortions such as faulting, folding, or slumping.
c) Non bedding features such as fractures, burrowing, vugs, pebbles, concre-

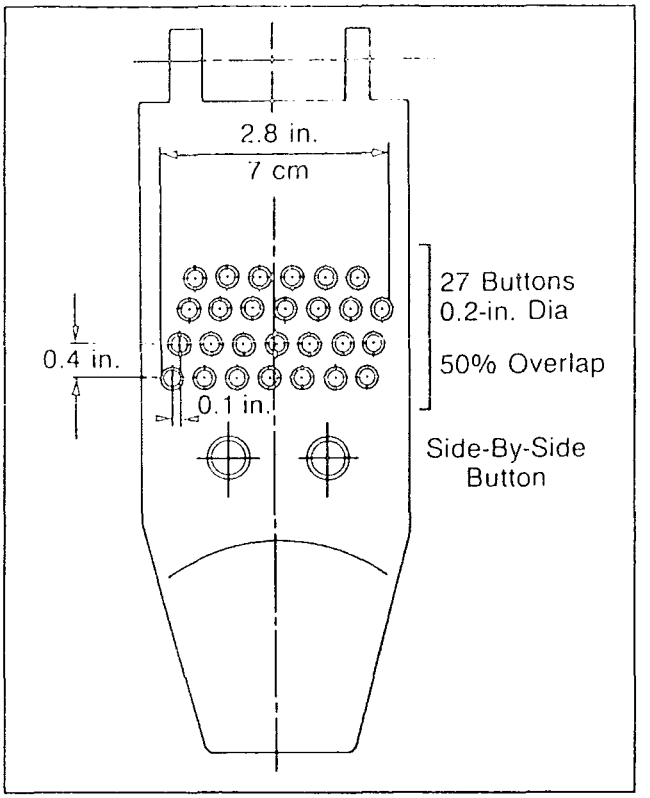

Figure 6-12. Formation Microscanner pad configuration. (Lloyd, Dahan, and Hutlin, 1986)

tions, fissures, stylolites, etc.

The log presentation includes the two-dimensional resistivity data and the grey-scale "core-like" borehole wall image mapped from the microresistivity data. The grey-scale mapping is on a relative resistivity scale where black and white correspond to low and high values of resistivity respectively. Colour images are also available. Figure 6-13 show the FMS display with a core photograph through a calcilutite sequence that has been subjcted to slumping. The individual laminae are broken up and present a brecciated appearance. A comparison of the FMS image and core photograph show that the tool is capable of defining individual clasts on a centimetre scale.

All the tools mentioned so far operate in conductive mud only. When non-conductive mud or oil-base mud is used, modification to the above tools is needed. Gearhart, Schlumberger and Western Atlas modify their FED, HDT and DIP tools respectively by using special knife-blade electrodes. Under these conditions, however, the microresistivity data that are recorded are seldom up to normal conductive mud standards. To overcome this problem, usually numerous passes are made over the interval concerned, and then used for interpretation.

Furthermore, for non-conductive mud operations Schlumberger has developed the Oil-Base Mud Dipmeter (OBDT) tool, and Gearhart has the 6-Arm Knife-Blade Dipmeter (SED) tool. The Gearhart SED tool is an improvement on the original FED tool by providing more information on two additional pads. The basic principle is still the same as before, and hence the quality of data of each pad is also still the same. Information from six pads should provide better determination of dip planes, but if the data quality from each pad is poor it could lead to a confusion rather than a result of high confidence.

However, the OBDT tool is a completely different tool which does not use knife-blade electrodes but uses a theory similar to an induction tool (see chapter 4.3.3). The difference is that the OBDT is designed to have a shallow depth of investigation. Because the tool is designed specifically for non-conductive mud the data quality is vastly improved. The inclinometry system in an OBDT tool is the same as the one in the SHDT tool.

In the field of dipmeter tools, Schlumberger offers a better range of services.

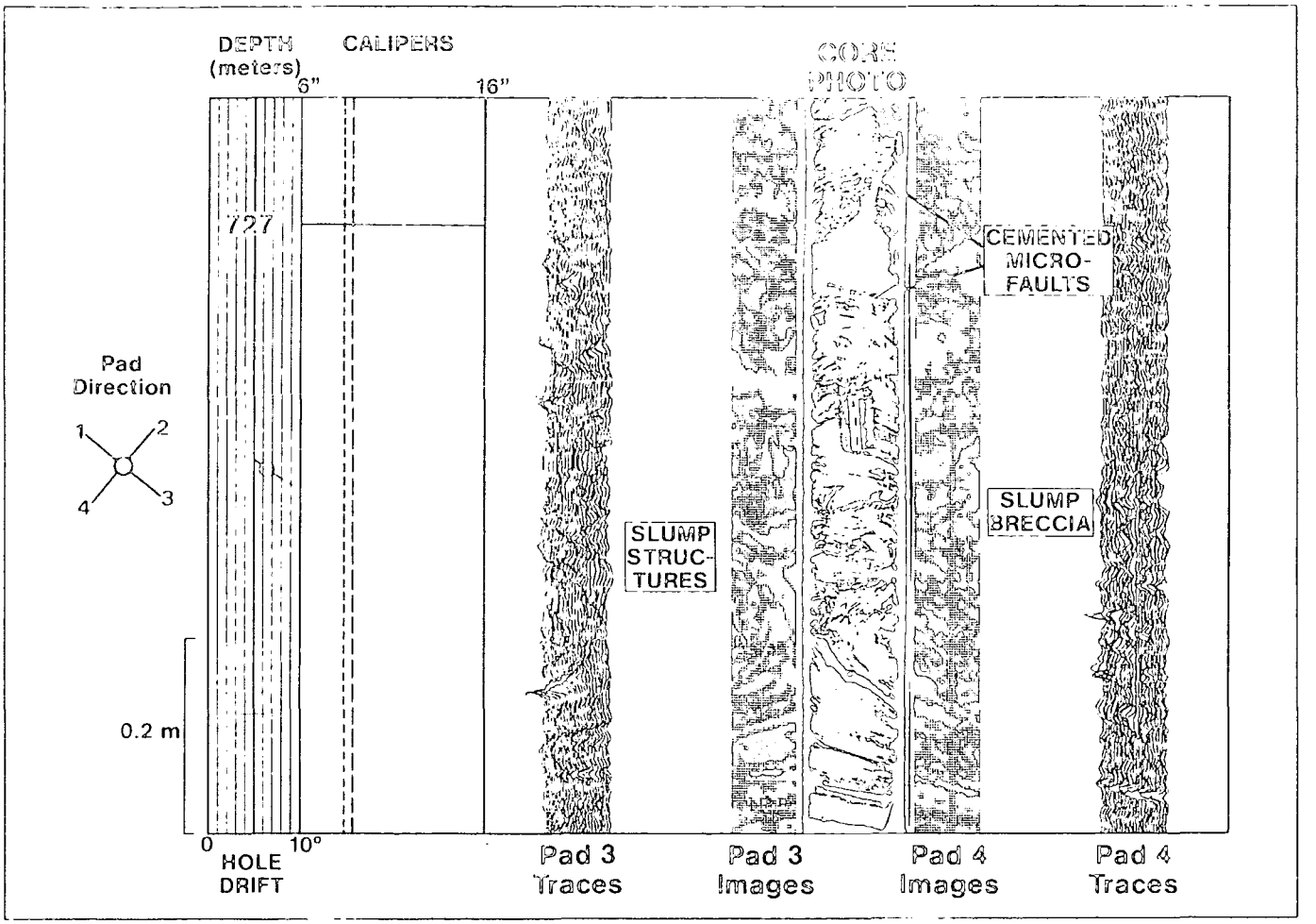

Figure 6-13. Slump breccia developed in a calcilutite sequence. (Lloyd, Dahan and Hutlin, 1986)

Their tools are more advanced and have the ability to provide the operator with accurate data with a higher degree of confidence. While both Gearhart and Western Atlas are still offering the service of the FED and DIP tools respectively, Schlumberger seems to have left them far behind with the introduction of both the SHDT and FMS.

6.3 Use and Detection of Natural Fractures

In addition to using the response of well-logging sensors to determine lithology and geologic parameters one can also use them to determine naturally fractured zones. These zones are important in reservoir rocks because of the extra drainage and considerable increase in permeability they promise. Although fractures can have a very significant effect on the total permeability of a rock they usually have very little effect on the porosity saturations or petrophysical characteristics of the rock. For example, a large number of the Middle East's prolific oil fields owe their fame to fractures which have formed the permeable highways through the reservoir along which oil can rapidly migrate. If the fractures were not present many of these well-known oil fields would not be viable.

Natural fractures generally exhibit certain constant characteristics:-

a) They are usually approximately perpendicular to the dip; this does not however exclude the possibility of horizontal fractures although horizontal fractures are much less frequent and less extensive than subvertical fractures.

b) They are usually oriented according to one (or more) prevailing strikes. Since fractures are often the result of tectonic stresses the prevailing strike of the fractures generally coincides with the orientation of the faults in the region.

c) They frequently cause small amounts of rock to be broken off from the borehole wall by the drill bit or drillstring during drilling.

d) They usually occur in compact, competent rocks where the hole would normally be cylindrical and in gauge in the absence of fractures.

Only fractures that are at least partially open are useful from the point of view of production.

6.4 Fracture Detection

Logging tools are designed to respond to different characteristics of the wellbore environment. Some tools respond primarily to lithology, some primarily to porosity, and others to fluid saturation. None unfortunately responds primarily to fractures, although fractures, particularly open ones, may affect the response of some logging tools. The effect however is usually rather subtle.

Measurement of density, caliper, or resistivity can help to detect a fracture zone, but generally are not used for this purpose. However the measurements of sonic and microresistivities of the dipmeter tool are used more often for fracture detection.

6.4.1 Dipmeter

A special presentation of dipmeter microresistivity measurements is perhaps one of the simplest and most effective methodsfor fracture detection. When mud filtrate invades a fracture system it usually causes a lower dipmeter microresistivity reading from the pad positioned opposite the fracture. A comparison of measurements from adjacent pads (i.e., 90° apart) indicates fractures. If no differences exist the probability of fractures is low; if large differences exist the probability is high. Such a difference is evident in figure 6-14. Dipmeter curves 1 and 3 are measuring much lower resistivities than curves 2 and 4 over a short interval of the example.

This method is not perfect since the pads covers only about 40 % of the borehole wall surface in an 8-inch borehole. Severely shattered intervals where all pads may read the same and thin fractures in a steeply dipping formations may not be easily detected by this method.

6.4.2 Formation MicroScanner Tool

As discussed earlier the tool has excellent vertical resolution and can distinguish two fractures as close as 0.4 inch. The FMS tool can also distinguish between opened and closed fractures. Figure 6-14 shows the dipping foreset beds in a carbonate grainstone. A steeply dipping series of linear conductive features are also evident. There are opened fractures filled by the conductive drilling fluid. The lack of displacement of the bedding surfaces across these fractures indicates they were induced by tensional stress and not by shear stress.

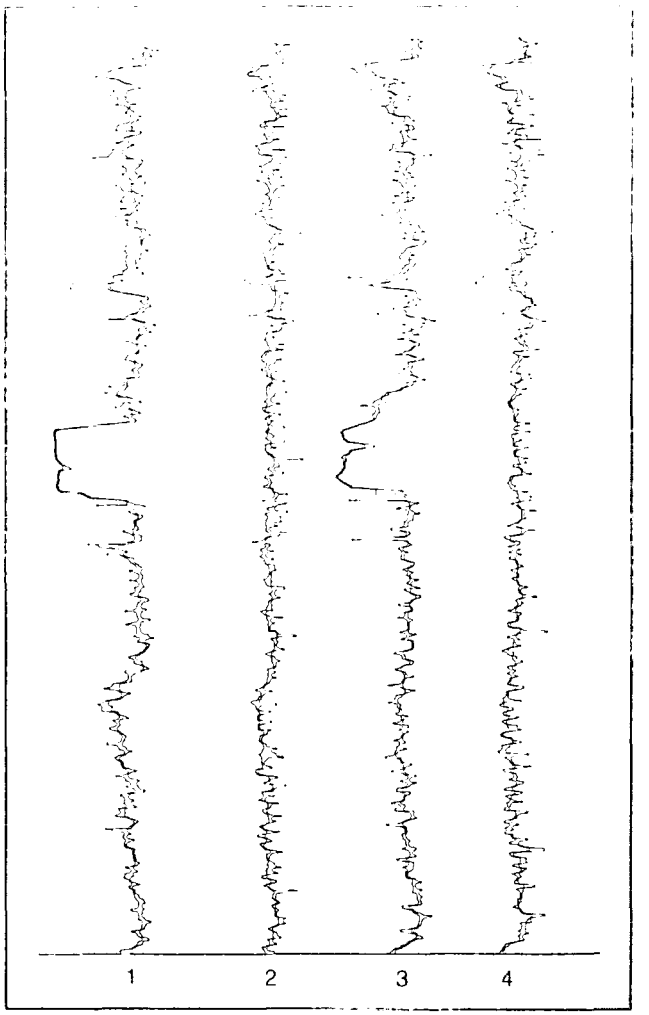

Figure 6-14. Dipmeter data indicate anisotropy and, perhaps, fractures. (Schlumberger, 1986)

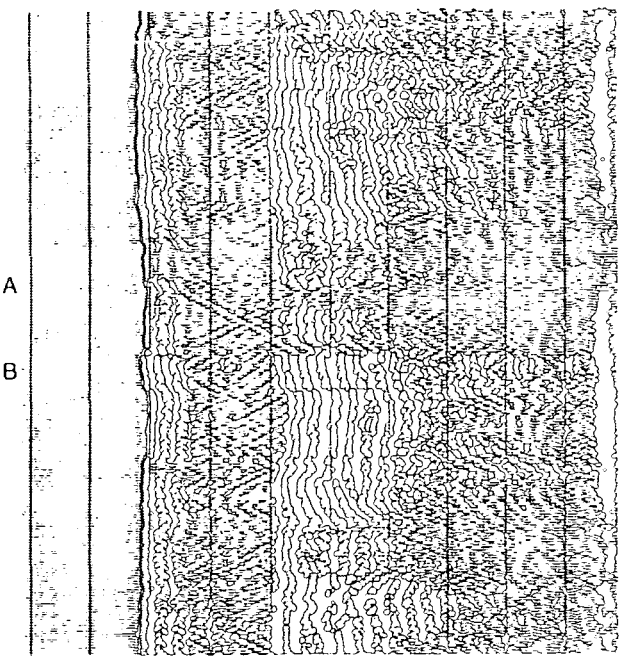

Figure 6-17. Sonic waveform response over a large horizontal fracture.

 (Noblett, Ferti and Guy, 1987)

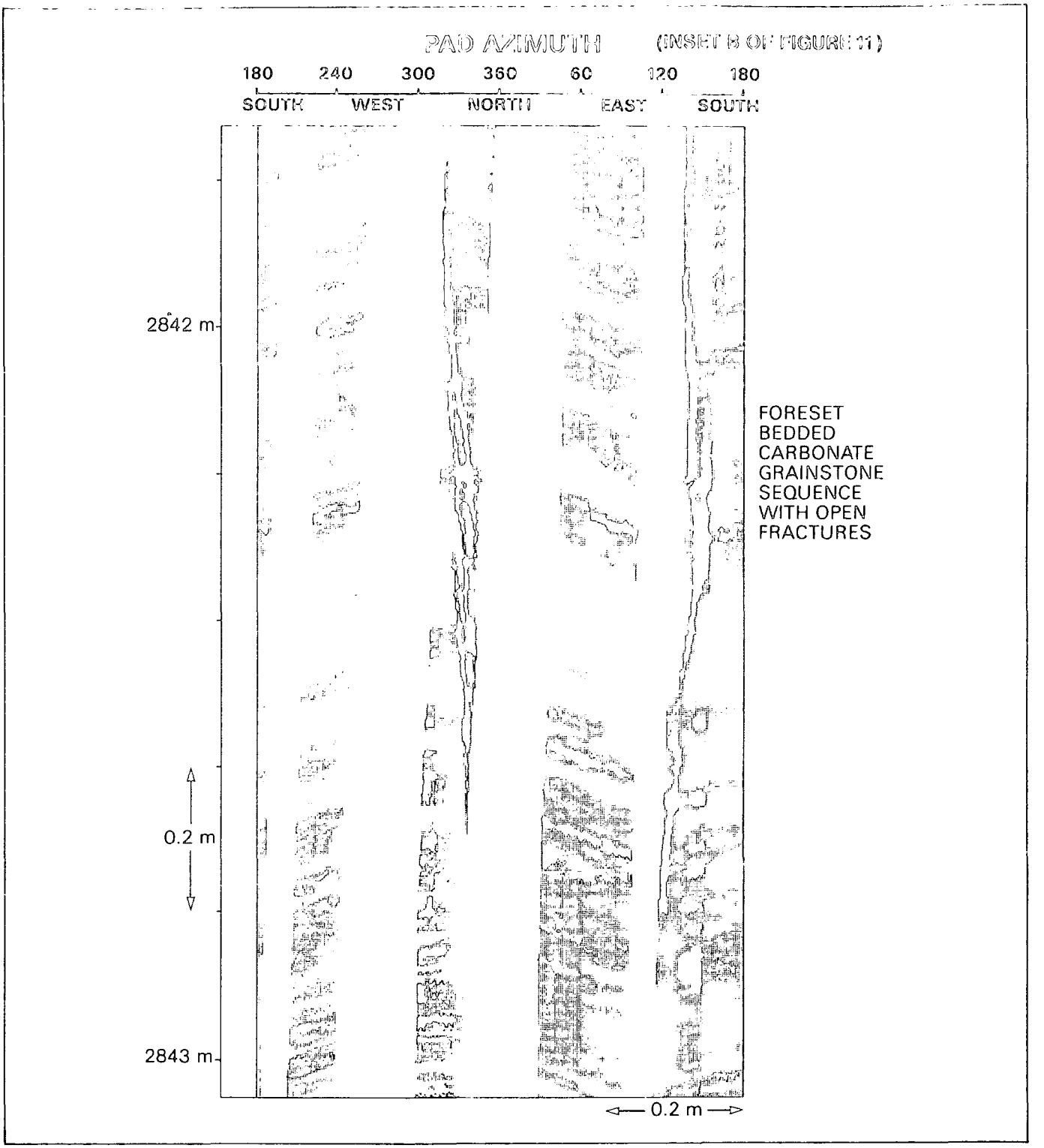

Figure 6-15. Foreset beds and a fracture in a carbonate grainstone. (Lloyd, Dahan and Hutlin, 1986)

6.4.3 Borehole Televiewer Tool

The Borehole Televiewer (BHTV) tool is an acoustic scanner. As it is pulled up the hole it scans the borehole wall with a rotating transducer that emits a pulsed ultrasonic beam. A visual representation of the pattern of acoustic reflection of the borehole wall is displayed both on film and on the monitor screen. The image shows the borehole wall as if it was split vertically and laid flat. Vertical fractures appear as straight lines, while fractures dipping between vertical and horizontal appear as sinusodial traces.

Both Schlumberger and Western Atlas are able to offer this service using tools of the same name. Both tools work on the principle described above. The Schlumberger's BHTV tool is rated at 350 °F and 20000 psi, while the Western Atlas's BHTV is rated at 300 °F and 15000 psi.

The problem with using this tool is its operational difficulty and its environmental limitations. The results are poor in elongated, rugose, or collapsing boreholes; and these conditions are common in fractured intervals.

6.4.4 Sonic Measurements

One of the oldest fracture indicators is the reverberation of sound waves in and around the borehole. Measurements based on sonic wave propagation respond to the mechanical properties of the rock and are little affected by the borehole environment.

In fractured zones, the appearance of the wavetrain as recorded on the Variable Density log (VDL) show sudden changes such as vague or blurred zones, chevron patterns, etc. (figure 6-16). These features suggest interfaces of differing acoustic impedance between the transmitter and receiver of the sonic tool. Such propagation anomalies can be caused by open fractures. Unfortunately similar anomalies can also occur with changes in the diameter of the borehole or because of thin beds of different lithology or even a "healed" (closed) fracture system.

Recently, the sonic tools have become popular for the recording of the sonic wavetrain (figure 5-1). Figure 6-17 shows a 12 foot spacing sonic waveform in the vicinity of a large horizontal fracture. Points A and B are, respectively, the positions where transmitter and receiver are directly opposite the fracture. A sharp increase in the amplitude of the compressional and shear first arrivals can be easily seen. Another feature, clearly discernible, is the criss-cross patterns origination in the compressional

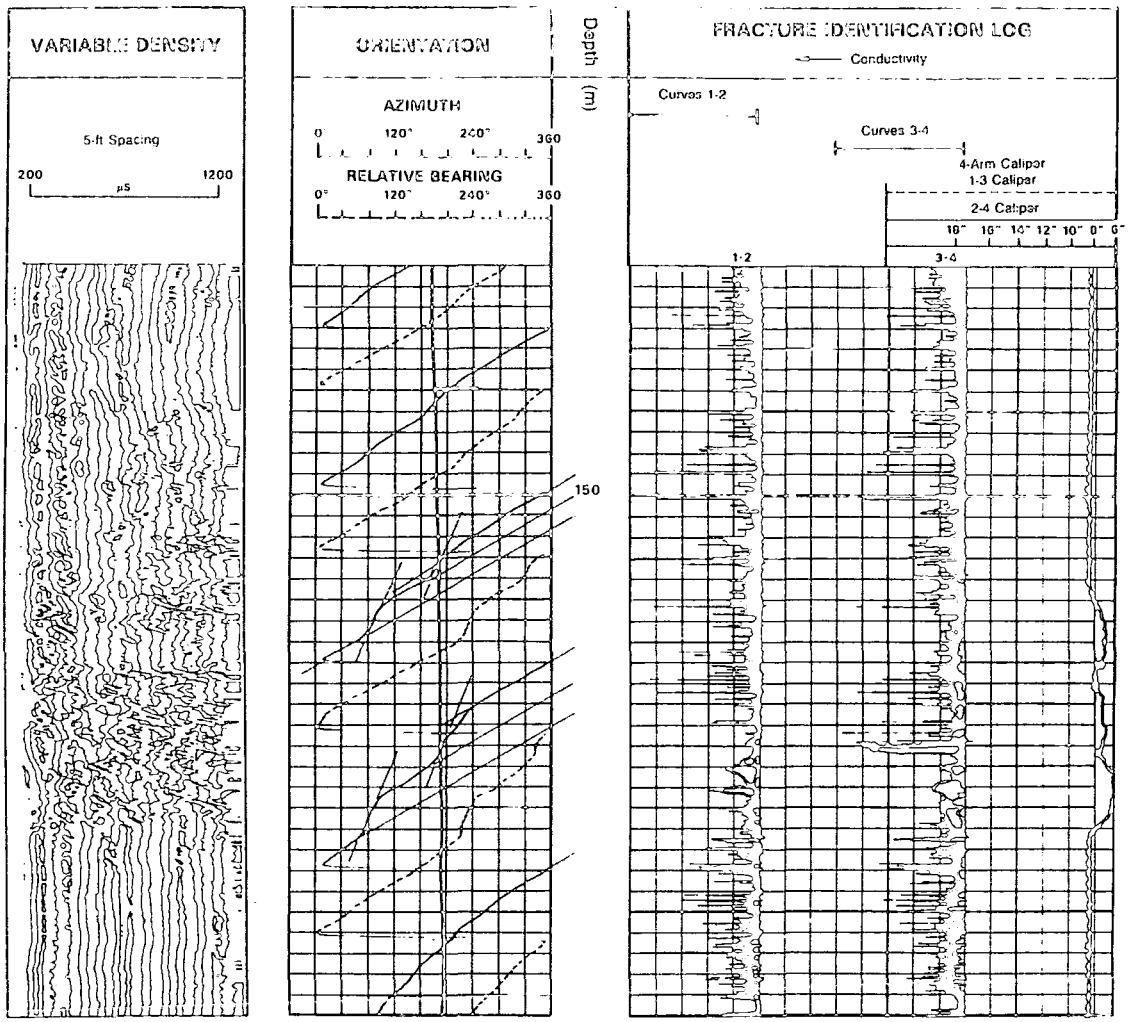

Figure 6-16. Fracture identification with VDL display and fracture identification log. (Noblett, Fertl and Guy, 1987)

and shear waves. However, anomalies caused by vertical fractures are more subtle.

The recording of full wavetrains are usually done by using the longer spacing sonic tools. This is to enable a better depth of investigation. Gearhart, Schlumberger (especially with the Array-Sonic (SDT) tool),and Western Atlas (especially with the Circumferential Acoustilog (CAC) tool) are all able to offer this service.

In addition to VDL and sonic wavefrom methods, the SDT can use the energy that arrives at the receiver to determine fracture. The SDT emits a fixed amount of energy with the amount arriving at the receiver indicating the competence and uniformity of the formation. High signal strength at the receiver suggests a competent rock with low probability of fractures; very low signal strength suggests a high probability of fractures. Figure 6-18 is an example of a decrease in shear energy opposite a zone where fractures are suspected. At the fracture interface some of the shear energy is reflected, some is converted to other modes of wave propagation, and some is refracted. The amount of shear energy reaching the receiver is therefore significantly reduced.

Western Atlas's CAC tool was designed to indicate the presence of vertical or near-vertically oriented fractures in fluid-filled boreholes. Based on a logging method proposed by Vogel et al, a circumferentially oriented acoustic transmitter-receiver array was developed for this purpose. The CAC employs the principle of generating and detecting circumferentially propagating acoustic boundary waves (Setser, 1981; Guy, et al., 1981; Guy,et al., 1986; Noblett, et al., 1987). The logging instrument has been designed to enhance the recording of Rayleigh and guided fluid waves by eliminating any direct fluid wave component. The tool has four pads which are used in contact with the borehole wall. Two opposing pads contain transmitting elements which generate acoustic waves that are converted to shear waves which travel circumferentially around the borehole. Two receiving elements detect the shear waves that have travelled one quarter of the circumference of the borehole. The loss of shear energy in two quadrants of the borehole incidates a near-vertical discountinuity, i.e., a vertical fracture.

The CAC tool also incorporates an orientation section into the logging string to measure deviation of boreholes from vertical plus the azimuth of the reference pad. This information is necessary for determining the directional subsurface trend of the

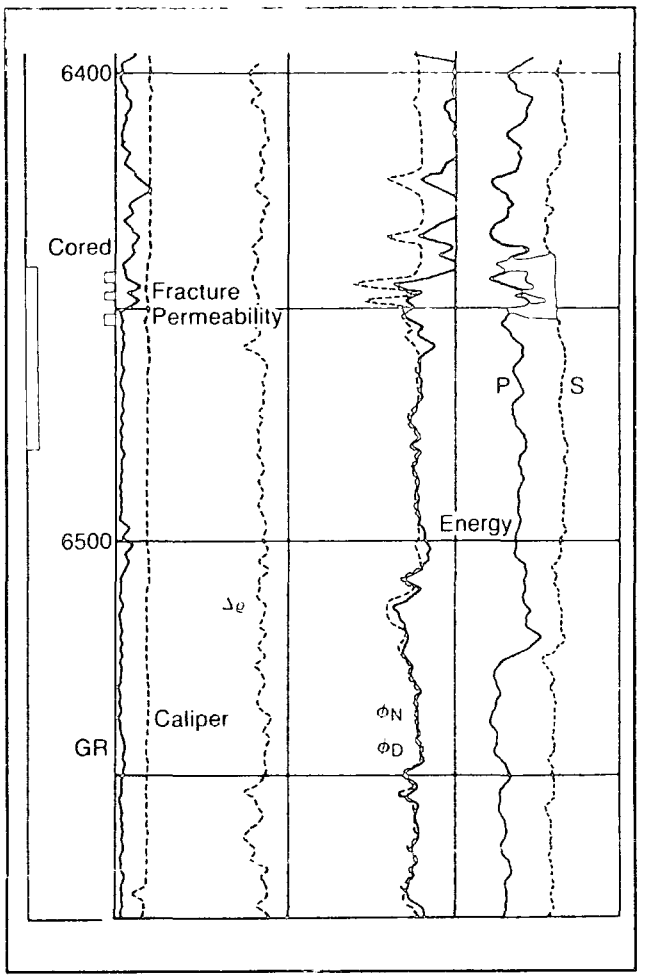

Figure 6-18. Drop in shear energy indicates fracture. (Noblett, Fertl and Guy, 1987)

detected fracture system.

It is apparent that both Schlumberger and Wester Atlas have done a lot of research in developing tools to detect fracture zones. It is certain that operators will be requiring these services more and more especially for their exploration wells to give them a better understanding of their reservoirs.

When confronted with a fracture zone it is worth examining whether it is induced fractures (from drilling) or natural fractures (figure 6-19). No log, used alone can furnish unequivocal proof of the presences of fractures. Fracture detection is most certain when several logs or techniques confirm their presence. The openhole logs would most likely display some of the following anomalous behaviour, normally considered as indications of natural fractures:-

a) A noisy delta-rho curve on the density log (see chapter 5.1.2.2).
b) A positive PEF anomaly if barite were present in the mud (see chapter 5.1.2.4).
c) A mismatch between the resistivity on the shallow and deep reading devices (see chapter 4).
d) The presence of conductivity spike anomalies on the conventional dipmeter.
e) The presence of disturbed patterns on the sonic waveforms.
f) The images of the borehole given by tools such as the BHTV, CAC and FMS.

The combination of methods best adapted to the solution of local fracture identification problems must be defined after some experimentation and study, during which most of the logs offering fracture detection promise should be used and the results carefully analysed.

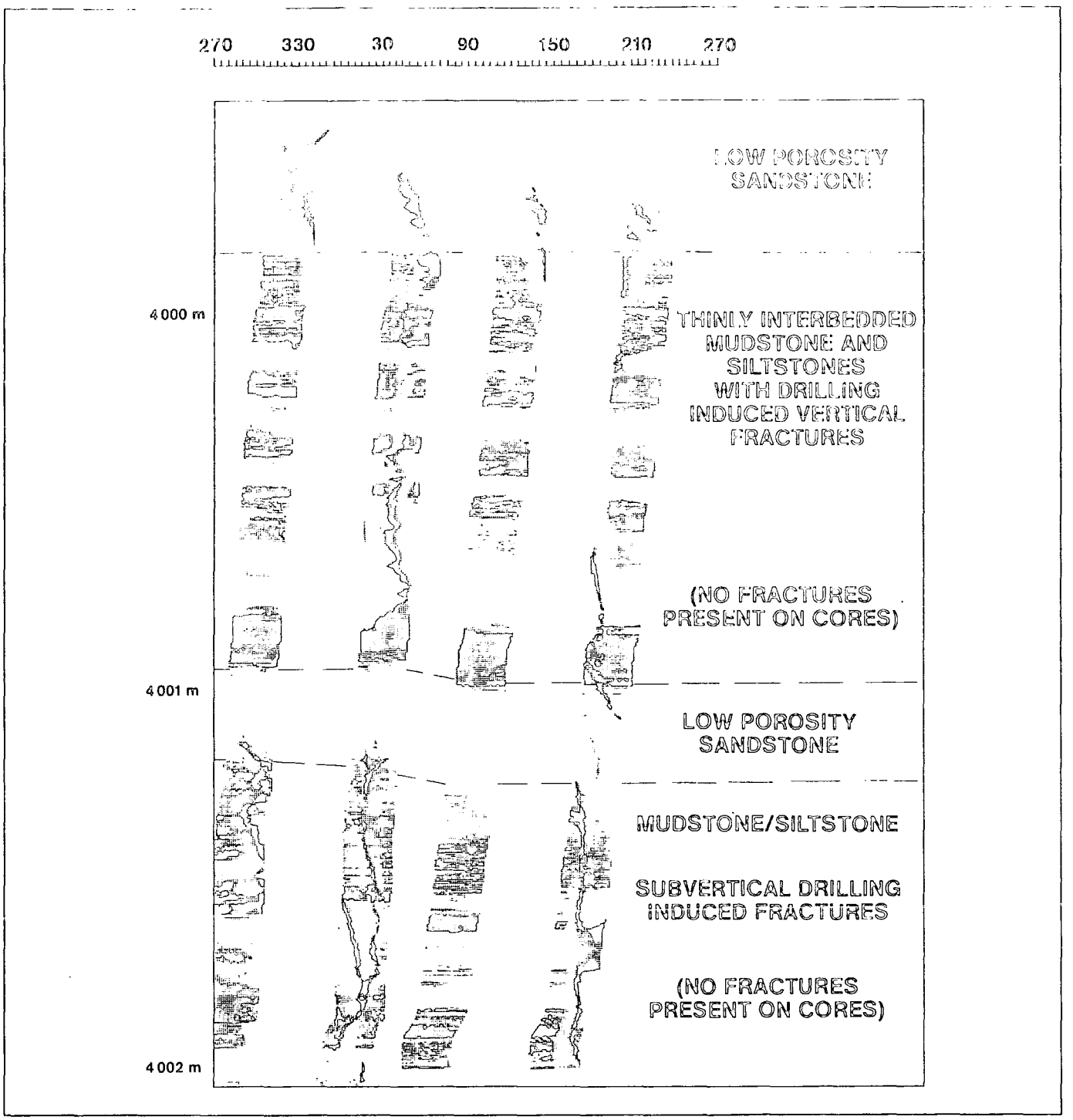

Figure 6-19. Drilling Induced Fractures in the Rotligendes Formation of Germany. (Lloyd, Dahan and Hutlin, 1986)

7. OPENHOLE SAMPLING

In addition to the conventional openhole logs such as resistivity and porosity it is also possible and desirable to run sampling tools down the hole. Essentially there are two main types of sampling tools: one for the formation fluid sample and another for the formation core sample. The depths (levels) at which these are taken are determined from the resistivity and porosity logs.

The information obtained from the sampling tools can enhance the original openhole log data with the interpretation of the well and furthermore it provides a fast and economical method for identifying the production potential of the targeted reservoirs without having to embark on an extensive coring and testing program. The recovery of the fluid sample can give the information on the resistivity of the formation water R_w if taken in the water zone or information on the type of hydrocarbon present if taken in the hydrocarbon zone. In addition to recovering formation fluid samples the same tool is capable of measuring the formation pressure at the same time. Also from the recovery data and pressure recording the permeability of the formation can be evaluated.

The recovery of the formation core sample on the other hand, gives geologic information at a very precise depth. The information when used in conjunction with the openhole log data should give a fairly accurate idea of the formation composition relative to the log readings. This should give the geologist first-hand answers on what type of formation e.g. clay compositions he has in his well and in doing so it should enhance his understanding of the log readings.

7.1 Formation Fluid Sampling

The recovery data and pressure recording taken during formation fluid sampling can have many reservoir engineering applications. The interpretation of the pressure curve can give an idea of the formation permeability and fluid mobility. Furthermore, the sampling tool provides an accurate in-situ pressure measurement at any desired depth in an open borehole and gives information on fluid type, fluid contacts, skin effect, reservoir communication, pore pressure, depleted zones and faults.

a) Permeability

Permeability is a measure of the ease with which a formation permits a fluid to flow through it. To be permeable a rock must have interconnected porosity (pores, vugs, capillaries, fissures, or fractures). Greater porosity usually corresponds to greater permeability but this is not always the case. Pore size, shape, and continuity, as well as the amount of porosity, influence formation permeability.

Some fine-grained sands can have high interconnected porosity, although the individual pores and pore channels are quite small. As a result the paths available through the narrow pores for the movement of fluid are quite restricted and tortuous. The permeabilities of very fine-grained formations may therefore be quite low.

Shales and clays which are composed of exceedingly fine-grained particles, often exhibit very high porosity. However, because of the pores and pore channels are equally small most shales and clays exhibit, for all practical purposes, zero permeability.

Other formations such as limestone may be composed of a dense rock broken by a few small fissures of great extent. The porosity of the dense formation would surely be very low but the permeability of a fissure can be enormous. Fissured limestones may thus have very low porosities but high permeabilities.

The unit of permeability is the darcy. One darcy is the permeability which will allow the flow of one cubic centimetre per second of a fluid of one centipoise viscosity through a cross-sectional area of one square centimetre under a pressure gradient of one atmosphere per centimetre. A darcy is a very large unit so, in practice the millidarcy (md) is the unit commonly used.

Using the sampling tool the local formation permeability can be derived from the pretest build-up curve. There is an upper limit (k_{max}) to the measurable permeability which is a function of the fluid properties, the gauge resolution (Sp) and the flowrate (see figure 7-1).

$$k_{max} = 390\left(\frac{q\mu}{Sp}\right)^{2/3}\left(\frac{\phi \quad C_t}{T}\right)^{1/3} \qquad (7\text{-}1)$$

(Stewart and Wittman, 1979)

where,

k = spherical permeability,

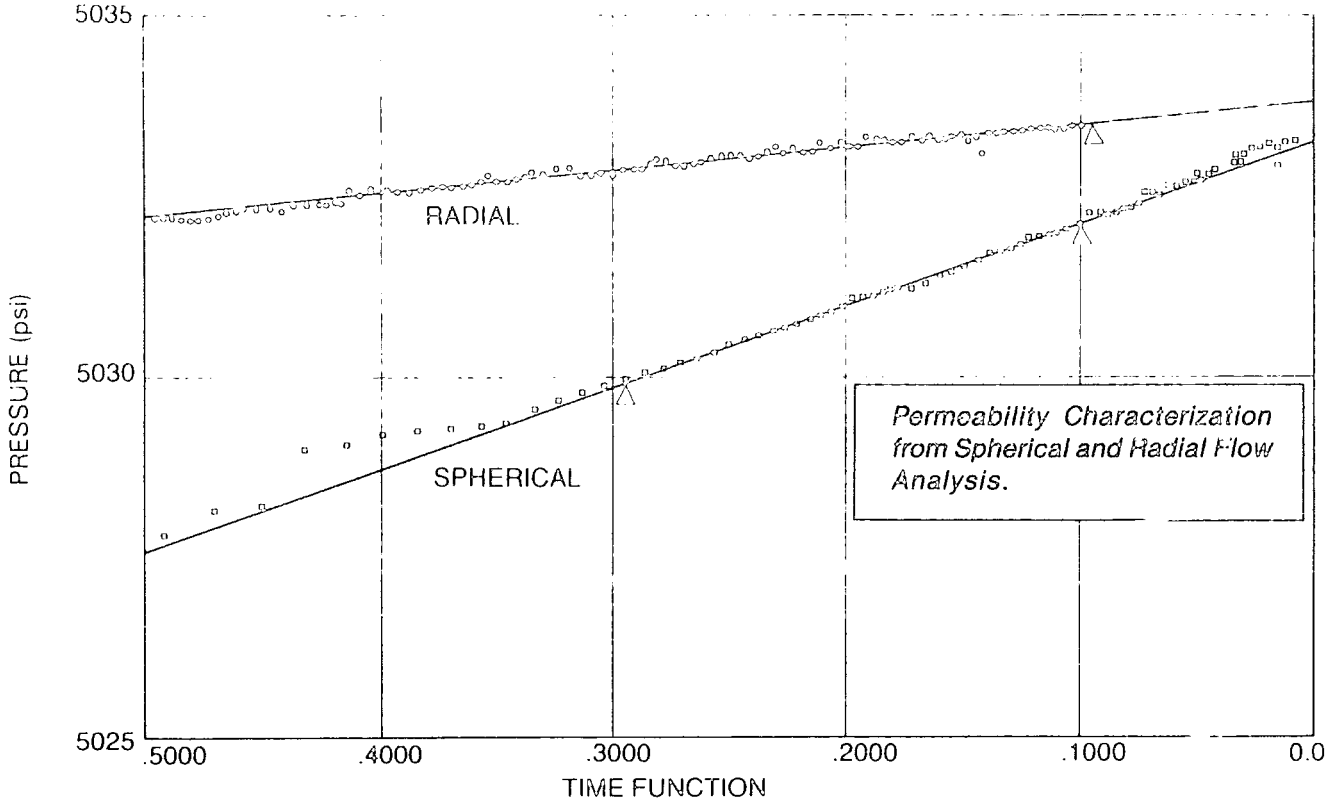

Figure 7-1. Permeability characterisation. (Schlumberger, 1981)

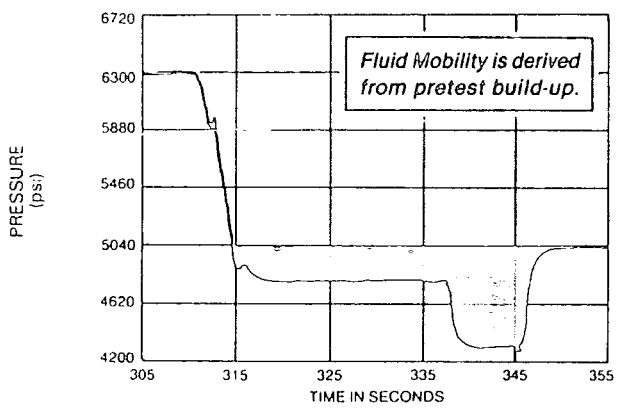

Figure 7-2. Pretest build-up plot. (Schlumberger, 1981)

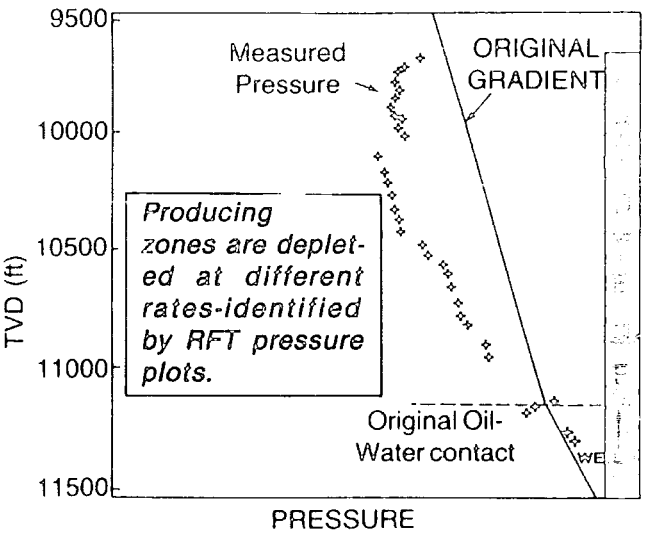

Figure 7-3. Application of Pressure data in developed reservoir. (Schlumberger, 1981)

q = probe flowrate in cc/sec,

μ = fluid viscosity in cp,

ϕ = formation porosity,

C_t = total system compressibility in psi^{-1},

and,

T = total probe flow time in sec.

b) Mobility

By integrating the area above the pressure curve in a pre-test (figure 7-2) it is possible to derive the fluid mobility (md/cp). In producing reservoirs a combination of poor vertical communication combined with differential depletion frequently leads to gradients independent of the fluid density as illustrated in figure 7-3. In such cases the wellsite plot of Mobility vs. True Vertical Depth (TVD) can successfully identify the fluid type.

c) Reservoir Fluid Identification

The pressure measurements alone can identify the reservoir fluid in fresh water or oil-base mud environment. (See figure 7-4) By presenting the plot of Pore Pressure v. TVD it is possible to identify the gas-oil contact and oil-water contact. The gradients also represent the density of the fluid in place.

d) Applications in Developed Reservoirs

In developed reservoirs the pressure recordings and recovery data can have the following applications (see figure 7-3):-

i) Characterisation of vertical and horizontal barriers.

ii) Information on vertical permeability.

iii) Identification of thief zones.

iv) Identification of reservoir length.

v) Detection of vertical flow and fluid segregation.

vi) Waterfront surveys.

In producing layered reservoirs the various layers are generally depleted at different rates. Differential depletion is revealed by the pressure depth profile, providing essential data for optimal reservoir completion design.

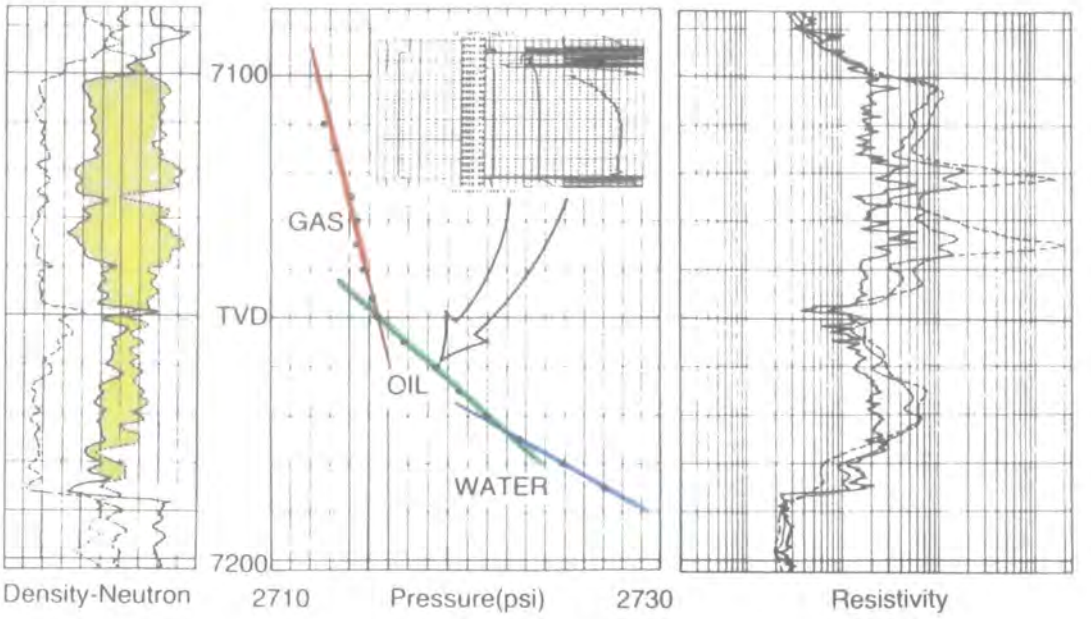

Figure 7-4. Fluid Identification example. (Schlumberger, 1981)

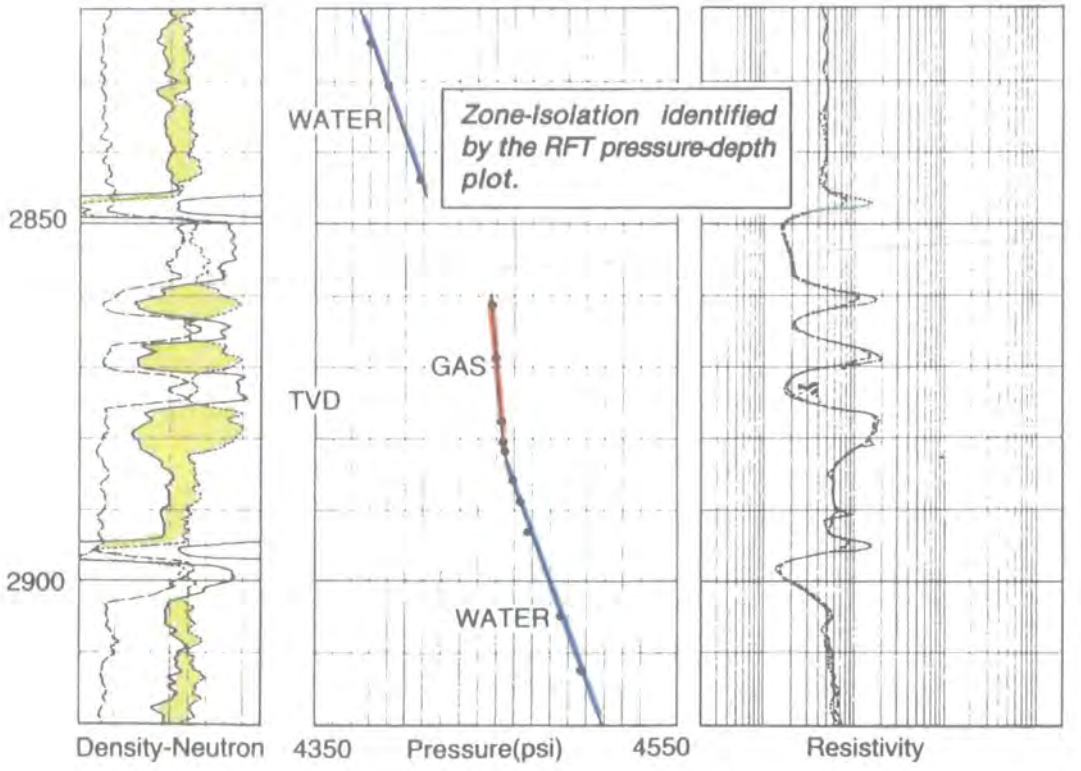

Figure 7-5. Zone-Isolation example. (Schlumberger, 1981)

e) Zone Isolation

Determination of the layering of a reservoir is particularly important in reservoir completion design and may not be apparent on openhole logs. In addition the effective design of secondary oil recovery processes based on fluid deplacement depends on the knowledge of permeability layering and the existence of horizontal or vertical barriers to flow. Figure 7-5 shows an example of zone-isolation. The precision pressure measurements provided by the sampling tool allow reliable reservoir delineation.

f) Supercharging

The sandface pressure, which is measured by the sampling tool, may differ from the undisturbed formation pressure as a result of mud filtrate invasion. This phenomenon known as "Supercharging" is significant only in low-permeability zones. The supercharging effect causes the observed formation pressure (near the wellbore) to be greater than the actual formation pressure. Supercharging is not to be confused with intrinsic formation overpressures. Two mud-related factors which affect the filtration rate are (1) the degree of pressure differential (or overpressure) between the mud and the formation and (2) the extent of mud cake buildup and its effectiveness in preventing further filtrate fluid loss into the formation. The Mud v. Formation Pressure plot (figure 7-6) produced at the wellsite provides good realtime quality control by highlighting supercharged zones. In non-produced reservoirs it also allows an accurate determination of formation fluid density.

g) Drilling Applications

The sampling tool pressure measurements provide useful data for the design of an optimal mud system. Figure 7-7 is a wellsite plot showing both the mud pressure and the pore pressure in the well. With this information it is possible to minimise the necessary overbalance and so improve the rate of penetration of the drilling bit.

Examination of the mud pressure recording permits control of the homogeneity of the mud, and the in-situ determination of mud weight in the wellbore. In figure 7-7 (enlarged portion) it is clear that the mud density increases at the bottom of the well and it may be concluded that the mud solids have begun to settle out.

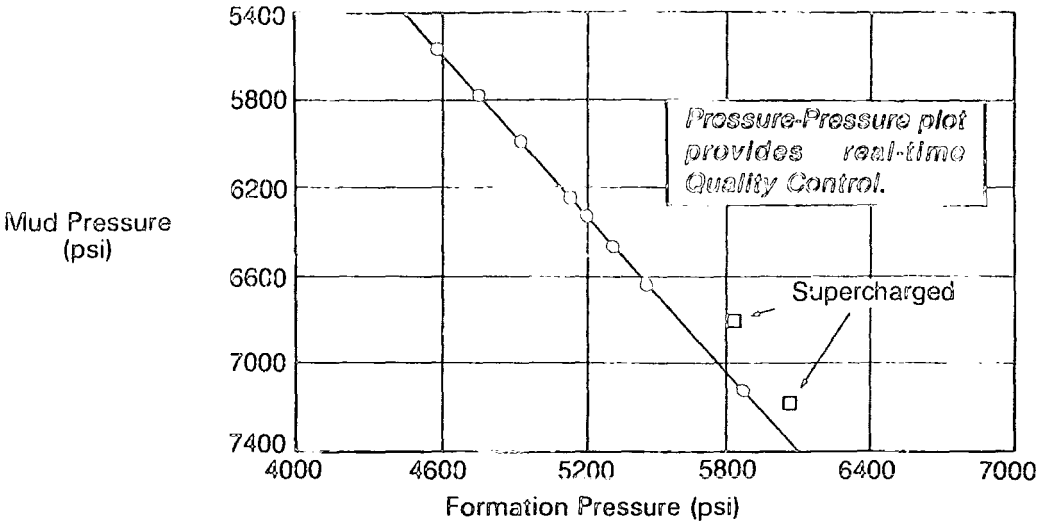

Figure 7-6. Supercharged example. (Schlumberger, 1981)

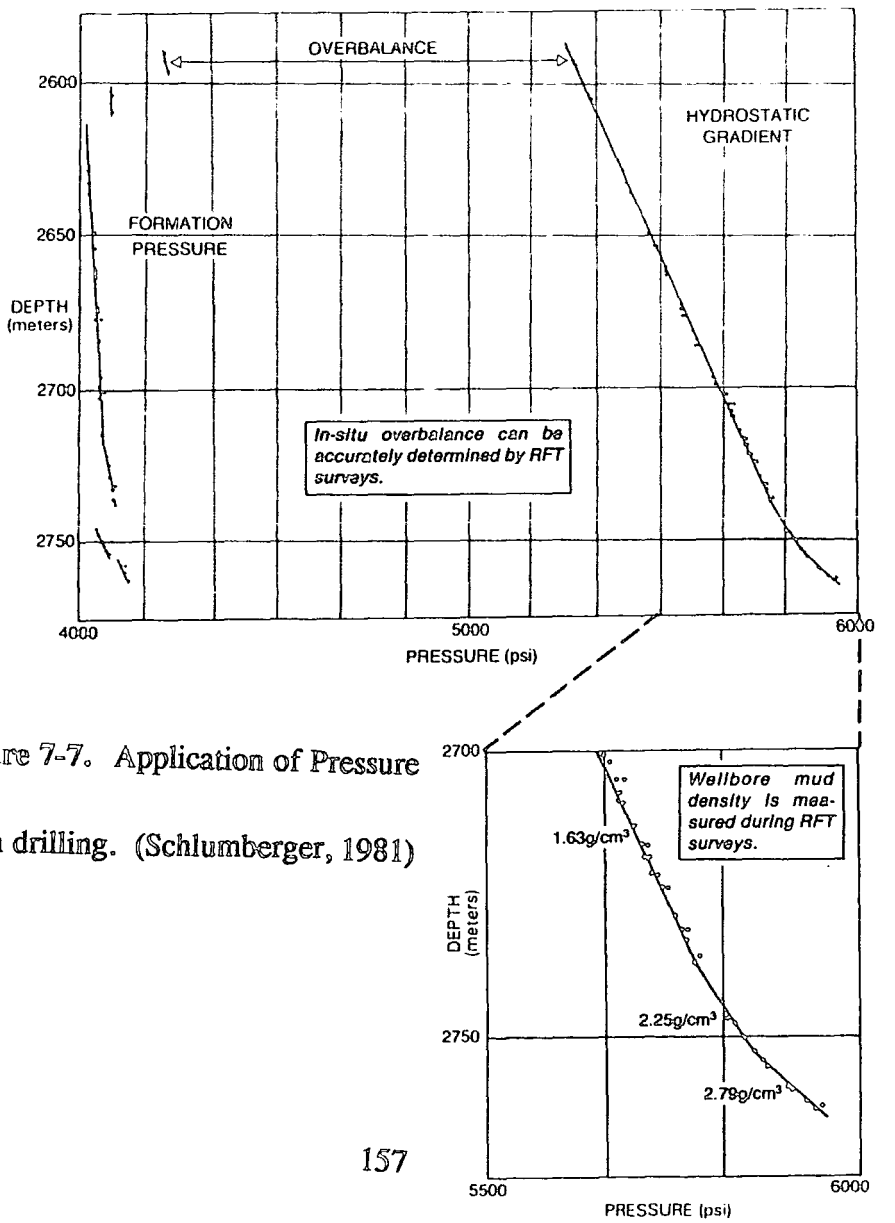

Figure 7-7. Application of Pressure data in drilling. (Schlumberger, 1981)

7.1.1 The Formation Fluid Sampling Tool.

In general, all the wireline companies use the same basic principles to design a formation fluid sampling tool. Schlumberger has the Repeat Formation Tester RFT tool, Western Atlas has the Formation Multi-Tester FMT tool, and Gearhart has the Selective Formation Tester SFT tool.

These tools provide a short production test. Once the tool is "packed-off" against the borehole wall a flow valve is opened and fluids from the formation flow into the tool's sample chamber. Sample chamber sizes vary depending on the company, from one or two small pretest chambers of 10 cm^3 each to regular 1-gallon, 2 3/4 -gallon, 4-litre, 10-litre, or larger chambers. Throughout the sampling (flow) period a continuous recording of pressure is made. Pressure recording continues after the chamber is filled in order to obtain pressure buildup data.

With this technique permeability can be estimated from the pressure drawdown data during fluid flow and from the pressure buildup data following the flow test.

The Schlumberger Repeat Formation Tester RFT tool (schematic as shown in figure 7-8) has two small pretest chambers of 10 cm^3 each and two larger sample chambers. The two pretest chambers open successively at different rates. Pretest chamber 1 opens in 15 seconds, and pretest chamber 2 opens in 6 seconds. Option to reduce the pretest chambers to 5 cm^3 for very low permeability is also possible. The sample chambers are 1-gallon, 2 3/4-gallon, or 6-gallon in size. Normally they are run in conjunction with a flow line restrictor (choke) or/and a water cushion to combat the problem of excessive drawdowns and excessive flow rates. The flow line restrictor is placed in the flow line upstream from the sample chamber to limit excessive flow. Water cushions are used to accomplish the same effect by causing the fluid filling the sample tank to displace a piston which pushes water through an orifice into an air-filled chamber. The flow rate is controlled by installing an appropriate sized orifice acting as a choke prior to the job.

Since the first generation RFT tool which was the RFT-A, Schlumberger has developed the RFT-B which, although mechanically it is the same tool, electrically it is fully digitised. With the advance in data acquisition both the tool accuracy and resolution have improved (table 7-1).

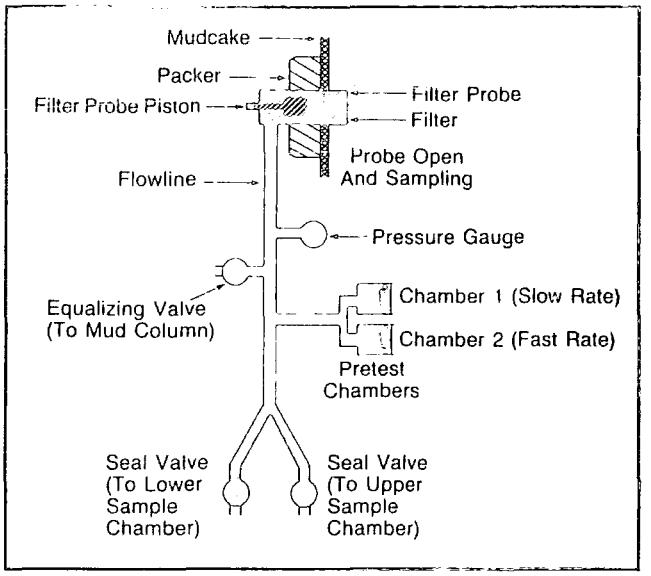

Figure 7-8. Schematic of the RFT tool. (Schlumberger, 1982)

Company	Gauge	Gauge Resolution psi	Accuracy with temp/pressure correction	kmax md
Schlumberger	RFT-A Strain guage	1	+/-0.13% of full scale	1
	RFT-A+Quartz gauge	0.1	+/-0.025% FS	5
	RFT-B Strain guage	0.1	+/-0.013% FS	5
	RFT-B+Quartz gauge	0.01	+/-0.025% FS	22
Western Atlas	FMT Strain gauge	1	+/-0.15% FS	1
	FMT+Quartz	0.1	+/-0.025% FS	5
Gearhart	SFT Strain gauge	1	+/-0.15% FS	1
	SFT+Quartz gauge	0.1	+/-0.025% FS	5

Table 7-1. Pressure Sampling Tools' Limitations.

The Western Atlas Formation Multi-Tester FMT tool works on the same basic principle as the RFT tool. However it only has one 10 cm^3 pretest chamber which can be reduced to 5 cm^3 for wells where extremely tight formations are expected. On sampling into larger chambers which can be 4-litre, 10-litre, or 20-litre in size, the flow is through a Variable Pressure Control VPC system. The schematic of the FMT system is shown in figure 7-9. The VPC is a variable orifice valve located upstream from the sample tank valve. Both valves are closed when no sample is being taken. To obtain a sample the tank valve is opened first followed by the variable orifice valve. The variable orifice valve is controlled from the surface and is opened only until a suitable flowing pressure is attained. The VPC avoids excessive pressure differentials and samples are obtained successfully without guesswork. This feature also prevents formation plugging in unconsolidated sands. The logging engineer can adjust the VPC to pressure increments as small as 5 to 10 psi. Samples can be obtained without damage or plugging from formation collapse. In addition, samples can also be taken above bubble point pressure, thereby eliminating non-representative gas/oil ratios caused by the effects of relative permeability.

The Gearhart Selective Formation Tester SFT tool works on the same basic principle of the two previously mentioned tools. Like the RFT tool, it has two 10 cm^3

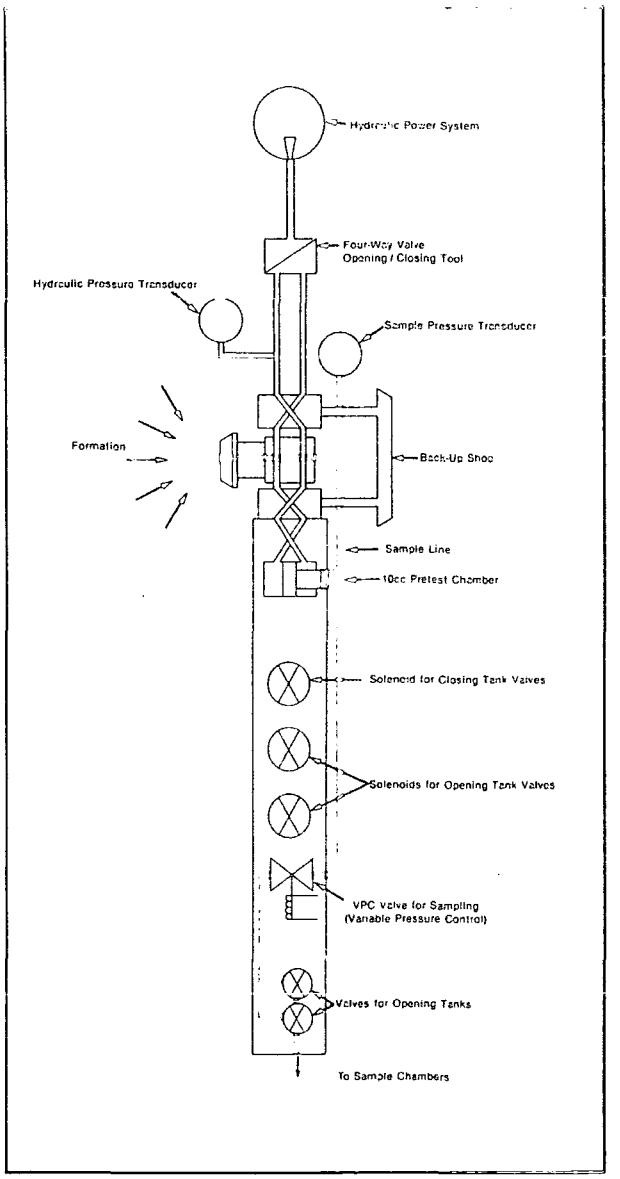

Figure 7-9. Schematic of the FMT tool. (Western Atlas, 1987)

pretest chambers. On sampling the chambers are equipped with water cushions and metered orifices. This system controls formation fluid entry by metering the transfer of the water cushion. This reduces the chance of formation fluid flowline plugging. When using smaller 1.32 gallon sample chambers the SFT has an advantage over the other two tools because it is able to attach three of these smaller sample chambers to the tool. Hence fluid samples may be taken up to three zones on a single trip into the well. In addition, the SFT's design includes a hinged connection above the sample chamber to minimise tool sticking.

Tool	Max. Pressure Rating (kpsi)	Max Temp. Rating (°F)
RFT	20	350
FMT	15	350
SFT	10 (400 min.)	350

Table 7-2 . Pressure Sampling Tools' Ratings

All the sampling tools are able to perform the same functions with a slight variation electrically and mechanically. Both the strain gauges and quartz gauges are made by an independent manufacturer so the accuracy and the resolution of the gauges themselves are not entirely dependent on the sampling tools. However if the sampling tool is fully digitised, as in the case of Schlumberger's RFT-B, the tool accuracy and resolution can be vastly improved. Also in such a case, accuracy and resolution now obtained by the strain gauge can match those normally obtained by a quartz gauge before, (see table 7-1).

Furthermore, the downhole conditions can also determine the choice of tool to be used, (see table 7-2), Gearhart SFT is only rated to 10000 psi, Western Atlas FMT to 15000 psi, and Schlumberger RFT to 20000 psi. Therefore if the well is deep and high pressures are expected, the RFT tool would be the obvious choice.

Mechanically, the Western Atlas FMT is the only tool which uses the Variable Pressure Control (VPC) valve instead of a flow line restrictor and/or water cushion. This is an advantage since it allows control while sampling and eliminates the need

to choose the correct size of flow line restrictor. In terms of taking samples the Gearhart SFT is the only tool which is able to obtain three 1.32 gallon samples during one trip into the well. This is a distinct advantage in being able to save the time needed for an extra trip into the well. The FMT and RFT tools are capable of obtaining only two samples during a trip into the well. Furthermore the SFT's design includes a hinged connection above the sample chamber to minimise tool sticking. In the case of a sticky borehole this should lessen the chance of differential sticking of the tool to the borehole wall.

In terms of operation the FMT is the only tool which has one pretest chamber. Having two pretest chambers which open at different rates can be advantageous in the case of plugging due to excessive drawdowns and flow rates. Sometimes the formation permeability may favour a pretest chamber opening at a slower rate than a faster rate. At best, with the option of two pretest chambers, pretest for permeability and mobility evaluation is more likely to be obtained.

On examining the tool specifications, the Schlumberger RFT and Gearhart SFT seem to be more desirable. In terms of resolution, accuracy, and tool ratings the RFT seems quite superior (see tables 7-1 and 7-2). This is even more so when the newer fully digitised RFT-B tool is considered. However, the SFT although at the lower range in tool ratings, does have the attraction of being capable of obtaining three samples in a single trip into the well. The Western Atlas FMT tool can operate in much the same way but it does not offer any extra feature when compared to the other two tools.

7.2 Formation Core Sampling.

Formation cores can substantiate data received from well logs as well as differentiate thin zones. Core-derived data integrated with logging information provides a more complete description of reservoir properties. In addition sidewall cores are less expensive and require less rig time than conventional cores, and faster turnaround of interpretive results is possible. Formation core samples recovered by wireline tools are commonly refered to as sidewall core samples and they aid the following :-

a) Building a lithological description.

b) Evaluating porosity/permeability.

c) Identifying thin producing intervals.

d) Recognising formation damage/sensitivity, including clay types.

e) Performing crude oil characterisation.

7.2.1 Principle

The fundamental principle of sidewall coring is simple and straight forward. A hollow cylinder is propelled at high velocity from a gun into the formation. The cylinder, containing a formation sample, is retrieved by means of a steel cable connected to the gun. Depending on the size of the hole and the type of guns the number of hollow cylinders in one trip into the well can range from 22 to 66 shots.

Sidewall coring theory was previously based on the concept that a high velocity is needed to drive the core barrel into the formation. Later and more careful studies of energy requirements for obtaining acceptable core samples have shown that this is not the case.

When a rock is penetrated by brute force, displacement of the rock material occurs in the following manner :

a) As the penetrating object breaks the cementation between the grains then they become free to move where they are pushed.

b) The grains then break into smaller pieces resembling powder and this material along with the reservoir fluid surrounding the penetrating object is driven radially into the formation or back to the borehole.

c) This action disturbs the reservoir rock and can create localised fractures and a cratering effect. The amount of disturbance depends on the compressive strength of reservoir rock and the velocity of the penetration object.

When the penetrating object is a sidewall core barrel, the volume of pulverised and damaged material surrounding the core barrel is greater if increased velocity is required to obtain a unit length of core. High velocity also affects fluid pressures inside the core barrel. As the barrel aproaches the formation it carries fluid with it (figure 7-10). The fluid inside the barrel has its own velocity. Since the barrel fluid has mass and velocity considerable pressure can result when the formation tries to stop the fluid motion. The faster the barrel travels the higher the internal fluid pressure at impact. This hydraulic effect can reduce the length of the core.

To overcome the problems of exaggerated cratering and pulverising, poor

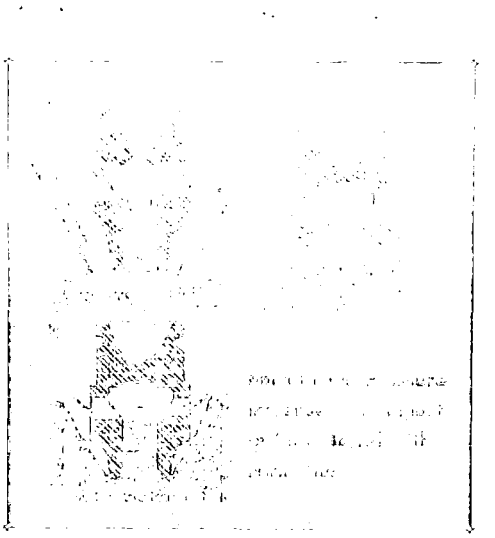

Figure 7-10. Impact of core barrel with formation. (Western Atlas, 1987)

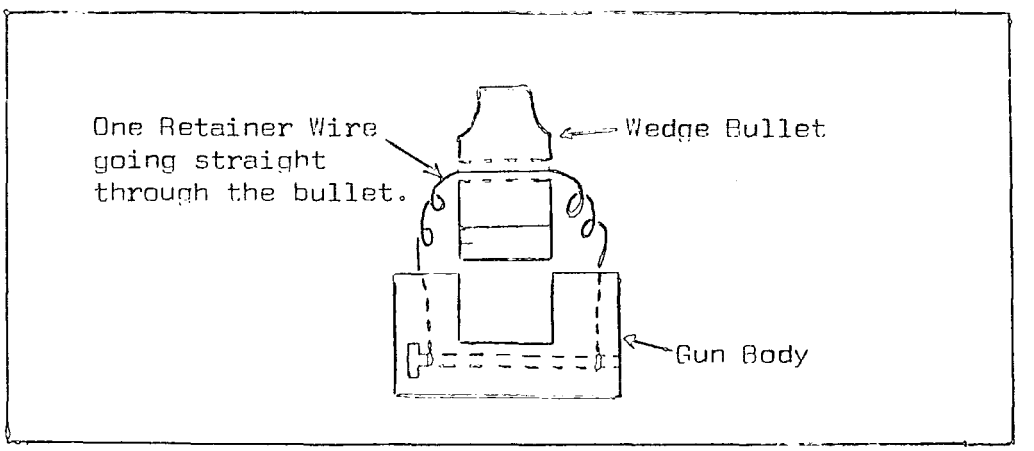

Figure 7-11. One cable retainer wire system. (Schlumberger, 1987)

quality samples, reduction in recovery rate, and damage to the core barrel resulting from the high-velocity concept, logging companies have made studies to obtain a more efficient use of the kinetic energy when the core barrel is fired from the gun body. This incorporates reduced velocity and redistribution of mass to solve the variety of problems experienced with the high-velocity technique. Thus the design of the core barrel is altered, and its velocity is decreased. These improvements can be summarised as follow :-

a) The velocity of the core barrel is reduced. The barrel is treated more like a piston than a bullet and its motion is better controlled to take advantage of inertia. This is done by shifting the mass to the rear of the barrel and more efficient vent placement and sizing to minimise the hydraulic effect.

b) Powder types and loads are changed for the new core barrels so that they are still tailored to the type of formation being cored.

c) The core barrel now strikes the formation with only the energy required to take a nominal length core. Excessive energy is detrimental to both the operation and the core.

d) Improved techniques are used to retrieve the core barrel after the gun is fired. The newer core barrel is designed to use only one cable. This system uses a centering effect to overcome problems of stress and snapping of dual cables during recovery. The design allows the cable to slide and centre itself in the barrel, resulting in a strengthened system (figure 7-11).

7.2.2 The Equipment

A formation core sampling tool is a percussion device that fires a hollow cylindrical core bullet into the formation wall to sample physically the formation. The core bullet is shot into the formation by a powder charge ignited by an electric current. The bullet containing a formation sample is then retrieved by either one wire or two wires attached to the gun. Only one core barrel (bullet) is fired at a time. A single gun can selectively core up to 30 samples on a single run and a tandem gun can selectively core up to 66 samples on a single run.

Core barrels are available to sample formations ranging from soft to very hard. The core samples are generally large enough to allow a comprehensive

core analysis. Cores range in size from 0.7 inch to 1.0 inch in diameter and up to 2 inches in length.

The SP or Gamma Ray curve, run simultaneously with the core sampling tool, provide depth comparisons with the primary suite of logs.

Company	Tool	Ratings		Hole Size (in)		No. of
		Temp. (° F)	Pressure (kpsi)	Min	Max	Shots
Gearhart	SCG	350	20	8	14	24
Schlumberger	CST-W	450	20	5 1/2	12 1/4	12
	CST-Z	450	20	8 1/2	14	30
	CAT-AA	450	20	8 1/2	14	30
Western Atlas	SCS	400	25	4 1/4	(7 5/8)	22
	(Corgun)	400	25	6	(60+)	25

Table 7-3 A selection of available formation core sampling tools.
(Figures quoted in parenthesis are for tools with positioners)

Logging companies provide a range of core sampling tools for various hole size (table 7-3). For larger hole size the tools are generally eccentralised using a positioning device attached to the tools. The tools can also be run in tandem giving the capability of more cores in a single trip into the hole.

Gearhart Sidewall Core Gun (SCG) has a capability of 24 cores and when run in tandem, 48 cores. Its charges are only rated up to 350 °F. Schlumberger has a range of Core Sample Taker (CST) tools and depending on the combination of tools being used a variable number of up to 66 cores. Its charges are rated up to 450 °F, the highest of the group of companies. Western Atlas Corgun (SCS) has a capability of up to 50 cores when run in tandem. Its charges are rated up to 400 °F.

Each core barrel is shot selectively by a powder charge ignited by an electric current. In general the logging companies use similar method to operate the coring tool. For example the Schlumberger CST-C (figure 7-12) uses cable line 1, 2 and 3 to shoot each core barrel. At first only core barrel 1, 2 and 3 are armed. Core barrel 1 uses cable line 1, core barrel 2 uses cable line 2 and core barrel 3 use cable line 3. Once core barrel 2 is shot it simultaneously pulls the arming wire which arms the next

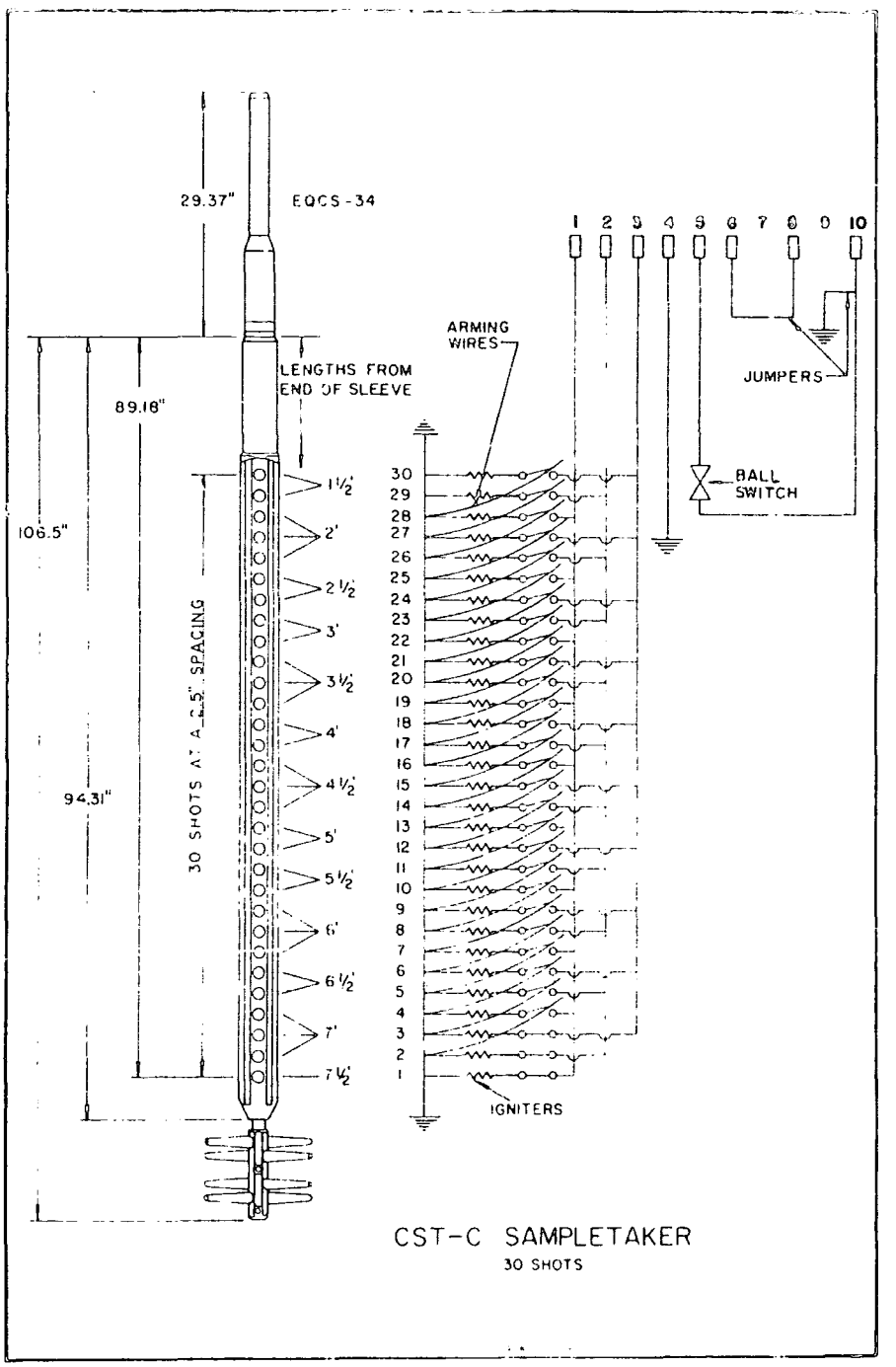

Figure 7-12. CST-C wiring diagram. (Schlumberger, 1987)

two core barrels which in this case are core barrel 3 and 4. Similarly when core barrel 3 is shot, core barrel 4 and 5 become armed. This continues until all the 30 core barrels are shot. In this way if one of the three lines goes down the operation can still continue because one core barrel arms the next two barrels of the other two lines. However if two lines are down, then the tool has to be pulled out of hole for redress.

Frequently the coring guns are run in tandem to increase the number of cores/ run. The same arming as above is still used and usually each gun is fired using current of different polarity. An alternate arming method also exists such as is the case of the Schlumberger CST-AA and CST-Z combination (figure 7.13). In each gun core barrel no. 1,2,3,10,17 and 24 are already armed and each gun uses 6 firing lines, and cable line 4 and armour cable line 10 for return. The lower gun, CST-AA, is fired by a current of positive polarity and the upper gun, CST-Z, is fired by a current of negative polarity. By using 6 firing lines, each gun is split into 4 blocks of core barrels. In this case if two successive misfired are encountered the operation can still continue by moving onto the next block of core barrels. The blocks of core barrels start at core barrel no. 1, 10, 17 and 24 respectively.

As previously mentioned, the core barrel design has also evolved over the years. Both Schlumberger and Western Atlas now have very similar wedge-shaped core barrels (figure 7-14), whereas Gearhart still operates with the core barrel of the older design (figure 7-15). The newer designs of core barrels are making more efficient use of kinetic energy and should in theory enable better core sample recovery. In addition to the equipment design, skill by the operator who pulls out the core barrel from the formation is also a very important consideration in terms of recovery. The operator must have a feel for the situation otherwise the wire joining the gun body to the core barrel would break before a formation core is recovered.

In addition to the core sampling tools mentioned, there are also core drilling tools available. Instead of using a percussion device the formation is mechanically drilled by a diamond core barrel. This type of mechanical coring tool is designed for hard rock applications where the normal percussion device may not be suitable.

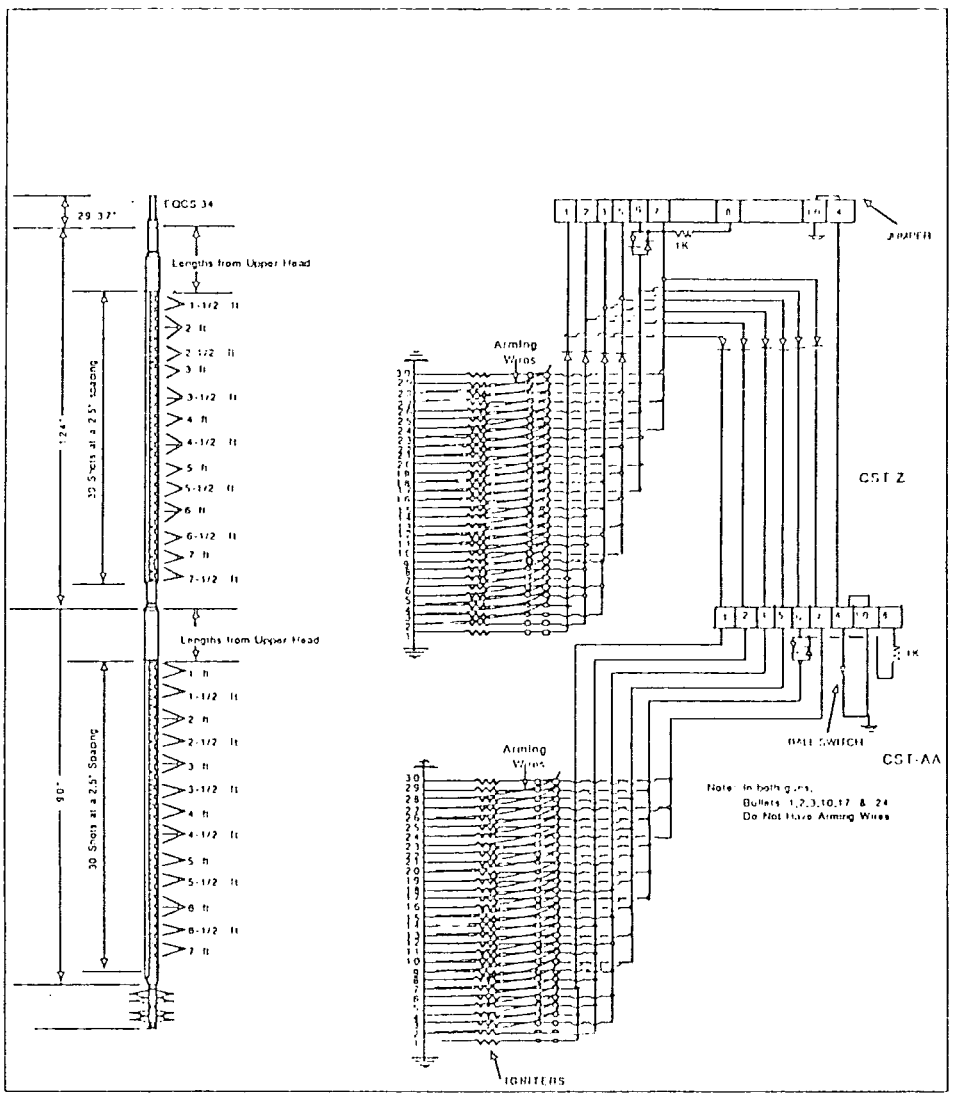

Figure 7-13. CST-AA, Z combination wiring diagram. (Schlumberger, 1987)

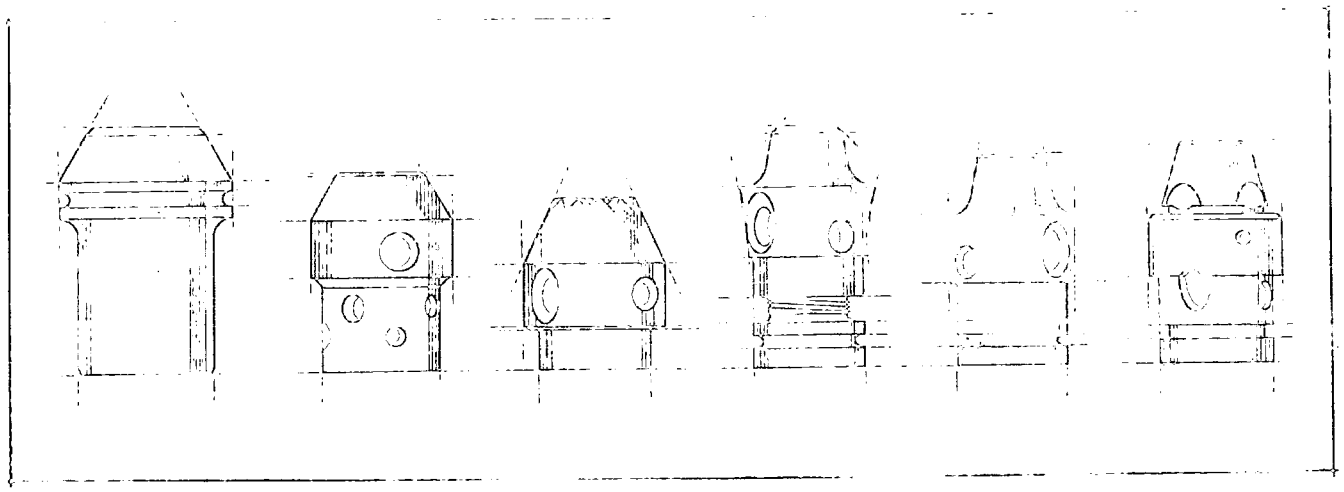

Figure 7-14. Evolution of the present day wedge bullet. (Western Atlas, 1987)

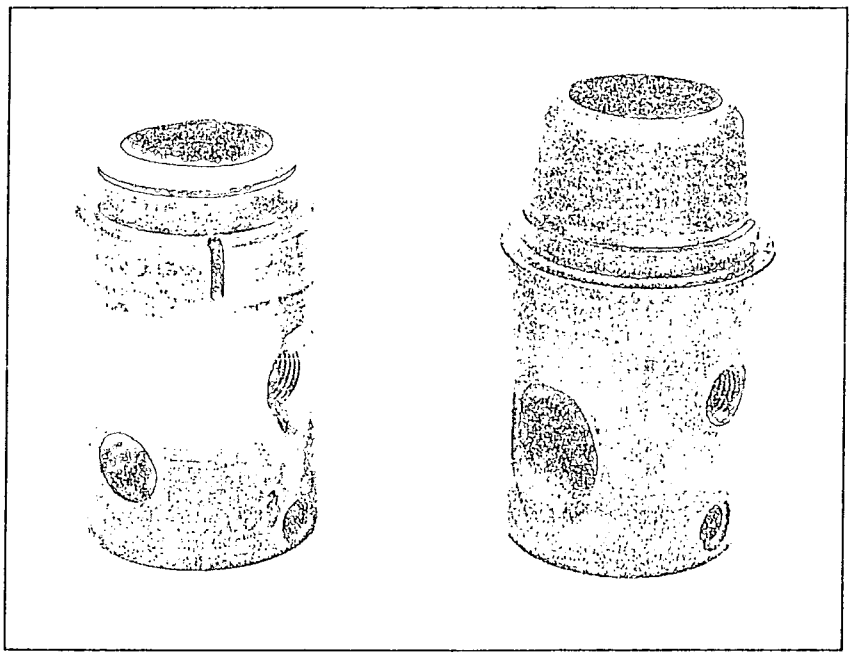

Figure 7-15. Old bullet (left) and new wedge bullet (right). (Schlumberger, 1987)

Company	Tool	Rating		Hole Size (in.)		No.of
		Temp.(°F)	Pressure (kpsi)	Min	Max	Cores
Gearhart	HRCT	350	20	6.5	13.0	12
Schlumberger	MSCT	400	20	6.25	12.75	20

Table 7-4. Mechanical Formation Core Sampling Tools' Ratings.

Gearhart and Schlumberger are the only two companies offering the service of a mechanical core sampling tool. Both tools operate by using a hydraulically driven diamond core barrel powered by an electric motor. Cores recovered by this method are not compacted as with percussion coring; thus, actual porosity and permeability can be more reliably measured. As in the case with all sampling tools, core points are selected from open hole logs and the gamma ray run with the coring tool assuring accurate location.

Although formation core sampling is regarded as an auxilary service the information gathered can better enhance the interpretation of the logs and the understanding of both the well and the reservoir. The type of coring tools available and on offer by logging companies are generally not a deciding factor for choosing a logging company.

8. ELECTROMAGNETIC PROPAGATION LOGS

8.1. Introduction

Historically water saturation in reservoir rocks has been determined from a measurement of true formation resistivity. Since most formation waters are quite saline, resistivity measurements are most effective in distinguishing between hydrocarbon and water-bearing formation. In addition, the resistivity measurement is somewhat unique in that, through proper tool design, it reflects the resistivity of the formation at some distance from the borehole with reasonable accuracy.

Unfortunately not all formation waters are saline nor are all formations always saturated with waters of a constant salinity. As a water becomes less saline, its resistivity increases. Indeed, a water containing no dissolved salts exhibits a very high resistivity, similar to that of oil or gas. It is obvious that as formation waters become fresher, resistivity measurements lose their ability to distinguish between hydrocarbons and water.

Quantitative interpretation of the resistivity measurement into water and oil saturations requires knowledge of the formation water salinity. In some geological sequences the salinity varies greatly over a relatively short interval. Similarly, in fields that have been under waterflood for some time, the injection water salinity may have varied greatly over the life of the waterflood and from well to well. As a result the formation water has become a mixture of waters of many chemical compositions.

A method that is less dependent upon water salinity and knowledge of water salinity, has long been needed to determine water saturation. The measurement of dielectric permittivity offers one alternative. Table 8-1 gives laboratory-measured values of dielectric permittivity, ε' (relative to air), of some typical reservoir materials. With the exception of water, most materials in sedimentary rocks have low values (less that 8). The measured dielectric permittivity therefore is primarily a function of the water-filled porosity. Although the dielectric permittivity of water is influenced by its salinity and its temperature the range is relatively modest and much smaller than its range of resistivity.

Electromagnetic propagation can be described by Maxwell's equation:-

Mineral	Relative Dielectric Constant	Propagation Time t_{pl}(ns/m)
Sandstone	4.65	7.2
Dolomite	6.8	8.7
Limestone	7.5-9.2	9.1-10.2
Anhydrite	6.35	8.4
Halite	5.6-6.35	7.9-8.4
Gypsum	4.16	6.8
Dry colloids	5.76	8
Shale	5-25	7.45-16.6
Oil	2-2.4	4.7-5.2
Gas	1	3.3
Water	56-80	25-30
Fresh water	78.3	29.5

Table 8-1. Dielectric constant. (Sen, 1980)

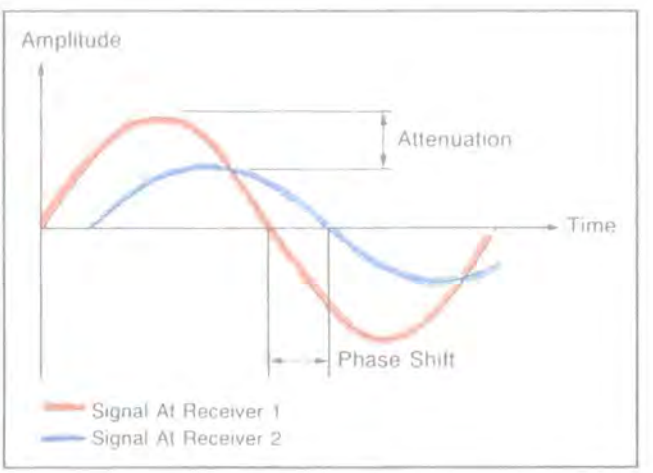

Figure 8-1. Electromagnetic propapation signals. (Wharton, Hazen, Rau, and Best, 1980)

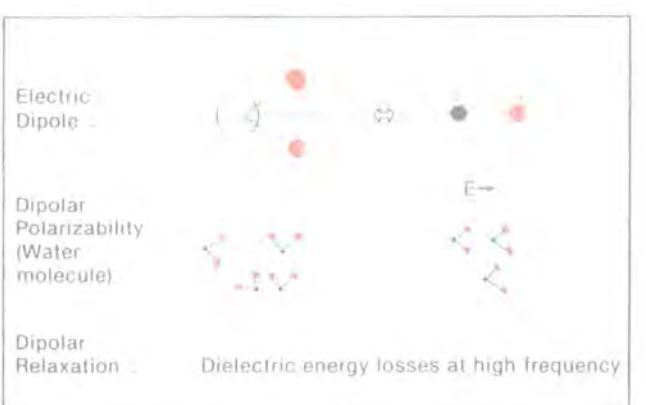

Figure 8-2. Polarisability. (Wharton, Hazen, Rau, and Best, 1980)

$\gamma = \alpha + j\beta$ (Eq. 8-1a)

$\omega^2\mu\varepsilon = \beta^2 - \alpha^2$ (Eq. 8-1b)

$\omega\mu C = 2\alpha\beta$ (Eq. 8-1c) (Calvert, Rau,& Well,1977)

where

γ is the electromagnetic wave propagation,

α is the attenuation of the wave,

β is its phase shift,

ω is its angular velocity,

μ is the magnetic permeability,

ε is the dielectric constant,

and

C is the conductivity.

A measurement of α and β can, therefore yield the dielectric constant (equation 8-1b) and the conductivity (equation 8-1c) of the formation in which the wave propagates (figure 8-1).

The toolscurrently being offered by the logging companies are:-

a) The Electromagnetic Propagation EPT tool by Schlumberger,

b) The Deep Propagation DPT tool by Schlumberger,

c) The 47-MHz Dielectric DCT tool by Western Atlas,

d) The 200-MHz Dielectric DCT tool by Western Atlas, and

e) The Dielectric Constant DCT tool by Gearhart.

The EPT is a shallow investigating device that operates at a frequency of 1.1 GHz . The DPT tool is a much deeper investigating device that operates at a frequency of about 25 MHz . Similar to Schlumberger Western Atlas has the 47 MHz DCT tool for deeper investigation and the 200 MHz DCT tool for shallower investigation. Gearhart on the other hand presently has only one tool, which operates at 500 MHz, to offer the customer.

8.2 Principle

Polarisability, dipolar relaxation and conductivity are the electrical characteristics of a medium. They can be represented altogether by a constant ε' which is called dielectric permittivity of the medium.

Polarisability is the ability of electrically charged particles of a medium to

orientate or distort themselves in an electrical field. Practically, all particles containing electric charges (atoms, molecules, etc.) are more or less subject to polarisation in an electric field. Some molecules are assymmetric and the centres of "gravity" of their positive and negative charges do not overlap. In this case they constitute a permanent electric dipole. Water is about the only material in geological formation that exhibits electrical dipole characteristics. The dipole formed by the electric charges of the atoms of hydrogen and oxygen will polarise itself in the direction of an applied electric field (figure 8-2). However at high frequency the water molecule cannot "follow" perfectly the fast variations of the direction of the electric field because of its inertia; the lag in the molecule movement with respect to the electrical field at high frequency introduces an energy loss which is dissipated in the form of heat in the medium. This phenomenon is called dipolar relaxation.

Figure 8-3 shows the above parameters related to the dielectric permittivity, ε°, and their variations as a function of the frequency of the applied electric field:

$$\varepsilon^{\circ} = \varepsilon - j\frac{\sigma}{\omega} - j\,\varepsilon_{\chi} \qquad (8\text{-}2)$$

(Sen, 1980)

C/ω is a parameter related to the conductivity losses,

ε_{χ} represents the dipolar relaxation losses, and

ε' is related to the polarisability phenomena.

8.2.1 Interpretation Methods

The shallower investigating tools (equation 8-2) respond mainly to the water content of a formation, rather than to the matrix or any other fluid. The water can be the original connate formation water, mud filtrate or bound water associated with shales. Because of the tool's shallow depth of investigation (1 to 6 inches) it can usually be assumed that only the flushed zone is influencing the measurement and that the water is primarily mud filtrate.

Under normal fresh mud conditions, t_{pl} is essentially unaffected by water salinity (figure 8-4). However, for waters with resisitivites less than 0.3 ohm-m, t_{pl} increases. Attenuation A also increases as water salintiy increases. If salt-saturated fluids are encountered, the attenuation increases to the extent that the electromagnetic waves are highly attenuated, and measurement can become difficult. A variation of

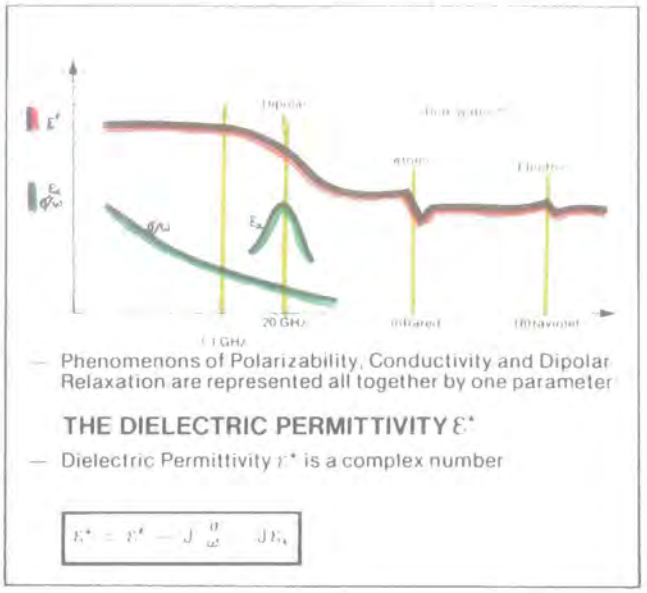

Figure 8-3. Dielectric permittivity. (Wharton, Hazen, Rau, and Best, 1980)

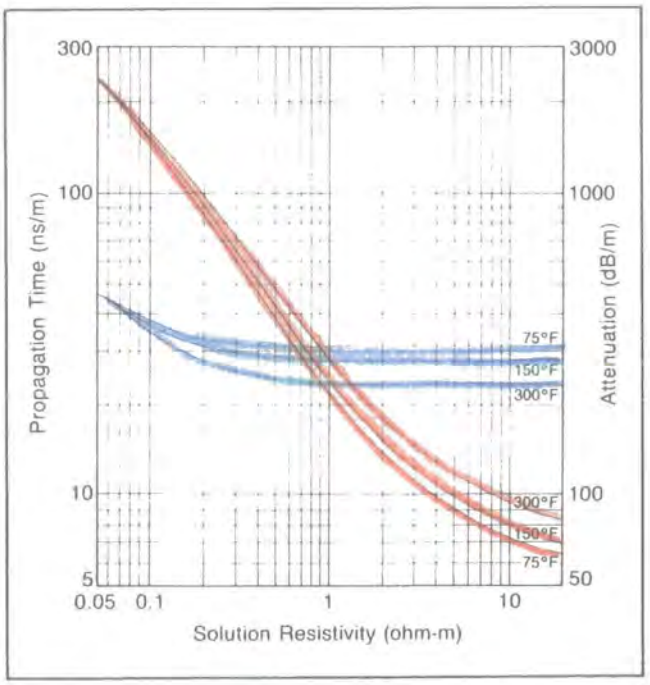

Figure 8-4. Variation of t_{pf} and A_t versus salinity and temperature. (Sen, 1980)

propagation time and attenuation because of changes in water salinity and temperature are presented in Charts 8-1 (EPT cor-1) and 8-2 (EPT cor-2).

Electromagnetic wave propagation in mixtures of materials of differing electromagnetic wave propagation, dielectric constant, and conductivity has been explored theoretically and experimentally by several investigators. The most popular relationship to emerge from these studies is a simple weight-average equation (similar to that used in density evaluation of mixtures):

$$\gamma^{\circ} = \phi \gamma_f^{\circ} + (1 - \phi) \gamma_{ma}^{\circ} \qquad (8\text{-}3)$$

(Calvert, Rau, & Well, 1977)

where,

γ° is the resultant electromagnetic wave propagation in the mixture,

γ_f° is the electromagnetic wave propagation in the fluid saturating the pores,

γ_{ma}° is the electromagnetic wave propagation in the rock matrix, and,

ϕ is the porosity.

Applying equation 8-3, individually, to the t_{pl} (phase shift), the relationship becomes

$$t_{pl} = \phi_{EPT}\, t_{pw} + (1 - \phi_{EPT})\, t_{pma}, \qquad (8\text{-}4\ a)$$

(Calvert, Rau, & Well, 1977)

and to the A_c (attenuation) it becomes

$$A_c = \phi_{EPT}\, A_w \qquad (8\text{-}4\ b)$$

(Calvert, Rau, & Well, 1977)

The subscripts, EPT, w and ma refer to EPT measurement, formation water and matrix respectively.

In each, the porosity determined is the water-filled porosity. The methods assume that the tool responds to hydrocarbons in much the same manner as it responds to matrix. Equation 8-4b also assumes that little signal attenuation occurs in the matrix.

Comparing ϕ_{EPT} with the actual porosity, ϕ, of the formation gives the water saturation of the zone investigated, most likely the flushed zone:

$$S_{XO} = \frac{\phi_{EPT}}{\phi} \qquad (8\text{-}5)$$

(Calvert, Rau, & Well, 1977)

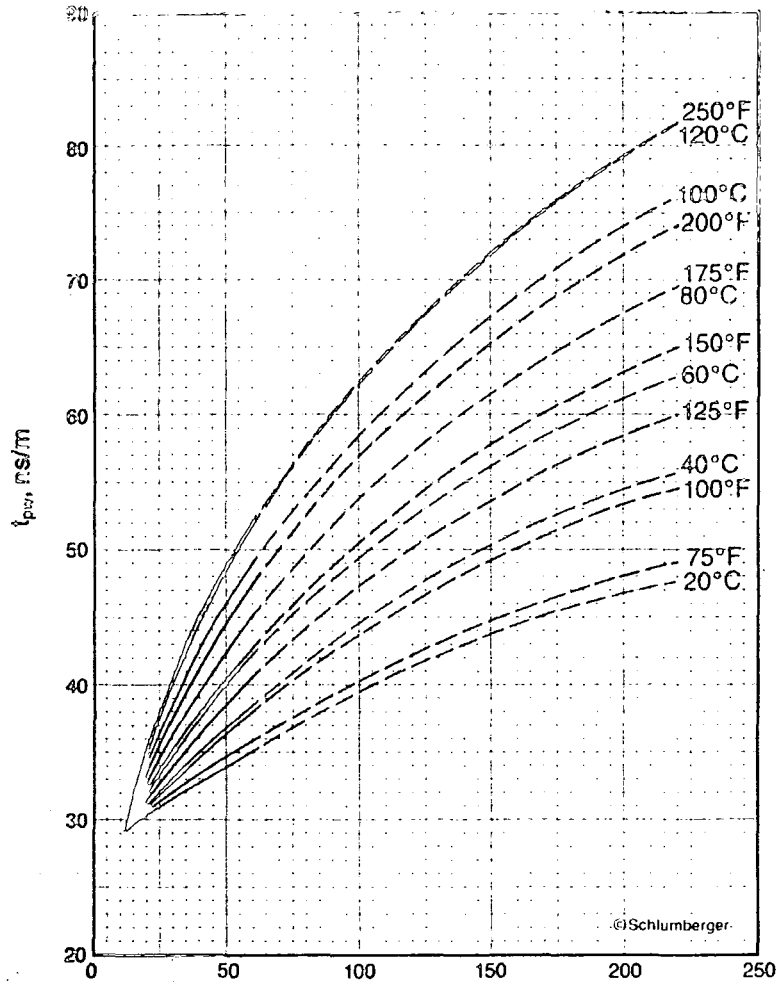

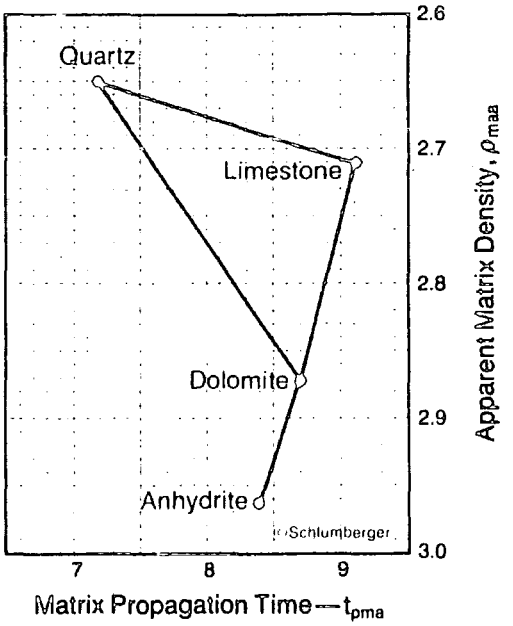

EPT Matrix Propagation Travel Time

*Mark of Schlumberger

EPTcor-1

Chart 8-1. EPT Cor-1 chart. (Schlumberger, 1987)

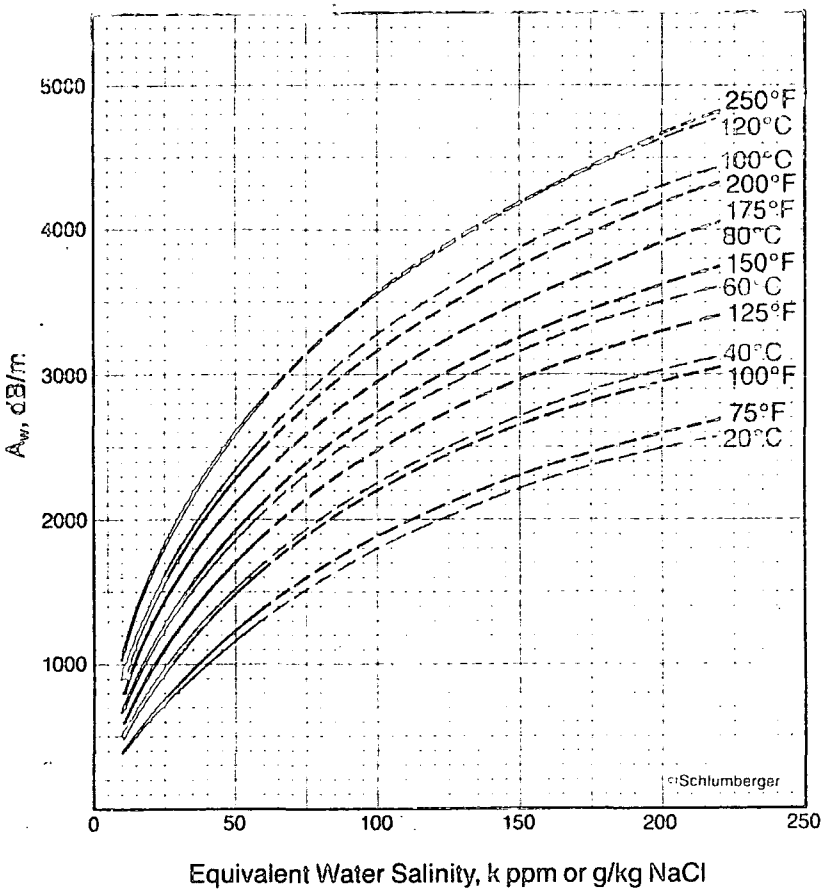

EPT Spreading Loss

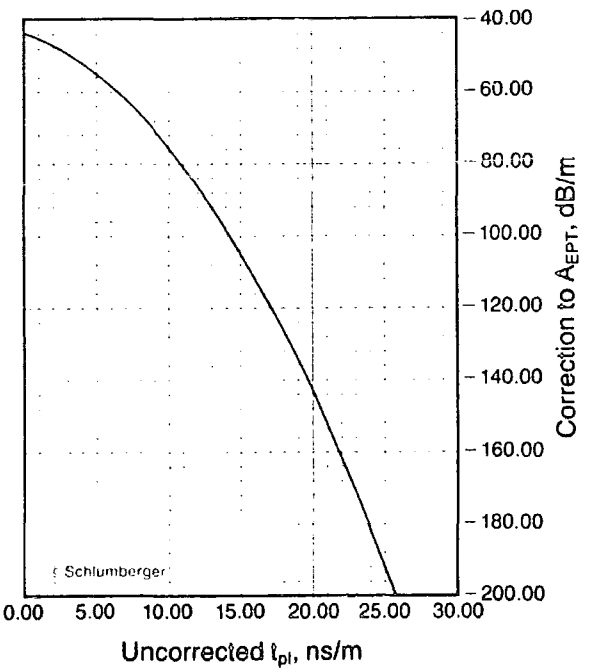

*Mark of Schlumberger

EPTcor-2

Chart 8-2. EPT Cor-2 chart. (Schlumberger, 1987)

Chart 8-3 (S_{XO} -1) graphically solves equation 8-4a and 8-5 to yield S_{XO} from t_{pl}. Chart 8-1 (EPT cor-1) provides estimates of t_{pw} and t_{pma} for use in equation 8-4a and Chart 8-3 (S_{XO} -1).

Chart 8-4 (S_{XO} - 2) graphically solves equation 8-4b and 8-5 to yield S_{XO} from A_c. Chart 8-2 (EPT cor-2) is used to estimate the attenuation in the saturating water, A_w, as a function of formation temperation temperature and water salinity.

The interpretation of deeper investigating tools is more complicated because the technique has to accomodate''dispersion'' and changes in dispersion. Dispersion is the term used to describe the changes with frequency in the dielectric constant and conductivity. It also appears to be a function of salinity (e.g. in a water-saturated rock dispersion increases as formation water resistivity, R_w, decreases).

In constant-salinity or freshwater environments the relationship between the water saturation, S_w, and the dielectric constants is:

$$\sqrt{\varepsilon_{DPT}} = \phi S_w \sqrt[p]{\varepsilon_w} + \phi (1 - S_w) \sqrt{\varepsilon_h} + (1 - \phi) \sqrt{\varepsilon_{ma}} \qquad (8\text{-}6)$$

(Huchital, Hutin, Thoraval, and Clark, 1981)

where

ε is the dielectric constant, and

p is a polarisation exponent.

The subscripts, DPT, w, h and ma refer to the DPT measurement, formation water, hydrocarbon, and matrix, respectively. The exponent p can be estimated from chart 8-5 as a function of water resistivity.

8.3 The Equipment

The Schlumberger EPT sonde is a pad-type tool with an antenna pad attached rigidly to the body of the tool (figure 8-5). A backup arm has the dual purpose of forcing the pad against the borehole wall and providing a caliper measurement (figure 8-6). A standard microlog pad attached to the main arm allows a resistivity measurement to be made with a vertical resolution similar to that of the electromagnetic measurement. A smaller arm which exerts less force, is mounted on the same side of the tool as the pad and is used to detect rugosity of the borehole. The borehole diameter is the sum of the measurements from these two independent arms.

Flushed Zone Saturation from EPT* Propagation Time

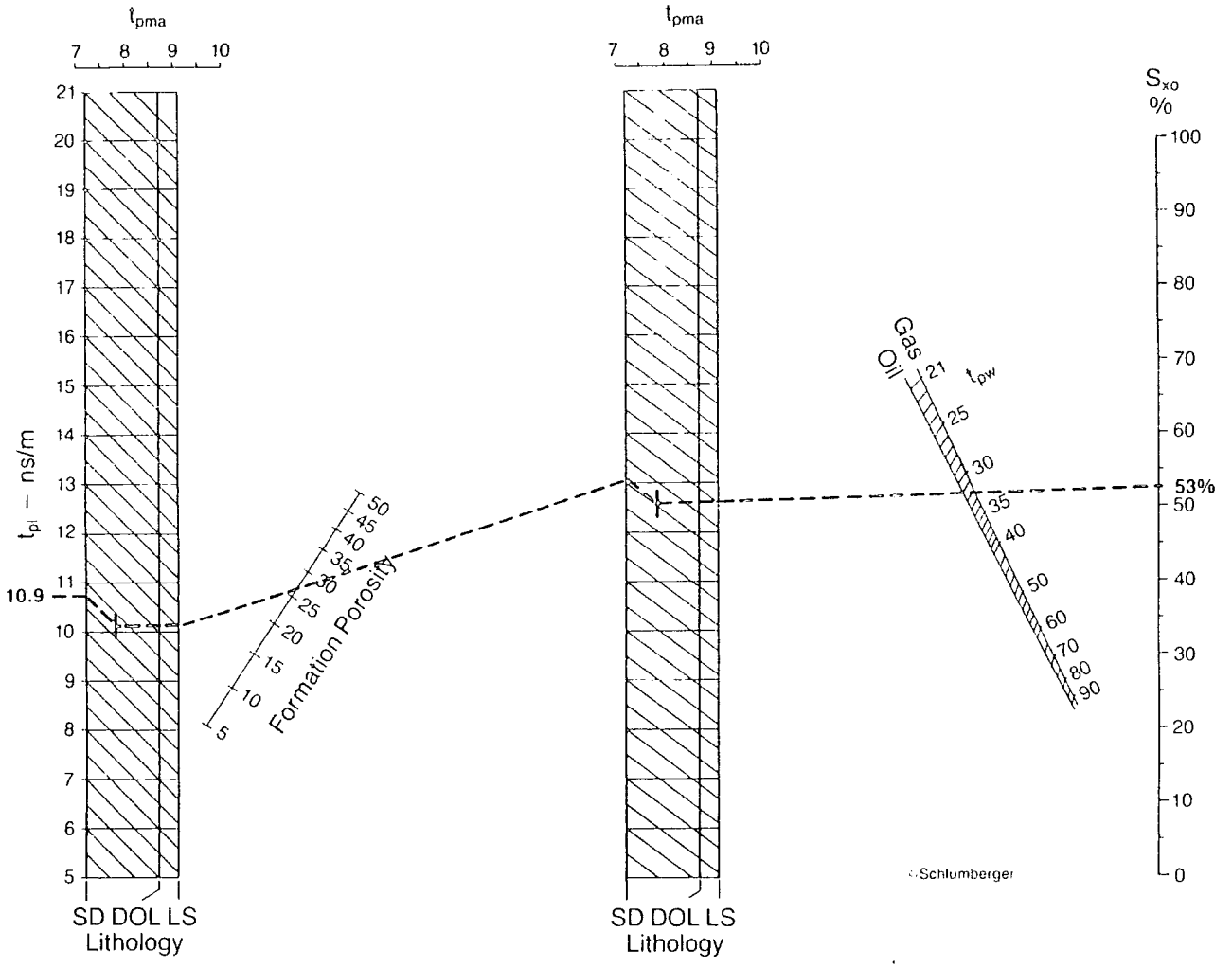

This nomograph defines water saturation in the rock immediately adjacent to the borehole, S_{xo}, using the EPT propagation time measurement, t_{pl}. It requires knowledge of reservoir lithology or matrix propagation time (t_{pma}), the saturating water propagation time (t_{pw}), porosity, and the expected hydrocarbon type.

Water propagation time, t_{pw}, can be estimated from the appropriate chart on the opposite page as a function of equivalent water salinity and formation temperature. Rock lithology must be known from other sources. For rock mixtures the chart on the opposite page can be used to estimate matrix propagation time, t_{pma}, when the apparent matrix density, ρ_{ma}, is known. The estimation does require some knowledge of the expected mineral mixture.

To use the nomograph, t_{pl} is entered on the left grid; follow the diagonal lines to the appropriate t_{pma} value, then horizontal to the right edge of the grid. From this point, a straight line is extended through the porosity to the center grid; again follow the diagonal lines to the appropriate t_{pma} value, then horizontal to the right edge of the grid. From this point, extend a straight line through the intersection of the t_{pw} and hydrocarbon type point to the S_{xo} axis. For additional information see Reference 25.

EXAMPLE: t_{pl} = 10.9 ns/m
ϕ = 28%
Limy sandstone with ρ_{ma} = 2.67 g/cc
Water salinity ≃ 20 k ppm, BHT = 150°F
Gas saturation expected.

Giving, t_{pma} = 7.8 ns/m (sand-lime mixture)
t_{pw} = 32 ns/m

And, S_{xo} = 53%

*Mark of Schlumberger

Sxo-1

Chart 8-3. S_{XO} - 1 Chart (Schlumberger, 1987)

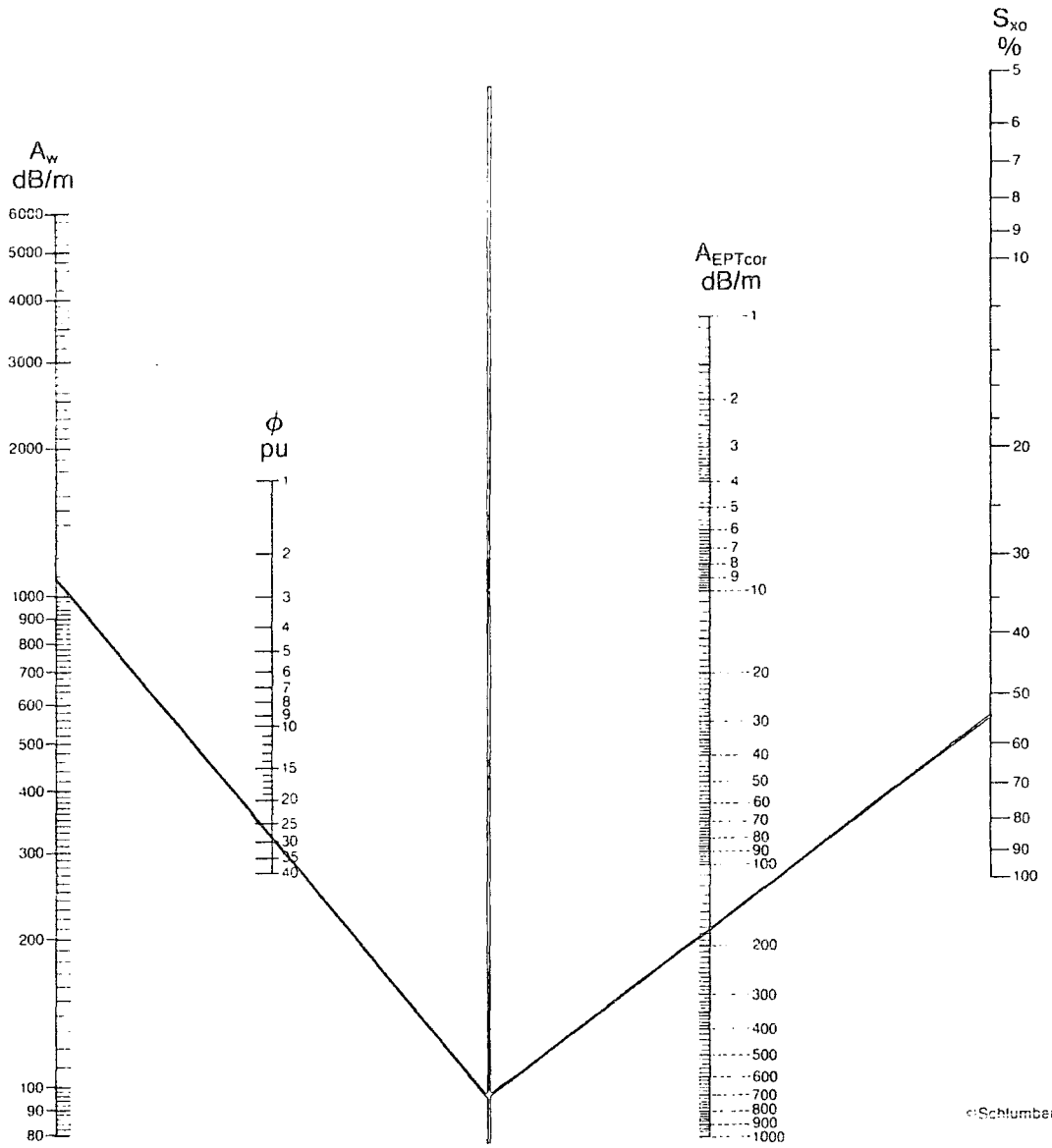

The nomograph defines water saturation in the rock immediately adjacent to the borehole, S_{xo}, using the EPT attenuation measurement. It requires knowledge of saturating fluid (usually mud filtrate) attenuation (A_w), porosity, and the EPT attenuation (A_{EPTcor}) corrected for spreading loss.

Fluid attenuation (A_w) can be estimated from the appropriate chart on the opposite page knowing the equivalent water salinity and formation temperature. EPT spreading loss is also determined from a chart on the opposite page based on the uncorrected EPT t_{pl} measurement. The spreading loss correction algebraically added to the EPT attenuation measurement gives the corrected EPT attenuation, A_{EPTcor}.

These values, together with porosity, inserted into the nomograph lead to the flushed zone water saturation, S_{xo}.

EXAMPLE: A_{EPT} = 250 ns/m
t_{pl} = 10.9 ns/m
ϕ = 28%
Water salinity = 20 k ppm, BHT = 150°F

Giving, spreading loss = −82 dB/m
A_{EPT} = 250 − 82 = 168 dB/m
A_w = 1100 dB/m

And, S_{xo} = 54%

*Mark of Schlumberger

Chart 8-4. Sxo - 2 Chart (Schlumberger, 1987)

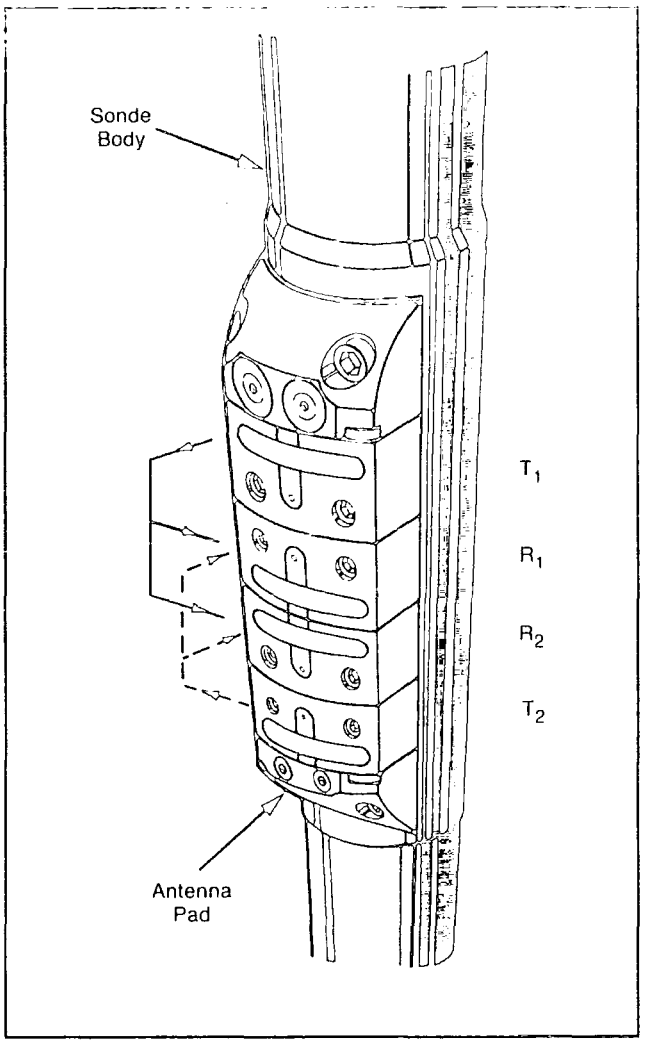

Figure 8-5. Antenna pad of the EPT sonde. (Schlumberger, 1984)

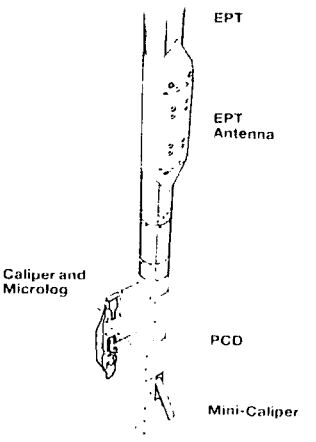

Figure 8-6. EPT tool. (Schlumberger, 1984)

Two microwave transmitters and two receivers are mounted in the antenna pad assembly in a borehole compensated array that minimises the effects of borehole rugosity and tool tilt (figure 8-5). The two transmitter receiver spacings of 8 cm and 12 cm provide an acceptable depth of investigation; at the same time, the detected signals have sufficient amplitude and no possibility of phase wrap-around. A 1.1 GHz electromagnetic wave is sent sequentially from each of the two transmitters; at each of the receivers, the amplitude and the phase shift of the wavetrain are measured (figure 8-1).

With reference to figure 8-3 and equation 8-2 it is important to note that around 1.1 GHz ε is constant, ε_χ is negligeable (versus ε) ,and C/ω is small (versus ε' if C is not too large). Thus, all measurements of dielectric permittivity made at 1.1 GHz will mainly read the part ε of the dielectric permittivity, provided that the conductivity of the formation is not too large. ε' which is also called the dielectric constant (table 8-1) is in fact a function of the temperature of the medium and, to some extent, of its salinity (constant for low salinity). This is therefore the optimum frequency at which the tool operates.

The propagation time of the wave, t_{pl}, , (where $t_{pl} = \beta/\omega$) and the attenuation, A, over the receiver-spacing are determined from the individual measurements . In each case an average is taken of the measurements derived from the two transmitters. A complete borehole-compensated measurement is made 60 times per second; these individual measurements are accumulated and averaged over an interval of either 2 or 6 inches of formation prior to recording on film and magnetic tape.

Because of the close proximity of the receivers to the transmitters, spherical waves are being measured; therefore a correction factor must be applied to the measured attenuation to compensate for the spherical spreading loss, SL. The corrected attenuation is given by the relationship

$A_c = A - SL$ (8-7) (Wharton, Hazen,Rau, & Best, 1980)

where

A_c is the corrected attenuation

A is the measured attenuation,

and

SL is the spherical attenuation loss.

The Western Altas 200-MHz DCT instrument is a pad-type device with two transmitters and two receivers (figure 8-7). The transmitters are alternately fired to provide compensation for pad tilt, borehole rugosity, or small instrumentation imbalances. This is a similar idea to the Schlumberger EPT tool. The distances of transmitter to receiver no. 1 and no. 2 are 10 inches and 13 inches respectively. Chart 8-6 is the response chart of this tool. The optimum operating conditions for the 200-MHz DCT are when the flushed zone resistivities are greater than 0.6 ohm-m and the boreholes are less than 20 inches.

The Gearhart 500-MHz DCT tool concept is similar to both the EPT and the Western Atlas's 200-MHz DCT tools. The optimum operating conditions are when the flushed zone activities are greater than 0.4 ohm-m and the boreholes are less than 18 inches.

The Schlumberger DPT tool is a deep-investigating device. As with the EPT tool an electromagnetic wave is launched from a transmitting antenna and its signal level and relative phase are measured at axially spaced receivers. These measurements are then transformed into attenuations and phase shifts. (For the EPT tool the measured propagation time is in reality also a phase shift measurement.) The computed attenuations and phase shifts can be used to determine the dielectric constant and resistivity or the formation.

The DPT tool is a mandrel device. Its operating frequency of 25 MHz is about midway between that of the standard induction tools (20 kHz) and the EPT tool (1.1 GHz) It has one transmitting loop antenna which radiates electromagnetic energy into the formation surrounding the borehole. Four receivers also loop antennas are located at staggered distances above the transmitting antenna (figure 8-8).

The receivers are grouped in two pairs (the "far" pair and the "near" pair); the signal attenuations and phase shifts between the two receivers of each pair are recorded. These attenuations and phase shifts are then used to compute, through equation 8-1, the apparent formation dielectric constant and apparent formation resistivity. Chart 8-5 graphically illustrates the solution.

Depending on the signal origin, several computations of dielectric constant and

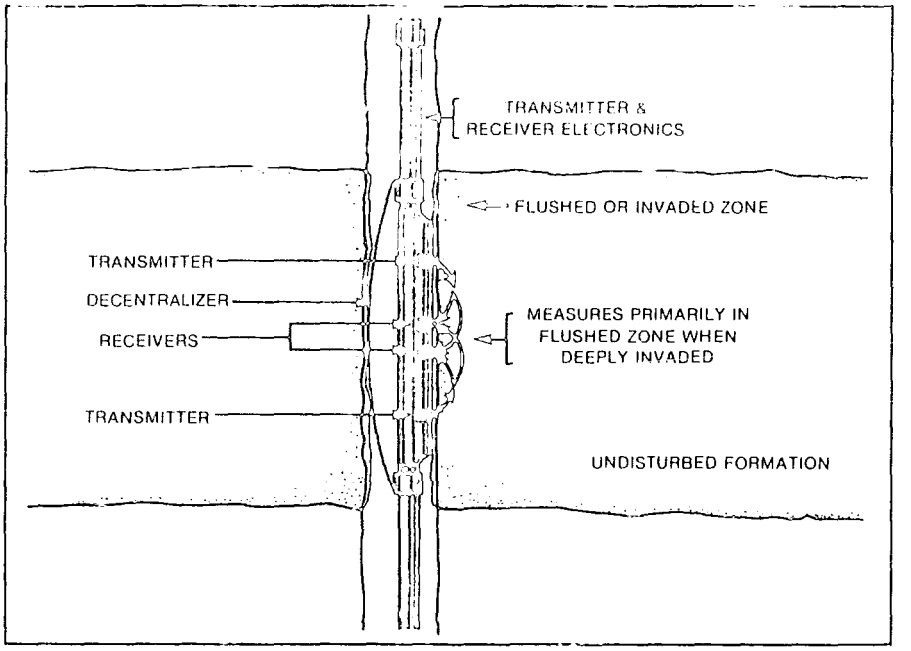

Figure 8-7. 200-MHz DCT tool configuration. (Western Atlas, 1988)

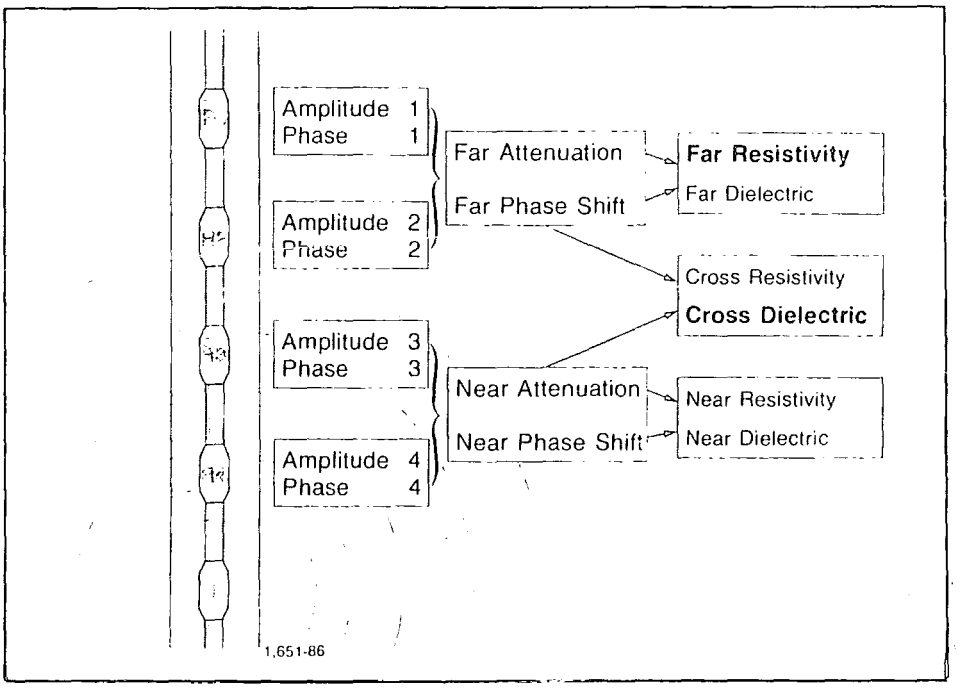

Figure 8-8. Deep Propagation tool. (Huchital, Hutlin, Thoraval, and Clark, 1981)

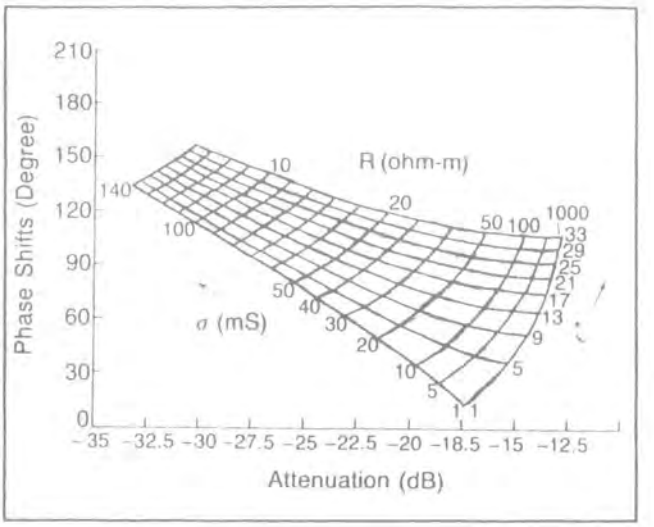

Chart 8-5. DPT phase shift/attenuation to epsilon/sigma conversion chart. (Huchital, Huthin, Thoraval, and Clark, 1981)

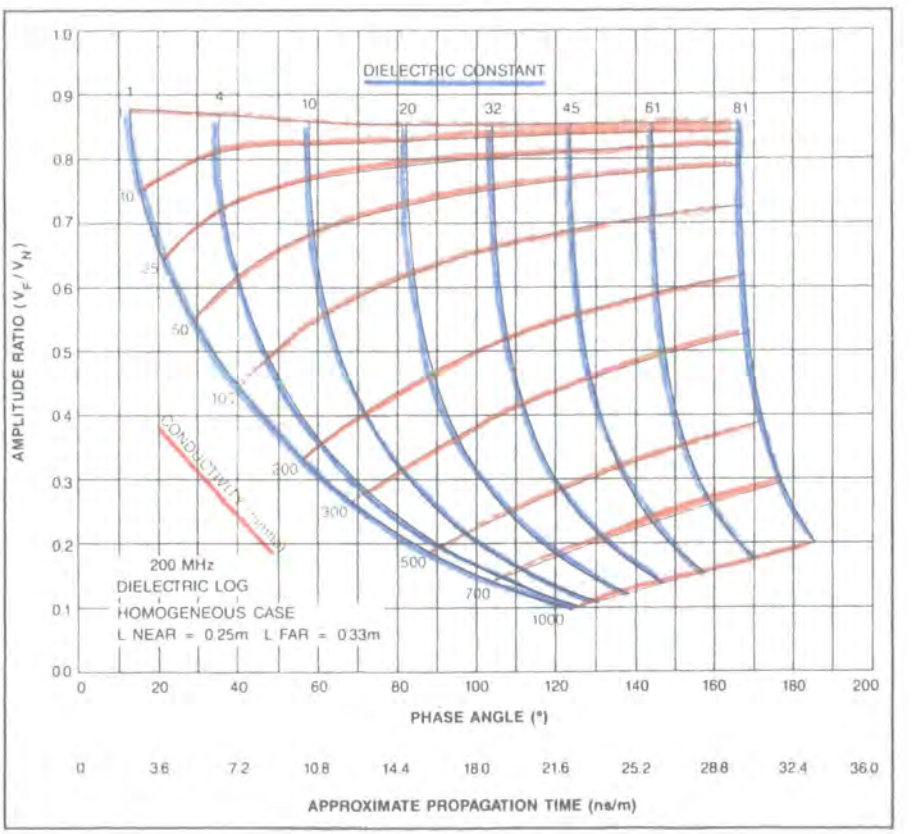

Chart 8-6. 200-MHz DCT tool response chart.(Western Atlas, 1988)

resistivity are made. These are:-

a) The DPT ''near'' measurements which use the near pair attenuation and phase shift.

b) The DPT ''far'' measurements which use the far pair attenuation and phase shift.

c) The DPT ''cross'' measurements which use the near pair attenuation and the far pair phase shift.

d) The DPT ''deep'' measurements which use a combination of attenuations and phase shifts from both receiver pairs.

The near measurement is the shallowest, followed by the far, and then the cross or the deep. These curves correctly indicate the invasion profile. Generally the cross, far, and deep are rather similar. Since their accuracy starts to degrade when they separate a comparison of the three provides a built-in quality control.

The receiver spacings and operating frequency for the DPT tool are chosen to be as sensitive as possible to the virgin, noninvaded formation parameters of dielectric constant and resistivity, over a large range of mud and formation parameters of dielectric constant and resistivity. Unfortunately the depth of investigation cannot be characterised in a simple fashion. It depends on the characteristics of both the virgin and invaded zones. Typical depths of investigations (diameters) are:

	Rt > Rxo	Rt < Rxo
Near	25 inches	20 inches
Far	45 inches	30 inches

Both mud and formation resistivity limit the tool's use. The lower the mud or formation resistivity the lower are the received signal levels. In addition the lower the formation resistivity, the less resolution there is in the measurement of dielectric constant. Acceptable accuracy is obtained in conditions where $R_{mud} \geq 0.2$ ohm-m, $R_T \geq 10$ ohm-m, and in 8-inch-diameter boreholes. If there is little invasion an acceptable dielectric constant measurement can be obtained in conditions where $R_{mud} \geq 0.1$ ohm-m and $R_T \geq 3$ ohm-m using the near receivers. In this case, the resistivity measurement is accurate to 1 ohm-m.

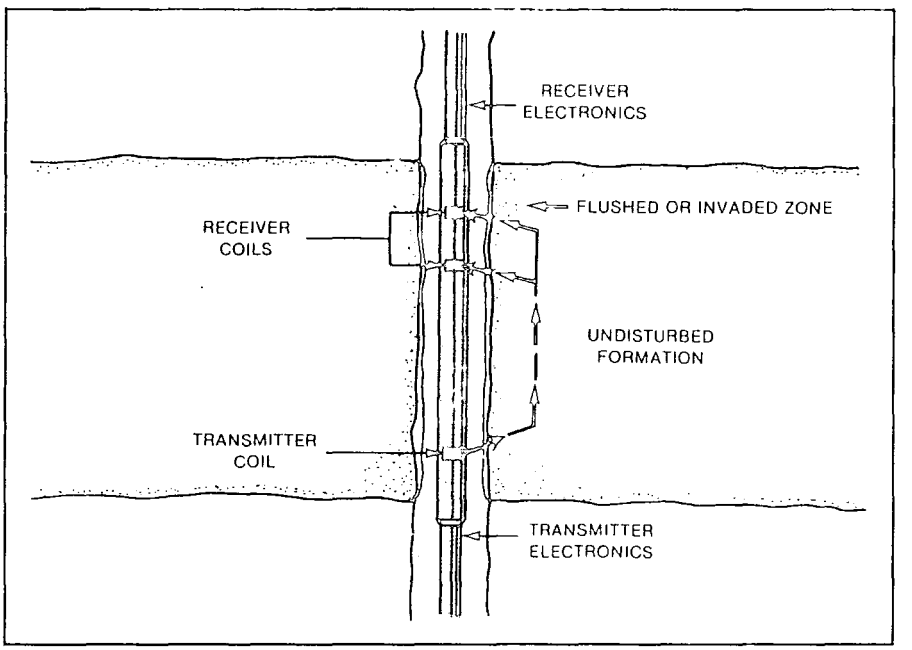

Figure 8-9. 47-MHz DCT tool configuration. (Western Atlas, 1988)

Qualitative results can be obtained in beds 4 feet thick; for quantitative applications bed thickness of 8 feet is required. Both the dielectric constant and the conductivity are frequency dependent and also salinity dependent. The term dispersion is normally used to describe these changes of the dielectric constant and conductivity with frequency. Therefore the interpretation technique should accomodate dispersion and changes in dispersion. Two groups of DPT interpretation techniques have evolved. One assumes dispersion remains relatively constant; the other accomodates changes.

The Western Atlas 47-MHz DCT instrument is a mandrel-type device with one transmitter and two receivers (figure 8-9). Attenuation is determined by the ratio of the signal amplitude measured at the far receiver relative to that at the near receiver. The wave velocity is obtained by measuring the phase difference between the signals at the two receivers. The propagation time, t_{pl} ,derived from the phase difference measurement and inversely related to the velocity is presented as a logging curve:

$$t_{pl} = \frac{\theta}{360\, f\, L} \times 109 \qquad (8\text{-}4)$$

(Huchital, Hutin; Thoraval, and Clark, 1981)

where

f = the frequency of the transmitted wave in Hz,

L = receiver spacing in m, and

θ = phase difference measurement in degrees.

Unlike the Schlumberger DPT tool, the Western Atlas DCT tool has only two receivers with distances of 31.50 inches and 39.37 inches respectively from the transmitter. This gives the tool a vertical resolution of 7.78 inches (0.2m). The response is numerically modelled as shown in chart 8-7. The tool operates better in relatively fresh mud systems and where the formation resistivities are greater than 3 ohm-m.

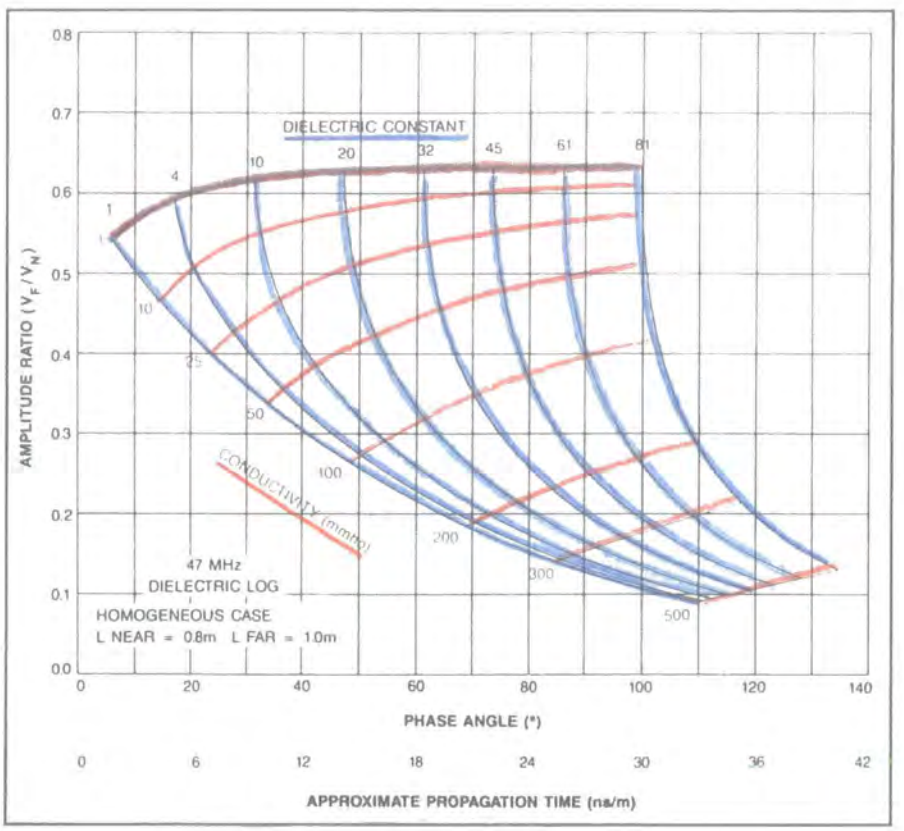

Chart 8-7. 47-MHz DCT tool response chart. (Western Atlas, 1988)

Company	Tool	Max. Temp (°F)	Max.Pressure (kpsi)	Operating Frequency (MHz)
Gearhart	DCL	205	0.7	500
Schlumberger	DPT	350	20	25
	EPT	350	20	1100
Western Atlas	DCT	350	20	47
	DCT	350	20	200

Table 8-2. Electromagnetic Propagation Tools' Ratings.

With reference to figure 8-3 and equation 8-2, it is clear that the Schlumberger EPT tool is operating near an optimum frequency. The Gearhart DCL tool is operating at 500-MHz, but has low temperature and pressure ratings. The lower the frequency at which a tool operates the less accurate will be the estimation for S_{xo} determination. Hence it seems that the Schlumberger will probably give a more accurate S_{xo} determination followed by Gearhart and then Western Atlas.

On the deeper investigating devices, even though there is little difference in the operating frequency of the Schlumberger DPT and Western Atlas DCT tools, the DPT tool is probably better because it has four receivers instead of only two. The two extra receivers act as a build-in quality control of the data and also provides the invasion profile.

9. WELLBORE SEISMIC

9.1 Introduction

In the early stages of planning the exploration and development in a new area, surface seismic surveys are used extensively to delineate prospective structure or stratigraphic traps. Recent improvements in digital filtering and processing techniques have led to high-quality results in favourable conditions. The resolution of seismic surveys however, is still fundamentally limited by low operating frequencies.

When drilling commences, opportunities exist to improve this situation through the use of well logs. After editing and calibrating against check shots the sonic and density logs can be used to generate synthetic seismograms. These synthetics are extremely valuble in verifying reflection events in a seismic section and relating seismic features to geological structures. Velocity anomalies or inversions which may cause exploration wells to be drilled off-structure can be resolved.

The physical property being measured is the formation velocity. The velocities of the formations are obtained by measuring the time required for a wavelet generated by a surface energy source to reach the seismic tool which is positioned at various depths in a well (figure 9-1). The recorded travel times of the direct arrivals (figure 9-2) are used to adjust the sonic log for drift (difference between seismic and integrated sonic times) which is caused mainly by dispersion and borehole effects. Sonic logs which have been calibrated in this way by check-shot surveys are the basic references needed to scale a surface seismic section in depth.

Borehole seismic records can be obtained by recording several seconds of waveform data at one level and repeating the process at frequent downhole intervals (figure 9-2). This type of recording is known as a Vertical Seismic Profile (VSP) (figure 9-3).

The total wavefield recorded by the tool in the well consists of both downgoing and upgoing events (figure 9-2) which will be separated by computer processing. The study of upgoing and downgoing waveforms provides the means of analysing the acoustic response of the earth in detail. The complete seismic wavetrains (figure 9-2) are recorded digitally and standard signal processing techniques are used in order to enhance the primary response of earth.

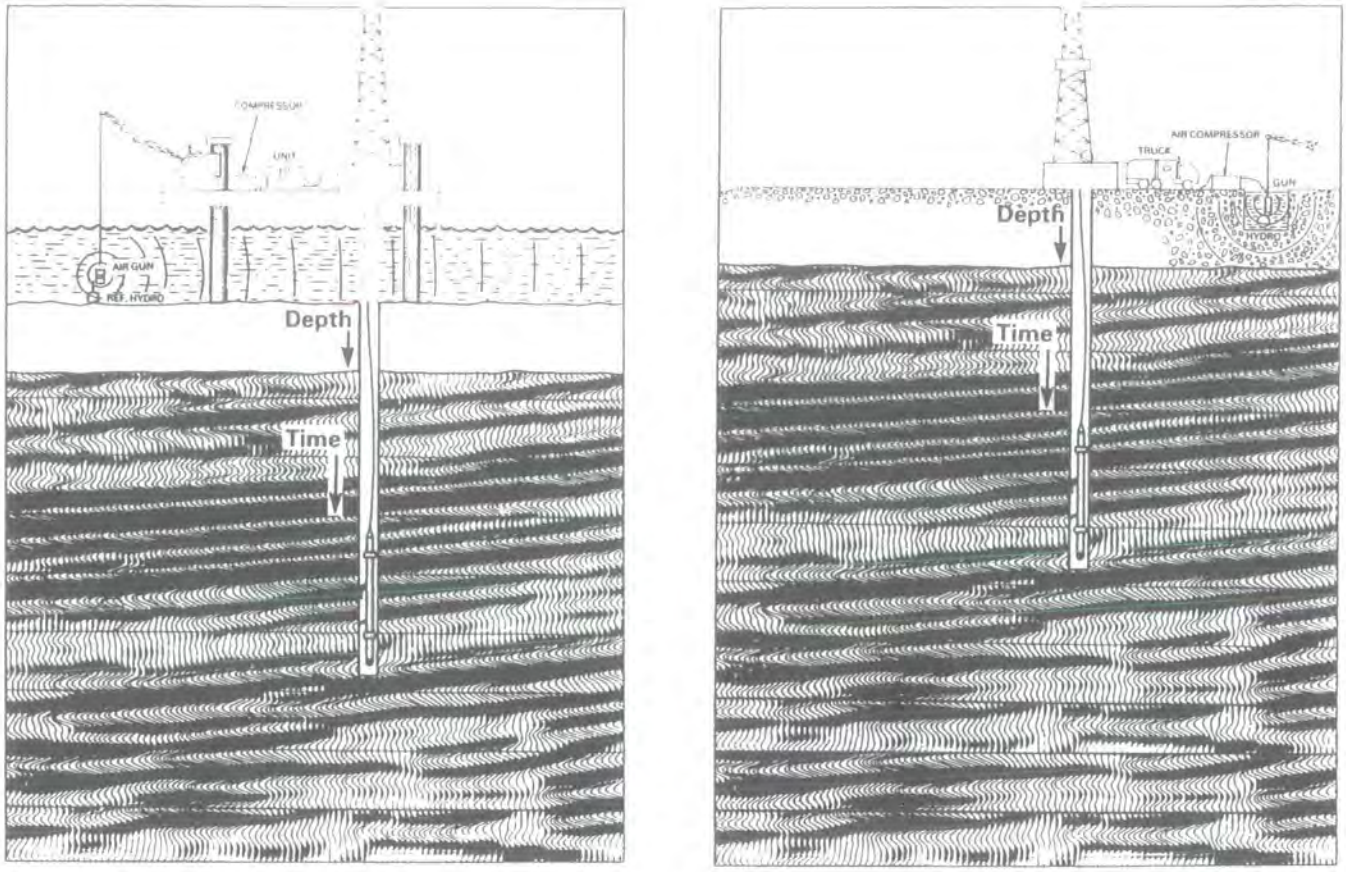

Figure 9-1. Well Seismic field set up, offshore (left) and land (right). (Schlumberger, 1987)

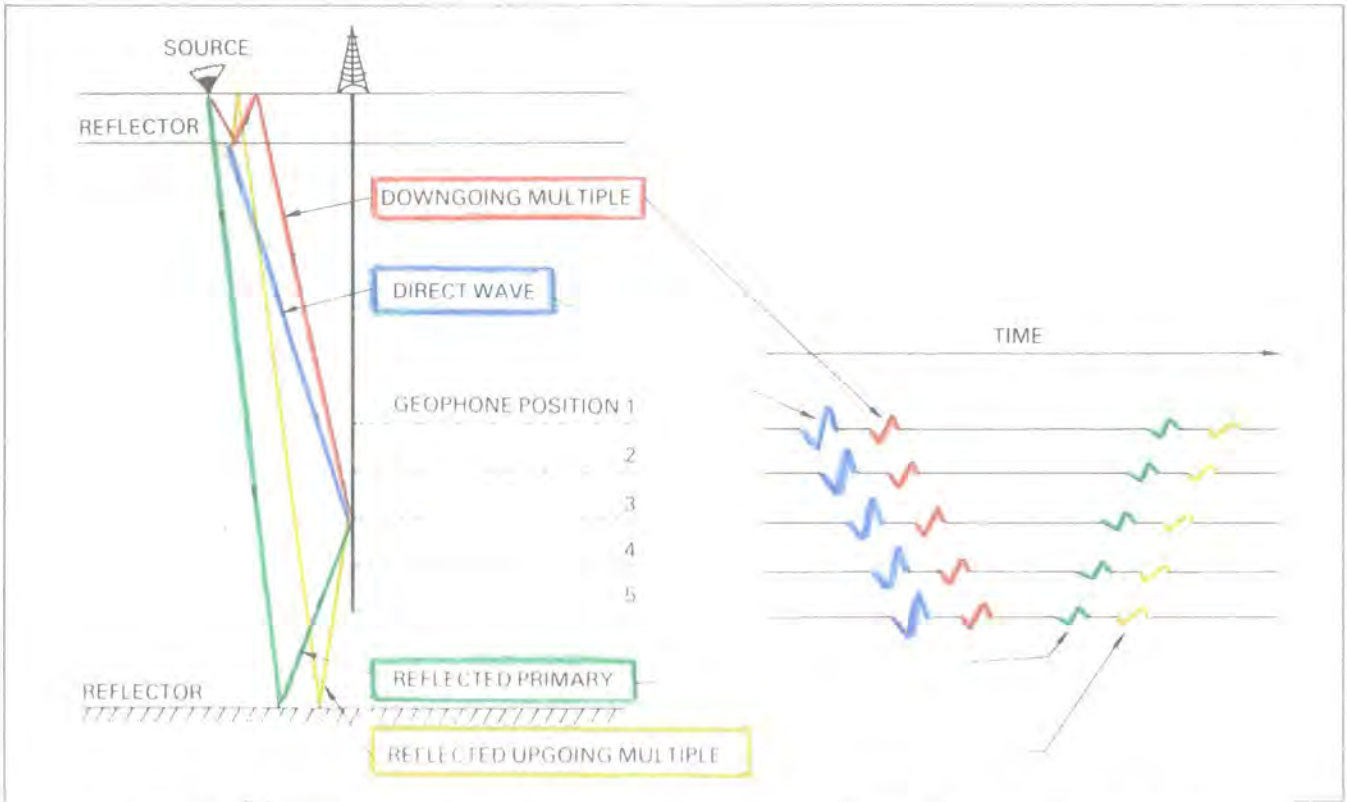

Figure 9-2. Seismic wavetrain. Recordings at multiple levels produce a Vertical Seismic Profile (VSP). Multiples can be seen clearly on the display. (Schlumberger, 1987)

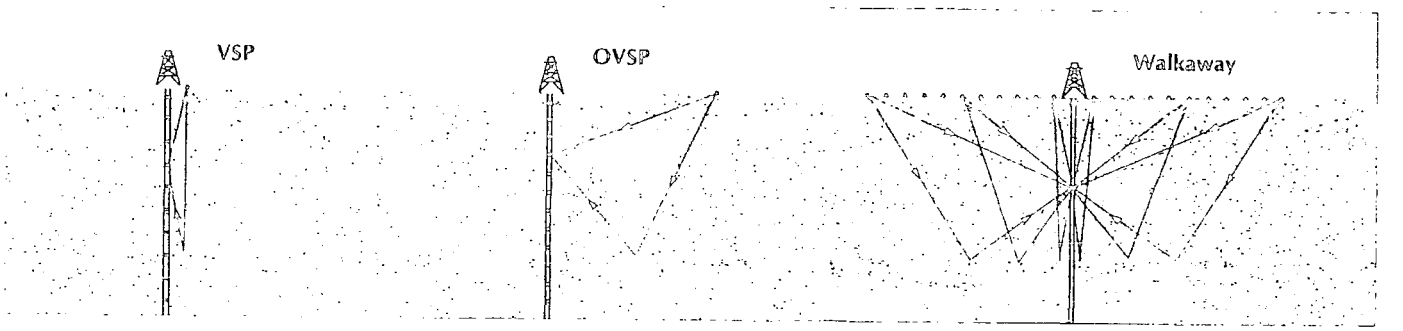

Figure 9-3. Typical ray path configurations for borehole seismics: from left, vertical seismic profile (VSP), offset vertical seismic profile (OVSP), and walkaway. (Belaud, Christie, de Montmollin, Dodds, James, Kamata, and Schaffner, 1988)

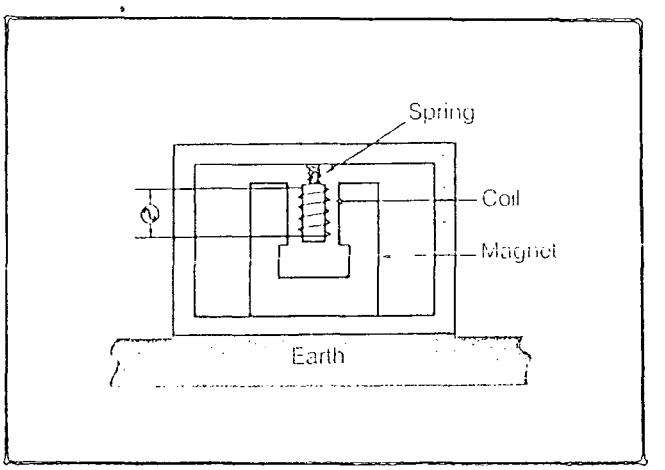

Figure 9-4. Schematic diagram of an electromagnetic geophone. The magnet is mounted to the geophone casing and the coil is wrapped around a cylinder and suspended from the case by a spring. Relative motion between the magnet and coil induces a voltage across the coil proportional to the velocity of the particles along the axis of the coil. (Schlumberger, 1987)

The simultaneous recording and subsequent separation of upgoing and downgoing waves leads to a better understanding of the acoustic properties of the earth through a study of the two wavefields. Well seismic data give better lithology correlation than surface seismic data because the borehole signal is less attenuated and has a higher signal-to-noise content. Also the precise depth of the reflection and therefore its correlation with lithology is known.

Applications of well seismic services include: adjustment of a sonic log for drift, time-depth conversion, determination of processing parameters, identification of multiples, prediction below the bit and more generally the calibration of all surface seismic interpretations.

9.2 Well Seismic Equipment

The equipment generally consists of downhole tool with geophones (figure 9.4), surface recording system, offset shooting equipment, and an air gun system. The most commonly used offshore energy source is the air gun. Its safety, reliability, cost, broad spectrum, simple signature, and transportability make the air gun a convenient seismic source. An array of synchronised air guns can be used if a large power output for deeper penetration is needed. The air gun firing chambers incorporate a wave-shaping kit that significantly reduces the bubble effect and produces a clean signal. The portable air compressor and air storage bottles provide an adequate air supply for fast, uninterrupted operations.

Other sound sources such as a vibrating truck unit or water gun are routinely used in the field depending on specific applications and local conditions.

When using an impulsive source such as a water or air gun the source signal is recorded at the surface by a hydrophone. This allows a precise determination of time break and permits continuous monitoring of the gun signature. The recorded source signature is used to enhance the signals recorded by the geophone in VSP processing.

The data are recorded digitally on magnetic tape with the surface recording system. The seismic waveforms can also be presented in analog form on film. Several shots recorded at the same level can be stacked to improve the signal-to-noise ratio (figure 9-5).

Gearhart has the Seismic Well Survey (SWS) tool whose seismic source is by

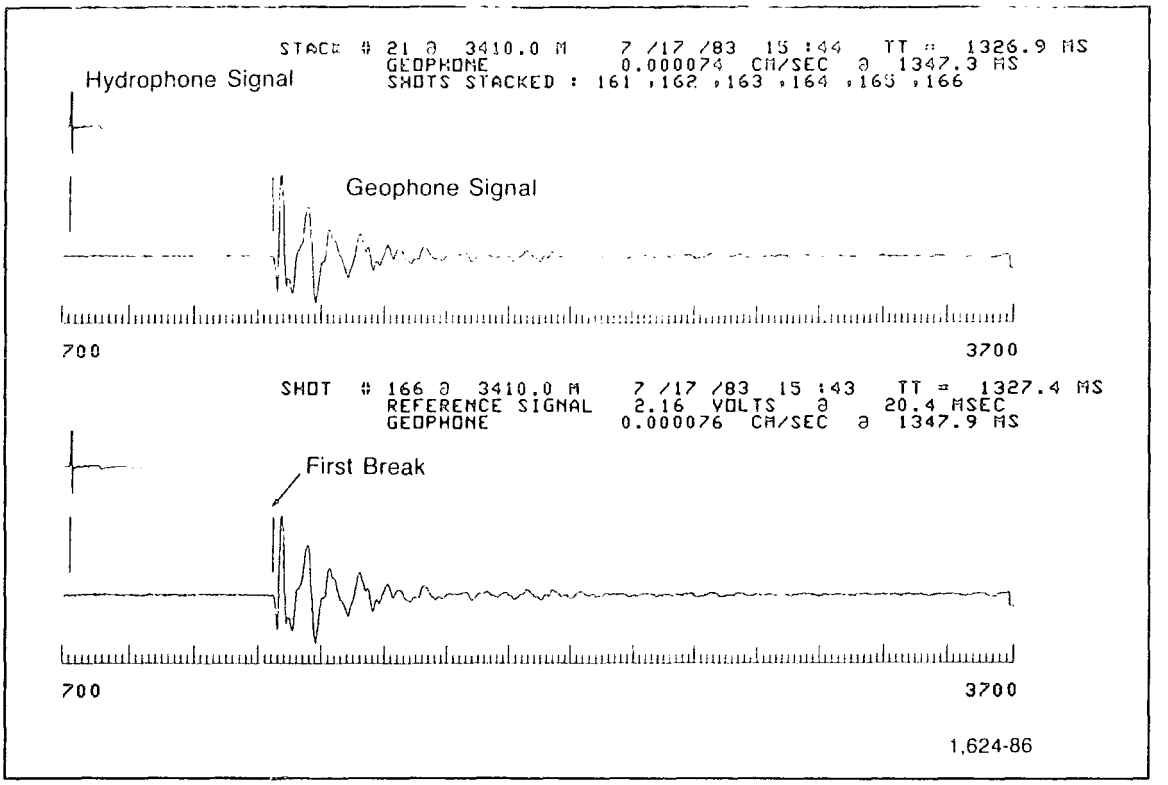

Figure 9-5. Field recordings of well seismic signals. (Schlumberger, 1987)

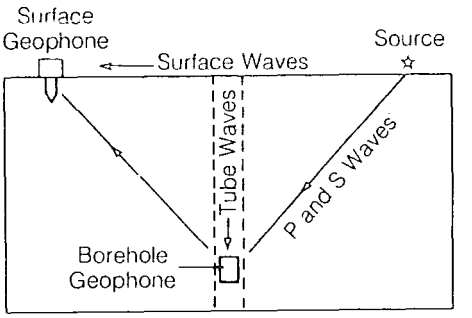

Figure 9-6. Tube waves generated when surface waves emitted by the source encounter a borehole. Tube waves usually travel more slowly than compressional and shear body waves and thus may dominate geophone response at late times. (Babour, Joli, Landgren, and Piazza, 1987)

means of shot-holes, airguns, or vibrators. The data is recorded via geophones downhole which are contained in a 2-arm probe hydraulically positioned against the borehole.

Schlumberger offers a variety of seismic tools: the Well Seismic (WST) tool, the Seismic Acquisition (SAT) tool, the Downhole Seimic Array (DSA) tool, and the Combined Seismic Acquisition (CSAT) tool. The latter three are discussed in more details later on. The WST tool is a "single-axis" tool orginally designed to record check shots, and was adapted to record waveforms on tape for further processing. The basic theory behind the tool and its operations are much the same as the Gearhart design.

Similarly, Western Atlas offers much the same package in their Seismic Reference tool (SRS). Table 9-1 gives a temperature and pressure ratings under which the tools mentioned can operate.

Company	Tool	Max.Temp. (°F)	Max. Pressure (kpsi)
Gearhart	SWS	350	18.5
Schlumberger	WST	350	20
	SAT	350	20
	DSA	350	20
	CSAT	350	20
Western Atlas	SRS	350	20

Table 9-1 Seismic Tools' Ratings.

As can be seen, all logging companies are able to offer the basic seismic services required by an operator. The check shot survey which is concerned only with the first arrival break-time measurement is a relatively simple service which does not require tools of high technical details. However when running vertical and offset seismic profiles which are concerned with both arrival times and with the processing of the reflected and direct wavefields seen by the downhole sensors, the information required is greater than what the SWS, WST, or SRS tool can provide because of its "single-axis" nature.

The first generation of borehole seismic tools used a single geophone to

measure only the vertical component of the particle motion, due to compression (P) waves and shear vertical (SV) waves. Modern tools are designed to measure the two horizontal components of motion as well. These are the two components, upgoing and downgoing, due to the shear horizontal (SH) waves. Large horizontal components arise when the reflecting planes of a formation are not horizontal or the source is offset from the well geophone. A three-axis measurement contains the complete wavefield yielding improved imaging near the well and estimates of formation density, velocity, and anisotropy. With three-axis recording, geophysicists can determine the arrival angles of seismic signals and the formation's compressional and shear velocities and delineate salt domes, reef flanks, and faults.

As the understanding of how tools behave acoustically downhole improves the borehole seismic tool design has evolved too. Historically geophysicists perceived a gap between tool and formation as the most significant source of signal distortion downhole. They modelled this gap with an oscillating mass-spring system which indicated that distortion would occur whenever the resonant frequency of the tool-formation system fell within the seismic bandwidth. According to the model, raising the resonant frequency above the seismic bandwidth to avoid distortion meant reducing the tool's mass and increasing its contact area with the formation as shown in equation 9-1 below.

$$\text{Resonant Frequency} = \sqrt{k/m} \qquad (9\text{-}1)$$

(Washburn and Wiley, 1941)

where,

k is the rigidity of the soil supporting the geophone, and

m is the mass of the geophone.

Much of such work is based on the work done in 1941 by Washburn and Wiley of United Geophysical Co., Pasadena, California. They observed the resonance characteristics of surface geophones planted in the ground while altering factors such as geophone mass, soil type, and geophone base area. They confirmed that resonant frequency decreased with increasing geophone mass and decreasing soil rigidity. Furthermore, they discovered that the rigidity factor actually reflected the microscopic contact between the soil and the geophone. By placing a thin layer of cement between

the base of the geophone and the earth, they filled in surface irregularites and doubled the resonant frequency of their geophone-earth system. Applying these results to the borehole, geophysicists believed that a high ratio of anchoring force to tool mass flattens minor irregularities between the anchoring pad and the formation to increase the effective coupling area and raise the rigidity factor by local compaction.

Working on this principle, geophysicists also believed that reducing the tool mass minimises distortion from tube waves that occur when surface waves generated by the source encounter the borehole (figure 9-6). The borehole acts as a wave guide and traps seismic energy in the form of tube waves which suffer little attenuation compared to waves travelling through the earth. Because in most formations, tube waves (figure 9-6) travel more slowly than compressional and shear waves, they dominate the geophone response to late arriving body waves.

In the past few years, geophysicists have realised that the main source of distortion in borehole seismic comes from vibrations of the tool itself (called intrinsic modal vibrations). From the work by P.C. Wuenschel of Gulf Research and Development Co., Pittsburgh, in 1976, (figure 9-7), the basis of the triaxial tool developed. It was realised that these modal vibrations can be eliminated from the seismic bandwidth in two ways: dramatically reduce the tool mass and size which sacrifices space for important electronics or somehow decouple the sensors from the main body of the tool.

With the demand from the geophysicists for logging companies to provide seismic data of better quality, Schlumberger has managed to use the principles mentioned previously to come up with the Seismic Acquisition (SAT) tool, the Downhole Seismic Array (DSA) tool (figure 9-8) and presently under testing the Combinable Seismic Acquisition (CSAT) tool.

The SAT tool, made of titanium alloy, is lighter and more compact than its predecessor, the WST tool. It features triaxial geophones, downhole signal digitisation, and a shaker geophone for evaluating tool coupling. In the gimballed assembly, a weighted cylinder contains the three geophones. The y-axis geophone is fixed horizontally in the cylinder, and the x-and z-axis geophones are mounted in gimbals along the tool azimuth and vertical direction, respectively. Gravity ensures that the cylinder always lies on the low side of the well, keeping the y-axis geophone horizontal

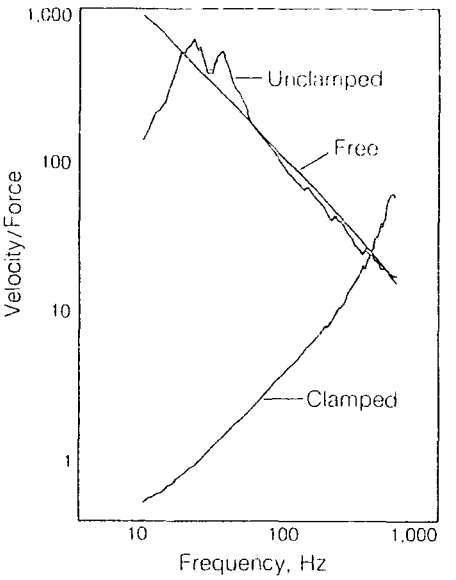

Figure 9-7. Vibration response versus frequency curves for three tool conditions: freely hanging, unclamped in the borehole, and clamped in the borehole. When the tool hangs freely outside the borehole, the velocity/force ratio monotonically decreases with frequency corresponding to an oscillator driven at frequencies above its resonant frequency. When the tool is left unclamped in the borehole, the same velocity/force decay with frequency occurs. The velocity/force peaks around 20 Hz are possibly due to contact with the borehole. Finally, when the geophone tool is clamped in the borehole, the velocity/force curve increases monotonically with frequency, corresponding to an oscillator driven at frequencies below its resonant frequency. The 500 Hz resonance frequency of the geophone tool is well above the normal seismic bandwidth. (Wuenschel, 1988)

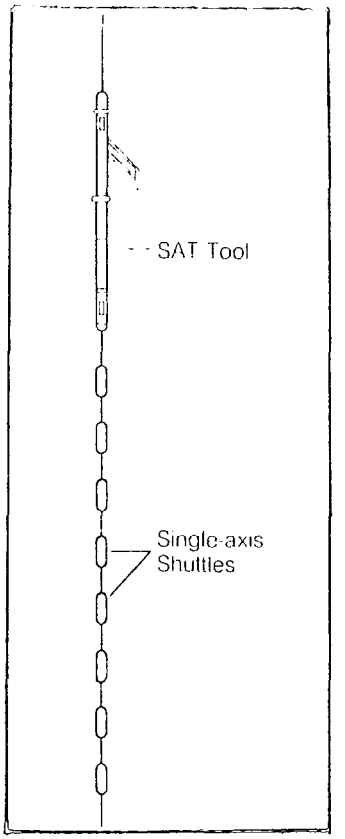

Figure 9-8. DSA tool. (Schlumberger, 1987)

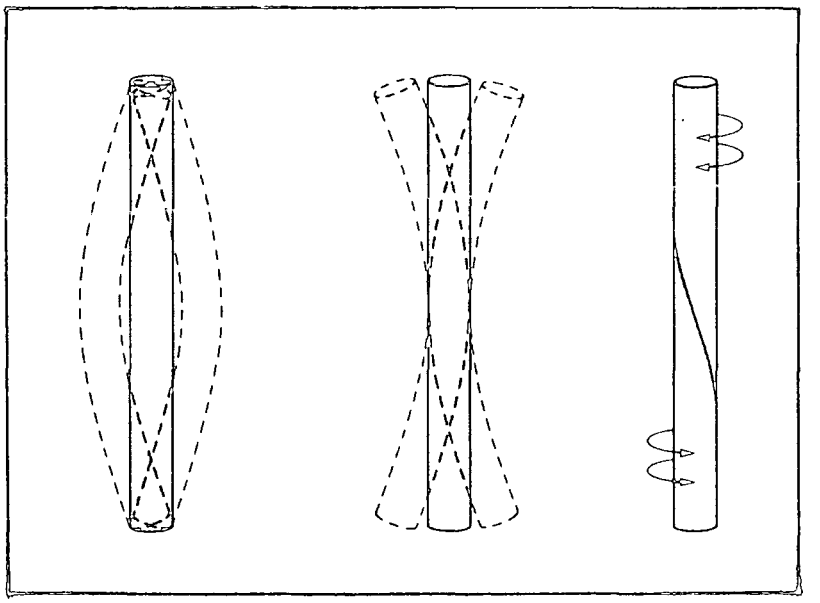

Figure 9-9. Some of the possible modes of vibration of an oscillating rod. (Babour, Joli, Landgren, and Piazza, 1987)

and perpendicular to the tool azimuth (the x-axis geophone direction). Similarly, the effect of gravity on the gimbals maintains the orientation of the x-and z-axis geophones. A fourth geophone called a "shaker" is used to estimate how well the tool is in contact with the formation. Instead of detecting vibrations, the shaker geophone works in reverse, vibrating the tool with a signal that sweeps from low to high frequencies. Its vibrations excite the entire tool which exhibits resonances that depend on the tool's contact with the borehole. These resonances are recorded by the three geophones. In case of poor tool contact, the anchoring force is withdrawn so that the tool can be pulled up, reanchored, and tested again with the shaker.

In the SAT tool the intrinsic modal frequencies which have a greater effect on the tool's acoustic performance than tool-formation resonances are still present. Any oscillating system, such as a metal rod, a pendulum, or any musical instrument, exhibits intrinsic modal frequencies that correspond to the system's different modal vibrations (figure 9-9). For the SAT tool or any borehole seismic tool these frequencies remain the same whether the tool is in the lab, cased hole, or open hole. They depend however, on how the tool makes contact with the formation and tool length, mass and stiffness.

Fortunately the SAT tool's intrinsic modal frequencies do not threaten the operation of the tool. Most of the modal frequencies are above 100 Hz whereas most seismic measurements occur between 5 and 80 Hz. Still, tube waves with high-frequency components can cause distortion by exciting these modal frequencies. From the work of Gaiser et al, stand-offs (sleeves that are clamped around the tool) help stabilise the tool by improving the contact area between the tool and formation.

As mentioned previously, modal frequencies can be raised by reducing the overall mass of the tool. However this tended to be impractical because it eliminated space needed for electronics. Instead, engineers at Schlumberger tried to isolate acoustically the geophone sensors from the rest of the tool. The resulting prototype DSA tool comprises eight single-axis sensor packages, called shuttles, for multilevel data acquisition in cased holes (figure 9-8). The shuttles, weighing 4.2 kilograms are spaced at either 15 or 20 metre intervals; each contains a vertical geophone, a magnetic clamper, a shaker, and electronics to transmit amplified signals to the SAT cartridge. The magnetic clamper (figure 9-10) which attaches the shuttles to casing applies a

force of 30 daN (66.1 lb) for a high force-to-weight ratio of 7.2. In one sense the DSA tool is an extension of the SAT tool. It borrows the SAT tool's electronics cartridge-by running downhole with the entire SAT tool to digitise and transmit data collected from an array of geophones which operate simultaneously.

The eight-geophone array reduces the number of shots needed to complete a walkaway survey (figure 9-3) by a factor of one-eighth. Decreasing the number of shots reduces source signature variations due to source positioning, air gun depth and pressure variations, gradual unconsolidation of the formation around the air-gun pit (on land), and tidal effects on water level (offshore). In an offshore walkaway for example, the DSA tool collects signals from eight levels while the seismic source moves by boat at a constant speed. Getting the same coverage with a single-level tool would require eight runs of the boat and the shot locations could never be exactly duplicated.

Although the DSA tool's shuttles are physically linked, they remain acoustically independent. This is accomplished with pairs of O-rings placed between the shuttle and its carrier. When tube waves arrive at the DSA tool any propagating noise is confined to the cable and the carriers. This helps protect the geophone from tube-wave interference. The DSA shuttle's high force-to-weight ratio of 7.2 guarantees that the shuttle will move only as much as the particles in the casing and hence the formation. A comparison of SAT and DSA data from the same test well in Texas shows that the DSA tool design eliminates tube waves visible on the SAT recording (figure 9-11).

In 1988, V. de Montmollin of Etudes et Productions Schlumberger, Clamart, France, tested an experimental version of the CSAT tool with a shaker and triaxial geophone located inside the tool housing, but decoupled from the main tool. The experimental CSAT tool showed intrinsic modal resonances above 300 Hz, well above the seismic bandwidth. Figure 9-12 shows a comparison of data from the SAT tool and an experimental CSAT tool. Decoupling maintains good acoustic performance of the sensors even though the mass of the entire tool system increases when the CSAT tool is combined with itself for multilevel recording or with other tools for orientation, depth control, or measurement efficiency. The CSAT tool has a variety of sampling rates in two modes of operation, depending on whether geophysicists want to detect signals in the seismic bandwidth or a higher frequency range around 1 kHz. Finally,

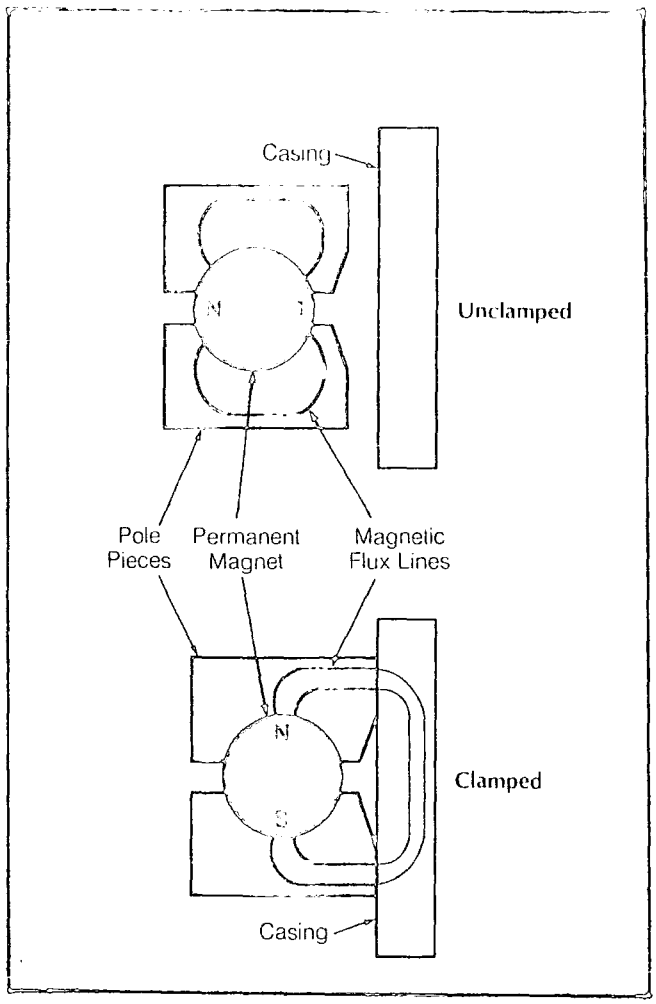

Figure 9-10. Principle of the DSA shuttle's magnetic clamper. When placed between two pole pieces with its north-south axis perpendicular to the casing. The permanent magnet generates a magnetic flux in the pole pieces (top). Rotating the magnet 90 degrees completes the magnetic flux circuit through the borehole casing for clamping the shuttle to the casing. (Schlumberger, 1987)

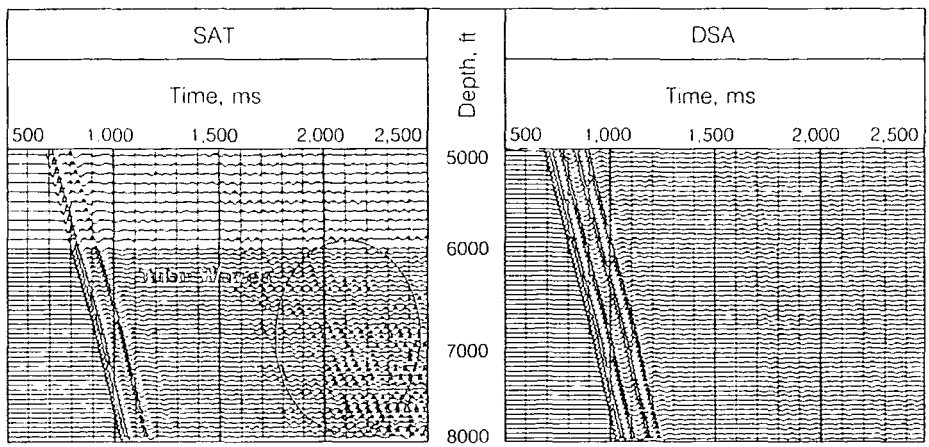

Figure 9-11. Comparison of SAT and DSA data from the same Texas well. The SAT data, made with a 120-cubic-inch air gun with a wave-shape kit that reduced bubble oscillation, show extensive tube wave distortion. The DSA data, made with a 230-cubic-inch air gun, are distortion-free because each of the DSA tool's eight shuttles is acoustically isolated and has a higher clamping force-to-weight ratio than the SAT tool. (Schlumberger, 1987)

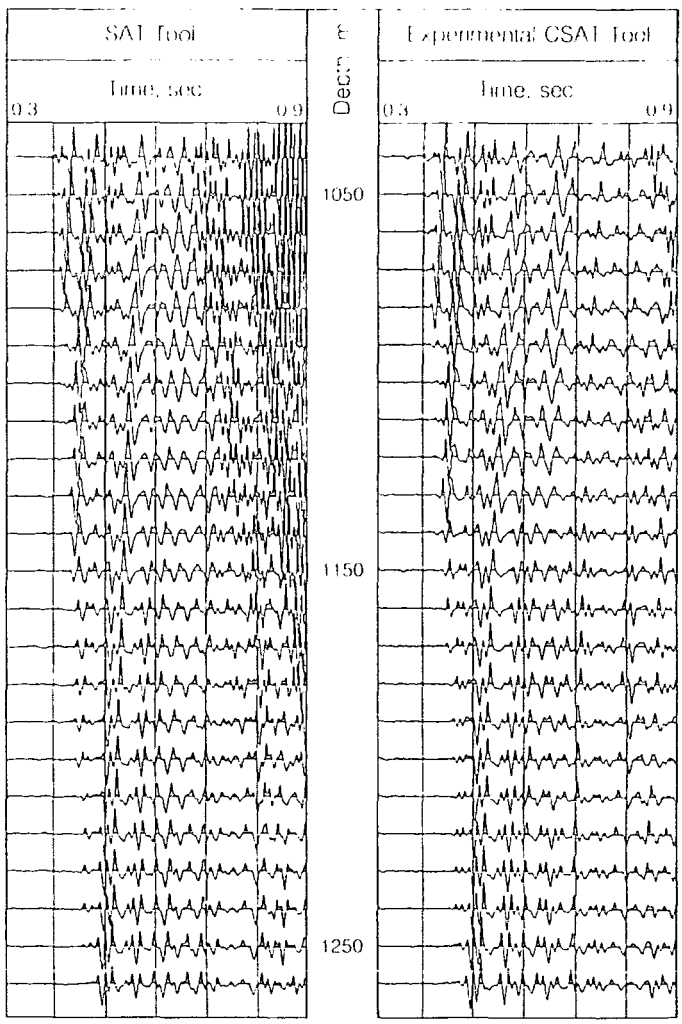

Figure 9-12. Comparison of data from the Seismic Acquisition (SAT) tool and an experimental Combinable Seismic Acquisition (CSAT) tool. The SAT data show tube wave interference. Data from the experimental CSAT tool having intrinsic modal frequencies above 300 Hz is unaffected by tube waves. (Schlumberger, 1987)

the CSAT tool will also be self-calibrating, allowing geophysicists to characterise the behaviour of geophones and electronics downhole.

10. PERFORATIONS

10.1 Introduction

The perforating of casing goes back to 1932, and is one of the most common of all the wireline cased hole operations. Its major purpose is to provide effective flow communication between the well bore and the reservoir. Bullet guns were used for many years, then after World War II, they were replaced by shaped charges (jet perforators) that stemmed from the bazooka weapon.

The ultimate goal of perforating is to provide adequate productivity. The accomplishment of effective flow communication does not hinge on perforating equipment alone but must be wedded to the proper completion technique, to achieve optimum results.

If the right combinations of techniques are not employed, damage may result to casing, reservoir or perforation, productive zones may be erroneously condemed or expensive diagnosis stimulation, repair and reperforating may be required in an attempt to correct the resulting problems.

The very fact that the perforating operation is irreversible in character argues strongly for good planning before the trigger is pulled on a gun. Test laboratories evolved over the years help to provide means of predicting and improving well performace. Today the performance of the charges is determined according to the procedures outlined in the "API RP-43 standard procedure for evaluation of well perforators, third edition, October 1974".

10.2 Shaped Charges (Jet Perforators)

In 1888, a man named Charles E.Monroe first observed that lettering embossed in blocks of explosives left their image on iron targets at the point of detonation. Although a full twenty-two years passed bebore the effect was again observed, this time by Egon Neuman in 1910, the phenomenon is still known as the Monroe effect.

The Monroe effect found little practical application until the observation of an effect caused by the dimpled end of a blasting cap at John Hopkins University. This eventually led to the development of the lined-cavity shaped charge by the military. Further developments of shaped charges for mining operations were reported during the late 1940's (Carl F. Austin).

The first description of a jet gun suitable for use in open hole completions appeared in 1946 (R.L. Mclemore, 1946). The individual charges were huge by modern standards and very inefficent as perforators. The amount of explosive used made them destructive when used in casing. In the spring of 1947, serious development work started. The objective was to produce an effective shaped charge of lesser explosive weight; one which could be encased in tubular gun body without undue damage to the tube.

10.2.1 Shaped Charge Effect

From the simple experiment shown in figure 10-1 (Birkhoff, Pugh and Taylor), it can be seen that the penetrating power of a cylinder of explosive is greatly increased by a cavity at the end opposite to the detonator. Taking exactly the same configuration as in (B) and placing a thin metallic liner in the cavity (C), penetration increases dramatically. This was work derived from hydrodynamic theory (Eichelberger and Pugh, 1952).

10.2.2 Shaped Charge Mechanism

In its most elementary form, a shaped charge consists of four basic elements: a cylinder of high explosive with a conical metallic liner at one end and a detonator and a booster at the other. Once the primer is initiated by detonating cord in the gun it in turn initiates detonation of the main charge. A detonation front sweeps through the charge at about 20,000 ft/sec. and generates pressures on the liner of two to four million psi. With forces of this magnitude acting on the liner its mechanical resistance is negligible and the process of jet formation can be predicted approximately from the laws of hydrodynamics (figure 10-2).

An oversimplification of the theory states that the shape of an explosive cavity focuses and propagates a progressive wave front against the outside surface of the metal liner. At the pressures generated, the metal acts as a fluid. Metal in droplet form is squirted into a focused jet stream. The resultant focusing force moves particles forward and relatively backward to form a jet which lengthens as the wave front advances from apex to base of the conical cavity (figure 10-3). The extremely high pressure, particle-laden jet stream breaks down and moves aside any material upon which it impinges (figure 10-4). Penetration is a result of the amount of pressure and

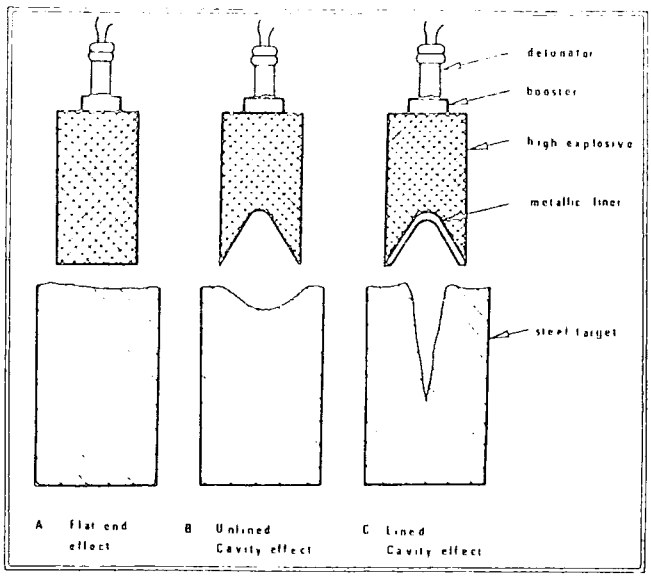

Figure 10-1. Shaped charge effect. (Birkoff, McDougal, Pugh, and Taylor, 1948)

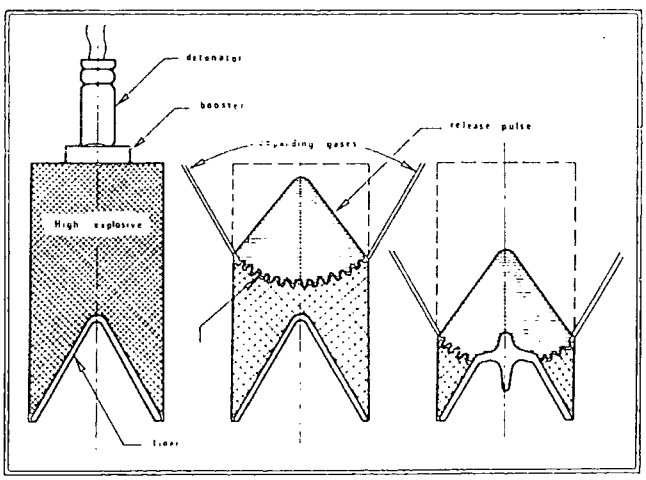

Figure 10-2. Shaped charge mechanism. (Birkoff, McDougal, Pugh, and Taylor, 1948)

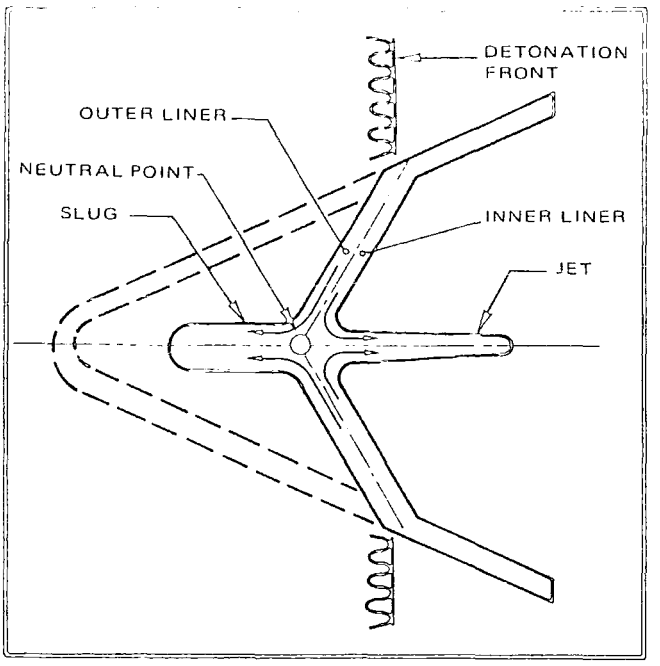

Figure 10-3. Jet slug mechanism. (Birkoff, McDougal, Pugh, and Taylor, 1948)

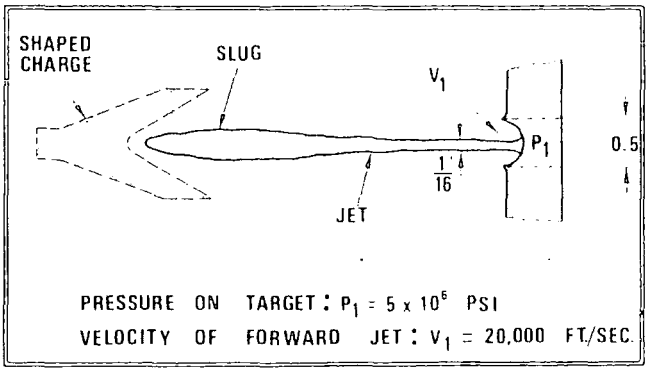

Figure 10-4. Jet penetrating mechanism. (Birkoff, McDougal, Pugh, and Taylor, 1948)

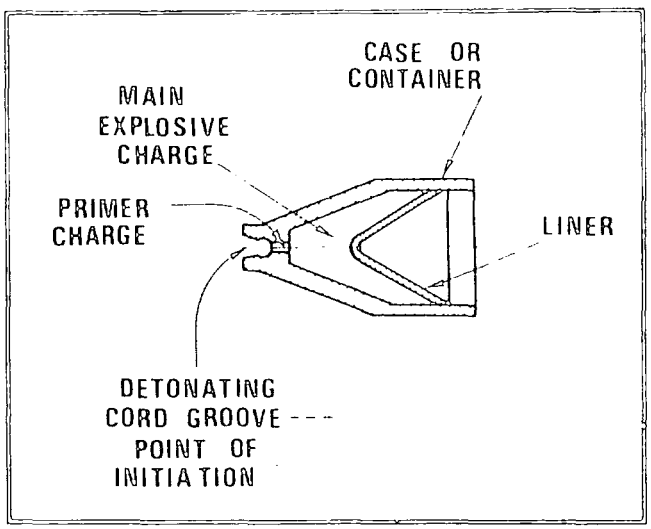

Figure 10-5. Typical shaped charge. (Birkoff, McDougal, Pugh, and Taylor, 1948)

the kinetic energy in the jet stream, i.e., velocity and mass. The greater the length of the jet stream the greater the depth of penetration. Temperature and explosion gases play a negligible role in the penetrating process. However crushing and compaction of formation material is to be expected and will be reviewed later.

The hydrodynamic theory best fits charges with true cone shaped liners. Other theories have been developed to explain the jet forming action in liners of hemispherical, parabolic and other forms. Figure 10-5 shows a typical shaped charge.

10.3 Perforating a Well

10.3.1 Casing Damage

The pressure attending detonation of high explosives used in the shaped charge guns can be as high as 4×10^6 psi. Therefore casing damage becomes the first concern when perforating a well : the shaped charge detonation should not ruin the casing. There is no damage to the casing if the charge is fired from a hollow steel carrier. (A more detailed description of the different types of gun follows later.) The expendable type of guns where the explosive energy is borne by the casing, lead to some casing deformation (Robinson, et al,1961).

The amount of damage depends upon:-

a) the explosive load and,

b) the well condition i.e.the amount of support provided to the casing by the cement (compression strength, thickness, etc.).

Figure 10-6 to 10-12 show laboratory test results of casing damage by perforation under different conditions. Non supported casing: equal water pressure inside and outside the pipe. Semi supported: cement 3/4 inch thick (compressive strength 35,000 psi) retained by a thin walled metal sheath.Well supported: cement 3/4 inch thick (compressive strength 35,000 psi) retained by a heavy walled steel cylinder.

10.3.2 Physical Parameters Affecting the Quality of Perforations and Productivity

The penetration of a perforation is very important for the following reasons:-

a) The further the jet goes in the formation, the easier it is for the fluid to flow into the well. (McDowell and Muskat, 1950)

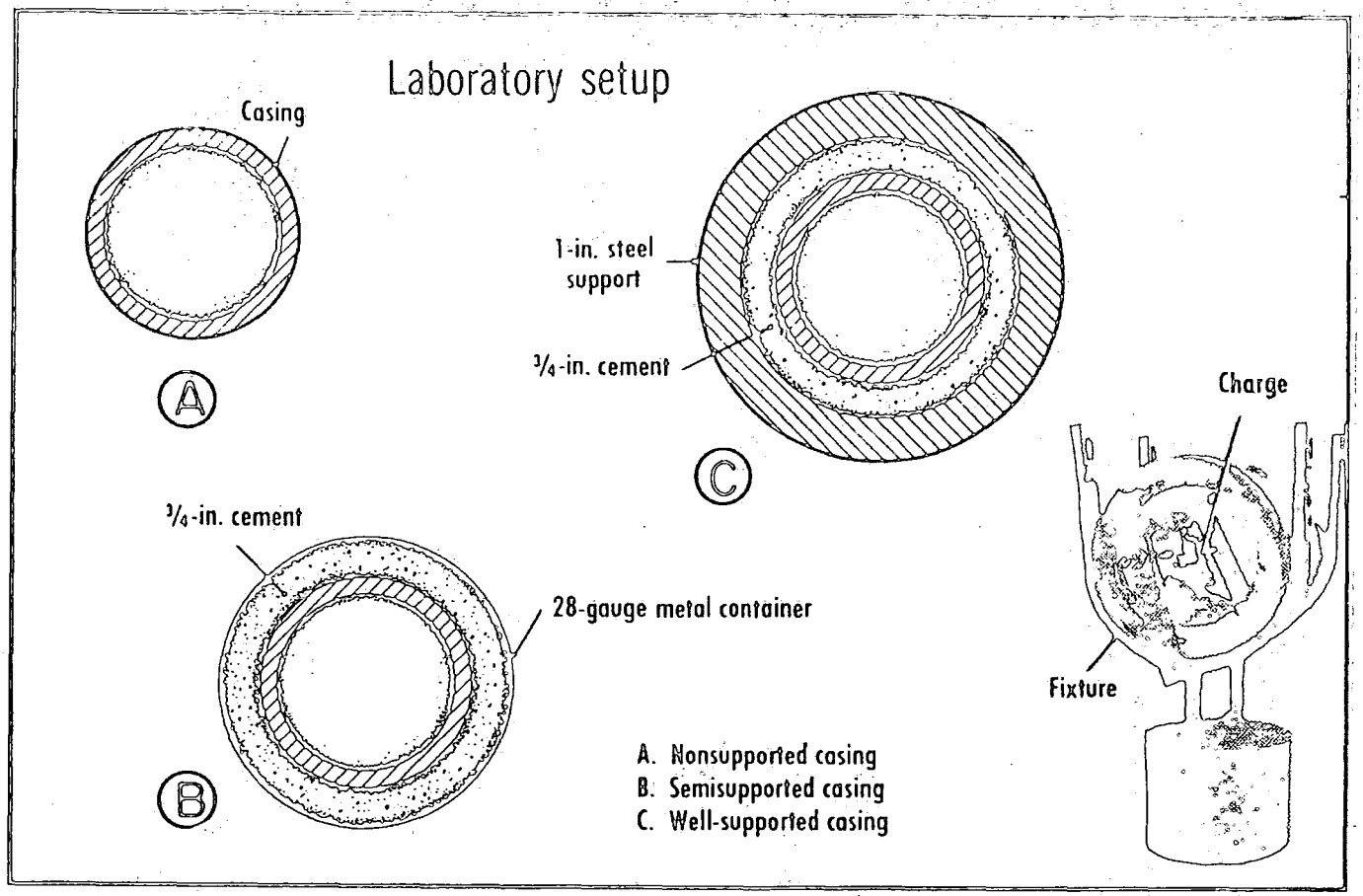

Figure 10-6. Laboratory setup of a casing test. (Robinson, Hermann, and De Frank, 1961)

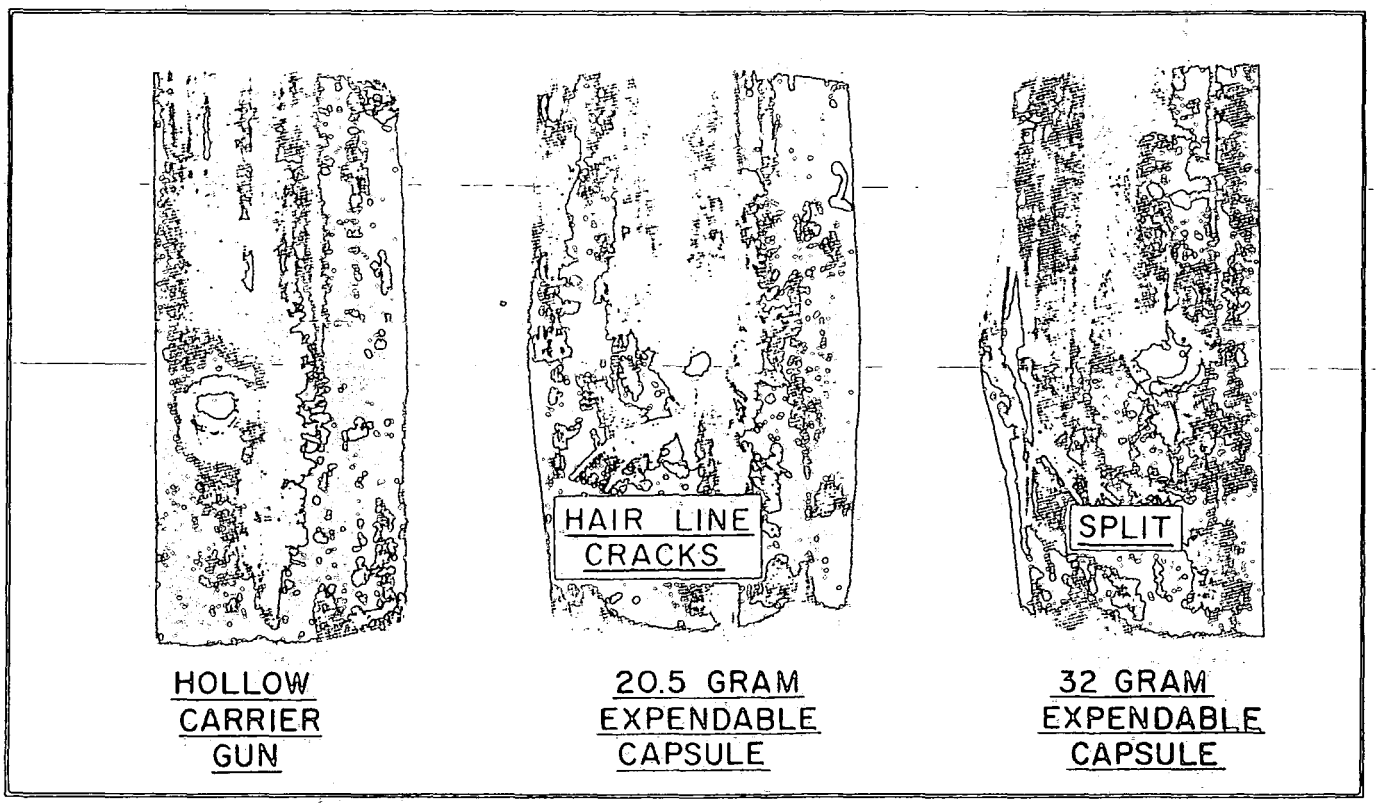

Figure 10-7. Damaged casings. (Robinson, Hermann, and De Frank, 1961)

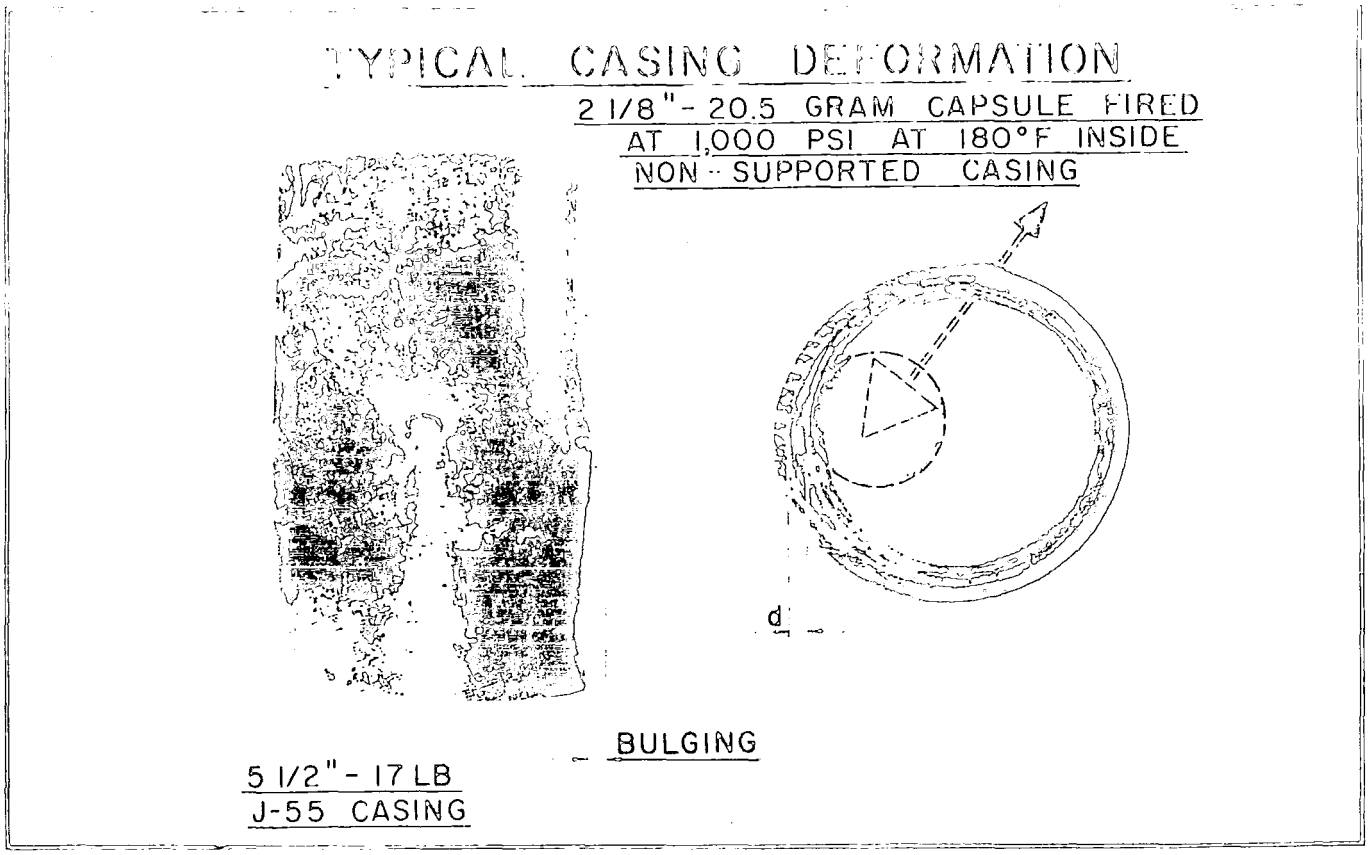

Figure 10-8. Typical casing deformation. (Robinson, Hermann, and De Frank, 1961)

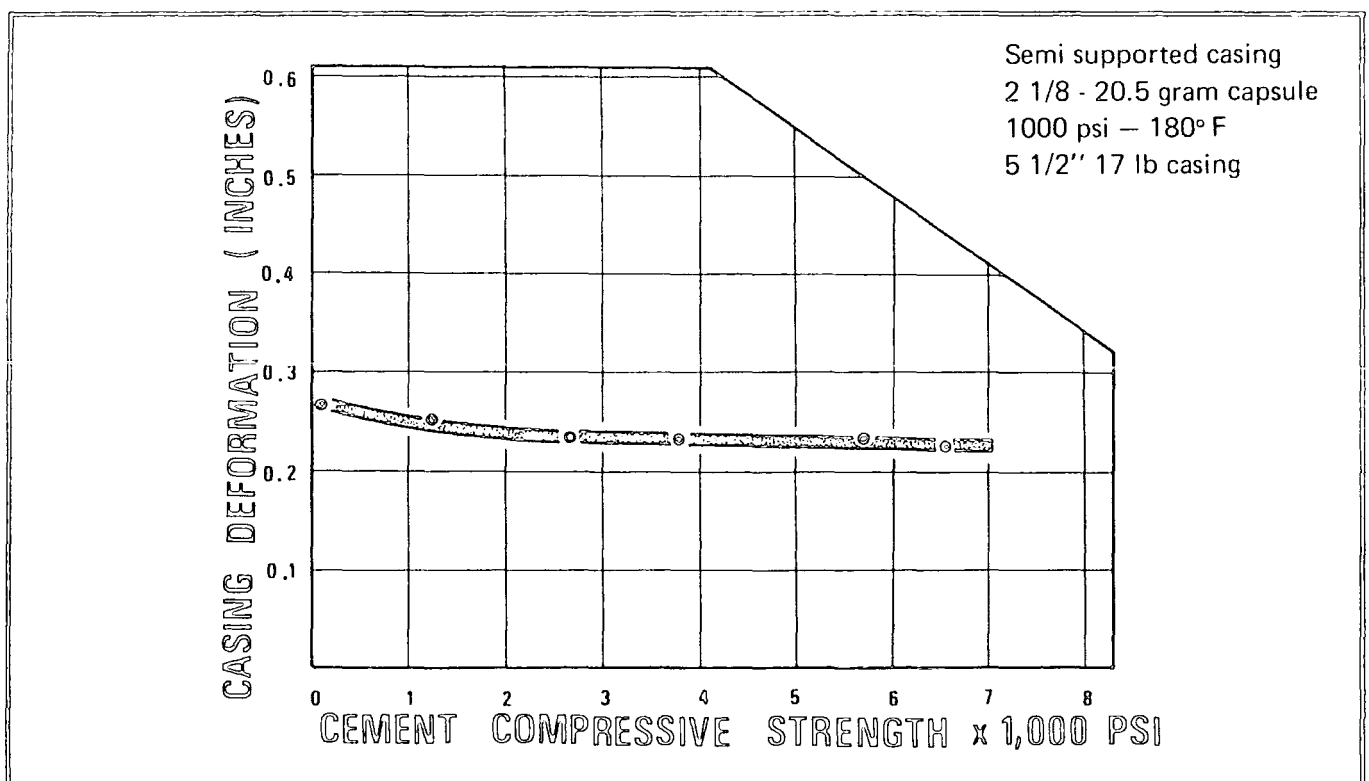

Figure 10-9. Cement strength has little effect on casing deformation. (Thompson, 1962)

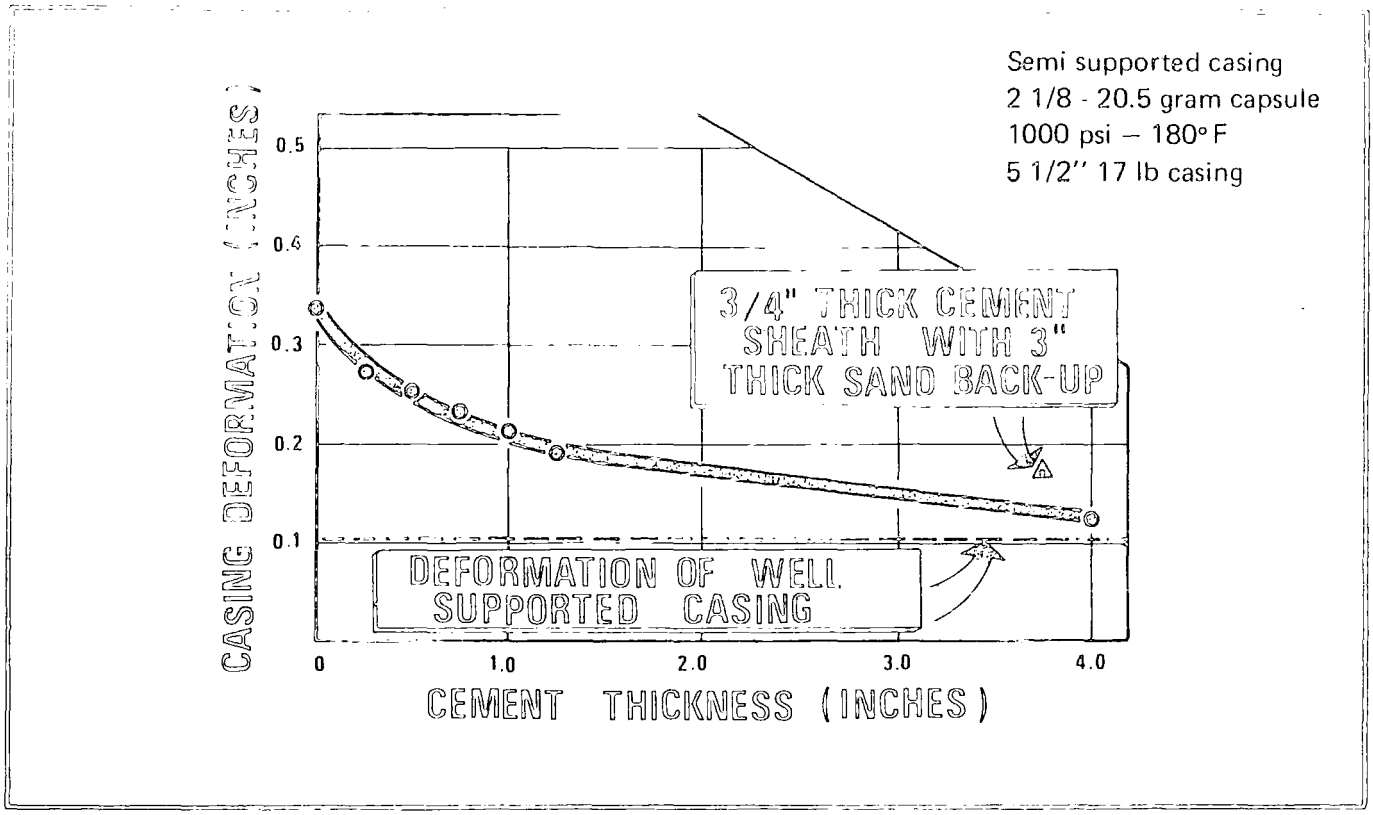

Figure 10-10. Cement thickness has large effect on casing deformation. (Thompson, 1962)

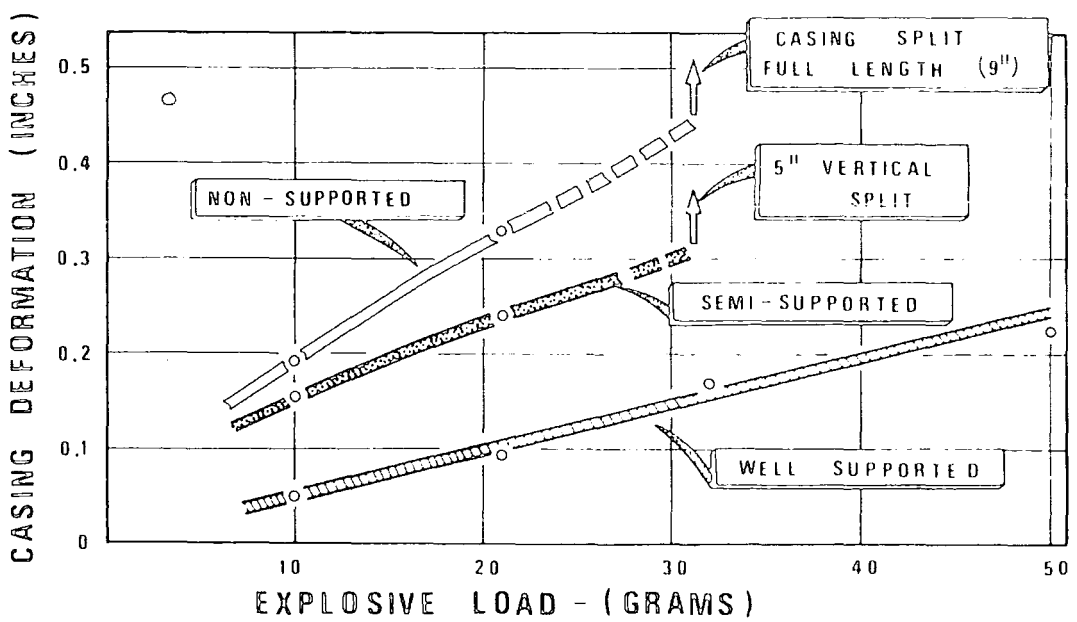

Figure 10-11. Casing deformation versus capsule explosive load measured and 180 °F. (Thompson, 1962)

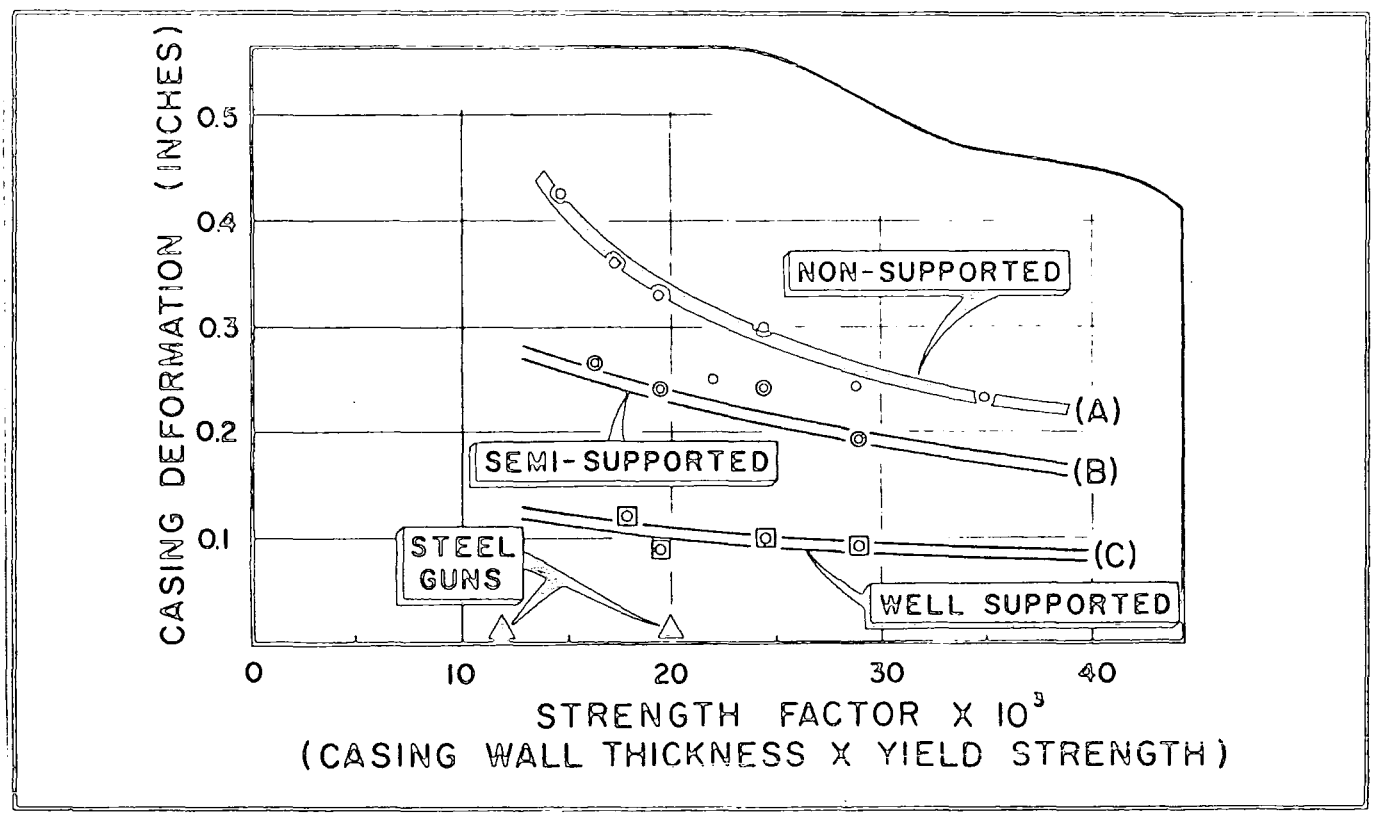

Figure 10-12. Casing deformation versus wall thickness, grade and confinement (20.5 grams capsule; 1000 psi at 180 °F. (Thompson, 1962)

b) The perforation must go beyond the damaged zones (see Fig. 10-13). Well bore damage (illustrated by the skin effect in pressure measurements) is caused during the drilling and may have different origins (Nowak and Kruegar, 1951):-

i) mud solid plugging,

ii) clay swelling,

iii) precipitates,

iv) particle tilting,

The penetration of a perforation is strongly influenced by the compressive strength of the formation: the more competent the formation, the smaller the penetration (Thompson,1962). (See figure10-14.)

One method used to reduce the plugging of the formation after perforation is to flow the perforated zone immediately after shooting (see figure 10-15). The influence of the clean-up is clearly illustrated on figure 10-16 where the Core Flow Efficiency is plotted against the time of flow or injection through the perforation in the laboratory tests. If fluid is injected rather than produced, the injection "CFE" is small.

10.3.3 Geometrical Parameters Influencing the Quality of Perforations and the Productivity of the Well.

a) Clearance

Gun clearance which is the distance from gun to casing along the axis of the jet, can have an important effect on the quality of the perforation (Harris, 1956). The best perforations (largest penetration and entrance hole) are obtained with clearance less than one inch. With large distances from gun to casing, the perforation characteristics are generally reduced (Godfrey,1986, and Robinson, et al, 1961).

b) Phasing

The perforation pattern changes the distribution of the flow around the well-bore: Harris showed that shooting in several directions(for a given number of shots per foot) increases the productivity ratio (see figure 10-17). (The productivity ratio is

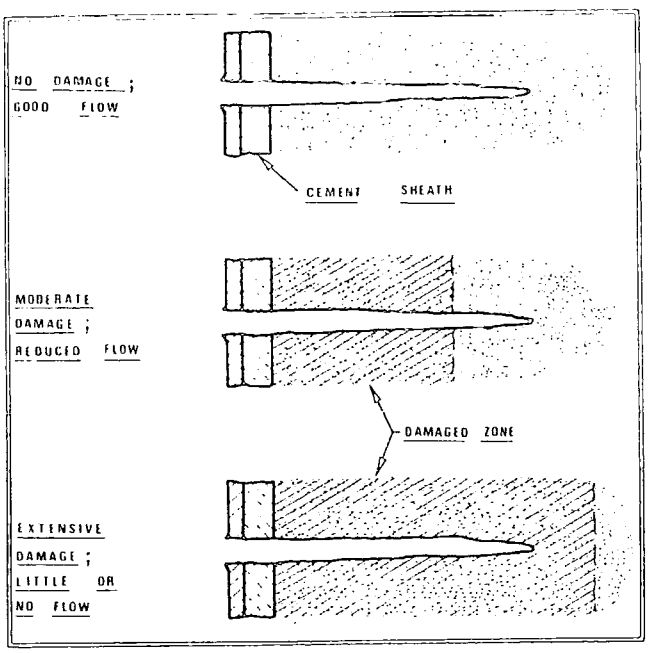

Figure 10-13. Influence of penetration in a damaged well bore. (McDowell and Muskat, 1950)

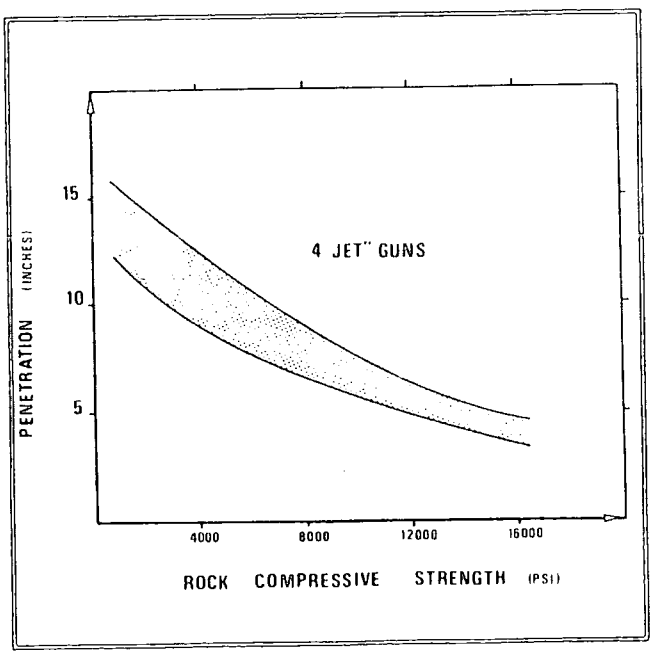

Figure 10-14. Penetration versus compressive strength. (McDowell and Muskat, 1950)

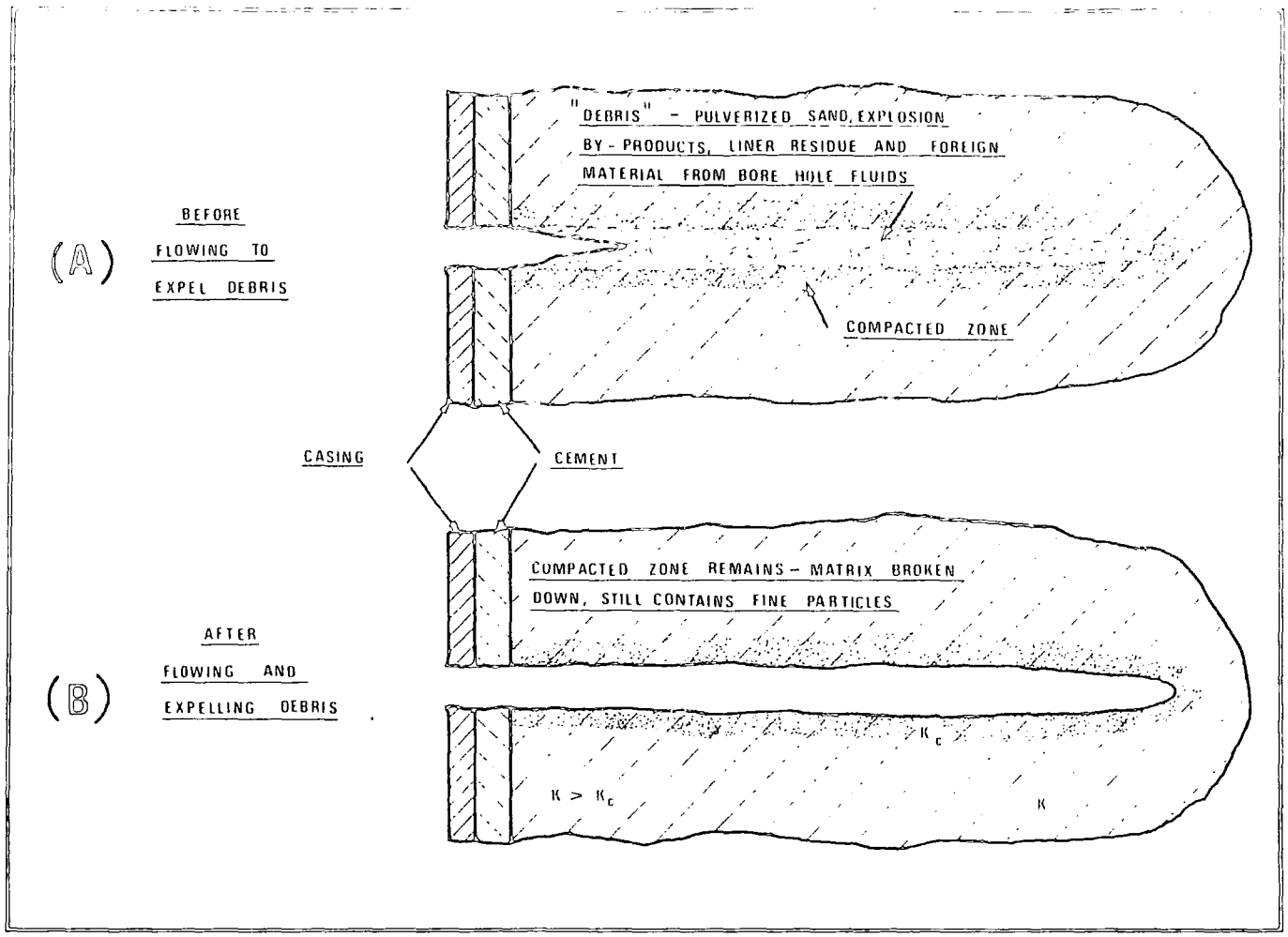

Figure 10-15. Perforation in Berea sandstone with and without clean ups. (McDowell and Muskat, 1962)

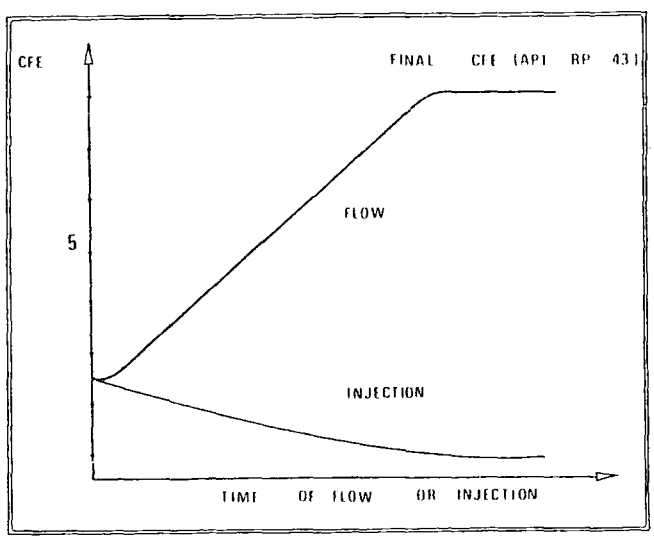

Figure 10-16. Core Flow Efficiency versus time of production (or injection), with constant pressure differential. (McDowell and Muskat, 1950)

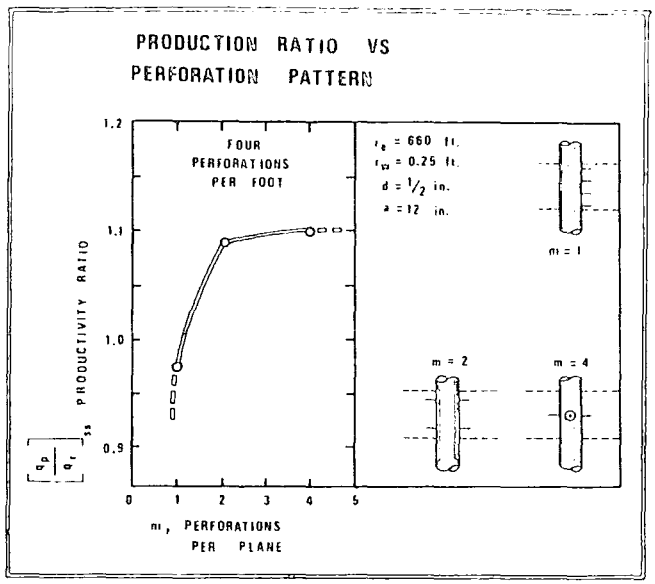

r_e = radius of extent of the reservoir

r_w = radius of the well bore

d : diameter of the entrance hole

a : penetration

Figure 10-17. Productivity ratio versus perforation pattern. (Harris, 1965)

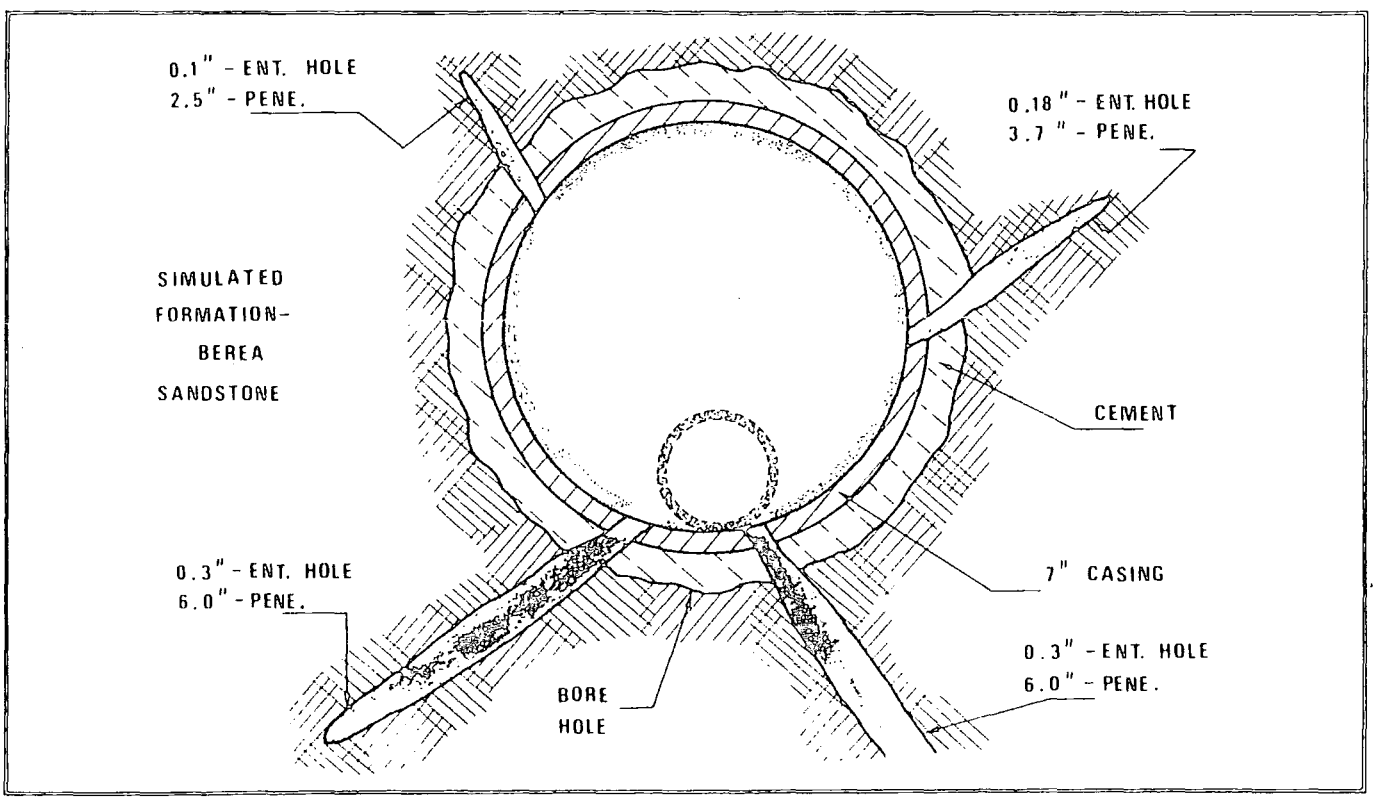

Figure 10-18. Random perforating pattern. Conventional $1^{11}/_{16}$ inch 90° phased (Harris, 1965)

the ratio of the productivity of the perforated cased hole to the productivity of the open hole). Note that the productivity ratio may be larger than one; this is because the perforations increase the "effective well bore radius".

The above leads to a dilemma: if a multiphased gun is used (i.e. a gun shooting in several directions), the clearance of some charges is not zero, and the penetration is smaller : the gain in productivity due to phasing may be more than lost by a high percentage of poor perforations (see figure 10-18).

As could be expected, the solution to the problem is a compromise:-

i) If the diameter of the gun is not too small in comparison with the diameter of the casing, the adverse effect of the clearance is not too important and then phasing helps.

ii) If a gun with small diameter (through-tubing gun) is used the clearance may become too large if the charges are shot at random. Therefore with that type of gun, in-line shooting is preferred and the quality of the perforations is helped by a positioning device (see figure 10-19) which is either magnetic or by meansof a spring.

c) Shot Density

Harris (1965) showed that increasing the number of shots increases the productivity ratio (see figure 10-20). Today the maximum shot density with available guns has increased from 4 shots per foot of early days to 12 shots per foot.

d) Completion Techniques

Ideally it would be most beneficial if all perforations could be done with large multi-phasing guns and at the same time if all perforations could be flowed immediately after shooting (reverse pressure perforation). However this is practically not possible because flowing the perforations means perforating with pressure at the well head: the tubing, packer, well head and flow line must be installed first and hence introducing a large gun into the well through this hardware is not possible.

Perforations are therefore carried out either by using a big hollow carrier casing gun (positive pressure perforating) or by shooting a small through-tubing gun with clean fluid in the well under reverse pressure (LeBourg and Hodgson, 1952). These two very different technique are best illustrated in figure 10-21.

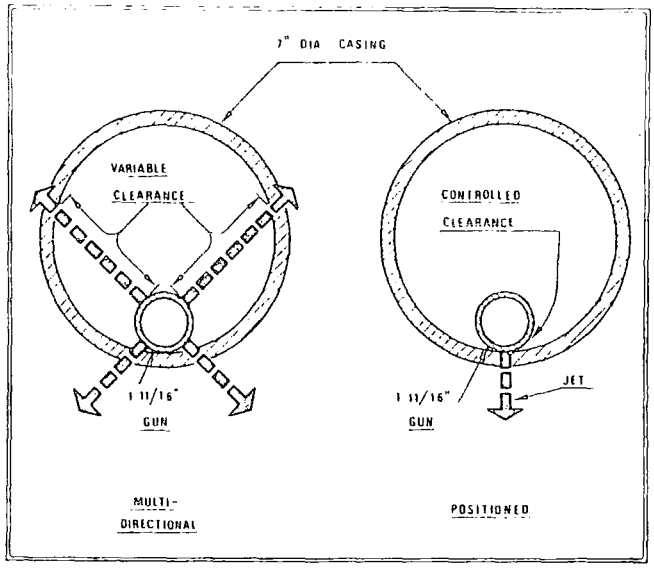

Figure 10-19. Through-tubing gun in a casing. (Lebourg and Hodgson, 1952)

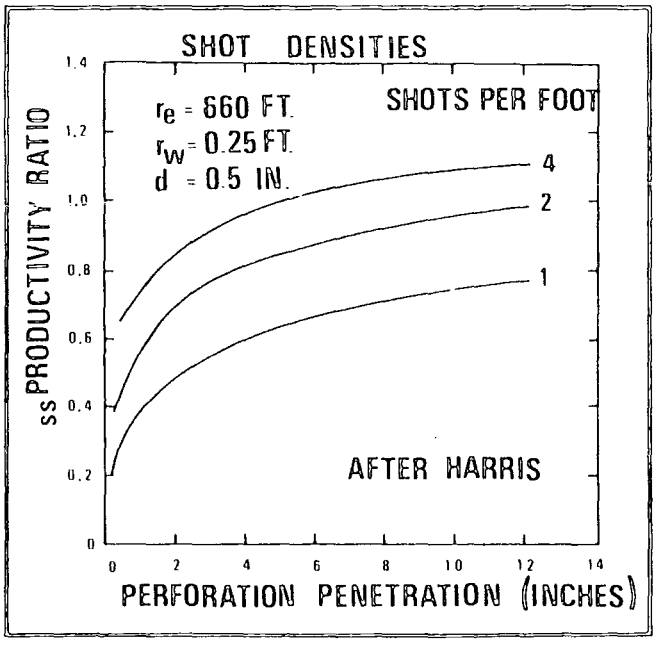

r_e = radius of extent of the reservoir
r_w = radius of the well bore
d = diameter of the entrance hole

Figure 10-20. Productivity ratio versus pentration for various shot densities. (Harris, 1965)

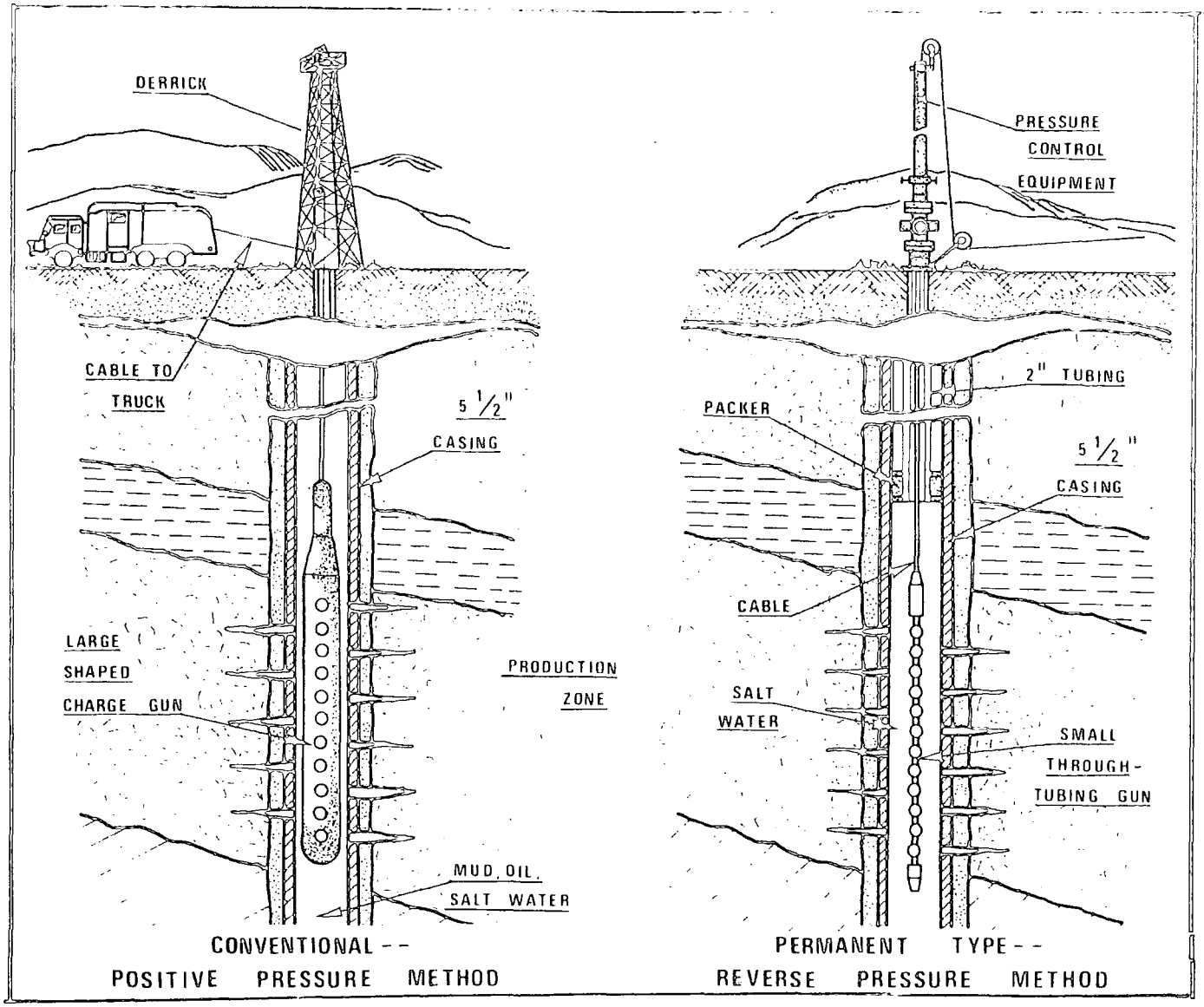

Figure 10-21. Comparison of completion techniques. (Lebourg and Hodgson, 1952)

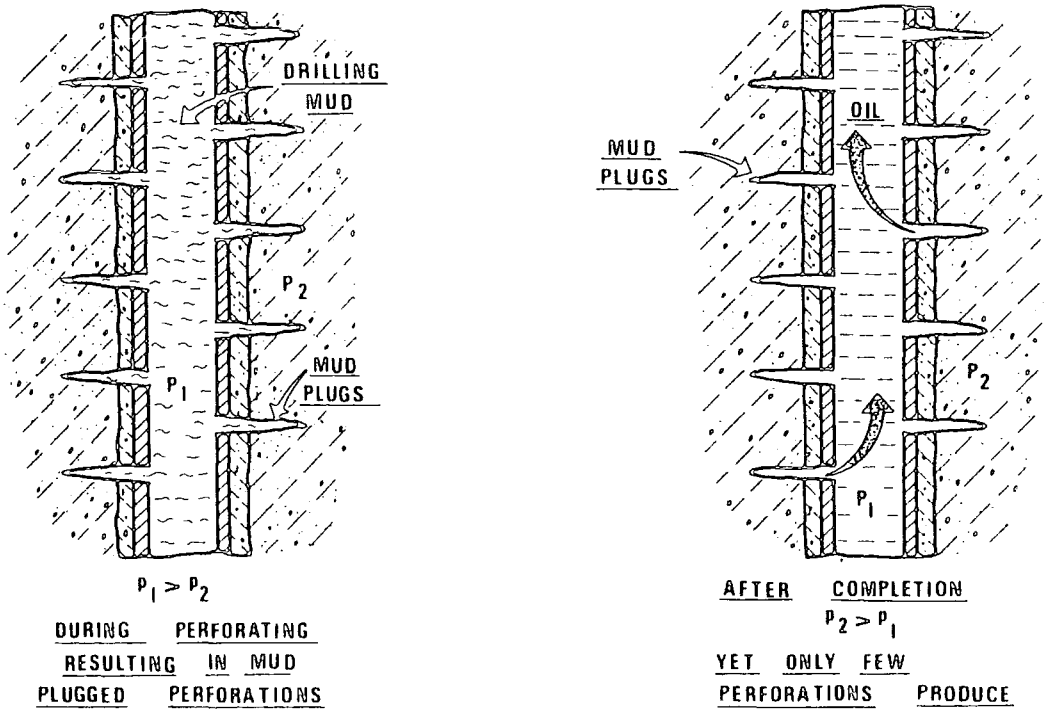

Figure 10-22. Positive pressure perforating in drilling mud. (Lebourg and Hodgson, 1952)

From the point of view of overall quality of the perforating (i.e. the final productivity of the well) the reverse pressure method is the best (Huber, et al, 1950) because with the positive pressure method only a few perforations may be unplugged when production starts(figure 10-22) while with the reverse pressure method the initial surge of fluids can clean most perforations (figure 10-23).

The versatility of the reverse pressure technique can be illustrated by the two stage method adopted for high production gas wells (see figure 10-24). Here, first a high-permeability zone near the bottom of the well (1-2 feet interval) is perforated by a debris-free gun as the trigger zone. The well is then allowed to flow until the completion fluid has been cleaned out of the well. This is followed by the (1st stage) perforation of the lower permeable zone. Expendable guns can be used later and the well is produced under the highest drawdown possible for several days. Finally the higher permeable zone (2nd stage) is perforated again with expendable guns. The well is then flowed, cleaned up and allowed to produce.

e) Depth Control

Depth control for perforating is most important for obvious reasons and is almost universally obtained through radioactivity instruments run in the cased hole in conjunction with the electromagnetic casing collar locator (CCL). Accurate correlation of radioactivity logs with open hole logs establishes the position of casing collars with respect to the formation to be perforated. A short "sub" in the casing string is highly desirable to eliminate ambiguities with CCL identification particularly when all joints of casing are about the same length. When a gun is run a CCL is attached to record a second collar log to compare with the first collar log for depth matching.

Generally a gamma ray tool is not run with a gun because of safety and practical reasons. When running a gun it is not desirable to send current down the wire unless the gun is downhole and on depth for shooting. Therefore, if a gamma ray tool is to be used it would have to be powered from a battery within the tool. Such gamma ray tool provides a log of poor resolution. Furthermore, there are problems which can arise from destruction of the detector crystal due to perforation shock and from the battery supply itself in the case of numerous runs or high temperature within the well. A perforation run is a simple service and by using a second collar log run with a gun

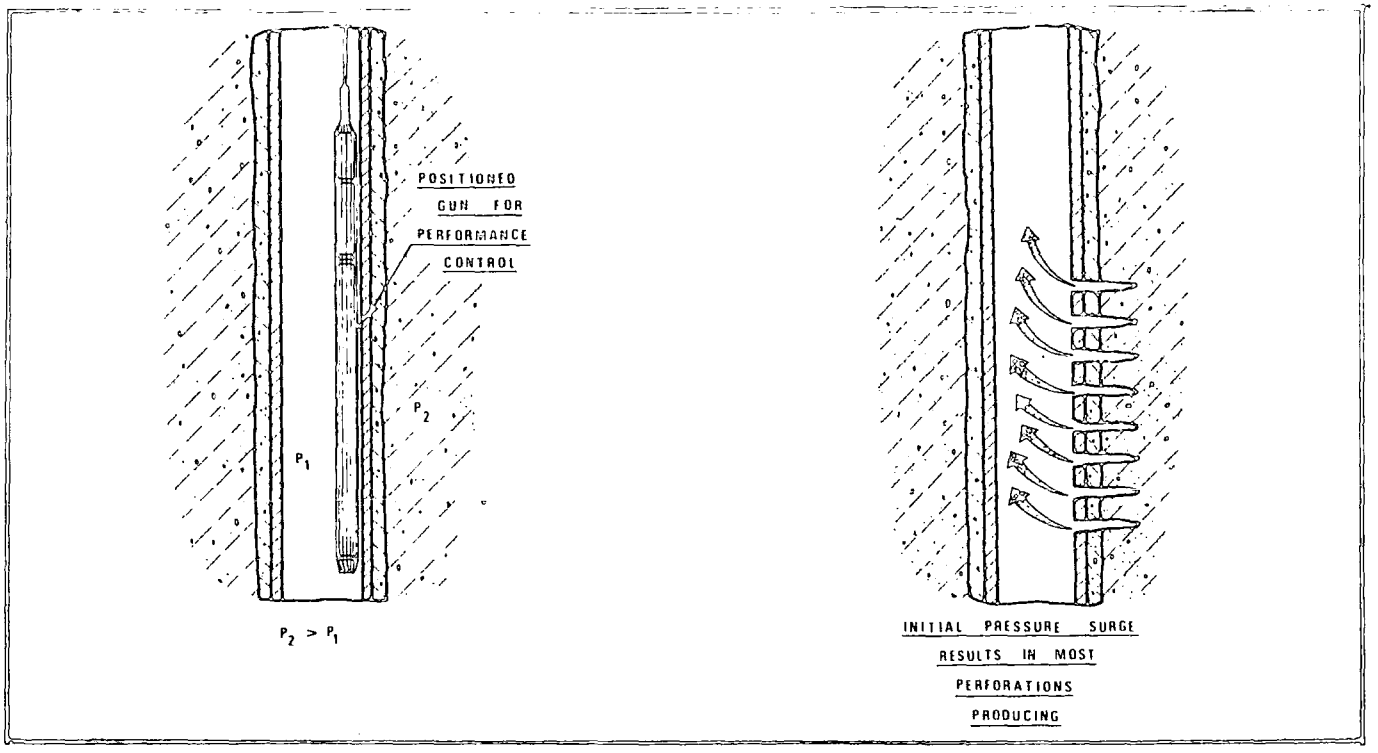

Figure 10-23. Reverse pressure perforating. (Lebourg and Hodgson, 1952)

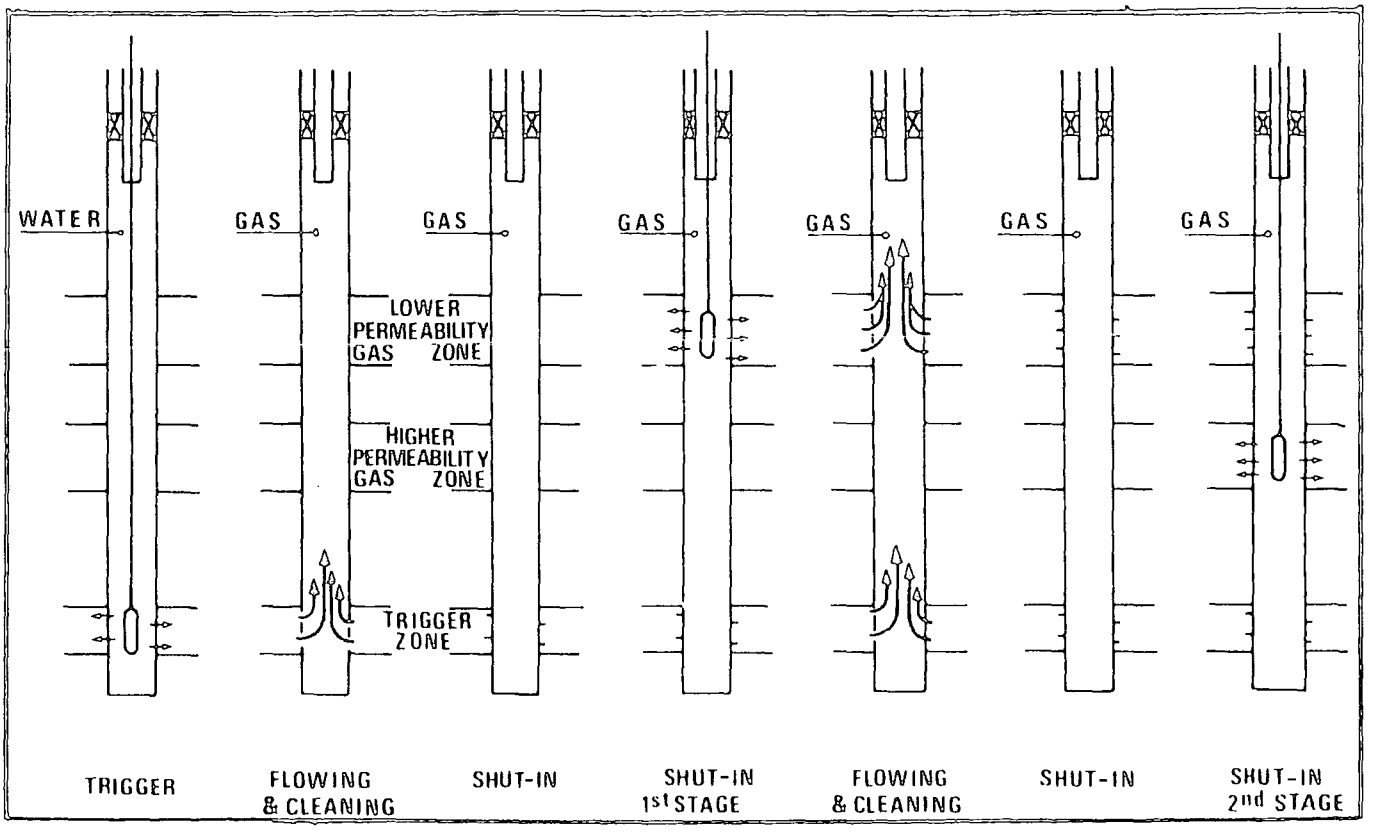

Figure 10-24. Two stage gas well completion with through-tubing guns. (Lebourg and Hodgson, 1952)

to correlate with the base collar log, depth control can be achieved accurately and efficiently in a short time.

10.4 The Guns

10.4.1 Detonating Components

All shaped charges within a gun are fired by mean of detonating components. There are two main types of detonating component, namely the electrical blasting cap and the detonation cord.

The electrical blasting caps are devices used to initiate detonation of high explosives. Electrical blasting caps operate in the following sequence:-

a) Electrical current passes through a wire causing it to heat.

b) The hot wire ignites a compound mix that burns.

c) The ignition mix heats the primary explosive (lead azide) causing the lead azide to detonate.

d) The detonation of the lead azide detonates the RDX (Cyclonite or Hexogene) base charge.

All electrical caps are generally fitted with safety resistors. They are safety devices to prevent accidental firing from stray voltages. Generally there are two main types of safety cap, namely fluid desensitised and pressure tight safety caps. The former is used for applications where the cap is not exposed to well pressure. The purpose of fluid desensitisation is to prevent cord detonation and charges of a hollow carrier gun into which well fluids have leaked. Should a liquid filled gun be allowed to fire it would swell and/or crack, ruining the carrier and possibly causing a fishing job to retrieve it. Desensitisation is accomplised by leaving an air gap between the main section of the detonator and the booster. If this gap becomes filled with liquid, detonation will not be transmitted across the gap (see figure 10-25). The pressure tight safety cap is made to withstand several thousand pound pressure because it is exposed to the well fluid (see figure 10-26).

The electrical cap detonates the detonating cord which transmits explosion from the blasting cap to a number of individual charges. Since the velocity of detonating wave is about 7000 m/s, initiation of all charges is practically simutaneous. The detonating cord consists of RDX, PETN (Pentaerythritol tetranitrate) or sulphone

explosives covered by a plasticised braid jacket or in some cases lead sheathed.

10.4.2 Guns

The myriad of shaped charges and guns commercially available today may be generally classified into categories for the purpose of considering their operational characteristics and applications. These are :-

a) The retrievable hollow carrier gun.

b) The non-retrievable or expendable gun.

The retrievable hollow carrier gun (figure 10-27) consists of a steel tube into which the explosive shaped charge is suitably secured. The gun tube is sealed against hydrostatic pressure. Therefore the charge is surrounded by air at atmospheric pressure. When the charge is fired the explosive forces slightly expand the carrier wall, but the gun and debris within are fully retrieved from the well.

The non-retrievable or expendable gun on the other hand, consists of individually pressure sealed cases made of some frangible material such as aluminium, ceramic, glass, cast iron or steel. A charge is contained within each case and, when detonated blasts the case into small pieces. There is no carrier to contain the blast. Case debris remain in the well. There are two types of non-retrievable guns:-

a) Fully expendable (capsule guns): everything is left in the hole (charge and carrier strip).

b) Semi-expendable : the carrier strip can be retrieved hence debris is reduced (figure 10-28). This is an improvement over fully expendable guns.

Service companies who offer perforation service, all have a selection of guns for their client. Depending on the type of completion the guns are designed for casing operations or through-tubing operations. For casing operations, generally retrievable hollow carrier guns are used because they are reliable, debris-free, resistant to well bore chemicals, fast running, inflict no casing deformation, and have multi-firing capability for shooting numerous guns. For through-tubing operations the gun size is reduced, and the well completion program will decide on the choice of either retrievable guns or expendable guns. The expendable gun has the advantages of being light and flexible and has the ability to use stronger charges. With through-tubing operations, the amount of explosive that can be used is limited by the swelling of the

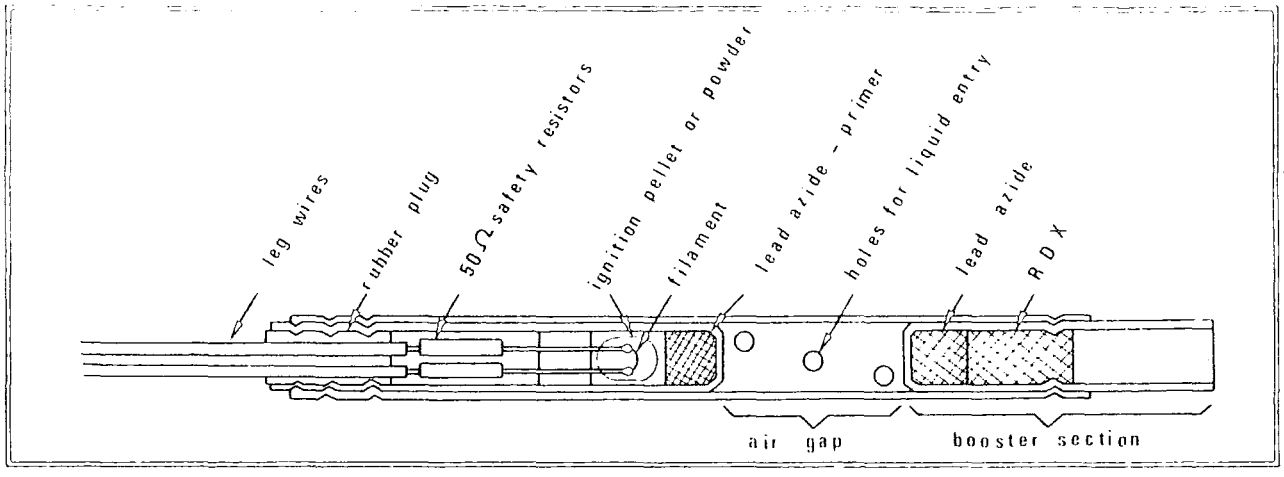

Figure 10-25. Schematic of fluid desensitised blasting cap. (Schlumberger, 1987)

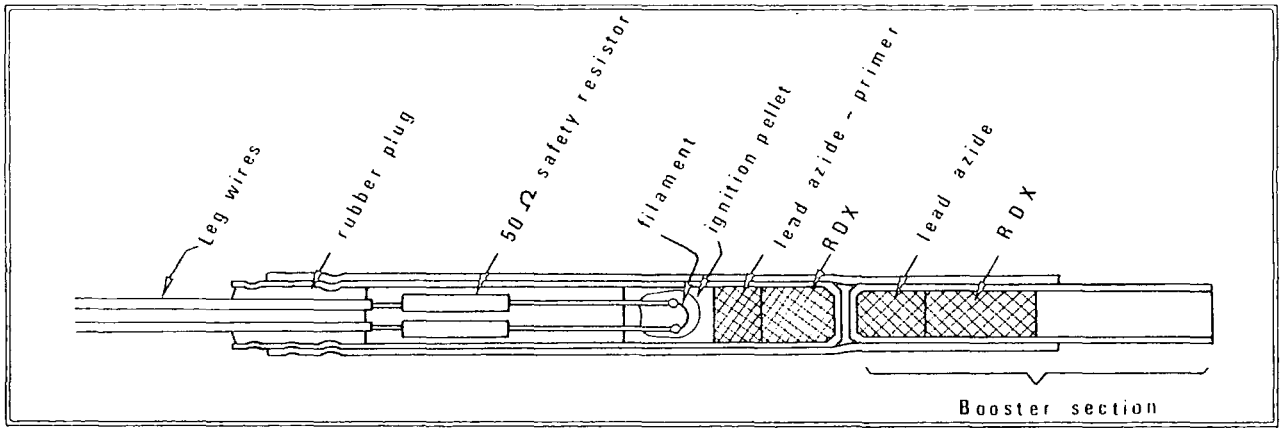

Figure 10-26. Schematic of pressure-tight safety blasting cap. (Schlumberger, 1987)

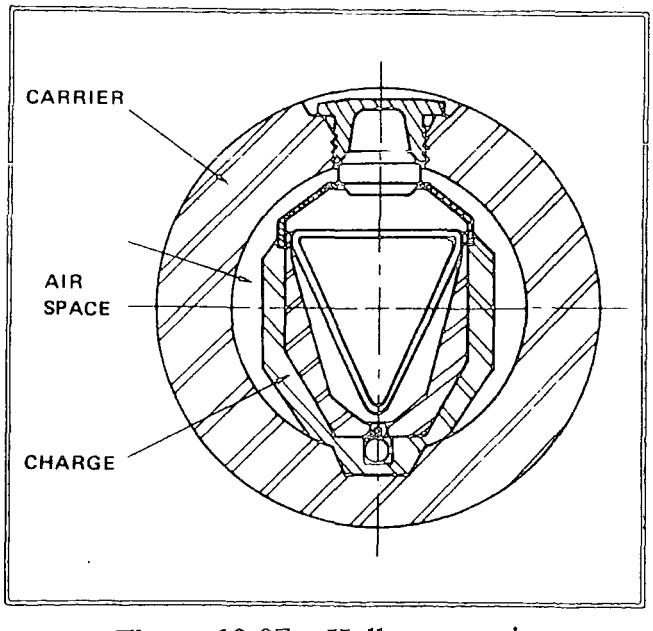

Figure 10-27. Hollow carrier gun.. (Schlumberger, 1987)

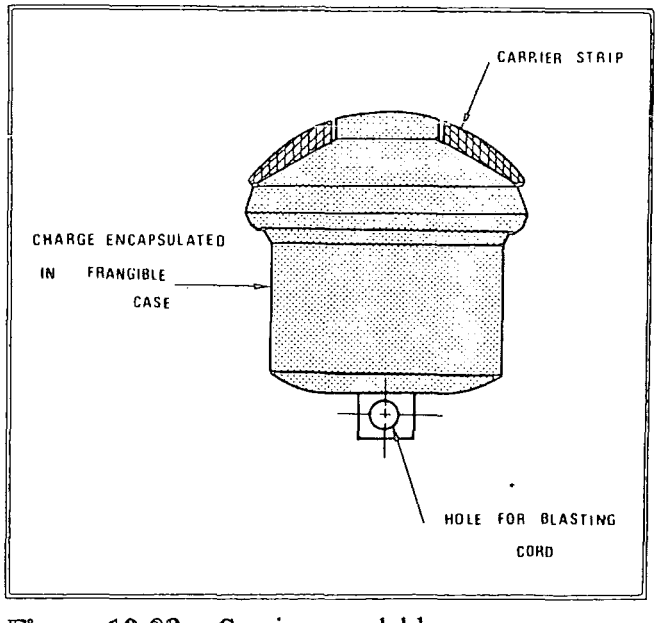

Figure 10-28. Semi-expendable gun. (Schlumberger, 1987)

carrier, therefore the performance is reduced as compared to an equivalent diameter expendable gun.

Examples of guns available are as listed in table 10-1 below. Obviously the names will vary but the basic principles are still the same.

Company	Gun Type	Gun Size (in.)	Shots/ft	Max Temp Temp.(°F)	Max Press (kpsi)
Gearhart	Hollow Carrier	4	4	325	20
	Gowinder	2	4	325	20
	Strap Jet*	2	4	325	7
	Tornado*	2	4	325	15
NL McCullough	Hollow Carrier	4	4	340	20
	Omega Dome	2	4	340	20
	Steel Wire*	2	4	325	15
	Tornado*	2	4	325	12
Schlumberger	High Shot Density Carrier	3	6	340	20
	Hollow Carrier	4	4	340	20
	Hyperdome	2	4	340	15
	Enerjet*	2	4	340	15
Western Atlas	Hollow Carrier	4	4	325	20
	Slim Kone	2	4	325	20
	Link Kone*	2	4	300	10

Table 10-1 A selection of gun types.((*) denotes expendable guns)

10.4.3 Charges

The choice of charges available is vast. An operator generally chooses the charges which he thinks are best for the well performance. The type of completion can determine the type of gun to be used and hence the charge type too. Depending on the terms of the contract, the perforating company generally is the same as the one

who carried out the logging too. Appendix B gives API RP-43 Test Data for perforating charges of Gearhart, L.L. McCullough, Schlumberger, and Western Atlas.

As Appendix B shows, the choice is vast and almost limitless. The main question for an operator is who gives the best charge performance for his needs? Generally he is also limited by economic and logistic reasons. It would be most impractical to use charge "A" which is only manufactured and used by company "A" in the U.S.A. to perforate in the dense jungle of Indonesia a well which company "B" has the logging contract and charge "B" readily available . The problem envisaged naturally favours the job to be perforated with charge "B" even though charge "A" may give slightly better performance.

Furthermore, the API RP-43 Test Data should not be treated as the perfect standard for comparison. The Test is merely a procedure laid down by the American Petroleum Institute, but it is not actually carried out by the API or any other independent body. All testing is carried out by individual manufacturing companies themselves. Therefore there is no guarantee that the full RP-43 procedure is followed or not. For example, the charges tested may not be a true representative sample of the batches which are on the market. Until there is an independent body to control and supervise the testing, all published RP-43 data should only be used as a guideline with limitations.

11. PRODUCTION LOGGING

11.1 Introduction

When a well is put on production it is often desirable for the operator to monitor the performance of the well not only at the surface but also downhole. At the surface by means of pressure gauges, flowmeters, separation tanks etc., he is able to determine the well performance in terms of flowrate, well-head pressure, gas-oil ratio, water cut, and the densities of the gas, oil and water being produced. However the surface data merely gives him an overall picture of the well's performance and does not give him a full understanding of what is happening downhole. It is important that the operator knows how well each of the perforated zones is performing and the percentage gas, oil and water produced from each zone.

To enable a better understanding of the well at downhole conditions, it is necessary to run some logs to evaluate the performance of the well. Generally, the types of logs run are as follow:

a) Water saturation logs.

b) Production logs.

11.2 Water Saturation Logs

Throughout the production life of a well there will be changes in the water saturation within the produced zones. Generally, it is desirable for an operator to know the water saturation within the produced zones. From this data he can predict how water influx has affected his well performance and hence how it will affect his well in the future.

Depending on the water salinity within the wellbore, there are two principal methods to evaluate water saturation :

a) The Pulsed Neutron System.

b) The Neutron-Gamma Spectral Method.

11.2.1 The Pulsed Neutron System

When the water salinity is high and known, this method is preferable to determine water saturation and to detect changes in water saturation throughout the production life of the well.

11.2.1.1 Principle

Pulsed Neutron Capture (PNC) logging was originally developed to measure the quantity Sigma (Σ), (Youmans, et al.). Sigma is the thermal neutron absorption cross-section of the formation surrounding the instrument. The measurement is made by analysing the time rate of decay of the thermal neutron population. Sometimes it is also referred to as the "Thermal Neutron Decay Time" method.

Many improvements were made later to PNC techniques, and new systems were introduced. The most noteworthy improvements were in the increase in the statistical accuracy of the Sigma measurement. Several parameters were added to monitor system operation and log quality but the basic applications of PNC logging remained the same. The recent introduction of PNC logging systems with the borehole decay component as well as the formation Sigma represents a significant departure from past trends.

The PNC log provides a measurement which indicates the rate at which thermal neutrons are captured by the elements of a formation. Chlorine is the strongest neutron absorber of the common earth elements so these logs primarily reflect the amount of chlorine (sodium chloride) in the formation water. Sigma, the macroscopic neutron capture cross section of the bulk formation, discriminates between hydrocarbon and salt water. In saline formation waters the Sigma curve resembles an openhole resistivity log with which it is easily correlated. The display of the two neutron count-rate curves provides a quicklook indicator of gas, and the ratio of the count rates provides a porosity index.

11.2.1.2 Equipment

Tools which are available for the thermal neutron decay time log are listed in table 11-1:

Company	Tool	Max. Temp. (°F)	Max. Pressure (kpsi)
Schlumberger	TDT-M	325	17
	TDT-P	325	17
Western Atlas	NLL	300	20

Table 11-1. Thermal Neutron Decay Time Tools' Ratings.

Western Atlas offers the service of the Dual Detector Neutron Lifetime log (NLL). This tool uses two detectors to measure the macroscopic thermal neutron absorption cross-section, Sigma. The tool uses the new state-of-the-art electronic technology developed by Western Atlas known as the PDK-100 system. It is a new downhole microprocessor which enables better processing of the raw data.

Schlumberger offers the services of the Dual-Spacing Thermal Neutron Decay Time (TDT) tools which are either type "M" or "P". In the TDT-M, measurements of the thermal neutron decay time constant are made a short time after the neutron source is turned off. The capture gamma-rays are detected by two scintillation detectors which are placed at different spacing to provide "near" and "far" data. Each detector counts gamma-rays over 16 different Time Gates. The duration of these time gates depends on a Gates Scaling Factor selected by the software while the log is being run.

The TDT-P, however, is a new generation tool and is substantially different. The TDT-P is different from the TDT-M in both the way neutrons are generated and in the way gamma ray radiation is collected and processed. Neutron pulses are generated in pairs, a short pulse followed by a long pulse. Using the sixteen available gates to collect data from a dual neutron burst dictates that background radiation can no longer be estimated by using the trailing gates during each burst cycle. Thus, in the new tool the background counts are collected using the "Burst-off Background" method (neutron generation is inhibited every sixteenth cycle for background collection).

The sixteen collection gates are grouped into four sections:-

a) Short duration pulse inelastic gate, during the short neutron burst.

b) Short duration pulse decay gates.

c) Long duration pulse inelastic gate, during the long neutron burst.

d) Long duration pulse decay gates.

Two methods have been developed to implement the diffusion processing. One is a fast, real-time wellsite computation based on a single-component diffusion model of the media. It simultaneously uses information provided by both short and long neutron bursts and from both near and far detectors to obtain a diffusion and borehole contamination free formation capture cross section.

The second is a slower, modified nonlinear least squares fit to all of the data using the full two-component diffusion model. It performs a level-by-level fit of the diffusion coefficients to provide the best agreement between the model and the measured decay curve. Data from the dual burst arrangement is used in such a manner that a borehole sigma is obtained by measuring the decay rate of capture data following the short burst. A formation sigma is obtained from capture data following the long burst. The capture data is background substracted and dead-time corrected before the computation of Sigma.

The time-dependent transport of thermal neutrons in the borehole and surrounding formation is approximated by the neutron diffusion equation:

$$\frac{1}{v} \cdot \frac{\delta\phi(\vec{r},t)}{\delta t} - D(\vec{r})\nabla^2\phi(\vec{r},t) + \Sigma_a(\vec{r})\phi(\vec{r},t) = S(\vec{r},t) \quad (11.1)$$

(Olesen, Mahdavi and Steinman, 1987)

where

$\phi(\vec{r},t)$	=	neutron flux;
$D(\vec{r})$	=	thermal diffusion constant;
$\Sigma_a(\vec{r})$	=	macroscopic absorption cross section of the medium;
$S(\vec{r},t)$	=	thermal neutron source;
v	=	speed of a thermal neutron; and
∇^2	=	the Laplacian operator.

The above model accounts for the nonexponential neutron diffusion and capture in the formation and the wellbore. The benefit of the method is that the measured cross section is the intrinsic formation capture cross section and its value is independent of the borehole fluid. Analysis of the decay curve by this method also makes the results independent of tool design features such as neutron burst width, counting gate widths, and counting gate positions. Thus the stable answers needed for monitoring projects can be provided over many years even though tool hardware may be modified or wellbore conditions may change. In addition, in operations such as a log-inject-log project where a higher degree of accuracy is required, the tool is ideally suited.

Furthermore, a porosity computation is made from the ratio of selected gates of the near and far detectors following the long burst. This ratio is transformed into

a porosity that has a response similar to other neutron porosity tools (see chapter 5.3).

The Dual-Burst Thermal Decay Time (TDT-P) logging tool with an innovative neutron burst timing technique and a physically realistic model of capture gamma ray detection seems to offer a better answer than the old TDT-M and Western Atlas's NLL tool. Its data processing accounts for neutron diffusion effects directly rather than treating the decay as a sum of exponentials from the formation and the borehole environment. Hence, the TDT-P service seems to provide a more accurate formation sigma with better statistical precision in common wellbore situations.

11.2.2 The Neutron-Gamma Spectral Method

The Neutron-Gamma Spectral method is useful for formation evaluation in reservoirs where formation water salinities are either unknown, or too low for the PNC log interpretation.

11.2.2.1 Principle

In the Neutron-Gamma Spectral method both the inelastic and the capture gamma ray spectra, providing a detailed measurment of formation response to neutron bombardment. Eight essential elements are identified and their concentrations are determined. Measurements of carbon, oxygen, silicon, calcium, iron, chlorine, hydrogen, and sulphur are used to compute the hydrocarbon saturation, salinity, lithology, porosity, and shaliness of the formation.

Unlike the PNC method, the principles of induced gamma ray spectroscopy are applied to the in-situ measurement and detection of hydrocarbons (Heflin, et al.). Using a similar pulsed neutron device, the energy and intensity of gamma rays resulting from neutron irradiation of the formation are measured, rather than thermal decay.

11.2.2.2 Equipment

Company	Tool	Max. Temp. (°F)	Max Pressure (kpsi)
Schlumberger	GST	300	20
Western Atlas	MSI	300	15

Table 11-2. Neutron-Gamma Spectral Tools' Ratings.

Schlumberger offers the service of the Gamma Spectrometry (GST) tool, and

Western Atlas offers the service of the Multiparameter Spectroscopy Instrument (MSI). Both tools look at the gamma ray spectrosopy emitted from excited nuclei in the formation and borehole. The excitation is either naturally occuring (Natural Gamma Ray Spectroscopy) or induced through bombardment by some particle such as the neutron (Induced Gamma Ray Spectroscopy).

11.3 Production Logs.

Production logs are most often used to determine the nature of fluid flows in producing wells such that decisions may be made on how to rework the well to improve the oil or gas production. Normally there are three pieces of information that are desired:

a) Where are the inflow/exit points of fluid?

b) What kind of fluid is coming or leaving (oil, gas, or water)?

c) How fast is the fluid moving?

Knowing where water is coming in identifies the zones that need to be closed off such that unwanted water production can be reduced. Knowing which zones are actually producing oil and gas also provides guidance for making completion decisions on other wells producing from the same reservoir.

Frequently the task of determining the nature of downhole flow is complicated considerably by the fact that the downhole flows are very turbulent and composed of several phases. This makes the interpretation considerably more difficult and requires the engineer to have a good understanding of both tool physics and fluid dynamics to obtain good results. A wide variety of sensors are required to provide a reasonable database for this interpretation.

Sometimes a production logging string is also used for well tests. This is normally an area of interest for reservoir engineers, whereas classic production logging runs are more a concern for production engineers. The purpose of well testing is to:-

a) Determine the ultimate flow potential of the reservoir.

b) Decide from the skin effect number whether flow is being choked off at the borehole by either poor completion efficiency or drilling damage and if so, choose a remedy (acidising or reperforating).

c) Determine the area extent of the reservoir.

(These are determined by measuring permeability (k) + skin effect)

The downhole data are often acquired simultaneously with surface flow and separation equipment.

11.3.1 Equipment

A production logging string combines numerous sensors to provide wellbore measurements needed for analysis simultaneously. Generally it combines the following measurement sensors:

a) Flow Rate

b) Fluid Density

c) Temperature

d) Pressure

e) Caliper

f) Gamma Ray

g) Collar Locator

The Gamma Ray and Collar Locator tools are run for depth correlation purpose. The caliper, using a potentiometer, measures the inner diameter of the casing. This data is used to evatuate the flowrate.

11.3.1.1 Flow Rate

A flowmeter tool incorporates an impeller which is rotated by a moving fluid The rotation impeller is arranged to generate a series of electrical pulses which are transmitted by the wireline for receipt by surface equipment. At the surface, the pulse frequency is detected, permitting measurement of the number of revolutions per second (RPS) of the impeller. The flowmeter tool continuously generates useful measurements even as the cable is moved with or against the direction of fluid flow.

Because the purpose of the flowmeter tool is to measure the velocity of the moving fluid it is necessary to relate revolutions per second to fluid velocity. This relationship, called the response curve, is presented in figure 11-1, where revolutions per second are represented on the vertical axis and fluid velocity appears on the horizontal. It should be noted that until the fluid reaches or exceeds the value V_T (the threshold velocity), the impeller does not rotate. As the fluid velocity increases above

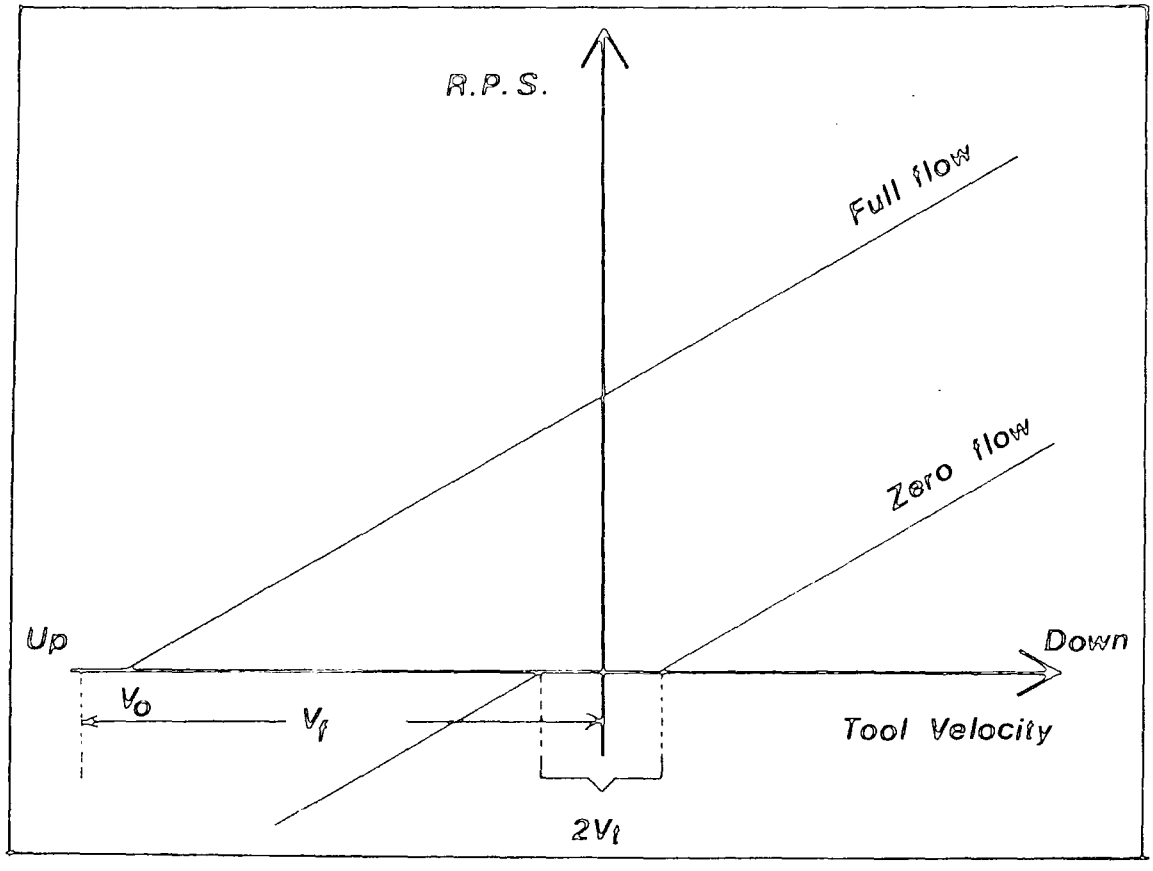

Figure 11-1. Flowmeter response curve. (Schlumberger, 1984)

V_T, the RPS values increase linearly with fluid velocity; therefore, the fluid velocity, is readily obtained from a measured RPS value, provided that the relationship depicted by the response curve is known.

There are a number of important considerations related to the response curve which are summarised here. First, the response curve is somewhat idealised especially at low fluid velocities. Second, the response curve relates revolutions per second to fluid velocity when the flowmeter tool is stationary in the moving fluid. Third, the slope of the response curve depends on the diameter of the pipe in which the fluid moves. Also, the slope of the response curve is significantly affected by the viscosity of the moving fluid. Finally, the value of V_T varies somewhat with the adjustment of the impeller shaft bearings and with the viscosity and density of the moving fluid.

It is possible to derive response curves from surface data that are applicable generally to all flowmeter tools in all surveys. But one of the most accurate response curves is derived by calibrating a particular flowmeter tool in its downhole environment, whereby the effects of diameter, viscosity, etc., are compensated automatically.

Company	Tool	Max.Temp (°F)	Max Pressure (kpsi)
Gearhart	HSF	300	15
Schlumberger	CFS	350	15
	FBS	390	20
Western Atlas	CSF	350	18

Table. 11-3. Flowmeter Tools' Ratings.

Gearhart offers the High Sensitive flowmeter (HSF) tool; Schlumberger offers two tools: the Continuous Flowmeter Sensor (CFS) tool for high flowrate and the Fullbore Flowmeter Sensor (FBS) tool; and Western Atlas offers the Continuous Spinner Flowmeter (CSF) tool. All these spinner tools work on the same basic principle described earlier.

11.3.1.2 Temperature

During a temperature survey, the temperature instrument is suspended in the

wellbore by the cable, which transmits measured wellbore temperatures to related surface equipment for recording and display. In fluids the temperatures may be recorded continuously, i.e., while the instrument is in motion. However, in gas environments, stationary measurements may be necessary.

Company	Tool	Max. Temp. (°F)	Max.Pressure(kpsi)
Gearhart	DTT	400	15
Schlumberger	MTS	350	20
	PTS	350	20
Western Atlas	Tl	350	17

Table 11-4. Temperature Tools' Ratings.

All the logging companies use a linear wirewound sensor element to detect changes in temperature. The resistance of the wire changes with the temperature. A Wheatstone bridge is usually employed to measure very accurately changes in the measuring filament resistance.

Gearhart has the Differential Temperature (DTT) tool; Schlumberger has the Manometer Temperature Sensor (MTS) tool and the Pressure Temperature Sensor (PTS) tool ; and Western Atlas has the Temperature Log (TL) tool. The Schlumberger PTS is a new generation tool which combines the pressure, temperature and fluid density sensors into one tool.

11.3.1.3 Fluid Density

The Fluid Density instrument measures the density of a downhole fluid, and transmits a signal representing the measured value through a cable to the surface, where the density is logged typically in units of grams per cubic centimetre.

Company	Tool	Max.Temp. (°F)	Max. Pressure (kpsi)
Gearhart	FDL	375	15
Schlumberger	GMS	350	20
	PTS	350	20
Western Atlas	FDL	400	15

Table 11-5. Fluid Density Tools' Ratings.

Both Gearhart and Western Atlas use a nuclear measurement technique to record density of the well fluids. Using a chemical gamma ray source, the density measurement is made by observing the relative absorption of gamma rays passing through the borehole fluid in a sampling channel. The basic unit of measure is a count of residual gamma rays. This counting rate is inversely proportional to the density of the sample and is a function of the activity of the gamma ray source. For example, the Gearhart tool output is approximately 600 counts per second in free air and 250 counts per second at 1.2 g/cc fluid density.

Meanwhile the Schlumberger tool uses the pressure technique. Figure 11-2 shows the schematic of the Gradiomanometer (GMS) tool. The pressure difference measured by the two sensing bellows is converted by a semiconductor device to an electrical signal, which is then related to the density of the fluid. Similarly, the PTS tool uses the pressure technique. The pressure difference between two ports connected by a tube of silicone oil and spaced two feet apart is detected by a transducer and related to the density of the fluid.

11.3.1.4 Pressure

Wellbore pressures may be surveyed with a high resolution gauge or a strain gauge. A high resolution gauge transmits frequency signals representative of measured values through a cable to a surface computer. At the surface a received frequency value is converted to its corresponding pressure value in psia. A strain gauge uses the same principle as those found in openhole pressure sampling tools. Often the temperature of the gauge is also measured, and this is used to compensate the detected pressure

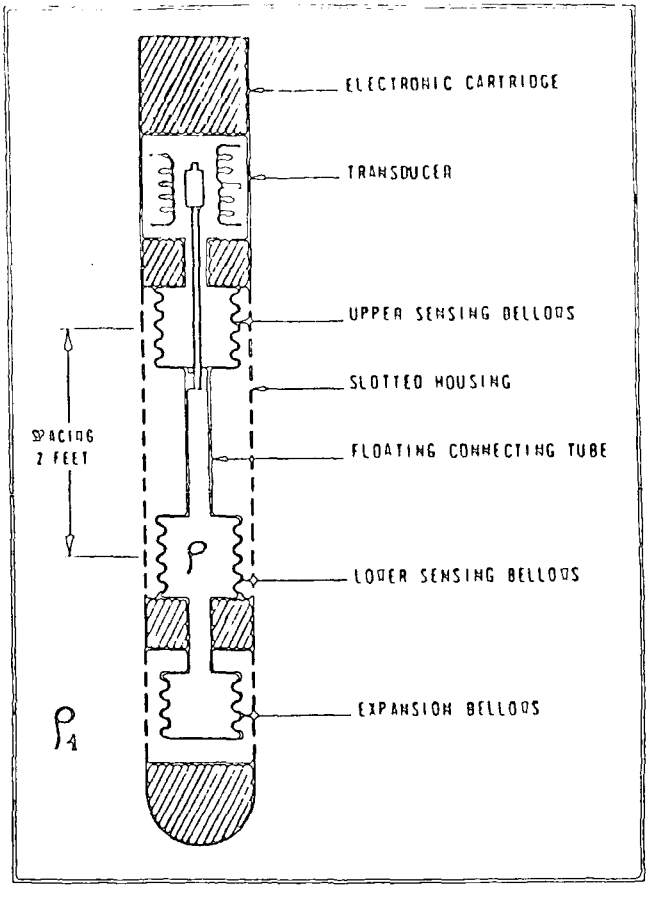

Figure 11-2. Schlumberger Gradiomanometer. (Schlumberger, 1984)

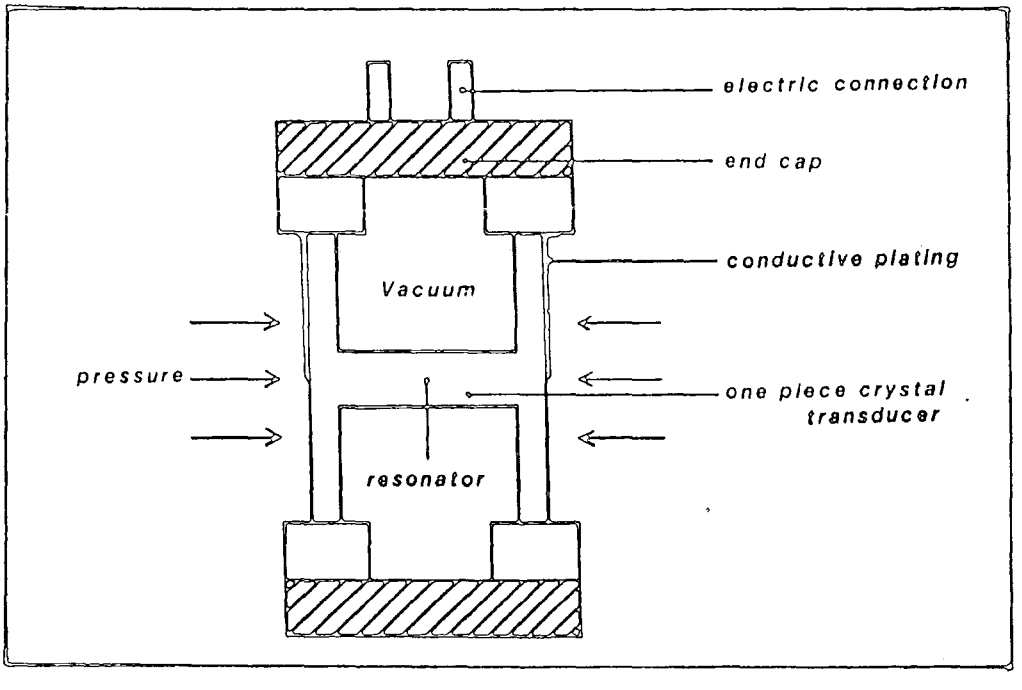

Figure 11-3. Schematic of the measuring section of a crystal gauge. (Schlumberger, 1984)

value, achieving greater accuracy of measured pressures.

Company	Tool	Max. Temp. (°F)	Max. Pressure (kpsi)
Gearhart	BHP	300	20
Schlumberger	MTS	350	15
	HMS	350	15
	PTS	350	15
Western Atlas	HP	300	20

Table 11-6. Pressure Tools' Ratings.

All the logging companies offer the use of the quartz pressure gauge, usually made by Hewlett Packard, to detect the pressure and the change in pressure. When the pressure is exerted on a crystal, it changes the frequency under which the crystal oscillates. Figure 11-3 shows a schematic of the measuring section of a crystal gauge.

However, in some cases a pressure measurement from a strain gauge may be sufficient. Such a service is offered by the Schlumberger MTS and PTS.

Production logging, as in openhole logging, is generally done with numerous sensors downhole simultaneously. All the logging companies are able to provide such a service. However it should be noted that the Schlumberger collection of production tools seem to have both better accuracy and resolution (see table 11-7).

The Schlumberger fluid density sensor tools have the better accuracy and resolution. This could probably be explained by the difference in measurement technique used. Schlumberger uses the pressure technique, whereas Gearhart and Western Atlas rely on radioactivity technique which is more dependent on statistical variation and hence is both less accurate and has worse resolution.

Concerning the temperature sensors all the companies use a similar method to measure the wellbore temperature. Hence all the tools have similar accuracy and resolution. However the PTS has better accuracy and resolution. This is probably because of the digitised hardware used downhole in the gathering and transmission of data.

Generally quartz pressure gauges are bought off the shelf from Hewett-Packard and there are therefore no differences in the tool performance. When a strain gauge is used, the accuracy and resolution are reduced. The figures quoted are similar

to those quoted for the openhole pressure sampling tools (see table 7.1). Again, the PTS has better accuracy and resolution because the tool electronics are fully digitised.

		Schlumberger		Western Atlas	Gearhart
		PLT	PTS		
FLUID	Acc	+/-3%	+/-3%	+/-5%	+/-5%
DENSITY	Res	0.005 g/cc	0.005 g/cc	0.01 g/cc	0.01 g/cc
TEMPERA-	Acc	+/-1%	+/-0.5%FS	+/-1%	+/-1%
TURE	Res	0.1 °F	0.02 °F	0.1 °F	0.1 °F
MANO	Acc	+/-0.15%FS	+/-0.3%FS	+/-0.15%FS	+/-0.15% FS
STRAIN G.	Res	0.5 PSI	0.1 PSI	1 PSI	1 PSI
MANO HP	Acc	+/-0.025% of reading		ditto	ditto
QUARTZ G.	Res	0.01 PSI	0.01 PSI	0.01 PSI	0.01 PSI
FLOW-	Acc	+/-3%(FBS):+/-10%(CFS)		+/-10%	+/-10%
METER		of the total flowrate		of the total flowrate	
	Res	0.1(FBS): 0.5(CFS) RPS		0.5 RPS	0.5 RPS
CALIPER	Acc	+/-1.4% FS		+/-2% FS	+/-2% FS
	Res	0.1 inch		0.1 inch	0.1 inch

Table 11-7. Production Logging Tools' Accuracy and Resolution.

The accuracy quoted for each flowmeter sensor are similar. However, the FBS has a better accuracy and resolution because it has larger impeller blades. Also the tool has six coils to measure each revolution of the impeller whereas all the other tools have only two coils. The final accuracy of the flowmeter data also depends on the response curve. In most cases, the data will be more qualitative than quantitative i.e. percentage contribution of each individual zone to the total amount is generally of more importance than the exact amount in terms of barrels per day.

12. CASE HOLE AUXILIARY SERVICES

So far, it is noticeable that electrical well-logging has primarily been used for gathering data in the open hole. However,even when the well has been cased there are still some useful logs that could help evaluate the performance of the well and hence the reservior. These logs are usually from a family of production logs as mentioned in chapter 11.

In addition to production logs, there are also quite a few other services in the case hole which could prove most valuable. These services can be termed "auxiliary services", and the major auxiliary services can be grouped as follow :

a) Directional.

b) Cement Evaluation.

c) Corrosion Monitoring.

12.1 Directional

When deviated wells are drilled it is in the operator's interest to know the bottom hole location and well trajectory. Originally, while the well was drilled, the direction and trajectory are controlled but in some cases this may not be sufficient. If there are many wells being drilled in the area a more accurate determination of bottom hole location and well trajectory may be needed especially during and after the well is drilled. For example, this is the a case in the North Sea where there are numerous operators and numerous blocks being leased out by the government. In fact it is a requirement by law that all wells drilled in the North Sea are to be surveyed directionally. This is to ensure that an operator is not drilling into another operator's block. However, in some other places, an operator may control such a vast area that he feels carrying out a directional survey only while drilling is sufficient.

Being in a cased hole environment it is not possible to use tools which contain compasses. However, tools which use accelerometers to determine hole direction and trajectory can still be used. These tools have already been mentioned earlier in chapter 6.

With the advancement in technology, some logging companies have incorporated the use of a gyroscope (figure 12-1) into their tools. In doing so, it is possible to obtain a very accurate measurement of bottom hole location and well trajectory.

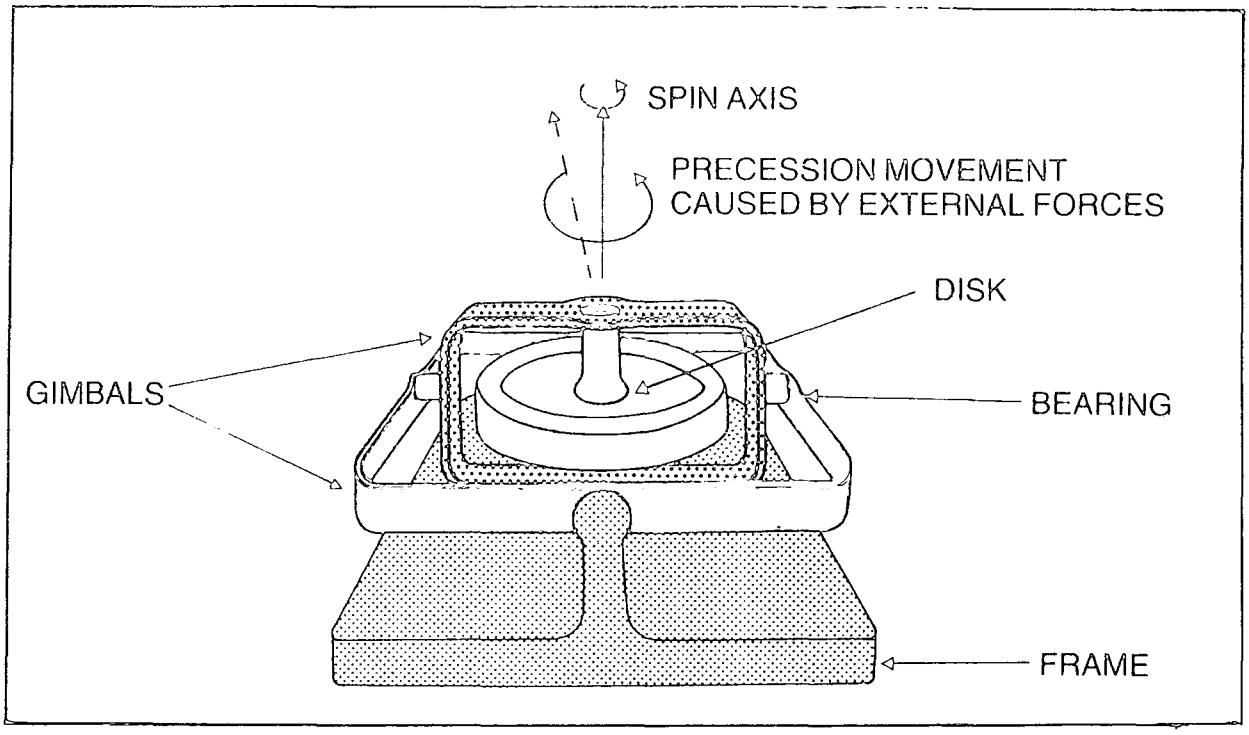

Figure 12-1. Gyroscope. (Schlumberger, 1987)

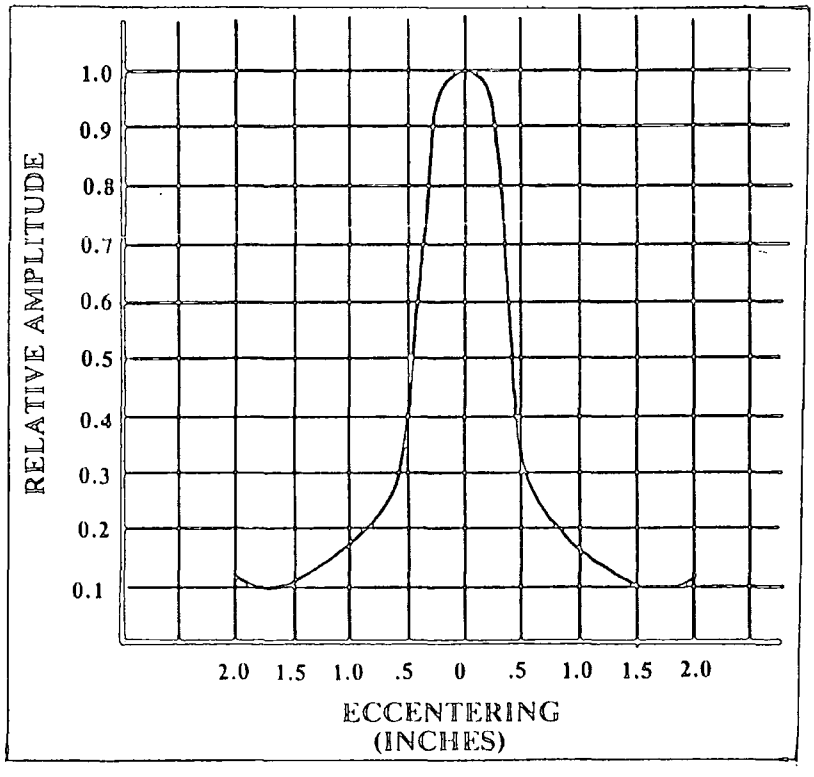

Figure 12-2. Tool Eccentering v. Relative Amplitude. (Schlumberger, 1986)

12.1.1 Principle

The principle of the above tool is based on an inertial platform with a gyroscope and accelerometers. The tool houses a gyroscope stabilised platform which contains sensors that allow the exact position of the tool within the earth to be determined when it is moved from a known starting position. Thus, a directional tool, having been given the X-Y-Z coordinates of the drilling rig may be run in the hole and be used to establish the precise vertical and horizontal departure of the hole at every point in the well.

By the use of a self-calibrating inertial guidance system similar in function to the types used in aircraft the tool in calibration mode aligns its internal gyros with the earth's spin axis. This is accomplished by fixing the tool stationary within the surface casing just under the rig and waiting several minutes while the rotation of the earth has a chance to cause the gyro's to precess a few fractions of a degree.

12.1.2 Equipment

There are presently only two companies who can offer the service based on the principle described above. This service is generally referred to as a continuous guidance survey. Schlumberger offers the Gyro-Continuous (GCT) tool, and Christiansen offers the Ferranti Gyro tool. Both tools work on the same basic principle. The Ferranti gyro tool is a larger tool due to the size of its gyroscope and hence will only work in wells which have 13 inch casing or larger. This unfortunately is a slight limitation since most wells use 13 inch casing or larger only at the surface levels.

The tolerances of the GCT tool measurements are:

a) 0.1 degree on the azimuth measurement.

b) 0.03 degree on the deviation measurement.

c) Geographic north direction is found within +/- 0.15 degree (at 45 degree latitude).

d) Maximum reference azimuth drift during the survey is less than 0.1 degree per hour.

In a 4000 metre deep well, with a 2000 metre horizontal departure, the GCT tool will determine the position of the bottom of the hole with a maximum error of 10.5 metres in the horizontal plane. The Ferranti Gyro tool also has a similar

accuracy, but unfortunately its diameter is over 10 inches and its temperature rating is only upto 150 °F. The GCT is 3 5/8 inches in diameter, and is rated to 300 °F.

Both continuous guidance tools have found their best application in areas where compasses do not work well due to the proximity of the magnetic poles, such as in Alaska and the North Sea. With more and more development wells being drilled in clusters, these tools will probably be used increasingly to reduce the risk of well collision and to position accurately a well within a reservoir.

12.2 Cement Evaluation

Once casing is run into the open hole and cementing is completed, it is often desirable to evaluate the bonding between the casing and the cement and between the cement and the formation. A poor cementing job could be the cause of the following:-

a) Communication between zones. The communication between gas-oil-water zones is undesirable, especially when it is uncontrolled.

b) Pressure trap in the annulus. If there is pressure trap in the annulus (between the casing and the borehole) this may build up large enough to cause a blow-out.

c) A blow-out. If the casing is totally free in the borehole, sooner or later it will blown-out of the hole.

The cement bond log (CBL) becomes a valuable source of data pertaining to the effectiveness of the cement sheath surrounding the casing.

12.2.1 Principle

Using the sonic tool principles and in most cases probably the same tools, the data are obtained by evaluating the effect of the casing, the cement sheath and the formation on an acoustic wave emanating from the cement bond log instrument. The amplitude curve of the reflected acoustic wave is maximum in unsupported casing and minimum in those sections in which the cement is bonded to the casing. This amplitude of sound pulses is generally produced by a transmitter-receiver pair spaced 3 feet apart.

One of the essential requirements when running a cement bond log is the centralisation of the tool. Eccentering of the tool even by 1/4 inch can cause the

amplitude signal level to drop drastically (figure 12-2). If the tool is poorly centralised a poor bonded section would be seen by the tool as a good bonded section.

In addition to the CBL curve a second log generally from the transmitter-receiver spaced 5 feet apart is also presented. This is usually presented as a wavetrain or/and as a "peak and valley-width" bar chart (variable density). Figure 12-3 shows a typical cement bond log presentation with the variable density log. Note the gamma curve and the casing collars are also recorded. The former is used for correlation to the base open hole log and the casing collars is used for correlation when a perforation service is run. The variable density (VDL) log is used to identify the wave path and confirm the interpretation of the CBL curve. When complete bonding is indicated, the through-the-formation wave is identifiable and can be used much like the open hole acoustic log.

12.2.2 Equipment

The tools used for a cement bond log are the same sonic tools which are used for open hole logging. The only difference is the mode setting for the tool operation, and this is usually software controlled.

With further development, Schlumberger has two more tools to evaluate cement bond. The first tool is the cement bond (CBT) tool, which gives a continuous measurement of the attenuation of sound pulses. This measurement gives attenuation independent of casing fluid and transducer sensitivity, as well as being self calibrating and less sensitive to eccentralisation and sonde tilt. Standard spacings are 2.4 feet and 3.4 feet The CBT additionally gives the attenuation of sound pulses from a receiver spaced at 0.8 foot from the transmitter that is used in fast formations where the formation signal may arrive before the casing signal at the longer spacings.

A CBL curve is computed from the three attenuations available to allow comparison with CBL logs made on 3 foot spacing. This computed CBL continuously discriminates between the three attenuations to choose the one most suited to the well conditions. This results in a CBL log which is less sensitive to noise and is less affected by fast formation signals. An interval transit time curve for the casing and a VDL log from a receiver on a 5 foot spacing are also recorded for interpre-

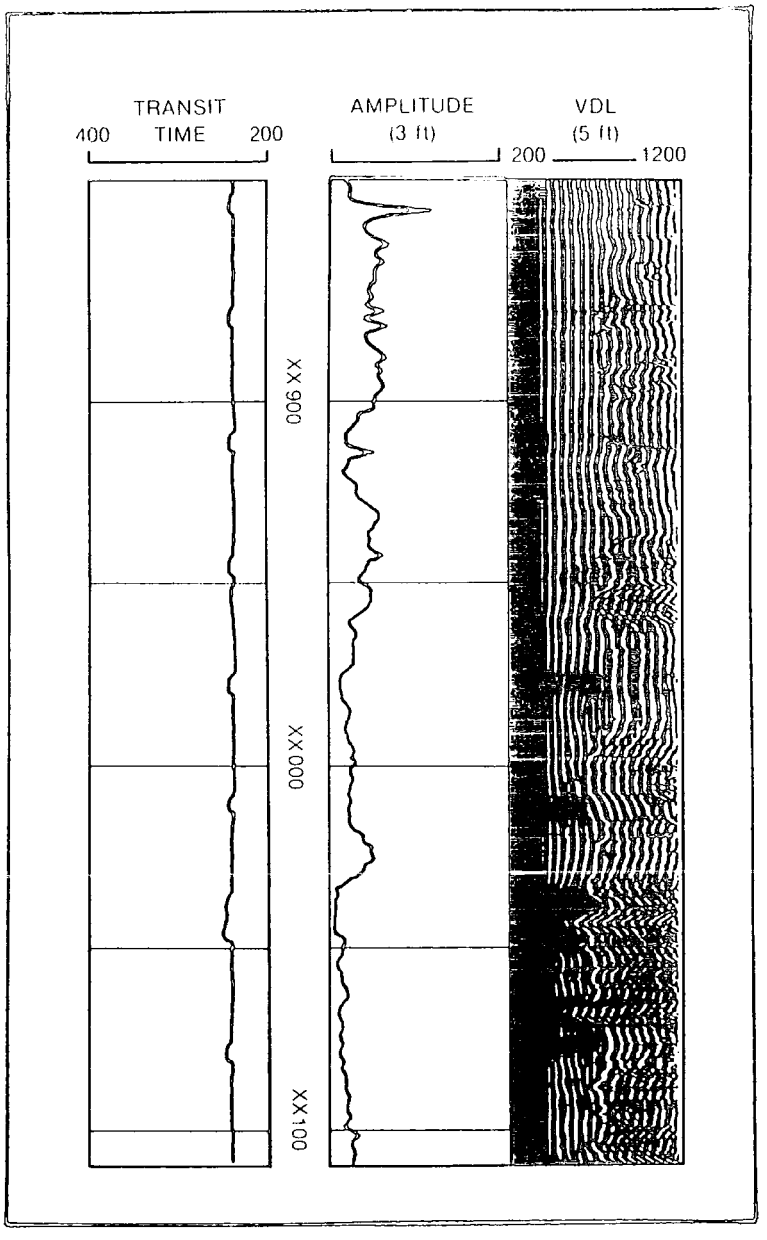

Figure 12-3. CBL-VDL Presentation. (Schlumberger, 1986)

tation of the cement job.

The second tool is the cement evaluation log (CET) tool. The CET tool investigates the cement radially and gives eight separate indications of cement distribution and quality in addition to measurements of casing diameter, casing roundness and tool eccentering.

Eight ultrasonic transducers, operating as both transmitters and receivers, are positioned radially around the CET sonde 45 degree apart. Each transducer emits a beam of ultrasonic energy in 300 to 600 kHz band which covers the resonant frequency range of most oilfield casing thicknesses.

The energy pulse from the transducers is directed perpendicular to the casing wall. The sound energy enters the casing and bounces back and forth between the impedance boundaries at the front and back face of the casing. With each bounce of the sound pulses at the boundaries, diminishing portions of the sound pulse are returned to the transducer. The transducer sees these returning pulses as a decaying oscillating waveform. The vibrations die out quickly or slowly, depending on the material behind the casing. The majority of the energy is reflected back to the transducer where it is measured and the remainder passes into the casing wall and echoes back and forth until it is totally attenuated. Each time the pulse is reflected off the inner casing wall, some energy passes through the interface and reaches the transducer. A ninth transducer continually measures acoustic travel time of the casing fluid column so that the eight transducer travel times can be converted to distance measurements. This fluid travel time can be presented on the log, if desired, to indicate the type of casing fluid. Figure 12-4 shows a typical CET log presentation.

12.3 Corrosion Monitoring

As the life of a well increases, the casing within such a well will most likely be affected by corrosion. There could be sufficient decrease in the casing wall thickness that the casing may not be able withstand the formation pressure. Or there could be cases where holes have developed on the surface of the casing, or else are beginning to develop.

Therefore, it may be desirable for the operator to investigate the condition of the casing in his wells. Obivously, it is impossible and impractical to pull the

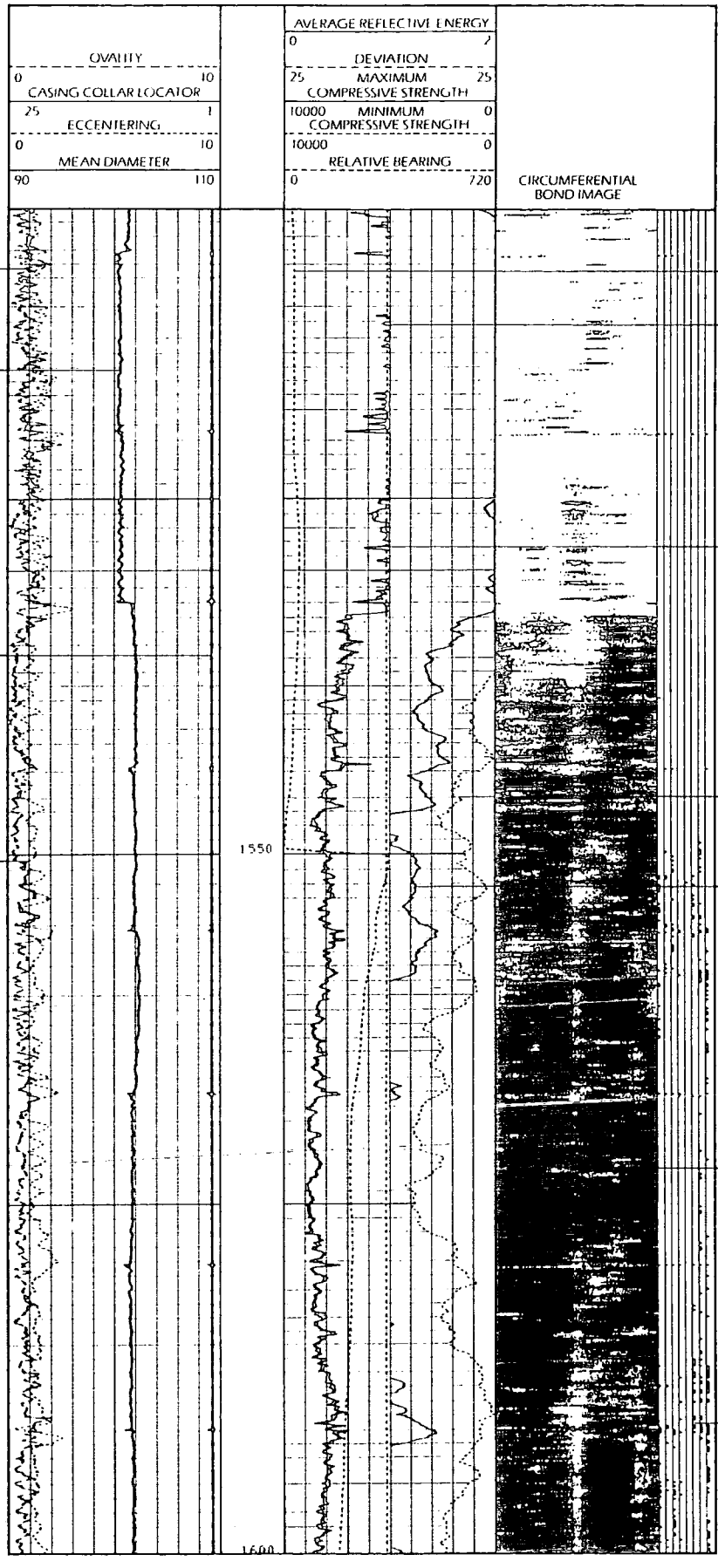

1. CASING OVALITY

2. MEAN DIAMETER

An acoustic caliper records 8 radii measurements that are accurate to within 0.004 inches. The ovality and mean diameter of the casing are also presented.

3. CASING COLLAR LOG

The Gamma Ray and Casing Collar log are correlated with open hole logs for accurate depth control.

4. ECCENTERING

Tool eccentering is computed for monitoring data accuracy.

5. DEVIATION

6. RELATIVE BEARING

The well deviation and the relative bearing of the first transducer are recorded. The orientation of a channel in the cement can be determined when the well is deviated by 3° or more.

7. WWM

The reflective energy average or acoustic impedance of the eight transducers is displayed. This curve is related to the amplitude attenuation of a Cement Bond log and is an indicator of cement quality.

8. MINIMUM COMPRESSIVE STRENGTH

9. MAXIMUM COMPRESSIVE STRENGTH

The compressive strength of the cement is computed for all of the eight segments and the maximum and minimum values are displayed on the log.

10. CIRCUMFERENTIAL BOND IMAGE

The responses of the eight transducers are presented for visual indications of cement quality and channeling.

11. GAS FLAGS & FAST FORMATION FLAGS

These additional graphic presentations aid interpretations and are displayed for the eight transducers.

Figure 12-4. CET Presentation. (Schlumberger, 1985)

casing out from the hole. Thus he will have to rely on the services offered by the logging companies to inspect the extent of corrosion developed on the casing within the wells. Downhole corrosion problems are many and varied, requiring many techniques for their detection and monitoring. A combination of measurements are available, and their principles are acoustic, electrical and mechanical.

Corosion monitoring has many applications, and these can include:-

- Internal Diameter.
- Casing Thickness.
- Scale Detection.
- Pipe Sections.
- Hole Detection.
- Metal Loss Detection.
- Mechanical Wear.
- Corrosion Rate.
- Condition of Multiple Strings.
- String Composition.
- Monitor Effectiveness of Anti-Corrosion system.

12.3.1 Acoustic Tool

Presently, Schlumberger is the only company which uses acoustic principle to provide data on corrosion. The tool used is the cement evaluation (CET) tool, whose principle has already been described earlier. In addition to giving cementation quality logs, the CET can also provide via its eight ultrasonic transducers:

a) 8 oriented acoustic radii with a resolution of 0.1 mm. (0.004 inch).
b) 8 absolute casing thickness measurements with a resolution of 0.7 mm (0.0275 inch).
c) Pipe roughness indicator.

The advantages of the CET tool are the fact that it is a non destructive ultrasonic measurement, and that the cementation quality can be obtained at the same time. Figure 12-5 shows a presentation of the CET calipers.

12.3.2 Electrical Tool

Electrical corrosion montoring tools generally use electromagnetic principles to provide the required measurements. The tools available are:-

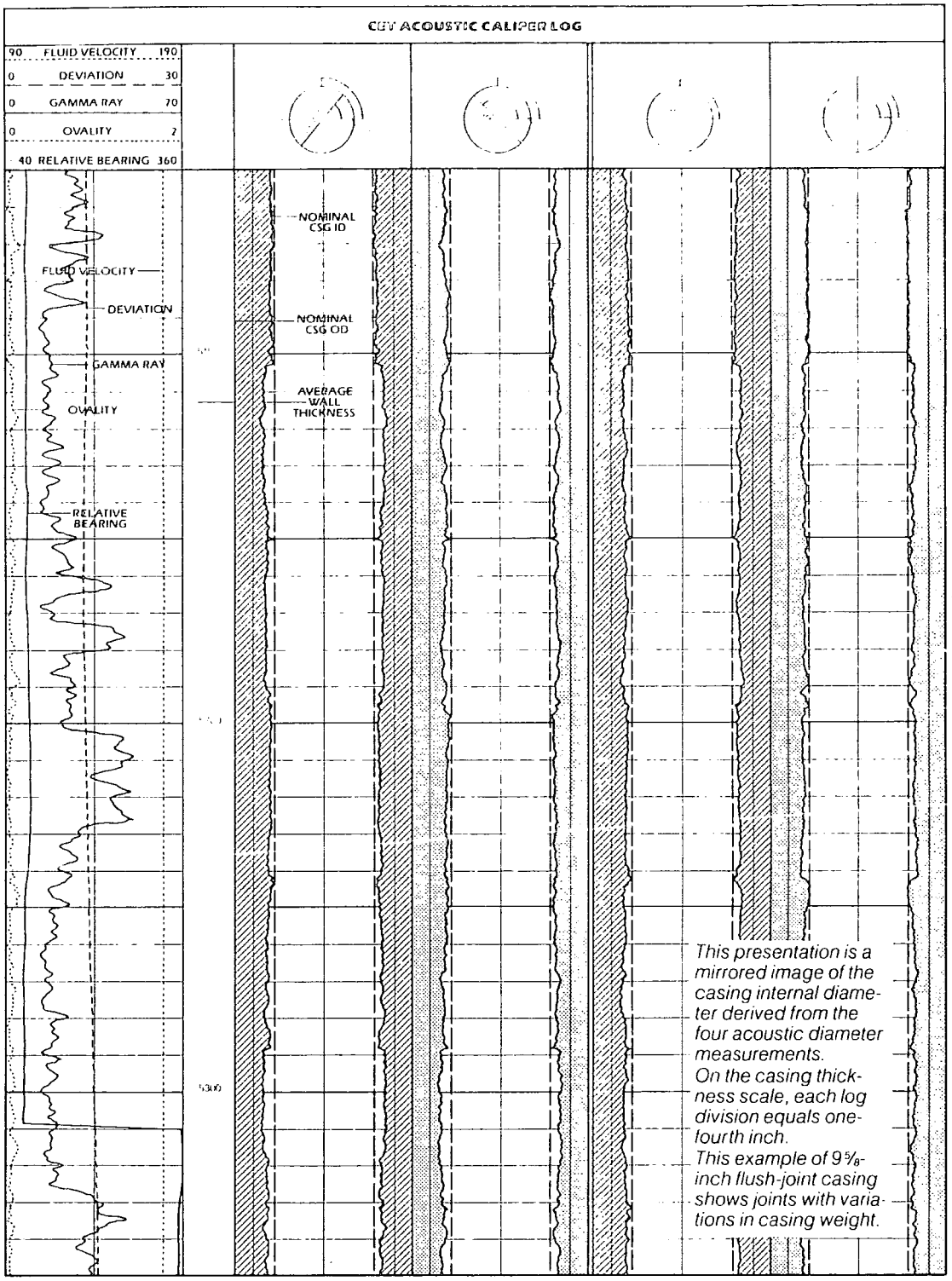

Figure 12-5. CET Calipers Presentation. (Schlumberger, 1985)

Company	Tool	Casing Range(in).	Max.Temp.(°F)	Max.Pressure(kpsi)
Schlumberger	ETT	3.50 - 10.75	350	20
	PAT	4.65 - 10.20	350	20
Western Atlas	CPP	4.50 - 13.38	300	20
	MGL	4.50 - 10.75	300	20
	VTL	3.50 - 10.75	280	12

Table 12-1 Electrical (Corrosion) Tool's Ratings.

Schlumberger has the Electromagnetic Thickness (ETT) tool and the Pipe Analysis tool (PAT). And Western Atlas has the Casing Potential Profile (CPP) tool, the Magnelog (MGL) tool, and the Vertilog (VTL) tool.

The Schlumberger ETT tool uses a transmitter coil to generate a magnetic field and a receiver coil to measure the created electromotive force. This electromotive force is out of phase with the transmitted signal and the difference is primarily proportional to the average thickness of the casing in front of both coils. This information can be used for a macroscopic evaluation of the casing condition but it cannot provide details on small defects or identify whether a defect is on the inner or outer wall of the casing. Interpretation is greatly enhanced by having a base log, run early in the life of the casing, to compare with subsequent logs. The ETT wall thickness measurement sums through all concentric strings.

The Schlumberger PAT tool uses a high-frequency eddy-current test to detect flaws on the inner surface of casing and a magnetic-flux-leakage test to inspect the full casing thickness. With these measurements, small defects and corroded areas in pipes can be detected and defects on the inner and outer walls of a single string of casing can be identified. Although small defects are easily seen on the PAT log, larger defects such as casing splits often cannot be identified.

However, using data from both the PAT and ETT logs, severe corrosion and defects can be detected and identified as on the inner or outer casing of a double string.

Western Atlas CCP survey records a succession of voltage differences measured along the inside casing wall. Each recording is made with the tool stationary, while it measures the voltage difference between two depths whose

spacing is selected before the survey. Examination of a depth plot of the measured voltage differences identifies intervals over which electrochemical corrosion is actively removing metal from the outside casing wall. Generally, it can be used to forecast corrosive damage, probable rate, and where cathodic protection would be effective.

The Western Atlas MGL tool uses ac electromagnetic measurements to record information which determine the circumferential average of the casing wall thickness. Other measurements recorded by the MGL tool indicate the presence of small defects on the inside casing wall as well as variations of the circumferential average of the casing's internal diameter. While the MGL curve may be used to detect corrosion of large aerial extent, its principle uses are to assess internal pipe wear, detect weight changes in a mixed casing string and to identify the bottom of external casing strings. The MGL tool responds to metal loss both internally and externally.

The Western Atlas VTL tool uses dc electromagnetic measurements to determine the degree of penetration of casing defect, whether the defect is internal or external, and the defect's circumferential extent. Figures 12-6 and 12-7 show flux lines of the VTL tool in non-defective casing and in defective casing respectively.

12.3.3 Mechanical Tool

Corrosion monitoring is also possible by mechanical means. Generally it is done by using a tool with caliper arms. Table 12-2 shows the tools currently available. Gearhart has the Pipe Inspection Caliper (PIC) tool, Schlumberger

Company	Tool	Casing Range (in.)	Max.Temp.(°F)	Max.Pressure (kpsi)
Gearhart	PIC	2.38 - 10.75	350	10
Schlumberger	MFC	4.50 - 13.38	350	20
Western Atlas	MCL	2.38 - 10.75	350	16.5

Table 12-2 Mechanical (Corrosion) Tool's Ratings.

has the Multi-Finger caliper (MFC) tool and Western Atlas has the Multi-Finger caliper (MCL) tool also. All the tools use the same basic principle of using multiple caliper arms on the tool. The number of arms can range

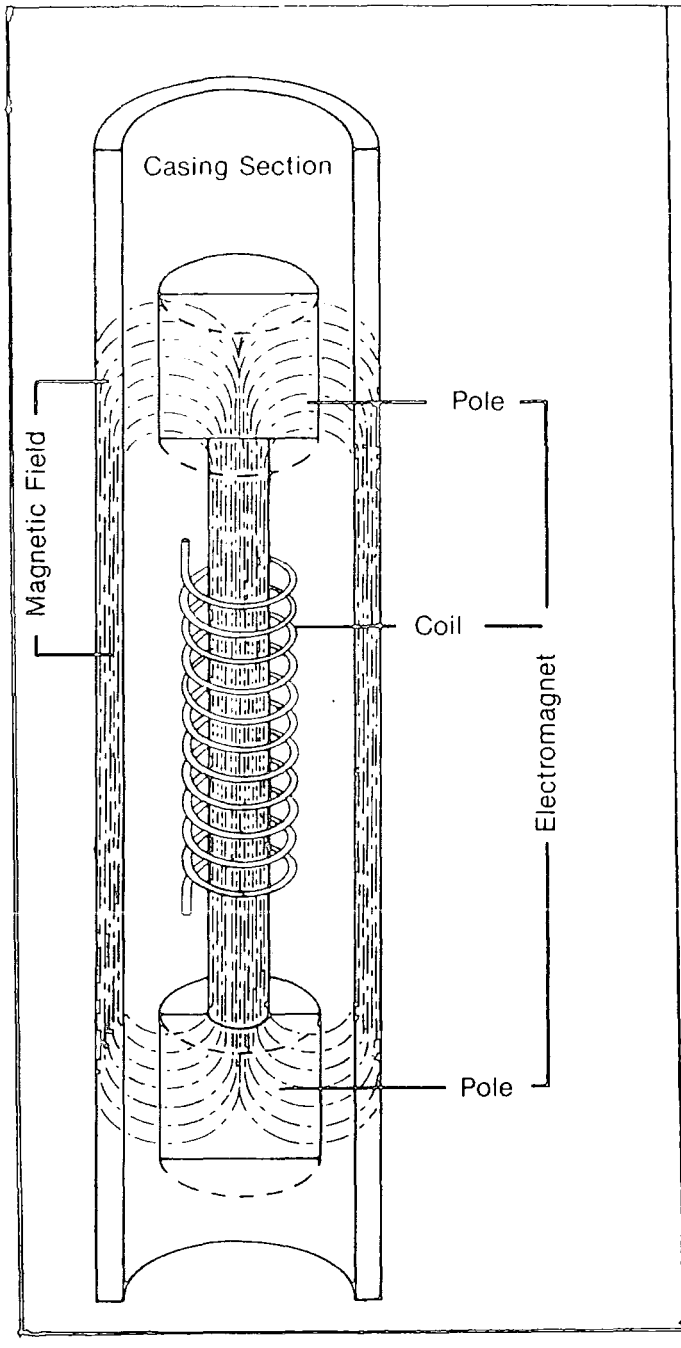

Figure 12-6. Flux lines in non-defective casing. (Western Atlas,1985)

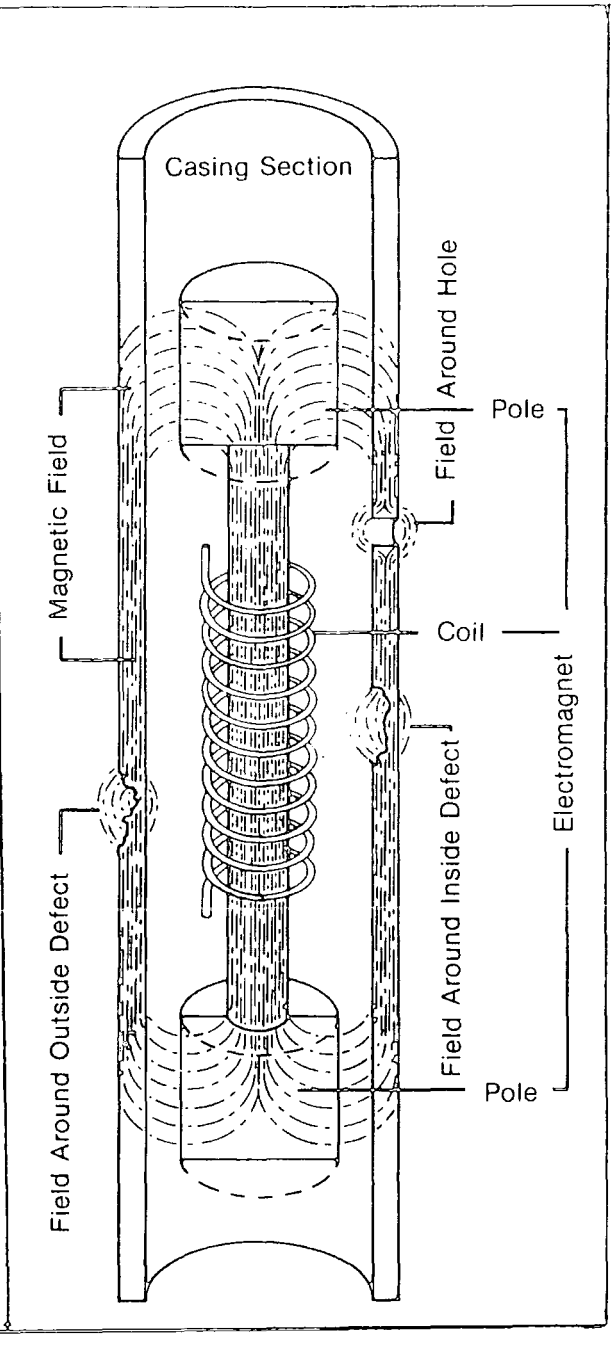

Figure 12-7. Flux lines in defective casing. (Western Atlas, 1985)

from 30 to 72 depending on the tool size and casing size. The measurements generally show the greatest and least internal radius of the casing. The Schlumberger MFC tool is the only tool which divides the caliper fingers into three sections thus giving three minimum and three maximum radius readings. The tool can also be arranged to give six maximum radius readings.

Case hole auxiliary services will for the near future remain auxiliary. The industry is in a slump and an operator is unlikely to decide to run an auxiliary log unless absolutely necessary. Generally, by the time a corrosion log is run the full benefit of the log is lost. A corrosion monitoring log, as the name implies, monitors the corrosion within a well. As already mentioned, the nature of corrosion can be electromagnetic, chemical or/and mechanical. If proper planning is followed it is desirable to monitor the corrosion within a well from the start of production and to continue monitoring annually, or more often if necessary. The importance of most case hole auxiliary services is generally overlooked and this is mainly due to the unwillingness to spend more money.

13 .THE FUTURE

The unsettled economic climate that oil industry recently experienced has resulted in lower and unstable oil prices, and in record cuts in exploration budgets. Back in 1985, the oil price was around $ 35 a barrel. Then in 1986, it fell to around $ 15 a barrel and kept fluctuating. Towards the end of 1987 and early 1988, it stablilised at around $16-$18, but then the world political situation made the price dropped again to $10-$12. Even now, the price is fluctuating between $10 - $16 . This being the case, the operators have had to rethink their plans. The smaller operators have been bankrupted or else have to re-evaluate their resources. The larger operators have become more conservative and also have to re-evaluate their resources.

Offsetting the drop in high risk exploration has been a rise in re-evalution and re-exploration of oil fields using improved or new technologies. Economic factors aside, the main reason for renewed interest in old fields is the refinement of reservoir models. A key element in this refinement has been the improvement of wireline methods, tools, data processing, and interpretation. The wireline companies have tried to respond as best they could. Unfortunately with the economic climate, some of the smaller wireline companies have been unable to compete and have thus been bought out by the larger companies. Alternatively their resources have been limited and thus they have been unable to expand and carry out a large program of research and development. Take-overs and mergers are becoming the norm in the oil industry as in the rest of world industry.

One such example is the case of Gearhart Industries In 1984-85, Gearhart used up a vast amount of their resources to avoid a take-over bid, then came the oil price collapse of 1986 which left Gearhart in the red. Presently it has been acquired by Halliburton Co. Ltd. Since 1984, Gearhart having limited resources were unable to continue their normal research and development program. This was reflected by the services they were able to offer when compared to other major logging companies.

The major reason for mergers and take-overs is the fact that the service company can come up with a complete package offer starting from surface seismic to finally putting the well into production. To the operating companies especially

the smaller few, this is an economic advantage and can ease the whole work process. However, some larger operating companies with more resources may still prefer to work with a range of service companies. Thus a competitive atmosphere is achieved and this to the operator, can be to his advantage.

As shown through this thesis all the logging companies can provide the same basic group of services. These basic services especially in the development fields, can be sufficient to bring a well into production. This raises the question as to why Schlumberger have more of the market share (82%) than all the others. Schlumberger was the first company in this field and it managed to expand with the oil industry expansion to cover the globe. By the time the competition arrived on the scene it already was in a dominant position. It already had the necessary network to provide field support and to offset the high cost of starting remote operation bases. The competitors generally are unable to compete especially in remote environment due to the high cost to establish the initial base. Schlumberger can therefore fund a large research and development program and hence it is the logging company which has monopolised the overall world market until now. However, in the U.S.A. and Europe where communication and logistics are convenient, companies such as Western Atlas are able to obtain a fair amount of the market share.

With most of the major fields already discovered the operators are now renewing their interest in old fields . The refinement in reservoir models is achieving better quantification of basic reservoir parameters (via the logging companies) in zones where bed thickness varies from a few inches to several feet. This has always been a long-recognised logging problem.

Therefore, more attention is being given to thin beds as exploration and development have increased in so-called down-dip, or deep water, sandstone facies. These sand-shale sequences are commonly composed of sandstone bed thinner than the resolution limit of the typical logging suite. In these facies, better estimates of basic reservoir parameters are critical in assessing the commercial value of wells and fields. Without this knowledge, reserves will be bypassed from too pessimistic an interpretation or money will be wasted from decisions based on too optimistic an interpretation.

There is no internationally recognised definition of a thin bed but the consensus of opinion has been to place the dividing line between thick and thin beds at about 15 centimetres (six inches). Efforts have been made, however, to classify rock strata according to thickness. The arbitrary nature of thin bed classifications probably arose because practical difficulties limited the apparent vertical resolution of logging tools to 15 centimetres or greater. At the time many logging tools were developed but digital transmission of data along logging cables and surface computers had not been introduced.

However with the improvement in surface computer hardware and software more data can be obtained and better interpreted. This has led to "High-Resolution Logging". Using the conventional logging tools and if the tools' hardware permit one can obtain a more detailed sampling rate to gather data. Today however new technology tools and new data processing methods are available to bring the vertical resolution of bulk volume analysis of formation to a resolution of two inches. The enhancing of density and neutron logs (using higher sampling rate and better processing) associated with the Digital Sonic Array tool (6 inches vertical resolution) can provide better effective porosity evaluation. The PHASOR tool will help to provide a more accurate R_t log. Then there are other tools such as the Electromagnetic Propagation tool, the Stratigrahic High Resolution Dipmeter, the Formation Micro Scanner tool, and the Circumferential Acousilog tool, all of which should enhance a high vertical resolution evaluation of reserves and accurate reservoir boundary definition.

One of the methods used to obtain better processing is known as "Enhanced Resolution Processing". This is a method used by Schlumberger. Enhanced Resolution Processing is ideally suited to tools in the nuclear family which generally have one and two detectors.

The near detector will provide data of higher vertical resolution but the data are highly affected by borehole fluids and mudcake and thus are less accurate. In contrast the far detector has a deeper depth of investigation and hence lower vertical resolution. Its data however suffer far less from borehole effects. Enhanced Resolution Processing combines the high resolution of the near detector

with the more accurate averaging of the far one. This procedure is explained with the aid of figures 13.1-13-4:

Figure 13-1: This shows the raw data as recorded by the near (green) and far (red) detectors. The blue line shows the true reading.

Figure 13-2: In order to commence Enhanced Resolution Processing the two readings must be depth matched to ensure accurate results.

Figure 13-3: The near detector curve is resolution-matched to the standard far detector reading. The difference between this curve and the uncorrected one is the high frequency information, the thin bed and boundary layer signals, missed by the far detector (green and red shaded areas).

Figure 13-4: Differences between near detector readings (green and red shading) are added to the standard far detector readings. The resultant curve is the vertically enhanced far detector signal.

This process involves depth and resolution matching of the near and far detector responses (figures 13-3 and 13-4). This means that the near detector reading is averaged so that its resolution matches that of the far detector. This has the adverse affect of smoothing the near detector's signal, but it does reduce the influence of environmental effects. By combining this averaged near detector response with the far detector signal using the "spine-and-rib" technique (chapter 5.2.2), a resolution-matched compensated response is obtained. Then, substracting this new response from the original near detector response, we obtain the information missing from the resolution-matched compensated measurement (figure 13-4).

Typically, with a sampling rate of 6 inches (15 cm), this process improves the resolution of litho-density data from 18 inches (56 cm) to 12 inches (30cm). With a 1.2 inch (3 cm) sampling rate this value decreases to a mere 4 inches (10cm). With the CNL tools, a 24 inch (60) resolution becomes only 12 inches (30cm), at a sampling rate of 6 inches while at a 1.2 inch sampling interval this value becomes 8 inches (20 cm).

The only drawback with the higher sampling rate is that it requires a logging speed of 900 ft/hr (260 m/hr) as opposed to the usual 1800 ft/hr (520 m/hr). Poor borehole conditions can limit the use of higher sampling rates as the effects of the borehole on the near detector can become very pronounced.

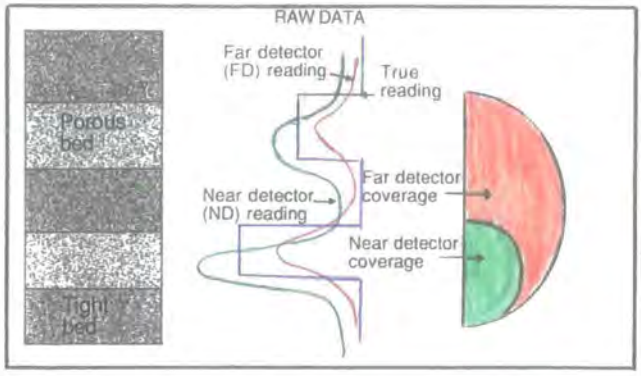

Figure 13-1. Raw data of near and far detectors.

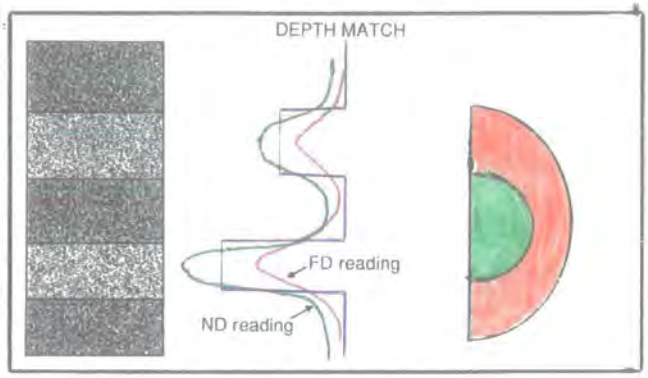

Figure 13-2. Depth matching of near and far detector data.

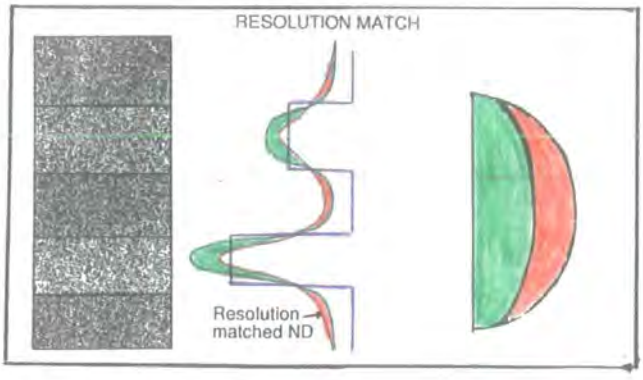

Figure 13-3. Resolution matching of near and far detector data.

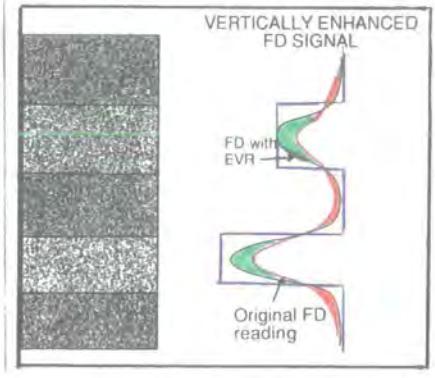

Figure 13-4. Vertically enhanced far detector signal.

N.B. Figures 13-1 to 13-4 are referenced to Johnston, Watfa, Nurmi, Andreani, and Flaum, 1989.

Furthermore, to enhance the high-resolution logging and data handling capability, the possibility of using fiber-optic cable instead of wire cable has already been experimented by Schlumberger. The primary advantage of the optical system is a 50-fold increase in bandwidth resulting in a new type of telemetry protocol for well logging. Its most significant feature, transparency, allows for simpler two-way communication between the surface computer (CSU) system and tools (i.e., data is delivered as if they are hardwired). This removes many of the restrictions, such as fixed sample rates and limited combinability of tools, that formerly hindered tool designs. Although the main motive behind the optical system is to allow development of tomorrow's data-intensive tools, the system also offers several advantages to users of existing tools:

a) New types of tool combinability.

b) Faster logging time.

c) Improved data reliability.

This system is still experimental, although some engineering challenges have been solved:

a) Fibre purity: By the early 1980's, when Schlumberger's optical-telemetry system was just evolving, glass-fibre manufacturers had perfected fibres with low losses in the 840-nanometer(nm) range, but achieving equally low losses in the 1,300-nm range eluded them. In 1982, Corning Glass Works and several Japanese manufacturers found ways to reduce concentrations of hydroxyl radicals in the glass, which lowered attenuation in the higher waverlength.

b) Optical emitter/ fibre alignment: Making optical emitters work at 200 °c is not as big a problem as assuring their axial alignment with optical fibres within 1 ppm over temperatures ranging from below 0 °c to above 200 °c. This problem was solved by mounting the emitter and fibre together in a rigid, hermetic package using novel assembly techniques and materials.

There are still problems unresolved:

a) Crystal oscillator technology in the downhole tool: A quartz crystal oscillator in the downhole telemetry cartridge serves as the clock for the logic chip that demodulates all transmissions as they pass through. To do this within an acceptable digitisation error, each bit of the 5 Mb/s must be segmented into eight

subdivisions. The crystal must therefore oscillate at 40 MHz with a tight tolerance of 0.01 prcent. In the past, suitable downhole designs had a 20 MHz limit, which permits only a 2.5 Mb/s maximum data rate.

b) Gate-array technology in the downhole tool: Much of the downhole electronics employs gate arrays. Existing technology supports only a 2.5 Mb/s telemetry rate reliably at borehole temperatures. Engineers are trying to extend the range of gate arrays to support 5 Mb/s at 200 °c. Typically, at high temperatures, gate arrays slow down, lose bandwidth, and latch up.

c) Downhole printed-circuit (PC) board design : A PC board that can handle 1 to 2 MHz is easy to design, build, and use. The parts are spread out and long lead lengths have little effect on performance. With analog circuitry designed for a 300-Hz gain-bandwidth product, long leads create inductive and capacitive parasitics that degrade the circuitry performance.

d) Ease of fibre-optic cable splicing : The first fibre-optic logging cable had one splice performed under controlled, laboratory conditions. Making the splice was not difficult but the process must be simplified before it can be done in a field service centre. Splicing now requires several steps, including the use of a high-power laser to weld the fibre.

e) Handling increased data volume : The optical system is expected to get data to the computer 40 to 50 times faster than the current system. Engineers are working on the next system generation to be able to handle this faster rate.

The next generation of well logging methods are already emerging. How quickly they are introduced will depend largely on the economic climate worldwide. If and when the price of oil is perceived as high and stable enough then newer technology should be applied more routinely and frequently, but until then the well logging methods will be limited to the basic services with additional extra services when needed.

14. DISCUSSION AND CONCLUSION

An overview of electrologging within the petroleum industry together with the principles of the methods used has been presented. For the survey and comparison the tools and their specifications have been chosen from the logging companies of Gearhart, Schlumberger and Western Atlas who together have 93% of the world market.

Although the tool ratings from the three logging companies are generally the same in practice the operator seems to obtain better result both in terms of accuracy and repeatability of the data from Schlumberger especially in exploration wells and in wells which are deep (> 10000 m) and hot (> 280 °F). When deep and hot well conditions are expected logging tools are normally heat-checked in an oven prior to the operation. In general it has been shown that the tools developed and used by Schlumberger provide the operator with a better service and reliability, although this is not always the least expensive.

The principle of the resistivity tools is relatively simple however in practice the determination of the virgin zone has proved to be more complicated. Even though all the logging companies are able to provide this service Gearhart and Schlumberger stand out in being able to offer the High Resolution Induction tool and the PHASOR Induction tool respectively. Both these tools have better accuracy and provide data of better resolution.

The operation of nuclear tools is dependent on measurement of radioactive counts which can vary due to statistics. The improvement has been made by means of generating higher counts and the use of two detectors to compensate for one another. Also the data obtained from each porosity tool is used to compliment each other. In the family of nuclear tools, the Schlumberger Litho-Density tool and the Western Atlas Compensated Z-Densilog tool stand out in being able to offer more than just bulk density and porosity data. They also offer lithology information through the use of the photoelectric absorption index.

The acoustic tool can also offer porosity information but nowadays the operator seeks a more detailed analysis of the data to provide him with information on fracture systems and rock elastic and inelastic properties. Hence more data acquistion

with the acoustic tool is necessary. Schlumberger has foreseen this market with the introduction of the Array-Sonic tool. The applications and full potential of this tool still remain to be tapped. Western Atlas has also developed the Circumferential Acoustilog tool to cater for the determination of fracture systems to compliment their existing sonic tool.

The determination of geological structure is very important to the operator. From this information a program is carefully planned and followed. The tools which can determine accurate dips of the geological structure within a wellbore therefore become very useful instruments. The introduction of the Stratigraphic High Resolution Dipmeter tool, Formation MicroScanner tool and the Oil Base Mud Dipmeter tool by Schlumberger makes them the leader in this field.

The acquisition of downhole pressure, fluid pressure and formation core sample further enhance the understanding of the log response within a wellbore. All the companies seem capable of providing the operator with this information.

The use of electromagnetic properties to enhance the determination of water saturation is still relatively new. The difficulty seems to be in designing the tool hardware capable of measuring the dielectric permittivity accurately. Schlumberger leads this field with the Electromagnetic Propagation tool and the Deep Propagation tool. These tools operate at the more optimum frequencies and have the means to crosscheck the acquired data.

The importance of borehole seismic is generally overlooked. However through detailed analysis of this data with reference to the logs and surface seismic data the operator can enhance the knowledge of the reservoir. The introduction of the Seismic Acquisition tool, the Downhole Seismic Array tool, and the Combined Seismic Aquesition tool by Schlumberger shows that they understand the importance of this field and hence, makes them the leader of this field too.

The decision to perforate a well to bring production is very important. Hence the selection of the correct charges and guns are also important. An operator has a vast selection of charges and guns on the market from which to choose. However he may be constrained by the terms of the contract of the whole electrologging operation.

Once a well is produced the importance of monitoring the production is sometimes overlooked. All the logging companies can provide downhole information

of the production. The use of the thermal decay time log can help monitor the water influx within a reservoir and hence help plan the production of the reservoir. The introduction of the Dual Burst Thermal Decay Time tool which uses the diffusion model to determine the intrinsic formation capture cross section independent of borehole environment is a welcome instrument to help reservoir monitoring over a period of many years.

Furthermore there are other auxiliary services such as directional survey, cement evaluation and corrosion monitoring. The decline in the oil market has at present (1989) made these services secondary. These services are generally not requested unless circumstances force the operator to request them.

The next generation of well logging method will look towards data-intensive technology. Hence there are needs for better surface equipment (i.e., computer hardware and software), cable system, and downhole equipment. Already, high resolution data acquisition is being used to enhance evaluation of reserves and accurate reservoir boundary definition.

Overall, the three logging companies using basically the same established principles are able to provide the full range of basic services. However Schlumberger seems to stand out ahead of the three by offering a more complete range of services which are more informative to an operator. This together with the fact that they started in the electrologging field very much ahead of their competitors and have the available resources to conduct an active on-going research and development program, have made them the leader and have enabled them to obtain the majority of the market share.

of the production. The use of the thermal decay time log can help monitor the water influx within a reservoir and hence help plan the production of the reservoir. The introduction of the Dual Burst Thermal Decay Time tool which uses the diffusion model to determine the intrinsic formation capture cross section independent of borehole environment is a welcome instrument to help reservoir monitoring over a period of many years.

Furthermore there are other auxiliary services such as directional survey, cement evaluation and corrosion monitoring. The decline in the oil market has at present (1989) made these services secondary. These services are generally not requested unless circumstances force the operator to request them.

The next generation of well logging method will look towards data-intensive technology. Hence there are needs for better surface equipment (i.e., computer hardware and software), cable system, and downhole equipment. Already, high resolution data acquisition is being used to enhance evaluation of reserves and accurate reservoir boundary definition.

Overall, the three logging companies using basically the same established principles are able to provide the full range of basic services. However Schlumberger seems to stand out ahead of the three by offering a more commplete range of services which are more informative to an operator. This together with the fact that they started in the electrologging field very much ahead of their competitors and have the available resources to conduct an active on going research and development program, have made them the leader and have enabled them to obtain the majority of the market share.

15. REFERENCES

1. Alger, R.P., Locke, S., Nagel, W.A., and Sherman, H.:"The Dual Spacing Neutron Log," paper SPE 3565 presented at the 1971 SPE Annual Technical Conference and Exhibition.

2. Alger, R.P., Roymer, L.L., Hoyle, W.R., and Tixier, M.P.: "Formation Density Log Applications in Liquid-Filled Holes," J. Pet. Tech. (March 1963)

3. Allaud, L.A. and Ringot, J. : "The High Resolution Dipmeter Tool,"The Log Analyst (May-June 1969) 10, No.3.

4. American Petroleum Institute : "Recommended Practice for Standard Calibration and Form for Nuclear Logs", (Sept. 1959), API RP-33

5. API Recommended Practice : "Standard Procedure for Evaluation of well Perforators", API Division of Production, RP-43, end ed. (Oct. 1974).

6. Archie, G.E. : "The Electrical Resistivity as an Aid in Determining Some Reservoir Characteristics,"J. Pet. Tech. (Jan 1942) 5, No.1.

7. Austin, C.F.: Bulletin 69, New Mexico Institute of Mining Technology, 1948.

8. Babour, K., Joli, F., Landgren, K., and Piazza, J-I.: "Elements of Borehole Seismics," The Technical 35, no. 2. (April 1987) : 6-7.

9. Belaud, D., Christie, P., de Montmollin, V., Dodds, K., James, A., Kamata, M., and Schaffner, J.: "Detecting Seismic Waves in the Borehole." The Technical Review 36, no.3 (July 1988) : 18-29.

10. Bell, W.T., Brieger, E.F., and Harrigan, J.W., Jr : "Laboratory Flow Characteristics of Gun Perforations," J. Pet. Techn. (Sept.1972) 1095-1103.

11. Birkoff, McDougal, Pugh and Taylor : "Explosives with Lined Cavities," Journal of Applied Physics, Volume 10, (June, 1948).

12. Blanchard, A. and Dewar, J.T. : "Calibration of Gamma Ray Logs." Pet. Eng. (Aug. 1953).

13. Calvert, T.J., Rau, R.N., Wells, L.E. : "Electromagnetic Propagation a New Dimension in Logging," Paper SPE 6542 presented at the 1977 SPE California Regional Meeting.

14. Doll, H.G. : "The SP Log : Theoretical Analysis and Principles of Interpretation,"Trans., AIME (1944) 155.

15. Doll, H.G.: "Introduction to Induction Logging," J.Pet. Tech. (June 1949).

16. Doll, H.G. "The Laterlog," J.Pet. Tech. (Nov 1951).

17. Doll, H.G. : "The Microlog," Trans., AIME (1950) 189.

18. Eichelberger and Pugh : "Journal of Applied Physics," Volume 23, No 25, (May, 1952).

19. Gaiser, J.E., Fulp, T.J., Petermann, S., and Karner, G.M.: "Three-Component Vertical Seismic Profiles: Geophone-Sonde Stability," presented at the 54 th Annual International SEG Meeting, Atlanta, December 2-6, 1984.

20. Gardner, J.S. and Dumanoir, J.L. : "Litho-Density Log Interpretation," Trans., 1980 SPWLA Annual Logging Symposium, paper N.

21. Gearhart : "Direct Digital Logging, DDL," 1985.

22. Gearhart : "Interpretation of Spectral Gamma Ray", 1968.

23. W.K. Godfrey : "Perforations. Effect of Fluid Density, Hydrostatic Head, Yield Strength of Casing and Gun Clearance," (1968).

24. Guy, J.O., and Fertl, W.H. : "Circumferential Acoustic Measurements The CALog," Paper # 30, Trans. SAID 7th European Logging Symposium, Paris, France, Oct. 21-23, 1981.

25. Guy, J.O., Fertl, W.H., and Oliver, D.W. : "The Use of Circumferentially Propagated Acoustic Waves in Well Logging," : Paper SPE 15484 presented at the SPE of AIME 61st Fall Meeting, Oct. 5-8, New Orleans, L.A., 1986.

26. Harris, M.H.: "The Effect of Perforating on Well Productivity", J. Pet. Techn, (1965) -1103.

26.1 Huber, Allen and Aberdeath : "Effect of Hydrostatic Head on Depth of Penetration", Paper presented to API, (1950).

27. Huchital, G.S., Hutin, R., Thoraval, Y., and Clark, B. : "The Deep Propagation Tool (A New Electromagnetic Logging Tool)," Paper SPE 10988 presented at the 1981 SPE Annual Technical Conference and Exhibition.

28. Johnston, J., Watfa, M., Nurmi, R., Andreani, M., and Flaum, C: "Peak Viewing for Thin Beds", Middle East Well Evaluation Review, No.6., 1989.

29. Kolesh, F.P., Schwartz, R.J., Wall, W.S., and Morris, R.L. : "A New Approach to Sonic Logging and Other Acoustic Measurements," J. Pet. Tech. (March

1965) 17, No. 3.

30. LeBourg and Hodgson : "Through-Tubing Completion Techniques," Paper presented to AIME, (Oct. 1952).

31. Lloyd, P.M., Dahan, C., and Hutin, R. : "Formation Imaging from Microelectrical Scanning Arrays: A New Generation of Stratigraphic High Resolution Dipmeter Logging Tool," SPWLA 10the European Symposium, Aberdeen, April 23-24, 1986.

32.McDowell, J.M., and Muskat, M. : "The Effect on Well Productivity of Formation Penetration Beyond Perforated Casing", Trans ., AIME (1950) 189, 309-312.

33. McLemore, R.L. : "Shaped Charge Perforator in Oil Wells," World Oil, (July 1946).

34. Moran, J.H. and Kunz, K. S. : "Basic Theory of Induction Logging," Geophys. (Dec. 1962).

35. Morris, C.F., Little, T.M., and Letton, W. : "A New Sonic Array Tool for Full Waveform Logging," paper SPE 13285 presented at the 1984 SPE Annual Technical Conference and Exhibition.

36. Mounce, W.D. and Rust, W.M., Jr.: "Natural Potentials in Well Logging," Trans., AIME (1944) 155.

37. De Montmollin V: " Shaker Test on Downhole Seismic Tools," Geophysics 53, no. 9 (1988).

38. Noblett, B.R., Fertl, W.H., and Guy, J.O. : "Recent Advances in Fracture Evaluation," Paper SPE 16226 presented at the SPE Production Operations Symposium, Oklahoma City, March 8-10, 1987.

39. Nowak and Krueger : "The Effect of Mud Filtrates and Mud Particles Upon the Permeabilities of Cores", Paper presented to API, (1951).

40. Olesen, J-R., Mahdavi, M., and Steinman, D.K., : "Dual-Burst Thermal Decay Time Data Processing," SPWLA 28the Annual Logging Symposium, June 29-July 2, 1987.

41. Robinson, Hermann and DeFrank : "How Well Conditions Influence Perforators", (1961).

42. Schlumberger : "Cement Evaluation tool, CET," 1985.

43. Schlumberger : "Core Sampling tools, CST ," 1987.

44. Schlumberger : "Cyber Service Unit, CSU," 1987.

45. Schlumberger : "Electromagnetic Propagation tools," 1984.

46. Schlumberger : "Essentials of Cement Evaluation," 1986.

47. Schlumberger : "Fundamentals of Dipmeter Interpretation," 1986.

48. Schlumberger : "Guidance Continuous tool, GCT," 1987.

49. Schlumberger : "Log Interpretation Charts," 1987.

50. Schlumberger : "Perforations," 1987.

51. Schlumberger : "Porosity tools," 1987.

52. Schlumberger : "Production Logging tool," 1984.

53. Schlumberger : "Repeat Formation Tester tool, RFT," 1982.

54. Schlumberger : "RFT Essentials of Pressure Test Interpretation," 1981.

55. Schlumberger : "Resistivity Logging tools," 1984.

56. Schlumberger : "Wellbore Seismic," 1987.

57. Scott, H.D., Flaum, C., and Sherman, H. : "Dual Porosity CNL Count Rate Processing," paper SPE 11146 presented at the 1982 SPE Annual Technical Conference and Exhibition.

58. Sen, P.N. :"The Dielectric and Conductivity Response of Sedimentary Rocks," paper SPE 9373 presented at the 1980 SPE Annual Technical Conference and Exhibition.

59. Setser, G.G. "Fracture Detection by Circumferential Acoustic Energy," Paper SPE 10204 presented at the 56 the Annual SPE Fall Meeting, San Antonio, Oct. 5-7, 1981.

60. Stewart, G. and Wittman, M. : "Interpretation of the Pressure Response of the repeat Formation tester", paper SPE 8362 presented at the 1979 SPE Annual Technical Conference and Exhibition.

61. Thompson, G.D.: "Effects of Formation Compressive Strength on Perforation Performance", Drill and Prod., API (1962) 191.

62. Tittman, J.and Wahl, J.S.: "The Physical Foundations of Formation Density Logging (Gamma-Gamma)," Geophysics. (April 1965).

63. Vogel, C.B., and Herolz, R.A.: "The CAD-A Circumferential Acoustic Device for well Logging," J.Pet. Tech., 1981.

64. Wertern Atlas : "Casing Evaluation Services," 1985.

65. Western Atlas : "Computer Logging Service, CLS," 1985.

66. Western Atlas : "Dielectric Logging Service," 1988.

67. Western Atlas : "Formation Multi-tester, FMT," 1987.

68. Western Atlas: " Sidewell Coring System," 1987.

69. Wahl, J.S., Tittman, J., and Johnstone, C.W.: "The Dual Spacing Formation Density Log," J. Pet. Tech. (Dec 1964).

70. Washburn, H., and Wiley, H.: "The Effect of the Placement of a Seismometer on its Response Characteristics," Geophysics 6 (1941) : 166-131.

71. Wharton, R.P., Hazen, G.A., Rau, R.N., and Best, D.L. : "Electromagnetic Propagation Logging Advances in Technique and Interpretation," paper SPE 9267 presented at the 1980 SPE Annual Technical Conference and Exhibition.

72. Wuenschel, P.C.: "The Vertical Array in Reflection Seismology - Some Experiments," Geophysics 41 (1976) : 219-232.

73. Wuenschel, P.C. : "Removal of the Detector - Ground Coupling Effect in the Vertical Seismic Profiling Environment," Geophysics 53 (1988) : 359-364.

74. Wyllie, M.R.J.: "A Quantitative Analysis of the Electro-Chemical Component of the SP Curve," J. Pet. Tech. (1949) 1.

75. Wyllie, M.R.J. : "An Investigation of the Electrokinetic Component of the Self-Potential Curve," Trans., AIME, 192

76. Wyllie, M.R.J., Gregory, A.R., and Gardner, G.H.F.: "Elastic Wave Velocities in Heterogeneous and Porous Medium," Geophysics (Jan. 1956) 21, No. 1.

77. Wyllie, M.R.J., Gregory, A.R., and Gardner, G.H.F.:An Experimental Investigation of Factors Affecting Elastic Wave Velocities in Porous Media," Geophys. (July 1958) 23, No.3.

78. Youmans, A. H., Hopkinson, E. C., Bergan, R. A., and Oshry, H. I.: "Neutron Lifetime Log, A New Nuclear Log," J. Pet. Tech. (March 1964) 319-29; Trans, AIME, 231.

APPPENDIX A. API RP-43 INDUSTRY TESTING PROCEDURE

Testing of early bullet and jet perforators was carried out in a variety of target materials, such as mild steel, concrete, neat cement and aluminium, etc. for the most part at surface conditions (Krueger,1956).

To make realistic comparisons between the perforators offered by several companies, there was a need to standardise the testing procedure for the perforators. This lead to adoption of American Petroleum Institute Recommended Practice RP-43 Standard Procedure for Evaluation Well Perforators issued October 1961 which was last revised in October 1974 (figure A-1).

Each service company has the option of testing their charges under either one or both of two methods.

- API RP-43 Section 1, is an evaluation of penetration and hole size in a steel casing and concrete simulated formation at surface conditions (figure A-2).
- API RP-43 Section 2, is an evaluation for hole characteristics and flow efficiency from single perforation; in sandstone under simulated well conditions (figure A-3).

The API requires that charges are randomly selected from production stocks and will be substantially the same as the equipment which would be furnished to perforate a well for any operator.

1. API RP-43 Standard Procedure - Section 1

The purpose of this surface test is to determine the physical characteristics of holes made by a multiple perforating gun. Section 1 test data are developed in a simple concrete drum-type shown schematically in figure A-2. A regular field gun containing six or more shots is placed in the casing and eccentered to check clearance effects. Several shots are fired simultaneously to assure that charges being fired in close proximity do not interfere with one another (which could result in reduced performance or "charge interference"). Before firing, the concrete target must be cured for a minimum of 28 days and must have a minimum tensile strength of 400 psi, which corresponds to about 4000 psi compressive strength.

The Section 1 test provides data on penetration and entrance hole size: both average values and individual shot values at different clearances are reported (see

28. Original Effective Permeability, k_o. The original effective permeability of a Berea sandstone core target, described in Par. 44, 45, and 46, is the effective permeability to kerosine of a 3.9 16-in. diameter by 12-, 15-, 18-, 21-, 24-, or 27-in. length core cut in such a way that the bedding planes are parallel to the axis of the core target and to the direction of fluid flow.

29. Perforated Effective Permeability, k_p. The perforated effective permeability of a Berea sandstone core target is the effective permeability to kerosine of the core target after it has been perforated at the outflow end by a bullet or shaped charge, based on the original cross section and length of the core target.

30. Ideal Perforated Permeability, k_i. The ideal perforated permeability of a Berea sandstone core target is the calculated permeability to kerosine of the core target containing an ideal perforation at the outflow end based on the cross section and length of the Berea sandstone core used in determining the perforated effective permeability.

31. Experimental Permeability Ratio. The experimental permeability ratio (k_p/k_o) is the ratio of the perforated effective permeability to the original effective permeability. These permeabilities are determined from flow tests on the core target.

32. Theoretical Permeability Ratio. The theoretical permeability ratio (k_i/k_o) is the ratio of the ideal perforated permeability to the original effective permeability. These data are obtained from the table presented in Appendix A.

33. Total Target Penetration (TTP). Total target penetration, TTP, is the distance from the exterior steel face of the core target to the probe depth. The probe depth shall be determined by the maximum depth from the exterior steel face to the deepest point that can be probed with a 0.1-in. OD tube using 50 psi air pressure and a probe force not exceeding 10 pounds.

34. Total Core Penetration (TCP). Total core penetration, TCP, is the distance from the original Berea sandstone core face to the depth probed. It is obtained by subtracting from the total target penetration, TTP, the combined thickness of the steel and *Hydromite-CM**.

35. Core-flow Efficiency (CFE). Core-flow efficiency is the ratio of the experimental permeability ratio to the theoretical permeability ratio ($k_p/k_o \div k_i/k_o$) for the same total core penetration. Theoretical permeability ratios are calculated values for test core targets containing clean, undamaged perforations and are tabulated in Appendix A. Values are given for penetration depths ranging from 0.1 in. to 22 in. in increments of 0.1 in. Average perforation diameter was assumed to be 0.4 in. The core-flow efficiency, CFE, is one of the measures of the effectiveness of the perforating tool under conditions of the test. It represents the relative effectiveness of the perforation for conducting fluid compared to an undamaged hole. The core-flow efficiency for a perfectly clean, undamaged perforation will be 1.0. Perforations that are damaged (partially plugged) in the process of perforating the core target have less than theoretical flow capacity. Core-flow efficiency declines with degree of damage from 1.0 to zero for a completely plugged condition. Therefore, when two different perforators are compared, one providing unit depth of penetration and a core-flow efficiency of approximately 1.0 would have about the same effective flow capacity as one providing twice the penetration and a core-flow efficiency of approximately 0.5.

36. Effective Core Penetration (ECP). Effective core penetration, ECP, is the product of the total core penetration and the core-flow efficiency (TCP x CFE). The effective core penetration is another measure of the effectiveness of the perforating tool under conditions of the test and corresponds to a clean, undamaged hole that has the same flow capacity as the test perforation. It permits a comparison of the fluid-carrying capacity, under these test conditions, for two different perforations with different penetrations, the same length core, and different core-flow efficiencies. The perforation with the highest effective core penetration in a given core-target length, regardless of total core penetration or core-flow efficiency, will produce at a higher flow rate under a given differential test pressure.

37. Porosity (ϕ). Porosity, ϕ, is the percentage by volume of pore space within a sample. It is defined as the ratio of pore volume to bulk volume, multiplied by 100. The Berea sandstone core, after oven drying, is evacuated and saturated fully with salt water. It is weighed both in the dry state and in the saturated state. The difference in weight divided by the density of the salt water gives pore volume directly. The bulk volume is calculated using the physical dimensions of the core.

38. Fluid Saturation. Fluid saturation is the percent of the total pore volume occupied by salt water (or kerosine) distributed through a saturated Berea sandstone core.

39. Maximum Safe 24-Hour Temperature. Maximum safe 24-hour temperature is the maximum temperature at which a gun can be held for 24 hours in a well without self-ignition of the explosive.

40. Entrance Hole Diameter. Entrance hole diameter is the average diameter of the hole through the 3 8-in. steel face plate on the core target. It shall be measured twice at right angles and the average of the two measurements reported. If this cannot be done because of some obstruction, this information should be noted on API Form 43D, Certification Data Sheet.

41. Burr Height. Burr height will be measured as the maximum protrusion from the face plate. If a carrot or other debris is lodged in the hole and cannot be removed with finger pressure alone, the total height will be measured as burr and a note of explanation placed in the remarks section of API Form 43D.

42. Clearance. Clearance is the minimum distance along the axis of jet or bullet between the gun body or charge case and the surface of the core target.

43. Measurements. Measurements are to be made with appropriate instruments and are to be reported in inches and in decimal fractions thereof to the nearest 0.01 in., e.g., entrance hole diameter — 0.37 in., total target penetration — 6.78 in.

BEREA SANDSTONE CORE TARGET

44. Tests will be conducted using Berea sandstone core targets mounted as shown in Fig. 2. These targets will consist of: (1) a 3 8-in. hot-rolled, SAE — A-7 fully annealed, mild-steel end-plate which has been butt welded on 4½-in., 16.60-lb ft drill pipe (2) a ½-in. layer of *Hydromite-CM*; and (3) a Berea sandstone core having a porosity not less than 17 percent or more than 22 percent, and an original effective permeability not less than 100 md or more than 300 md.

PREPARATION OF BEREA SANDSTONE CORE FOR THE CORE TARGET

45. The Berea sandstone core shall be prepared as follows:

*Registered trade name, U. S. Gypsum Company, 300 W. Adams St., Chicago, Illinois, 60606, available on special order.

Terminology as Described in API 43

Figure A-1. API RP-43 Testing Procedures.

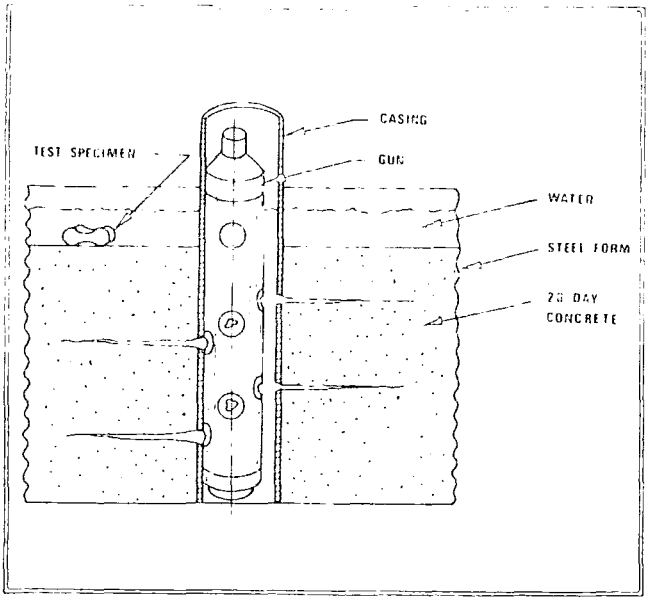

Figure A-2. API test. Section 1. (API, 1974)

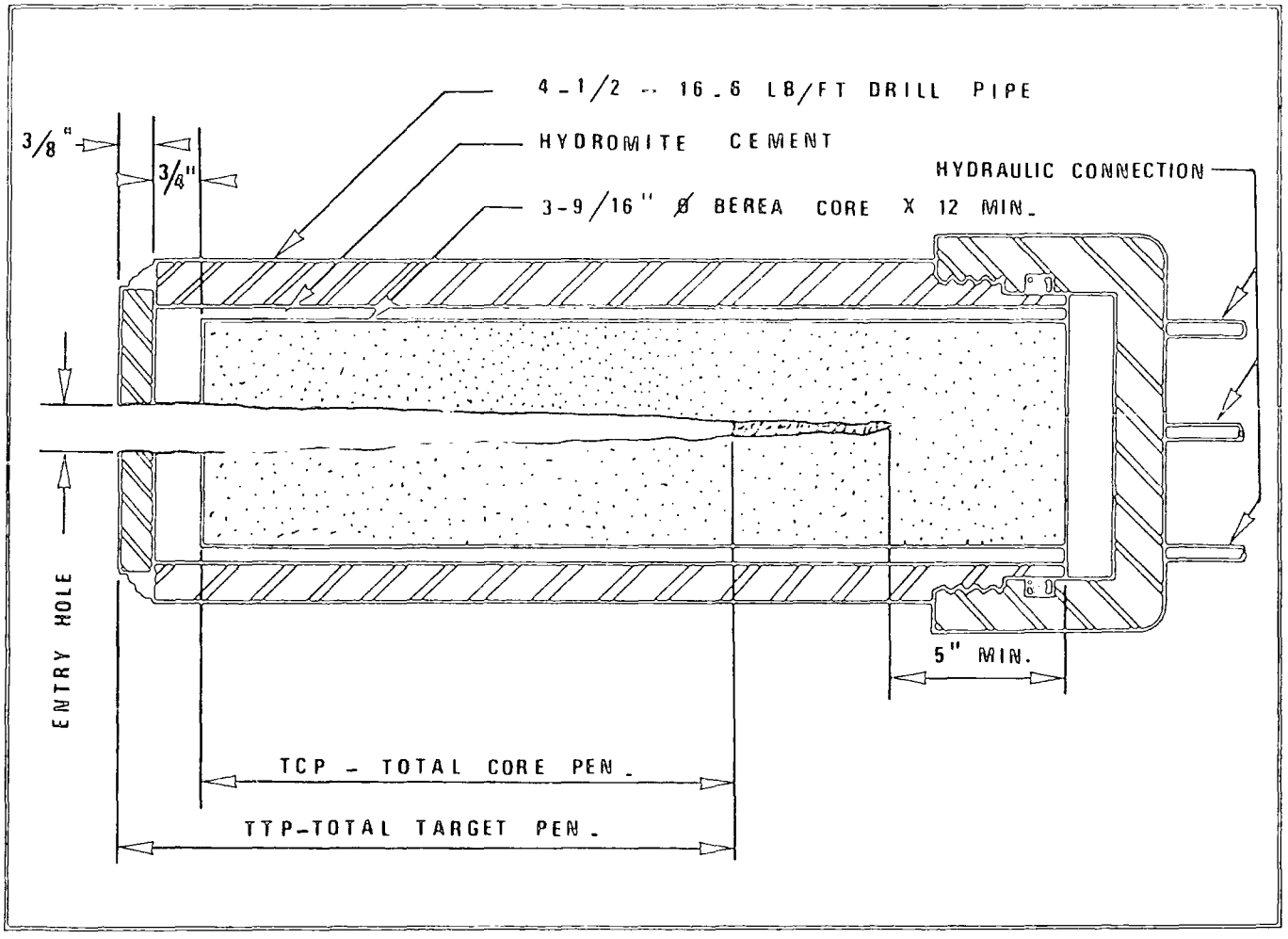

Figure A-3. API test. Section 2 - Berea sandstone target. (API, 1974)

figure A-2). Burr height (the lip of metal around the periphery of the perforated hole) is included.

The Section 1 test is not intended to throw light on cleanliness aspects of the perforation. This is left to the Section 2 flow test. Also the Section 1 test results are not representative if the formation is of different composition and compressive strength from that of the target. The slug and debris postition are not always indicative as tests are made at atmospheric pressure.

2. API RP-4 Standard Procedure - Section 2 (figure A-3)

The Section 2 test is a laboratory measurement of flow from a perforation in a berea sandstone target after shooting under specified pressure conditions at a temperature of 180 °F. It is intended to show whether the perforation will liberate debris resulting from the penetration process, and whether clean-up under the stimulus of fluid flow will occur (Bell,et al, 1972).

Depending upon the intended use of the charge that is fired, two types of test are performed: the positive pressure flow test (figure A-4) that simulates perforating in mud (casing operations) or the reverse pressure flow test (figure A-5), that simulates perforating through-tubing with flow into the well bore immediately after shooting.

After the test target is perforated, it is flowed with kerosene at a differential pressure of 200 psi until a stable flow rate is achieved. Following the procedures outlined in the latest edtion of API RP-43 , a Core Flow Efficiency (CFE) is then calculated as shown in figure A-6.

CFE is essentially a measure of the capability of the perforation to flow. The flow from the actual perforation is compared to flow from an ideal hole of the same diameter and with the same open hole depth as the shot perforation in the particular target. CFE is related to the perforation damage (e.g.,crushed zone).

CFE represents an improvement over the Well Flow Index (WFI) used in the original test procedure. WFI was strongly influenced by depth, particularly as the perforation approached the end of the 15 inch long target used. The relation of WFI with depth is shown in the plot of k_i / k_o (WFI of ideal perforation) versus depth in figure A-6. Since CFE is a ratio of shot-to-ideal perforations, the depth

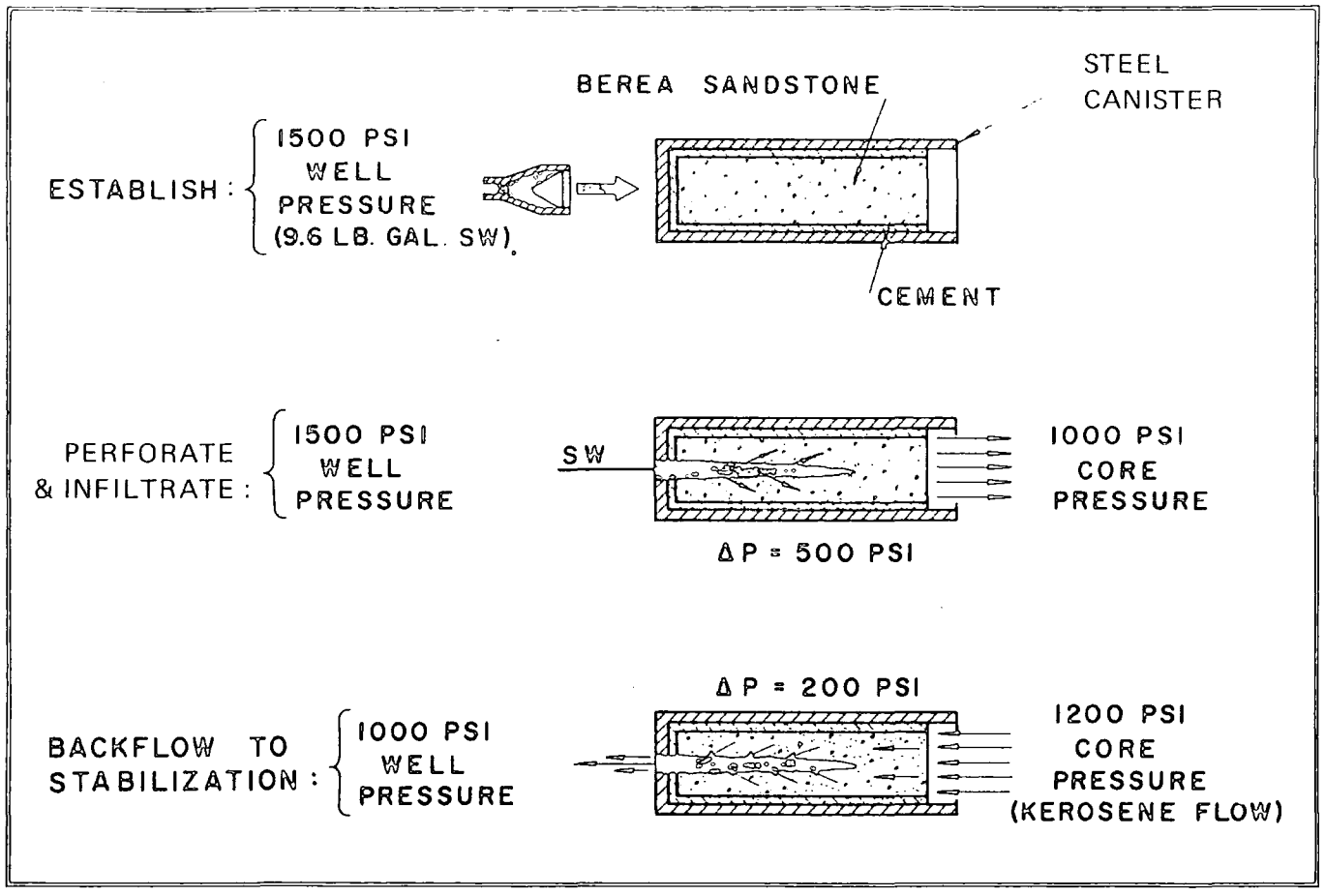

Figure A-4. Positive pressure flow test procedure. (API, 1974)

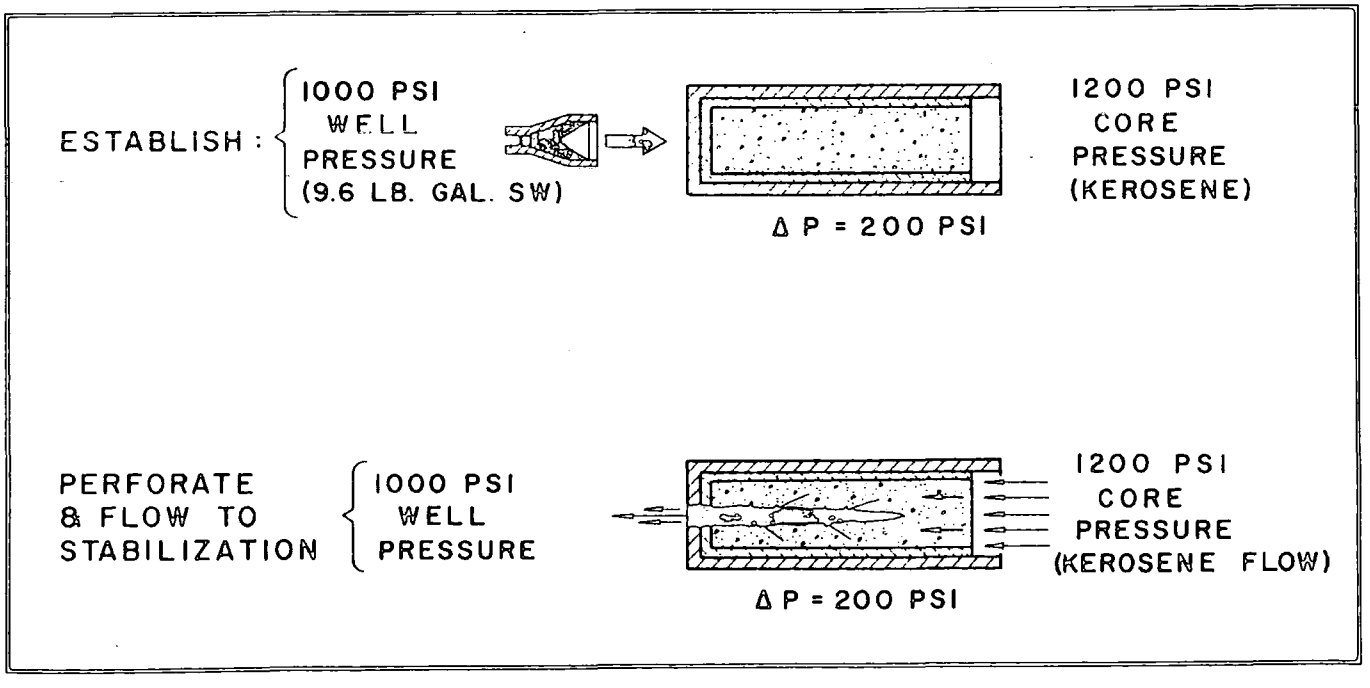

Figure A-5. Reverse pressure flow test procedure. (API, 1974)

A)-DETERMINE ORIGINAL K_0:

$$K_0 = \frac{Q_0 \mu_0 L_0}{A_0 \Delta P_0}$$

B)-CALCULATE PERFORATION K_P FROM TEST:

$$K_P = \frac{Q_P \mu_P L_0}{A_0 \Delta P_P}$$

C) $$CFE = \frac{K_P / K_0}{K_i / K_0} = \frac{K_P}{K_i}$$

--WHERE K_i / K_0 REPRESENTS THE RATIO OF THE EFFECTIVE PERMEABILITY OF A TARGET CONTAINING AN IDEAL (DRILLED) PERFORATION (OF THE SAME DEPTH & DIAMETER AS THE PERFORATED ONE) TO THE ORIGINAL TARGET PERMEABILITY K_0

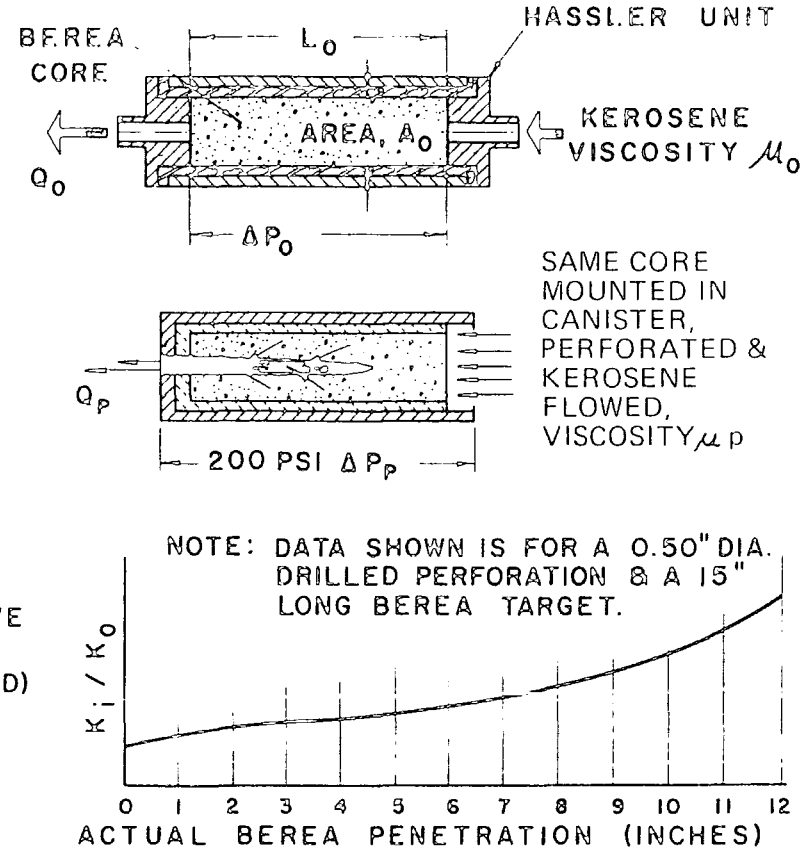

Figure A-6. Core Flow Efficiency (CFE) determination. (API, 1974)

sensitivity problem is avoided. Furthermore, the modified API procedure requires that the target length is selected so that a minimum of 5 inches of unpenetrated rock remains (as opposed to the original requirement of 3 inches), regardless of depth of penetration. Thus the possible influence of depth of penetration on perforation clean-up characteristics is minimised. Short and long shooting charges should show approximately the same CFE if equally clean (about 0.70 to 0.90).

Besides the CFE, more details on individual shots are provided on the certification sheets, including a perforation configuration and information on debris remaining in the perforation following flow test. The results given are (see figure A-3):-

a) Total Target penetration : TTP

b) Total core penetration : TCP = (TTP-1.12) inches

c) Overall penetration : OAP

The Effective Core Penetration (ECP) is the product.

$$ECP = TCP \times CFE$$

ECP is another measure of the effectiveness of the perforator under the conditions of the test. Figure A-7 is an example of an API Section 2 certification sheet.

API FORM 43D

CERTIFICATION DATA SHEET

Service Company: Schlumberger
Gun OD and Designation: 2 1/16" Enerjet
Charge Name: Enerjet
Type Perforator: Shaped charge
Recommended Minimum Pipe ID: 2 7/8 in.
Standard Gun Length: 10' ft
Maximum Gun One Run: 120 shots
Spacing Available: 1 to 4 shots/ft
Phasings Available: 0 degree
Firing Order: X Top down, ____ Bottom up
Available Firing: ____ Selective, X Simultaneous

Charge Weight: 11.5 gm RDX powder
Maximum 24 hour Temperature: 340 F
Maximum Pressure: 15,000 psi
Charge Case Material: Steel
Carrier Material: Steel
Bullet OD: ____ in., Length ____ in.
Debris Weight: Nil gm/charge
Debris Description: ____
Remarks: ____

SECTION 1 – CONCRETE TARGET

Casing Data: 5.5" OD, 17 lb/ft, J-55 API Grade
Target Data: 48" OD, Tensile Strength 441 psi, Compressive Strength 4860 psi
Date of Test: 7.29.1974, Age of Target 47 days

Shot No	No. 1	No. 2	No. 3	No. 4	No. 5	No. 6	Average
Clearance, in.	0	0	0	0	0	0	0
Casing Hole Diameter, Short Axis, in.	.34	.34	.32	.30	.30	.30	0.32
Casing Hole Diameter, Long Axis, in.	.34	.36	.37	.34	.38	.34	0.36
Average Casing Hole Diameter, in.	.34	.35	.35	.32	.34	.32	0.34
Total Depth, in.	17.25	18.42	20.32	18.42	18.40	17.64	18.41
Burr Height, in.	0.03	0.04	0.02	0.03	0.06	0.03	0.03
Depth to Jet Debris or Bullet, in.	17.25	18.42	20.32	18.42	18.40	17.84	18.41

Remarks: ____

SECTION 2 – BEREA SANDSTONE CORE TARGET

CORE DATA						SHOOTING CONDITIONS			FLOW CONDITIONS				RESULTS					
Test No	Test Date	Porosity, %	S_w, %	Core Length in	k_a, md	Pressure, psi Well	Pressure, psi Core Target	Clearance in	Pressure, psi Well	Pressure, psi Core Target	Total Flow, liters	k_e, md	Entrance Hole Diam in	CFE	TTP, in	TCP, in	ECP, in	d_f OAP in.
330	8.8.74	19.2	77.1	15	175	1000	1200	0	1000	1200	25	283	0.36	0.77	10.13	9.00	6.98	11.13
331	8.13.74	19.2	74.9	15	172	1000	1200	0	1000	1200	26	290	0.36	0.82	10.	8.88	7.29	10.75
332	8.14.74	19.3	76.4	15	169	1000	1200	0	1000	1200	25	295	0.36	0.78	1063	9.50	7.39	1113
												Average →	0.36	0.79	10.25	9.12	7.22	11.00

* See General Remarks

CERTIFICATION

I certify that three tests were made according to the procedures as outlined in *API RP 43, Standard Procedure for Evaluation of Well Perforators*, Second Edition, November 1971. All the equipment used in these tests, such as the guns, jet charges, detonator cord, etc., was standard equipment with our company for use in the gun being tested, and was not changed in any manner for the test. Furthermore, the equipment was chosen at random from stock and therefore will be substantially the same as the equipment which would be furnished to perforate a well for any operator.

CERTIFIED BY: ____ Aug.20,74 Date — Director of Engineering Title — P.O. Box 17, 92140 Clamart Address
RECERTIFIED BY: B. Vivet Date — Paris, Franco Address

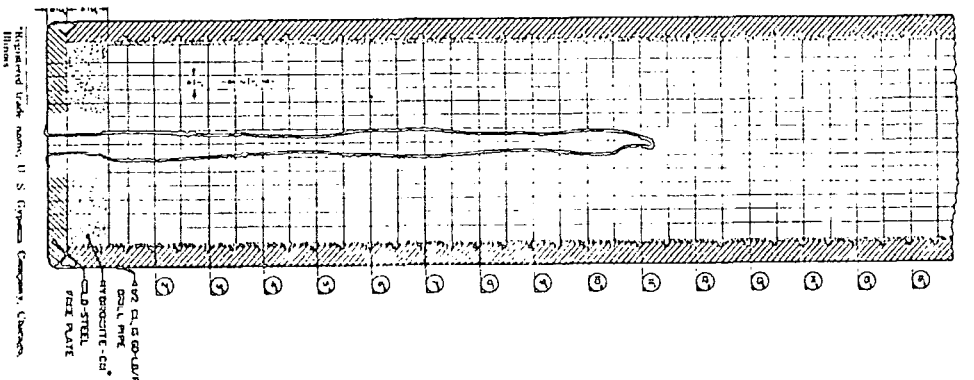

INDIVIDUAL SHOT RECORD
BEREA SANDSTONE CORE TARGET

Service Company: Schlumberger
Gun OD and Designation: 2 1/16" Enerjet
Charge Name: Enerjet
Type Perforator: Shaped charge
Test No.: 332

GENERAL REMARKS: OAP (overall penetration) is the distance from face plate to the tip of the perforation.

CERTIFICATION

I certify that three tests were made according to the procedures as outlined in *API RP 43, Standard Procedure for Evaluation of Well Perforators*, Second Edition, November 1971. All the equipment used in these tests, such as the guns, jet charges, detonator cord, etc., was standard equipment with our company for use in the gun being tested, and was not changed in any manner for the test. Furthermore, the equipment was chosen at random from stock and therefore will be substantially the same as the equipment which would be furnished to perforate a well for any operator.

CERTIFIED BY: B. Vivet Aug.20,1974 Date
Director of Engineering P.O. Box 17 Title
RECERTIFIED BY: 92140 Clamart, France Address
Title Date

API FORM 43D

CERTIFICATION DATA SHEET (CONT'D.)

Figure A-7. Copy of an API Certification Data Sheet.

APPENDIX B.
PUBLISHED API RP-43 DATA, 1985 CERTIFICATION.
(LISTED BY MAJOR COMPANIES)

	Jet Perforators	Part Number	Gun OD	Case Material	Gram Weight	Casing OD	Concrete Target EHD	Concrete Target Penetration	Berea Target EHD	Berea Target CFE	Berea Target TTP	Pressure Rating (psi) 60°F	Pressure Rating (psi) 325°F
HOLLOW STEEL CARRIERS	DML Densi Jet X	022-3701-041	3-1/8	Steel	10	4-1/2"	.31	10.20	.35	.87	7.82	20000	20000
	Densi Jet X	022-3701-008	3-1/8"	Steel	10	4-1/2"	.39	8.99	.45	.89	9.33	20000	20000
	DML Densi Jet XII	022-3701-101	3-1/8	Steel	12	4-1/2"	.36	12.37	.35	.88	10.04	20000	20000
	"600" Go Devil	022-3708-005	3-1/8"	Steel	10	4-1/2"	.59 ☆	9.02	.59	.02	7.24	20000	20000
	DML Densi Jet XIV	022-3705-003	3-3/8	Steel	14	4-1/2"	.38	12.38	.45	.88	8.83	20000	20000
	Tru Jet XVI	022-3705-009	3-3/8	Steel	16	4-1/2"	.49	19.15	.48	.89	11.25	20000	20000
	DML Densi Jet XIV	022-3705-003	3-5/8	Steel	14	4-1/2	.39	12.47	.42	.01	9.10	20000	20000
	Densi Jet X	022-3701-008	3-5/8	Steel	10	4-1/2"	.40	9.20	.40	.05	8.60	20000	20000
	Densi Jet X	022-3701-008	4"	Steel	10	5-1/2"	.37	9.30				20000	20000
	DML Densi Jet XIV	022-3705-003	4"	Steel	14	5-1/2"	.34	11.11				20000	20000
	DML Densi Jet XVIII	022-3703-039	4"	Steel	18	5-1/2"	.32	11.26	.35	.85	9.35	20000	20000
	DML Densi Jet XIX	022-3703-097	4"	Steel	19	5-1/2"	.48	16.65 ~	.53	.85	11.13	20000	20000
	Densi Jet XIX	022-3703-006	4"	Steel	19	5-1/2"	.50	12.31	.53	.75	11.10	20000	20000
	Densi Jet XIX	022-3703-006	4"	Steel	19	7"	.48	13.23	.53	.75	11.10	20000	20000
	Improved DML XXIII	022-3703-071	4"	Steel	22.7	5-1/2"	.43	23.14	.45	.83	14.70	20000	20000
	"720" Densi Jet	022-3703-090	4	Steel	20	5-1/2"	.69 ☆	11.01	.74	.79	8.97	20000	20000
	Tru Jet XXII	022-3703-079	4	Rub & Stl	22	7"	.375	19.90	.47	.88	11.58	20000	20000
	Densi Jet XXXII	022-3709-035	5	Steel	32	9-5/8"	.77	16.13	.80	.82	11.20	20000	20000
	○ Circulation	022-3710-020	3-1/8"	Steel	6		.51	1/4 to 3/8 △				20000	20000
	○ Circulation	022-3710-030	4"	Steel	6		.46	1/4 to 3/8 △				20000	20000
EXPENDABLE RETRIEVABLE STEEL WIRE BI-WIRE AND NEEDLE JETS	Tornado Jet Bi-Wire	017-3405-079	15/16"	Alum	1.25	4-1/2"	.12	2.84	.15	.23	2.52	20000	15000
	Tornado Jet Bi-Wire	017-3405-003	1"	Alum	2	4-1/2"	.15	3.00	.18	.50	2.65	16500	14000
	Tornado Jet Bi-Wire	017-3405-004	1-1/8"	Alum	2.5	4-1/2"	.19	3.55	.23	.68	3.19	15000	12000
	Tornado Jet Bi-Wire	017-3405-005	1-1/4"	Alum	5	2-3/8"	.30	4.51	.29	.69	3.91	14000	14000
	Tornado Jet Bi-Wire	017-3405-006	1-3/8"	Alum	6	2-3/8"	.30	5.68	.26	.86	4.80	15000	14000
	Tornado Jet Bi-Wire	017-3405-007	1-11/16"	Alum	13	2-7/8"	.36	7.39	.37	.90	6.35	14000	13000
	Tornado Jet Bi-Wire DML	017-3405-058	1-11/16	Alum	12							14000	13000
	Tornado Glasjet Bi-Wire	017-3405-011	1-11/16	Glass	13	2-3/8"	.36	6.34	.31	.86	5.82	8000	7000
	Tornado Ceramic Bi-Wire	017-3204-060	1-11/16"	Ceramic	12	5-1/2"	.25	5.33	.32	.80	5.42	20000	15000
	Tornado Ceramic Bi-Wire	017-3204-061	2-1/8"	Ceramic	22.7	5-1/2"	.33	8.05	.42	.84	7.58	20000	15000
	Tornado Jet Bi-Wire	017-3405-008	2-1/8"	Alum	22.7	2-7/8"	.44	8.92	.48	.91	7.89	15000	12000
	Tornado Jet Bi-Wire	017-3405-008	2-1/8"	Alum	22.7	5-1/2"	.41	8.52	.48	.91	7.00	15000	12000
	Tornado Jet Bi-Wire DML	017-3405-072	2-1/8"	Alum	22							15000	12000
	Tornado Glasjet Bi-Wire	017-3405-013	2-1/8"	Glass	22.7	2-7/8"	.43	8.31	.41	.85	7.53	8000	7000
	Tornado Glasjet Bi-Wire	017-3405-013	2-1/8"	Glass	22.7	7"	.32	7.13	.41	.05	7.53	8000	7000
	Twin Needle Bi-Wire	017-3212-005	1-11/16"	Alum	1.5	4-1/2"	.10**	2.68	.10		2.30	16000	12000
	Twin Needle Bi-Wire	017-3212-006	2-1/8"	Alum	3.5	5-1/2"	.12**	3.67	.12		3.15	16000	12000
	Twin Needle Bi-Wire	017-3212-007	2-3/4"	Alum	4	7"	.14**	4.77	.14		4.10	13500	12000
	○ Circulation — Red Nose	017-3405-082	15/16"	Alum	1		.24	1/8 to 1/4 △					15000
	○ Circulation — Red Nose	017-3405-083	1"	Alum	2		.30	1/8 to 1/4 △					14000
	○ Circulation — Red Nose	017-3405-095	1-1/8"	Alum	2		.36	1/8 to 1/4 △					12000
	○ Circulation — Green Nose	017-3405-043	1-1/4"	Alum	4		.36	3/8 to 1/2 △					14000
	○ Circulation — Red Nose	017-3405-044	1-1/4"	Alum	4		.43	1/4 to 3/8 △					14000
	○ Circulation — Green Nose	017-3405-085	1-3/8"	Alum	5		.45	7/16 to 5/8 △					14000
	○ Circulation — Red Nose	017-3405-090	1-3/8"	Alum	5		.45	5/16 to 7/16 △					14000
	○ Circulation — Red Nose	017-3405-053	1-11/16"	Alum	8		.53	5/8 △				14000	13000
EXPENDABLE RETRIEVABLE STEEL WIRE FORMED WIRE JETS	Tornado Jet—Formed Wire	017-3404-004	15/16"	Alum	1.25	4-1/2"	.12	2.84	.15	.23	2.52	20000	15000
	Tornado Jet—Formed Wire	017-3404-005	1"	Alum	2	4-1/2"	.15	3.06	.18	.59	2.65	16500	14000
	Tornado Jet—Formed Wire	017-3404-006	1-1/8	Alum	2.5	4-1/2	.19	3.55	.23	.68	3.15	15000	12000
	Tornado Jet—Formed Wire	017-3404-007	1-1/4	Alum	5	2-3/8"	.30	4.51	.29	.69	3.91	15000	14000
	Tornado Jet—Formed Wire	017-3404-008	1-3/8"	Alum	6	2-3/8"	.30	5.68	.26	.86	4.80	15000	14000
	Tornado Jet—Formed Wire	017-3404-009	1-11/16"	Alum	13	2-7/8"	.36	7.39	.37	.90	6.35	14000	13000
	Tor. Jet—Formed Wire DML	017-3404-065	1-11/16"	Alum	12							14000	13000
	Tor. Glasjet—Formed Wire	017-3204-005	1-11/16"	Glass	13	2-3/8"	.36	6.34	.31	.86	5.82	8000	7000
	Tor. Glasjet—Formed Wire	017-3204-005	1-11/16"	Glass	13	5-1/2"	.27	5.78	.31	.86	5.82	8000	7000
	Tor. Ceramic—Formed Wire	017-3204-012	1-11/16"	Ceramic	12	5-1/2"	.25	5.33	.32	.80	5.42	20000	15000
	Tor. Ceramic—Formed Wire	017-3204-013	2-1/8	Ceramic	22.7	5-1/2"	.33	8.05	.42	.84	7.58	20000	15000
	Tornado Jet—Formed Wire	017-3404-010	2-1/8	Alum	22.7	5-1/2"	.41	8.52	.48	.91	7.89	15000	12000
	Tornado Jet—Formed Wire	017-3404-010	2-1/8	Alum	22.7	7"	.42	8.14	.48	.91	7.89	15000	12000
	Tor. Jet—Formed Wire DML	017-3404-066	2-1/8	Alum	22							15000	12000
	Tor. Glasjet—Formed Wire	017-3204-011	2-1/8"	Glass	22.7	2-7/8"	.43	8.31	.41	.85	7.53	8000	7000
	Tor. Glasjet—Formed Wire	017-3204-011	2-1/8"	Glass	22.7	7"	.32	7.13	.41	.85	7.53	8000	7000
	Tor. Magnum—Formed Wire	017-3404-086	1-3/8"	Steel	6.5	2-7/8"	.30	6.07	.26	.81	5.35	15000	14000
	Tor. Magnum—Formed Wire	017-3404-092	1-1/2"	Steel	7	2-7/8"	.30	6.88	.26	.85	6.12	15000	14000
	Tor. Magnum—Formed Wire	017-3404-090	1-11/16"	Steel	13	5-1/2"	.31	8.14	.38	.88	7.37	14000	13000
	Tor. Magnum—Formed Wire	017-3404-045	1-13/16"	Steel	13	5-1/2"	.32	8.54	.39	.83	7.76	14000	14000
	Tor. Magnum—Formed Wire	017-3404-088	2-1/8"	Steel	22.7	5-1/2"	.42	9.64	.51	.93	8.82	15000	14000
EXPENDABLE ALUMINUM LINK JETS	Tornado Jet—Link	018-3101-004	1-1/4"	Alum	5	2-3/8	.30	4.51	.29	.69	3.91	14000	14000
	Tornado Jet—Link	018-3101-005	1-3/8	Alum	6	2-3/8	.30	5.63	.26	.86	4.80	15000	14000
	Tornado Jet—Link	018-3100-011	1-11/16	Alum	13	2-7/8"	.36	7.39	.37	.90	6.35	14000	13000
	Tornado Jet—Link	018-3100-011	1-11/16"	Alum	13	5-1/2"	.30	7.34	.37	.90	6.35	14000	13000
	"500" Tornado Jet—Link	018-3100-061	1-11/16"	Alum	13.5	4-1/2"	.51	5.02	.53	.89	3.39	14000	13000
	Tornado Jet—Link DML	018-3100-060	1-11/16"	Alum	12							14000	13000
	Tornado Jet—Link 1-way	018-3100-051	1-11/16"	Alum	13	5-1/2"	.30	7.34	.37	.90	6.35	14000	13000
	Stiff Jet DML 1-way	018-3102-005	1-11/16"	Alum	12							14000	13000
	Tornado Stiff Jet	018-3102-001	2-1/16"	Alum	21							15000	12000
	Tornado Stiff Jet DML	018-3102-002	2-1/16"	Alum	20							15000	12000
	Tornado Jet—Link	018-3100-045	2-1/8"	Alum	22.7	2-7/8"	.44	8.92	.48	.91	7.89	15000	12000
	Tornado Jet—Link	018-3100-045	2-1/8"	Alum	22.7	5-1/2	.41	8.52	.48	.91	7.89	15000	12000
	Tornado Jet—Link	018-3100-045	2-1/8	Alum	22.7	7"	.42	8.14	.48	.91	7.89	15000	12000
	Tornado Jet—Link DML	018-3100-075	2-1/8"	Alum	22							15000	12000
	Tornado Jet—Link 1-way	018-3100-053	2-1/8"	Alum	22.7	5-1/2"	.41	8.52	.48	.01	7.89	15000	12000
	Tornado Frac	018-3130-002	3-3/4"	Alum	90	4-1/2"	.66	18.02	.71		14.75	13000	12000
	Tornado Frac	018-3130-002	3-3/4"	Alum	90	5-1/2"	.67	18.62	.71		14.75	13000	12000
	Tornado Frac	018-3130-002	3-3/4"	Alum	80	7"	.71	17.21	.71		14.75	13000	12000
	○ Circulation—Green Nose	018-3101-030	1-1/4"	Alum	4		.36	3/8 to 1/2 △				14000	14000
	○ Circulation—Red Nose	018-3101-003	1-1/4"	Alum	4		.43	1/4 to 3/8 △				14000	14000
	○ Circulation—Green Nose	018-3101-008	1-3/8"	Alum	5		.45	7/16 to 3/8 △				15000	14000
	○ Circulation—Red Nose	018-3101-010	1-3/8"	Alum	5		.45	5/16 to 7/16 △				15000	14000
	○ Circulation—Red Nose	018-3101-032	1-11/16"	Alum	8		.53	5/8 △				14000	13000
	Strap Jet	020-3202-001	1-11/16"	Alum	6	2-7/8"	.28	6.19	.25	.86	5.89	14000	13000
	Strap Sand Control	020-3201-004	1-11/16"	Alum	1	2"	.10					15000	15000
	Strap Jet	020-3202-002	2-1/8"	Alum	10	2-7/8"	.41	7.75	.34	.60	7.37	6000	7000
	Strap Sand Control	020-3201-005	2-3/16"	Alum	2	2-7/8"	.11				3.25	15000	15000

	nado Jet Bi Wire	017-3405-008	2-1/8	Alum	22	2-7/8	.41	8.52	.48	.91	7.89	15000	12000
	Tornado Jet Bi Wire DML	017-3405-072	2-1/8	Alum	22							15000	12000
	Tornado Glasjet Bi Wire	017-3405-013	2-1/8	Glass	22.7	2-7/8	.43	8.31	.41	.85	7.53	8000	7000
	Tornado Glasjet Bi Wire	017-3405-013	2-1/8	Glass	22.7	7	.32	7.13	.41	.85	7.53	8000	7000
	Twin Needle Bi Wire	017-3212-005	1-11/16	Alum	15	4-1/2	.10**	2.68	.10		2.30	16000	12000
	Twin Needle Bi Wire	017-3212-006	2-1/8	Alum	3.5	5-1/2	.12**	3.67	.12		3.15	16000	12000
	Twin Needle Bi Wire	017-3212-007	2-3/4	Alum	4	7	.14**	4.77	.14		4.10	13500	12000
	o Circulation — Red Nose	017-3405-082	15/16	Alum	1		.24	1/8 to 1/4 Δ					15000
	o Circulation — Red Nose	017-3405-083	1"	Alum	2		.30	1/8 to 1/4 Δ					14000
	o Circulation — Red Nose	017-3405-095	1-1/8"	Alum	2		.36	1/8 to 1/4 Δ					12000
	o Circulation — Green Nose	017-3405-043	1-1/4"	Alum	4		.38	3/8 to 1/2 Δ					14000
	o Circulation — Red Nose	017-3405-044	1-1/4"	Alum	4		.43	1/4 to 3/8 Δ					14000
	o Circulation — Green Nose	017-3405-005	1-3/8"	Alum	5		.45	7/16 to 5/8 Δ					14000
	o Circulation — Red Nose	017-3405-050	1-3/8"	Alum	5		.45	5/16 to 7/16 Δ					14000
	o Circulation — Red Nose	017-3405-053	1-11/16	Alum	8		.53	5/8 Δ				14000	13000
	Tornado Jet — Formed Wire	017-3404-004	15/16	Alum	1.25	4-1/2	.12	2.84	.15	.23	2.52	20000	15000
	Tornado Jet — Formed Wire	017-3404-005	1"	Alum	2	4-1/2	.15	3.06	.18	.59	2.65	16500	14000
	Tornado Jet — Formed Wire	017-3404-008	1-1/8	Alum	2.5	4-1/2"	.19	3.55	.23	.68	3.15	15000	12000
	Tornado Jet — Formed Wire	017-3404-007	1-1/4"	Alum	5	2-3/8"	.30	4.51	.29	.69	3.91	15000	14000
	Tornado Jet — Formed Wire	017-3404-008	1-3/8"	Alum	6	2-3/8"	.30	5.68	.26	.86	4.80	15000	14000
	Tornado Jet — Formed Wire	017-3404-009	1-11/16"	Alum	13	2-7/8"	.36	7.39	.37	.90	6.35	14000	13000
	Tor. Jet — Formed Wire DML	017-3404-035	1-11/16"	Alum	12							14000	13000
	Tor. Glasjet — Formed Wire	017-3204-009	1-11/16"	Glass	13	2-3/8"	.36	6.34	.31	.88	5.82	8000	7000
EXPENDABLE	Tor. Glasjet — Formed Wire	017-3204-005	1-11/16"	Glass	13	5-1/2"	.27	5.76	.31	.88	5.82	8000	7000
RETRIEVABLE	Tor. Ceramic — Formed Wire	017-3204-012	1-11/16"	Ceramic	12	5-1/2"	.25	5.33	.32	.80	5.42	20000	15000
STEEL WIRE	Tor. Ceramic — Formed Wire	017-3204-013	2-1/8	Ceramic	22.7	5-1/2"	.33	8.05	.42	.84	7.58	20000	15000
FORMED WIRE	Tornado Jet — Formed Wire	017-3404-010	2-1/8	Alum	22.7	5-1/2"	.41	8.52	.48	.91	7.89	15000	12000
JETS	Tornado Jet — Formed Wire	017-3404-010	2-1/8	Alum	22.7	7"	.42	8.14	.48	.91	7.89	15000	12000
	Tor. Jet — Formed Wire DML	017-3404-066	2-1/8"	Alum	22							15000	12000
	Tor. Glasjet — Formed Wire	017-3204-011	2-1/8"	Glass	22.7	2-7/8"	.43	8.31	.41	.85	7.53	8000	7000
	Tor. Glasjet — Formed Wire	017-3204-011	2-1/8"	Glass	22.7	7"	.32	7.13	.41	.85	7.53	8000	7000
	Tor. Magnum — Formed Wire	017-3404-063	1-3/8"	Steel	6.5	2-7/8"	.30	6.07	.26	.81	5.35	15000	14000
	Tor. Magnum — Formed Wire	017-3404-062	1-1/2"	Steel	7	2-7/8"	.30	6.96	.26	.85	6.12	15000	14000
	Tor. Magnum — Formed Wire	017-3404-060	1-11/16"	Steel	13	5-1/2"	.31	8.14	.36	.88	7.37	14000	13000
	Tor. Magnum — Formed Wire	017-3404-045	1-13/16"	Steel	13	5-1/2"	.32	8.54	.39	.83	7.78	14000	14000
	Tor Magnum — Formed Wire	017-3404-068	2-1/8"	Steel	22.7	5-1/2"	.42	9.64	.51	.93	8.62	15000	14000
	Tornado Jet — Link	018-3101-004	1-1/4"	Alum	5	2-3/8"	.30	4.51	.29	.69	3.91	14000	14000
	Tornado Jet — Link	018-3101-005	1-3/8"	Alum	6	2-3/8"	.30	5.63	.26	.86	4.80	15000	14000
	Tornado Jet — Link	018-3100-011	1-11/16"	Alum	13	2-7/8"	.36	7.39	.37	.90	6.35	14000	13000
	Tornado Jet — Link	018-3100-011	1-11/16"	Alum	13	5-1/2"	.30	7.34	.37	.90	6.35	14000	13000
	"500" Tornado Jet — Link	018-3100-031	1-11/16"	Alum	13.5	4-1/2"	.51	5.02	.53	.89	3.39	14000	13000
	Tornado Jet — Link DML	018-3100-089	1-11/16"	Alum	12							14000	13000
	Tornado Jet — Link 1-way	018-3100-051	1-11/16"	Alum	13	5-1/2"	.30	7.34	.37	.90	6.35	14000	13000
	Stiff Jet DML 1-way	018-3102-008	1-11/16"	Alum	12							14000	13000
	Tornado Stiff Jet	018-3102-001	2-1/16"	Alum	21							15000	12000
EXPENDABLE	Tornado Stiff Jet DML	018-3102-002	2-1/16"	Alum	20							15000	12000
ALUMINUM	Tornado Jet — Link	018-3100-045	2-1/8"	Alum	22.7	2-7/8"	.44	8.92	.48	.91	7.89	15000	12000
LINK	Tornado Jet — Link	018-3100-045	2-1/8"	Alum	22.7	5-1/2"	.41	8.52	.48	.91	7.89	15000	12000
JETS	Tornado Jet — Link	018-3100-045	2-1/8"	Alum	22.7	7"	.42	8.14	.48	.91	7.89	15000	12000
	Tornado Jet — Link DML	018-3100-075	2-1/8"	Alum	22							15000	12000
	Tornado Jet — Link 1-way	018-3100-053	2-1/8"	Alum	22.7	5-1/2"	.41	8.52	.48	.91	7.89	15000	12000
	Tornado Frac	018-3130-002	3-3/4"	Alum	90	4-1/2"	.86	18.02	.71		14.75	13000	12000
	Tornado Frac	018-3130-002	3-3/4"	Alum	90	5-1/2"	.87	18.62	.71		14.75	13000	12000
	Tornado Frac	018-3130-002	3-3/4"	Alum	90	7"	.71	17.21	.71		14.75	13000	12000
	o Circulation — Green Nose	018-3101-030	1-1/4"	Alum	4		.38	3/8 to 1/2 Δ				14000	14000
	o Circulation — Red Nose	018-3101-003	1-1/4"	Alum	4		.43	1/4 to 3/8 Δ				14000	14000
	o Circulation — Green Nose	018-3101-009	1-3/8"	Alum	5		.45	7/16 to 3/8 Δ				15000	14000
	o Circulation — Red Nose	018-3101-010	1-3/8"	Alum	5		.45	5/16 to 7/16 Δ				15000	14000
	o Circulation — Red Nose	018-3101-032	1-11/16"	Alum	8		.53	5/8 Δ				14000	13000
	Strap Jet	020-3202-001	1-11/16"	Alum	6	2-7/8"	.28	6.19	.25	.86	5.89	14000	13000
	Strap Sand Control	020-3201-004	1-11/16"	Alum	1	2"	.10					15000	15000
	Strap Jet	020-3202-002	2-1/8"	Alum	10	2-7/8"	.41	7.75	.34	.80	7.37	8000	7000
	Strap Sand Control	020-3201-005	2-3/16"	Alum	2	2-7/8"	.11				3.25	15000	15000
	Tornado Ceramic Strip	020-3203-029	1-11/16"	Ceramic	12	5-1/2"	.25	5.33	.32	.80	5.42	20000	15000
	Tornado Glass Strip Jet	020-3203-004	1-11/16"	Glass	13	2-3/8"	.36	6.34	.31	.86	5.82		8000
	Tornado Glass Strip Jet	020-3203-004	1-11/16"	Glass	13	5-1/2"	.30	6.33	.31	.86	5.82		8000
	Tornado Ceramic Strip	020-3203-019	2-1/8"	Ceramic	22.7	5-1/2"	.33	8.05	.42	.84	7.58	20000	15000
EXPENDABLE	Tornado Glass Strip Jet	020-3203-003	2-1/8"	Glass	22.7	7"	.34	7.10	.41	.85	7.53	8000	7000
RETRIEVABLE	Glass DML Strip Jet	020-3207-040	3-1/2"	Glass								20000	20000
STEEL	Glass Strip Jet	020-3207-005	3-1/2"	Glass	22.7	4-1/2"	.50	10.21	.50	.78	9.95	20000	20000
STRIP	Glass Strip Jet	020-3207-005	3-1/2"	Glass	22.7	5-1/2"	.43	9.86	.50	.78	9.95	20000	20000
	Strip Jet	020-3207-008	3-1/2"	Alum	22.7	4-1/2"	.53	10.36	.61	.79	9.85	15000	15000
	Strip Jet	020-3207-003	3-1/2"	Alum	22.7	5-1/2"	.53	10.20	.61	.79	9.85	15000	15000
	Strip Jet	020-3207-003	3-1/2"	Alum	22.7	7"	.43	10.33	.61	.79	9.85	15000	15000
	Strip Jet DML	020-3207-041	3-1/2"	Alum								15000	15000
	Glass Sabor Jet	020-3199-001	3-5/8"	Glass	37	4-1/2"	.39	9.41	.42		8.62	12000	11000
	Glass Sabor Jet	020-3199-003	3-5/8"	Glass	80	4-1/2"	.73	17.94	.70		13.31	12000	11000
	Glass Sabor Jet	020-3199-002	4-5/8"	Glass	50	7"	.49	12.83	.53		11.08	12000	11000
	Glass Sabor Jet	020-3199-003	4-5/8"	Glass	80	7"	.82	17.39	.70		13.31	12000	11000
	Stick Jet	019-3000-001	3-1/2"	Alum	15	4-1/2"	.40	7.60	.41		7.58	12000	11000
EXPENDABLE	Stick Jet DML	019-3000-050	3-1/2"	Alum	13							12000	11000
ALUMINUM	Stick Jet	019-3000-002	4-1/4"	Alum	22.7	5-1/2"	.46	0.47	.51	.89	7.91	15000	12000
TUBING	Stick Jet DML	019-3000-081	4-1/4"	Alum	22							15000	12000
	Stick Jet	019-3000-003	5-1/2"	Alum	22.7	7"	.56	12.33	.63	.89	9.50	12000	11000
	Stick Jet DML	019-3000-052	5-1/2"	Alum	22.7							12000	11000
	DML Tru Jet III	021-3807-103	1-9/16"	Steel	3	5-1/2"	.24	5.32	.25	.68	4.82	20000	20000
	Donsi-Jet IV Big Hole	021-3809-033	1-9/16"	Steel	4	2-7/8"	.32	4.50	.33	.72	4.12	20000	20000
	DML Tru Jet VI	021-3802-123	2"	Steel	6	5-1/2"	.20	7.52	.32	.60	6.20	20000	20000
EXPENDABLE	Donsi-Jet VI Big Hole	021-3808-005	2"	Steel	6	5-1/2"	.34	5.63	.35	.73	5.25	20000	20000
HOLLOW	DML Donsi-Jet VI H. T	021-3808-010	2"	Steel	6	5-1/2"	.29	7.33	.31	.70	6.01	20000	20000
CARRIER	o Circulation	021-3809-050	1-9/16"	Steel	2		.39**	1/4 to 3/8 Δ				20000	20000
(GOWINDER)	o Circulation	021-3809-056	1-9/16"	Steel	2		.41**	3/8 to 1/2 Δ				20000	20000
	o Circulation	021-3818-010	2"	Steel	2		.42**	1/4 to 3/8 Δ				20000	20000
	o Circulation	021-3818-015	2"	Steel	2		.43**	3/8 to 1/2 Δ				20000	20000

Special Perforators and Cutters data available on request.

o These charges are used to penetrate the primary string without penetration into the secondary string.

ΔPenetration in steel at zero clearance. **Controlized *Decontrolized

COMPLETION CHARGE PERFORMANCE DATA

Casing Charges				API Cement			API Berea			(PSI) at °F	
Part #	Charge Designation	Explosive Gr. Wt.	Type Carrier	Pipe Size	Hole	Penetration	Hole	TTP	CPE	PSI	Temperature
HOLLOW GUN CHARGES											
525-5-1	3-1/8" S.D.J. Plus	8.0	Hollow Carrier	4-1/2"	.41	9.25	.46	6.18	.72	20,000	340
526-3701-8	3-1/8" Donol Jet II	10.0		4-1/2"	.39	8.99	.45	8.33	.89	20,000	325
525-75-0	3-1/8" Big Hole	10.0		4-1/2"	.61	7.54	.62	5.60	.76	20,000	340
*525-5-6	3-1/8" Omega II*	11.0		4-1/2	.34	15.36	.39	10.60	.80	20,000	340
*525-5-4	3-1/8" Omega Hi-Temp*	12.0		4-1/2"	.43	11.20	.42	9.62	.72	20,000	400
525-13-12	3-1/8" NL NU-LINE RPS**	12.0		4-1/2"	.38	19.36	.41	11.10	.83	20,000	340
*525-5-7	3-5/8" Omega II*	11.0		4-1/2"	.34	15.36	.39	10.60	.80	20,000	340
525-6-1	3-5/8" S.D.J. Plus	15.0		4-1/2"	.44	11.63	.53	8.15	.77	20,000	340
525-7-1	4" S.D.J. Plus	15.0		5-1/2"	.39	16.78	.46	9.38	.78	20,000	340
525-7-2	4" S.D.J. 10	18.0		5-1/2"	.47	17.30	.49	11.08	.86	20,000	340
525-7-5	4" S.D.J. 1/4" Hole	19.0		7"	.25	13.53	.29	8.75	.81	20,000	340
525-65-1	4" Big Hole	20.5		9-5/8"	.71	10.20	.75	7.14	.77	20,000	340
525-65-4	4" NL	21.0		5-1/2"	.92	5.01	.83	4.72	.78	20,000	340
525-13-13	4" NL NU-LINE RPS**	22.0		5-1/2"	.50	23.64	.56	14.86	.85	20,000	340
*525-8-5	4" Omega II*	22.0		5-1/2	.50	23.20	.56	14.73	.85	20,000	340
*525-8-3	4" Omega Hi-Temp*	23.0		5-1/2"	.51	20.63	.51	12.68	.82	20,000	400
*525-8-1	5" Omega*	32.0		9-5/8"	.78	17.56	.81	11.99	.83	15,000	340
*525-65-3	5" Big Hole	32.0		9-5/8"	.86	14.22	.79	12.10	.93	15,000	340
THRU TUBING CHARGES											
*525-12-1	1-9/16" Omega Hi-Temp*	2.5	Expendable Retrievable Hollow Carrier	5-1/2"	.23	6.04	.26	4.81	.76	20,000	400
*525-12-2	1-9/16" Omega II*	3.0		5-1/2"	.25	8.12	.29	5.48	.81	20,000	340
525-13-14	1-9/16" NL NU-LINE**	3.0		4-1/2"	.26	9.88	.29	5.68	.81	20,000	340
*525-13-1	2" Omega Hi-Temp*	4.5		5-1/2"	.31	8.35	.34	6.09	.78	20,000	400
*525-13	2" Omega*	5.5		5-1/2"	.33	7.87	.36	6.46	.80	20,000	340
525-13-5	2-1/8" Omega II* Hi-Temp	6.5		4-1/2"	.30	10.28	.35	6.90	.75	20,000	400
525-13-9	2-1/8" NL NU-LINE**	6.5		4-1/2	.32	10.37	.36	8.15	.79	20,000	340
525-13-11	2-3/4 NL NU-LINE**	11.0		4-1/2	.38	16.24	.37	10.55	.75	20,000	340
524-1	2-1/2" N-VADER**	12.0		4-1/2"	.35	15.59	.39	10.54	.85	20,000	340
**526-3404-7	1-1/4" Tornado Jet Formed Wire	5.0	Expendable Retrievable Stool Wire Expendable Aluminum Link	2-3/8"	.30	4.51	.29	3.91	.69	14,000	325
**526-3404-86	1-3/8" Tornado Jet Magnum	6.5		2-7/8"	.30	6.07	.26	5.35	.81	15,000	325
**526-3404-90	1-11/16" Tornado Jet Magnum	13.0		5-1/2"	.31	8.14	.38	7.37	.88	14,000	325
**526-3404-88	2-1/8" Tornado Jet Magnum	22.7		5-1/2	.42	9.64	.51	8.62	.93	15,000	325
**526-3100-11	1-11/16" Tornado Jet	13.0		5-1/2	.30	7.34	.37	6.35	.90	14,000	325
**526-3100-45	2-1/8" Tornado Jet	22.7		5-1/2"	.41	8.52	.48	7.89	.91	12,000	325

Rubber pop-up alignment system available in Hollow Carrier charges
*Available to 525°F by order
**Tornado Jet charges available to 20,000 PSI and 420 F by order

S.D.J. — Super Dyna Jet
API Data sheets for charges listed are available on request.

SCHLUMBERGER
CHARGE PERFORMANCE DATA
JANUARY 1984

STANDARD

Classification	Gun Size (in.)	Gun Type	Charge Type	Rating (psi/°F)	Gun Phasing (°)	Explosive Ld (g)	API RP-43 Section I Pene. (in.) Sand-Cement	API RP-43 Section I Casing Hole Dia. (in.)	API RP-43 Section II Berea Sand Formation EH	OAP	TTP	TCP	CFE	ECP
Through-Tubing Semi-Expendable	1-11/16	Enerjet	Enerjet II	20,000/340	0	11.0	13.26	0.33	0.34	8.11	7.35	6.22	0.90	5.60
	2-1/8	Enerjet	Enerjet	15,000/340	0	13.5	18.41	0.34	0.36	11.00	10.25	9.12	0.79	7.22
Through-Tubing Hollow Carrier	1-3/8	Domed Scallop	HyperDome	15,000/340	0	1.8	5.75	0.21	0.23	4.28	3.30	2.18	0.81	1.76
	1-11/16	Domed Scallop	HyperDome	15,000/340	0	3.2	7.94	0.25	0.29	5.46	5.03	3.91	0.80	3.11
	2-1/8	Domed Scallop	HyperDome	15,000/340	0,180	6.5	10.64	0.32	0.34	8.83	7.92	6.80	0.76	5.13
	2-1/8	Domed Scallop	Ultrajet	25,000/340	0,180	6.5	12.84	0.32	0.33	9.50	8.69	7.56	0.80	—
	2-7/8	Domed Scallop	HyperDome	15,000/340	0,180	14.0	16.12	0.37	0.40	10.98	10.63	9.50	0.76	7.44
Casing Hollow Carrier	3-3/8	Carrier	Ultrajet	20,000/340	90	14.0	22.04	0.33	0.35	13.08	12.45	11.33	0.87	—
	3-3/8	Carrier	Hyper-Jet II	20,000/340	90	14.0	19.36	0.38	0.38	11.30	10.85	9.73	0.81	7.88
	4	Carrier	Hyper-Jet II	20,000/340	90	22.0	23.07	0.40	0.46	16.13	14.13	13.01	0.84	10.88
Selective Shot-by-Shot	3-3/8	Selective Csg. Gun	Hyper-Select	20,000/340	0	10.0	17.70	0.37	0.37	10.80	9.50	8.38	0.73	6.11
Sand Control	4	Carrier	Big Hole Hyper-Jet	20,000/340	0	22.0	4.32	0.89	0.91	4.60	4.48	3.36	0.73	2.47
	4(1)	Carrier	Ultrapack	20,000/340	90	22.0	16.22	0.66	0.76	11.17	11.00	9.87	0.73	—
	4(2)	Carrier	Ultrapack	20,000/340	90	22.0	16.65	0.67	0.69	9.73	9.27	8.15	0.88	—
	5(3)	Carrier	Ultrapack	20,000/340	90	32.0	14.17	0.79	1.02	9.04	8.92	7.80	0.88	—
	5(4)	Carrier	Ultrapack	20,000/340	90	32.0	13.49	0.80	0.91	9.94	9.73	8.60	0.86	—
	5(5)	Carrier	Ultrapack	20,000/340	90	32.0	16.57	0.77	0.91	9.55	9.23	8.11	0.86	—
	5(6)	Carrier	Hyper-Pack	20,000/340	90	32.0	17.71	0.70	0.82	13.70	13.26	12.13	0.78	9.42
	5(7)	Carrier	Hyper-Pack	20,000/340	90	32.0	19.36	0.70	0.83	14.17	13.63	12.50	0.82	10.24
	5(8)	Carrier	Hyper-Pack	20,000/340	90	32.0	22.00	0.65	0.81	14.30	13.60	12.47	0.82	10.22
	(9)	Semi-Expendable	Big Hole Expendable	15,000/300	0,90,180	22.6	8.04	0.67	0.81	—	5.83	4.71	1.16	5.47

HIGH-TEMPERATURE

Through-Tubing Hollow Carrier	1-3/8	Domed Scallop	HyperDome	25,000/470	0	1.8	5.10	0.19	0.19	3.79	3.32	2.2	0.64	1.42
	1-11/16	Domed Scallop	HyperDome	25,000/470	0	3.2	6.02	0.23	0.25	4.03	3.85	2.73	0.76	2.07
	1-9/16	Scallop	Hyper-Jet	25,000/600	0	3.4	3.75	0.18	0.20	3.00	2.00	0.88	0.89	0.78
	2-1/8	Domed Scallop	HyperDome	25,000/470	0,180	6.5	10.36	0.30	0.33	7.40	6.6	5.40	0.70	3.82
	2-7/8	Domed Scallop	Ultrajet	25,000/470	0,180	15.0	14.40	0.30	0.34	10.17	9.54	8.42	0.80	—
Casing Hollow Carrier	3-3/8	Carrier	Hyper-Jet	25,000/470	90	13.5	10.65	0.34	0.43	7.73	5.67	4.55	0.67	3.11
	4	Carrier	Hyper-Jet II	25,000/470	90	22.0	20.28	0.38	0.40	11.88	11.80	10.67	0.84	8.92

(1) 5.5" 17.0# J-55
(2) 7.0" 23.0# J-55
(3) 7.0" 23.0# J-55
(4) 7 5/8" 26.4# J-55
(5) 9 5/8" 40.0# J-55
(6) 7.0" 23.0# N-80
(7) 7 5/8" 29.7# N-80
(8) 9 5/8" 40.0# N-80
(9) 9 5/8" K-55

EH = Entrance Hole
OAP = Overall Penetration
TTP = Total Target Penetration
TCP = Total Core Penetration
CFE = Core Flow Efficiency
ECP = Effective Core Penetration

SCHLUMBERGER WELL SERVICES - PERFORATING CENTER
14910 AIRLINE ROAD DRAWER A
ROSHARON, TEXAS 77583-0076 (713) 431-0211

SCHLUMBERGER API DATA SHEETS ON FILE WITH API OFFICE

Gun Designation	Charge Name	Part Number	1 Hr Temp. rate	Expl. Load Gms.	API RP43–Second Edition Section I Casing	Section I E.H.	Section I Penetr.	Section II E.H.	Section II CFE	Section II TTP	Section II OAP	Test Date
1 3/8" DS	16A HD, RDX (1 3/8" TTG)	H224509	330	1.8	4 1/2	0.21	5.75	0.23	0.81	3.30	4.28	11-74
1 3/8" DS	16A HD, PSF (1 3/8" TTG)	H247295	470	1.8	4 1/2	0.19	5.10	0.19	0.64	3.32	3.79	07-76
1 11/16" EJ	1 11/16" EJ II	P274035	330	11.0	5 1/2	0.33	13.26	0.34	0.90	7.35	8.11	09-78
1 11/16" DS	20A HD, RDX (1 11/16 TTG)	H224234	330	3.2	4 1/2	0.28	7.23	0.28	1.02	4.63	4.81	08-86
1 11/16" DS	20A HD, HMX (1 11/16 TTG)	H334639	400	3.2	4 1/2	0.21	6.89	0.27	0.87	4.54	5.21	12-84
1 11/16" DS	20A HD, PSF (1 11/16 TTG)	H224372	470	3.2	4 1/2	0.23	6.02	0.25	0.76	3.85	4.03	03-74
2 1/8" EJ	2 1/8" EJ	P273920	330	13.5	5 1/2	0.34	18.41	0.36	0.79	10.25	11.00	08-74
2 1/8" DS	25A HD, RDX (2 1/8" TTG)	H224470	330	6.5	4 1/2	0.32	10.64	0.34	0.76	7.92	8.83	09-74
2 1/8" DS	25A HD, PSF (2 1/8" TTG)	H224577	470	6.5	4 1/2	0.30	10.36	0.33	0.70	6.55	7.40	03-75
2 1/8" DS	25A UJ, RDX (2 1/8" TTG)	H304920	380	6.5	4 1/2	0.29	10.90	0.30	0.85	7.71	9.29	08-85
2 1/8" DS	25A UJ, HMX (2 1/8" TTG)	H334542	400	6.5	4 1/2	0.31	13.04	.35	0.69	7.98	8.33	10-85
2 7/8" DS	38B1 HD, RDX (2 7/8" TTG)	H224363	330	14.0	4 1/2	0.37	16.12	0.40	0.78	10.63	10.98	03-74
2 7/8" DS	38A1 UJ, PSF (2 7/8" TTG)	H304349	470	15.0	4 1/2	0.30	14.40	0.34	0.80	9.64	10.17	02-83
3 3/8" PPG	38B HJ, PSF (3 3/8" PPG)	H132439	470	13.5	5 1/2	0.34	10.65	0.43	0.67	5.67	7.73	07-72
3 3/8" PPG	38B HJ II, RDX (3 3/8 PPG)	H247247	330	14.0	4 1/2	0.38	19.36	0.38	0.81	10.85	11.30	04-73
3 3/8" PPG	38A UJ, RDX (3 3/8" PPG)	H247776	330	16.0	4 1/2	0.35	19.75	0.34	1.03	12.77	13.44	06-85
3 3/8" PPG	38A UJ, HMX (3 3/8" PPG)	H304637	400	14.0	4 1/2	0.30	20.44	0.36	0.73	12.09	12.61	03-84
3 3/8" PPG	38A UJ, HNS (3 3/8" PPG)	H304569	500	14.0	4 1/2	0.28	14.66	0.31	0.78	9.38	9.84	02-84
3 3/8" PPG	38F UP, RDX (3 3/8" PPG)	H304630	330	14.0	4 1/2	0.56	7.52	0.57	1.35	5.13	6.17	04-84
3 3/8" SCG	38B HYPER SELECT (3 3/8" SBS)	H247431	330	10.0	4 1/2	0.37	17.70	0.37	0.73	9.50	10.30	11-76
4"PPG	41A HJ III, RDX (4" PPG)	H421504	330	22.7	5 1/2	0.37	23.97	0.38	1.11	14.25	15.42	07-85
4" PPG	41B HJ II, RDX (4" PPG)	H224733	330	22.7	5 1/2	0.45	19.72	0.41	1.03	12.71	13.50	08-85
4" PPG	41B HJ II, HMX (4" PPG)	H334534	400	22.7	5 1/2	0.40	20.97	0.46	0.92	11.71	11.96	08-84
4" PPG	41B HJ II, PSF (4" PPG)	H247262	470	22.7	5 1/2	0.38	20.28	0.40	0.84	11.80	11.88	05-74
4" PPG	41B UP, RDX (4" PPG)	H247778	330	22.7	5 1/2	0.66	16.22	0.76	0.73	11.00	11.17	03-80
4" PPG	41B UP, RDX (4" PPG)	H247778	330	22.7	7	0.67	16.65	0.69	0.88	9.27	9.73	09-81
5" PPG	51B HJ II, RDX (5" PPG)	H334504	330	37.0	7	0.43	28.61	0.49	-	20.38	20.38	06-84
5" PPG	51B UP, RDX (5" PPG)	H304043	330	32.0	7	0.79	14.17	1.02	0.88	8.92	9.04	06-81
5" PPG	51B UP, RDX (5" PPG)	H304043	330	32.0	7 5/8	0.80	13.49	0.91	0.86	9.73	9.94	09-81
5" PPG	51B UP, RDX (5" PPG)	H304043	330	32.0	9 5/8	0.77	16.57	0.91	0.86	9.23	9.55	09-81
3 3/8" HSD	38A UJ, RDX	H304760	330	16.0	4 1/2	0.31	19.04	0.34	0.75	11.85	12.36	02-85
3 3/8" HSD	41B HJ II, RDX	H304953	330	22.7	4 1/2	0.42	19.73	0.46	0.80	12.25	12.57	11-84
5" 5 SPF HSD	51B HJ II, RDX	H334497	330	37.0	7	0.46	25.80	-	-	-	-	04-85
5" 5 SPF HSD	51B HJ II, HMX	H334498	400	37.0	7	0.56	26.13	-	-	-	-	04-85
5" HSD	41B HJ II, RDX	H304953	330	22.7	7	0.41	16.07	0.50	0.62	11.04	11.46	12-83
5" HSD	41B HJ II, PSF	H304978	470	22.7	7	0.35	10.94	0.43	0.70	8.29	8.46	01-85
5" HSD	41B UP II, RDX	H334852	330	22.7	7	0.68	8.80	-	-	-	-	11-84
5 1/2" HSD	41B HJ II, RDX	H304953	330	22.7	7 5/8	0.40	19.06	0.49	0.73	11.46	11.77	12-83
5 1/2" HSD	41B UP II, RDX	H334852	330	22.7	7 5/8	0.66	11.60	-	-	-	-	11-84
6" HSD	41B HJ II, RDX	H304953	330	22.7	9 5/8	0.38	21.07	0.47	0.75	11.73	12.00	12-83
6" HSD	41B HJ II, HMX	H304952	400	22.7	9 5/8	0.40	20.40	0.48	1.23	11.96	12.17	09-84
6" HSD	51C UP, RDX (6" HSD)°	H304930	330	32.0	9 5/8	0.83	6.65	-	-	-	-	01-85
6" HSD	51B UP II, RDX (6" HSD)°	H304885	330	32.0	9 5/8	0.76	9.40	-	-	-	-	01-85
7 1/4" HSD	51B HJ II, RDX (7 1/4" HSD)	H334497	330	37.0	9 5/8	0.47	27.86	0.54	-	18.67	18.67	06-84
7 1/4" HSD	51C UP II, RDX (7 1/4" HSD)	H334862	330	35.1	9 5/8	0.80	12.25	-	-	-	-	11-84

GUNS= DS: Domed Scallop, EJ: Enerjet, PPG: Port Plug Gun, SCG: Selective CSG Gun, HSD: High Shot Density
CHARGES= HD: Hyperdome, HJ: Hyperjet, UJ: Ultrajet, UP: Ultrapack
° Clip ring retained charge

28th October 1985

TEST DATA
FOR
DRESSER PERFORATORS
AS OBTAINED WITH
STANDARD PROCEDURE FOR EVALUATION OF WELL PERFORATORS

Name	Gun Diameter (O.D.)	Charge Weight (Grams)	Type Carrier	Min. Pipe Size (I.D.)	CONCRETE TARGET		BEREA TARGET					Temp. °F	Pressure PSI
					Total Penetration	Entry Hole Diameter	Entry Hole Diameter	CFE	TTP	TCP	ECP (TCP x CFE)		
Slim Kone-Hi Temp.		2.5			6.04	.23	.26	.76	4.81	3.68	2.80	400°†	20,000
Slim Kone-Sidewinder D.P.	1-11/16"	2.5	Steel	1.995	5.34	.25	.24	.74	5.03	3.90	2.89	325°*	20,000
Slim Kone-SSB		3.0			8.12	.25	.29	.81	5.48	4.35	3.52	325°*	20,000
Link Kone-Golden Jet	1-11/16"	13.0	Aluminum	1.995	7.87	.33	.41	.88	6.93	5.80	5.10	300°	10,000
Bar Kone II	1-11/16"	12.0	Steel	1.995	9.22	.34	.31	.83	6.95	5.83	4.84	300°	15,000
Link Kone-Rigid Jet	2-1/16"	19.0	Aluminum	2.441	8.83	.40	.45	.77	8.63	7.51	5.76	300°	10,000
Link Kone-Golden Jet	2-1/8"	22.0	Aluminum	2.441	9.59	.35	.45	.71	8.27	7.14	5.06	300°	10,000
Silver Jet	2-1/8"	16.0	Steel (Alloy)	2.441	17.56	.37	.39	.87	10.55	9.42	8.17	300°	15,000
Slim Kone-Big Hole	2-1/8"	6.0	Hollow	2.441	7.96	.39	.44	.77	6.40	5.27	4.06	325°*	20,000
Slim Kone-Jumbo Jet	2-5/8"	11.0	Hollow	2.750	13.32	.36	.36	.78	10.36	9.21	7.15	325°*	20,000
Slim Kone	3-3/8"	22 + 17	H.T. Steel	3.826	15.10	.47	.46	.79	10.28	9.14	7.27	325°	20,000
Kone Shot-Golden Jet		11.0			12.38	.30	.32	.86	8.74	7.61	6.52	325°*	20,000
Kone Shot-Jumbo Jet	3-1/8"	12.0	Hollow	3.548	13.37	.32	.40	.83	10.46	9.33	7.77	325°*	20,000
Big Hole, Burr Free		11.0			6.25	.61	.67	.81	5.48	4.35	3.51	325°*	20,000
Kone Shot-Jumbo Jet II	3-3/8"	14.5	Hollow	3.826	16.26	.37	.38	.84	11.81	10.68	8.93	325°*	20,000
Kone Shot-Golden Jet		11.0		4.026	12.87	.32	.31	.75	9.92	8.73	6.58	325°	20,000
Select Kone Golden Jet	3-1/2"	11.0	Hollow	4.026	12.87	.32	.31	.75	9.92	8.73	6.56	325°*	20,000
Kone Shot-Jumbo Jet		12.0		4.026	13.47	.34	.40	.83	10.46	9.33	7.77	325°	20,000
Kone Shot-Golden Jet	3-5/8"	17.0	Hollow	4.026	15.40	.38	.44	.80	12.79	11.66	9.31	325°*	20,000
Kone Shot-Jumbo Jet	3-5/8"	22.5			18.40	.42	.44	.78	14.01	12.88	10.00	325°*	20,000
Kone Shot-Golden Jet		17.0			16.37	.40	.44	.80	12.79	11.66	9.31	325°	20,000
Kone Shot-Jumbo Jet II	4"	22.5	Hollow	4.670	23.68	.39	.43	.84	15.07	13.93	11.74	325°*	20,000
Big Hole, Burr Free		20.0			7.29	.65	.76	.79	6.38	5.25	4.14	325°	20,000
Big Hole-Jumbo Jet	5"	32.0	Hollow	5.675	16.10	.78	.84	.82	11.60	10.40	8.49	325°*	15,000
Sequential H.D.	5"	20.0	Steel (Alloy)	5.675	16.14	.38	.41	.84	11.72	10.59	8.84	325°	20,000

*Charges available for temperatures to 525°F.
CFE — Core Flow Efficiency
TTP — Total Target Penetration
TCP — Total Core Pentration
ECP — Effective Core Penetration
†475° and 550°F available

N.B. Dresser Atlas is the old name for Western Atlas.

Both are parts of the Dresser Industries Group.